Durham E-Theses

Defoemational and physico-chemical properties of cereain sediments, with particular reference to colliery spoil

Taylor, Roy K.

How to cite:

Taylor, Roy K. (1971) *Defoemational and physico-chemical properties of cereain sediments, with particular reference to colliery spoil*, Durham theses, Durham University. Available at Durham E-Theses Online: http://etheses.dur.ac.uk/9085/

Use policy

The full-text may be used and/or reproduced, and given to third parties in any format or medium, without prior permission or charge, for personal research or study, educational, or not-for-profit purposes provided that:

- a full bibliographic reference is made to the original source
- a link is made to the metadata record in Durham E-Theses
- the full-text is not changed in any way

The full-text must not be sold in any format or medium without the formal permission of the copyright holders.

Please consult the full Durham E-Theses policy for further details.

Academic Support Office, Durham University, University Office, Old Elvet, Durham DH1 3HP
e-mail: e-theses.admin@dur.ac.uk Tel: +44 0191 334 6107
http://etheses.dur.ac.uk

DEFORMATIONAL AND PHYSICO-CHEMICAL PROPERTIES OF CERTAIN SEDIMENTS, WITH PARTICULAR REFERENCE TO COLLIERY SPOIL

A Thesis submitted for the Degree of

Doctor of Philosophy

in the

University of Durham

by

ROY K. TAYLOR

November, 1971

Acknowledgements

This work has been generously supported over the past four years by personal research grants to the writer from the National Coal Board. Without such support the scope of the work would necessarily have been limited. The unfailing help of numerous Board officials is greatly appreciated, particularly Mr. G. Armstrong (Chief Geologist) and Mr. G. McKechnie Thomson (Chief Civil Engineer), both of whom have negotiated grants on behalf of the writer and have offered considerable encouragement.

To my colleague Dr. Peter Attewell, warm thanks are due for useful discussions over the years and for critically reading this long manuscript. Similarly, Dr. Alan Spears of Sheffield University has been most helpful in geochemical matters.

Virtually all the Technical and Secretarial staff in the Geology Department at Durham have been inconvenienced on many occasions and the writer is deeply appreciative of their efforts. Technical staff and students have been of great assistance in the field, usually under adverse weather conditions. It is difficult to single out staff by name but three technicians who have been trained in soil mechanics methods by the writer should be mentioned: Mr. B. McEleavey (Engineering Geology), Mr. J. Higgins and Mr. W. Bayston (both with National Coal Board support, and now with the Teesside Greater Authority).

Sincere thanks are due to Mr. R.G. Hardy (now Experimental Officer in the Department of Geology) for his tireless efforts in developing the quantitative X-ray diffraction curves and for help with X-ray fluorescence methods. Dr. J.G. Holland and Mr. J.H. Peacock (Geology Department) and Dr. A.G. Hawkes (Mathematics Department) are other colleagues who have been consistently understanding and helpful with X-ray fluorescence analysis, seismic reflection techniques and statistical methods, respectively.

ABSTRACT

The present study is placed in the context of the disastrous Aberfan (Wales) colliery tip failure in 1966, particularly with respect to the singular lack of knowledge regarding the consequences of long-term weathering of coal-bearing strata.

Initial breakdown of fresh indurated sediments from underground workings (roof and floor measures) is shown to be a function of a) sedimentary structures b) capillarity (air-breakage) c) expandable mixed-layer 10Å clay content. A geographical variation in clay mineralogy implies that breakdown should generally be at a minimum in the Durham, Northumberland and Scottish coalfields.

An *in situ* study of a stratigraphic section containing all rock-types likely to be found in British colliery tips shows that chemical (weathering) processes are very restricted. Pyrite is the only mineral species which has completely broken down within the 8ft-deep weathering zone, over a period of about 10,000 years. Cohesion is the strength parameter most susceptible to *in situ* degradation and the shear strength parameters of the near-surface materials generally conform with those of jointed and fissured rocks, rather than soils. The residual (ultimate) strength of weathered-unweathered Coal Measures sediments is shown to be a function of the ratio quartz: clay minerals.

Major temperature-time dependent, mineralogical changes in the superficial zone of the very coaly, 100-year-old Brancepeth colliery tip are not matched by a large fall-off in shear strength. The composite internal friction value is similar to shale-fill dams in Britain; there is no statistically significant strength difference between upper slope (younger) and lower slope (older) samples, which are some 27 per cent higher than the residual spoil strength. Convincing chemical, physical and mechanical data

from a 50-year-old tip at Yorkshire Main Colliery show that small changes within the heap are more readily attributable to changing colliery practice, rather than to degradation processes. After initially rapid physical breakdown, the material has changed little after burial.

This study has shown that long-term weathering processes have little influence on the overall stability of colliery spoil.

CONTENTS

		Page
Chapter 1.	INTRODUCTION	1
Section 1.1	Aims of the work and method of approach	1-2
1.2	Colliery tips	2-8
1.3	Argillaceous rocks associated with colliery discard	9-14
1.4	Weathering and shear strength characteristics	14-19
1.5	Statistical treatment of results	19-23
1.6	Methods and general comments	23
Chapter 2.	THE BREAKDOWN OF EXCAVATED COAL MEASURES ROCKS	
Section 2.1	Introduction	24-25
2.2	The role of geological structures in disintegration	25-32
2.3	The influence of mineralogy on breakdown	32-42
	a) Clay minerals	32-38
	b) Pyrite (non-detrital mineral)	38-40
	c) Carbonates (non-detrital minerals)	40-41
2.4	Textural features	42-44
2.5	Water uptake by shales	44-47
2.6	Empirical suction pressure curves for weak rocks	47-51
2.7	Breakdown of shales and mudstones in water and other liquids	51-61
2.8	Conclusions	61-62
Chapter 3.	THE MINERALOGICAL AND DEFORMATIONAL CHARACTERISTICS OF A WEATHERED PROFILE DEVELOPED IN COAL MEASURES ROCKS	
Section 3.1	Introduction	63-64
3.2	Geological sequence and sampling	64-66
3.3	Visual weathering	66-77
3.4	Mineralogy and chemistry	77-78
3.5	Detrital minerals	78-81
3.6	Micaceous minerals	81-83
3.7	Kaolinite	83-85
3.8	Chlorite	85-88
3.9	Non-detrital minerals	88-91
3.10	Grain size and consistency limits	91-94
3.11	Specific gravity, density and Standard Penetration Tests	94-95

Chapter 3 (contd.) Page

Section 3.12 Shear strength measurements and treatment of results 95-103
3.13 Deviator stresses 103-105
3.14 Shear strength parameters 107-109
3.15 Deformation modulii 110-111
3.16 Conclusions 112-115

Chapter 4. THE CHEMICAL, MINERALOGICAL AND GEOTECHNICAL CHARACTERISTICS OF AN ANCIENT COLLIERY TIP

Section 4.1 Introduction 116
4.2 History of the heap 116-117
4.3 Sampling 117-120
4.4 Mineralogy of equivalent strata 120-122
4.5 Mineralogy and chemistry of the tip materials 122-123
4.6 Detrital minerals 123-132
a) Quartz 123-130
b) Feldspars 130
c) Clay minerals 130-132
4.7 Non-detrital and secondary minerals (excluding sulphates) 132-134
a) Pyrite 132-133
b) Carbonates 133
c) Iron oxides 133-134
4.8 Spontaneous combustion and sulphates in colliery tips 134-142
4.9 Chemical-mineralogical correlations 142-144
4.10 Fundamental properties 144-146
a) In situ density 144-146
b) Specific gravity (G_s) 146
4.11 Classification 146-149
a) Liquid and plastic limits 146-147
b) Particle size distribution 147-149
4.12 Shear strength 149-161
a) Triaxial tests 149-159
b) Deformation modulii 159
c) Large strain shear box tests 160-161
4.13 Correlation matrix; physical data versus mineralogy and chemistry 161-163

Chapter 4 (contd.)		Page
Section 4.14	Stability analyses	163-167
	a) 1957-58 reclamation period	164-166
	b) 1948 period - Reconstruction from aerial photographs	166-167
4.15	Compaction	167-170
4.16	Conclusions	170-172
Chapter 5.	**THE MINERALOGY AND GEOTECHNICAL PROPERTIES OF UNBURNT SPOIL - YORKSHIRE MAIN COLLIERY**	
Section 5.1	Introduction	173-177
5.2	Underground samples	177-178
5.3	Hand specimens and thin sections	178-179
5.4	Chemistry and mineralogy	179-187
5.5	Water sample analysis and tip permeability	187-190
5.6	Liquid and plastic limits	190-193
5.7	Density considerations with respect to the evolution of the tip	193-194
5.8	Particle size distribution	194-195
5.9	Specific gravity (G_s) and organic carbon content	195
5.10	Triaxial compression tests	195-204
	a) Colliery discard	195-203
	b) Fabricated equivalent roof and floor measures	203-204
5.11	Correlation of physical and mechanical data	204-206
5.12	Slope stability analyses	206-211
	a) Slope profile and geophysical survey	206-208
	b) Factor of safety-limit equilibrium analyses	208-211
5.13	Compaction characteristics	211
5.14	Shear strength characteristics with respect to degradation	211-215
5.15	Sample representability	215-218
Chapter 6.	**GENERAL SUMMARY AND CONCLUSIONS**	219-226
Bibliography		227-237
APPENDIX 1	X-ray fluorescence spectrometry Cation exchange capacity	A1-A4
APPENDIX 2	X-ray diffraction quantitative curves	A5-A6
APPENDIX 3	Triaxial tests- back-saturation	A7-A8
APPENDIX 4	Slope stability analysis	A9-A14

LIST OF TABLES

		Page
Chapter 2.		
Table 2.1	Cyclothemic sequences (after Edwards and Stubblefield (1947), Elliott (1968)	26
2.2	Chemical composition; a) Mansfield Marine Band shale, Little Smeaton Borehole. b) Durham High Main seam roof measures, Lumley	27-28
2.3	Cation exchange values	39
2.4	Long-term permeability-chemical changes; large strain direct shear box test results	41
2.5	Slaking test results	53
2.6	Fundamental properties	54
2.7	Swelling pressures and free swell data for two air-dried tonsteins	58
Chapter 3.		
Table 3.1	Modified RQD and core recovery	65
3.2	Quartz and clay minerals	68
3.3	Chemical analyses	69-72
3.4	Oxide ratios and selected chemical data	73-76
3.5	Kaolinite crystallinity factors	85
3.6	X-ray reflections - 14Å (smear mounts)	86
3.7	Non-detrital minerals; X-ray and thin section identification	89
3.8	Specific gravities, moisture contents, densities and Standard Penetration Tests	93
3.9	Triaxial and shear box tests	96-100
3.10	Principal stress difference at failure for lowest confining pressure	105

		Page
Table 3.11	Comparative shear strength parameters - Triaxial tests; shear box	106
3.12	Comparison of deformation modulii	111

Chapter 4.

Table 4.1	National Coal Board records relating to seams which have contributed to Brancepeth tip	118
4.2	Sample descriptions	119
4.3	Mineralogy of equivalent measures represented in the Brancepeth heap (samples from neighbouring collieries)	121
4.4	Minerals identified by X-ray diffraction in the Brancepeth tip	124
4.5	Normalized chemistry and oxide/alumina ratios	125-126
4.6	Clay minerals, mica shape factor, free silica, sulphate content, adsorbed moisture, hydrogen ion concentration	127
4.7	X-ray confirmation of unusual sulphates in Brancepeth spoil	136
4.8	Sulphate species from in situ and colliery tip materials	137
4.9	Chemistry of burnt shales from Co.Durham (Sherwood and Ryley, 1970) compared with Brancepeth	140
4.10	Correlation matrix - Chemistry/mineralogy	143
4.11	Physical properties	145
4.12	Consistency limits and grading parameters	148
4.13	Triaxial and Shear Box results (basic test data)	151-153
4.14	Triaxial shear strength parameters - statistics; Brancepeth	154-155

		Page
Table 4.15	Variance Ratio (F-test), Chow (1960). Difference between regression lines (Mohr circle top points)	156
4.16	Triaxial shear strength parameters - statistics; Aberfan	157
4.17	Correlation data - physical, mechanical, chemical and mineralogical data	162
4.18	Slope stability analyses	165
4.19	Compaction and field density data	169
Chapter 5.		
Table 5.1	Sampling and testing scheme	174-176
5.2	Average modal composition from thin sections (percentage)	179
5.3	Chemistry of S.P.T. and U4 samples (X.R.F., summed to 100 per cent)	180-181
5.4	Chemical composition of Yorkshire Main Spoil Heap (based on 25 samples)	182
5.5	Correlation matrix for elements and oxides in the Yorkshire Main tip	184
5.6	Ground-water analyses	188
5.7	Properties of Yorkshire Main discard	191-192
5.8	Triaxial test data	196-199
	a) Yorkshire Main tip	196-198
	b) Fabricated specimens from underground measures	199
5.9	Triaxial shear strength parameters. Yorkshire Main tip; fabricated underground samples	200-202
5.10	Correlation matrix-physical and mechanical data	205
5.11	Slope stability analyses	207
5.12	Compaction tests, Yorkshire Main	210
5.13	F-value on differences between regression lines (Chow test)	212

Page

Table 5.14 Comparison of shear strength parameters - spoil-heap and fabricated samples 213

5.15 Student t-test on U4 chemistry vs. S.P.T. chemistry 216

Chapter 6.

Table 6.1 Comparison of normalized chemistry; U4 samples of Brancepeth and Yorkshire Main 225

6.2 Variance Ratio (F-test) on differences between regression lines; Aberfan, Brancepeth and Yorkshire Main 225

Table A1.1 X-ray fluorescence analysis. Preliminary calibration of major element standards A3

A1.2 Comparison of X.R.F. and wet chemical analyses A3

A2.1 X-ray calibration data A6

A4.1 Example; circle (9) Brancepeth (slope stability program) A11

FIGURES

Chapter 1. Following page

Fig. 1.1 Conical tip construction (diagrammatic) 2

1.2 Aerial ropeway tip construction (Diagrammatic) 2

1.3 Consolidation characteristics, normally-consolidated and over-consolidated clay (after Skempton, 1970) 10

1.4 Shear box (diagrammatic) and large strain shear tests (b and c after Skempton, 1964) 17

1.5 Linear regression analyses (after Imbrie, 1956) 20

Chapter 2.

Fig. 2.1 Non-marine laminated silty mudstone - swelling characteristics in water 26

2.2 Joints and slickensides; Mansfield Marine Band cyclothem, Tinsley Park, Nr. Sheffield 28

2.3 Showing clay mineral components in 57 tailings samples from all N.C.B. Areas in Britain 34

2.4 End-over-end breakdown test results for seatearths, plotted against the rank of associated coal seam 37

2.5 Results of two consecutive long-term permeability tests on carbonate-rich lithorelicts of silty shale from Lumley, Co. Durham. 40

2.6 Details of X-ray texture goniometer operating in reflection mode 41

2.7 X-ray fabric diagrams: a- artificially sedimented specimen of b; b - non-marine mudstone; c - High Hazels roof shale; d - mudstone roof, Upper Nine Feet seam 42

2.8 X-ray texture analogue print-out for quartz ($\underline{d}$ = 1.817Å) 42

2.9 Seasonal variation in shear strength parameters for soil horizon developing on breakdown of silty mudstone at Lumley, Co.Durham 44

Following page

Fig. 2.10 Suction pressure curves for mudstone and siltstone samples 47

2.11 Suction pressure curves for High Hazels shale and chalk. (adapted from Philpott, 1970) 47

2.12 Stafford tonstein suction curves compared with compacted commercial clays (after Philpott, 1970) 49

2.13 Slaking test samples - X-ray data 57

2.14 Slaking test samples; breakdown vs. clay size fraction and 'shape factor'. 57

2.15 Simplified illustration of variation in calculated capillary pressures for roof rocks 57

Chapter 3.

Fig. 3.1 Cross section through boreholes at Wales (Grid. Ref. SK 476 821) 63

3.2 Natural particle size and fundamental particle size of samples from Wales 66

3.3 Showing profile of quartz and clay minerals 79

3.4 Shape of 10Å reflection for selected micas (X-ray diffraction) 81

3.5 Profile of sulphur content with depth 88

3.6 Wales samples shown on Casagrande plasticity chart 91

3.7 Relationship between liquid and plastic limits with quartz 92

3.8 Mohr circle 'top point' plot for all triaxial specimens (logarithmic scales) 103

3.9 Shale, mudstone, seatearth, upper siltstone specimens (excluding shale and mudstone from less than 6.5 ft) - Mohr circles 103

3.10 Mohr envelope for non-weathered lower siltstone, borehole 2 108

Following page

Fig. 3.11 Relationship between ϕ'_r (c'=o) and quartz to clay minerals ratio 108

3.12 Principal stress ratio at failure versus secant modulus at half failure stress 111

Chapter 4.

Fig. 4.1 Evolution of Brancepeth tip (Ordnance Sheets, 1898, 1924, 1938) 116

4.2 Brancepeth Colliery waste heap reclamation scheme. Plan from aerial survey 116

4.3 Silica (quartz) solubility data superimposed on solubility/pH stability fields of other oxides (adapted from Loughnan, 1962) 127

4.4 Relative frequencies of organic carbon retained on sieves after wet sieving 134

4.5 Relationship between water soluble and acid soluble sulphate (weight percentage SO_3), Yorkshire Main tip samples 140

4.6 Particle size distributions, Brancepeth - dry sieving 147

4.7 Particle size distributions, Brancepeth - wet analysis 147

4.8 Particle size distributions, Brancepeth, dry sieving - Rosin's-law probability scale 147

4.9 Particle size distributions, Brancepeth, wet analyses - Rosin's-law probability scale 147

4.10 Large strain shear box tests - Barnsley Day Bed Coal, Yorkshire Main Colliery 159

4.11 Relationship between deformation modulii, E_i and E_s 159

4.12 Shear box tests - Brancepeth 160

4.13 Cross section of Brancepeth tip for slope stability analyses 163

Following page

Chapter 5.

Fig. 5.1 Roof and floor measures, Yorkshire Main Colliery 177

5.2 Relative proportions of clay minerals 182

5.3 Variation in CaO, MgO, FeO and MnO through Yorkshire Main tip 185

5.4 Variation in acid-soluble sulphate, sulphur in pyrite and Al_2O_3 through Yorkshire Main tip 185

5.5 Permeability (field and laboratory) plotted against porosity of materials 188

5.6 Brancepeth and Yorkshire Main specimens, classified according to Casagrande plasticity chart 190

5.7 Profiles showing variation in physical parameters through Yorkshire Main tip 190

5.8 Particle size distributions relating to Yorkshire Main tip 193

5.9 Relative frequencies of organic carbon retained on sieves after wet sieving 193

5.10 Cross section of Yorkshire Main tip for seismic reflection work and slope stability analyses 206

5.11 Computation for hammer siesmograph used in simple reflection mode 206

Chapter 6.

Fig. 6.1 Composite shear strength parameters for Yorkshire Main (including fabricated samples), Aberfan and Brancepeth 223

Appendix 2

Fig. A.2.1 X-ray diffraction calibration curves for quantitative quartz, illite, kaolinite and chlorite A6

Following page

Appendix 3

Fig. A3.1 Diagrammatic layout of the triaxial test (after Bishop and Henkel, 1962) A7

Appendix 4

Fig. A4.1 To show forces and dimensions used in Bishop Simplified Method of Slices analysis A9

LIST OF PLATES

Chapter 1.

Plate 1.1 Slickensided shear plane, Littleton Colliery tip (natural size) 8

Chapter 2.

Plate 2.1 To show progressive breakdown of a suite of underground samples when exposed out of doors 28

Plate 2.2 Polygonal fracture development - High Main roof rocks (sample 18in long) 30

Plate2.3 Showing Suction Plate and Pressure Membrane apparatus for measurement of suction pressure 45

Chapter 3.

Plate 3.1 Selection of weathered and unweathered triaxial specimens after failure (with detailed description sheet) 66

Chapter 4.

Plate 4.1 Brancepeth tip (Aerial photograph, 1948) 116

Plate 4.2 Failed triaxial specimens, Brancepeth 147

Chapter 5.

Plate 5.1 View southern face Yorkshire Main tip 173

CHAPTER 1

INTRODUCTION

1.1 Aims of the work and method of approach

The principal aim of this study is to ascertain whether or not the material that is buried within colliery tips is subject to weathering, and if so to what degree the mechanical stability of the spoil is affected. When the work was started in 1967 there were no published physical or mechanical data relating to colliery spoil; even at the time of writing the Aberfan Technical Reports (1969), and to a lesser extent the National Coal Board Technical Handbook (1970), provide the only authoritative information on colliery spoil heaps. Consequently, the investigations of the 100-year-old Brancepeth tip, Co. Durham (Chapter 4) and the 50-year-old Yorkshire Main tip (Chapter 5) have been considered in detail because the sum total of information now available provides a basis for future research on tip stability.

The argillaceous rocks which make up the bulk of material in spoil-banks may be excavated in a relatively fresh condition from many thousands of feet underground. In Chapter 2 therefore the factors affecting the initial breakdown of the rock types which are most susceptible to degradation will be investigated. The longer term weathering is characterized by both physical and chemical processes, which to a great extent are inter-related. However, the relative importance of chemical (i.e. mineralogical) changes is not easy to assess in the spoil-bank environment due to two features:

a) Their heterogeneous nature, and the periodic disturbance of spoil, following regrading.

b) The older heaps in which any significant time-dependent chemical changes may have taken place have invariably been subject to

27 JAN 1972 LIBRARY

spontaneous combustion; changes affecting unburnt (possibly more degraded) spoil are consequently masked by combustion effects.

In order to circumvent this problem an in situ section of progressively weathered rocks consisting of all the types which are likely to be found in colliery tips has been studied (Chapter 3). This strata section has been subjected to natural weathering over a period of about 10,000 years. The resulting mineralogical findings, together with the strength characteristics of the more weathered and fragmental rock types provide a useful 'yard-stick' with which to compare the colliery spoil materials.

1.2 Colliery tips

The rocks immediately associated with exploitable coal seams, together with a certain amount of coal that has not been separated in the washeries will have been included in the spoil or discard found in colliery tips. In addition there is the relatively dry run-of-mine materials from the underground development drivages and shafts, which, when tipped over high faces, generally produces slopes which are approximately equal to the angle of shearing resistance of the loose material. It will be demonstrated subsequently (Chapter 4) that inferior coal may be present in considerable proportions in some of the older spoil-banks. Dominantly sand and silt sized reject wet fines (tailings; also pressed tailings cakes) from the froth flotation process are in places included in the discard (for example, Aberfan; Weeks, 1969). Tailings lagoons are outside the scope of the current work but it is pertinent to mention that the lagoons were often sited on top of a tip complex; failure of the retaining embankment may well give rise to a widespread 'mud run'.

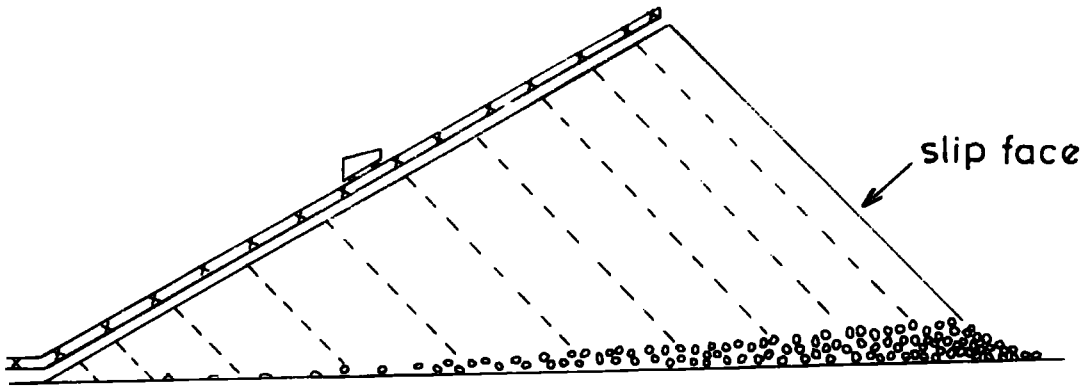

Fig 1.1 CONICAL TIP
(Like moving sand- dune)
e.g. Maclane type

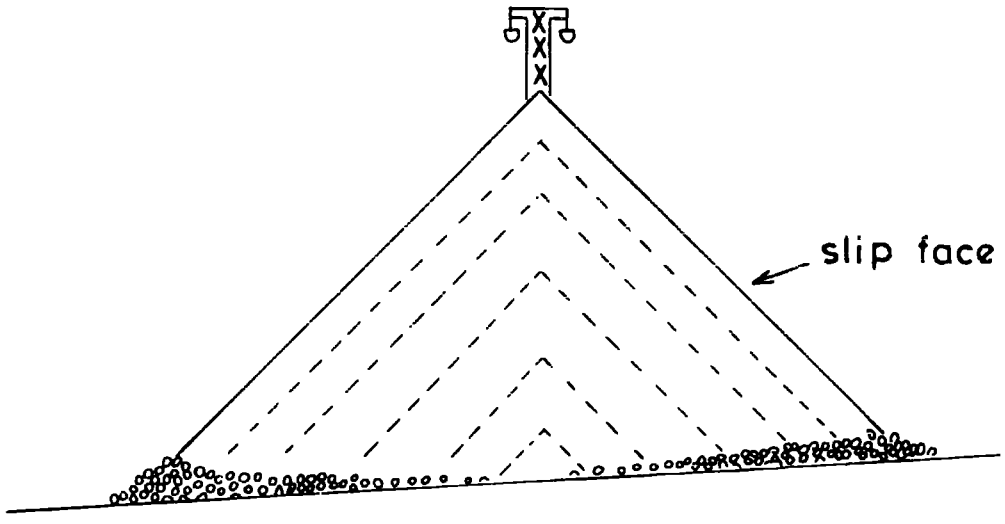

Fig 1.2 AERIAL ROPEWAY TIP
(Like seif dune)

Risk of spontaneous combustion due to segregation, particularly on faces subject to prevailing wind.
(Surfaces unstable to erosion.)

Such a phenomenon occurred in January 1966 when the embankment of a lagoon at Abernant Colliery failed and 3,000,000 gallons of tailings were released into the Upper Clydach River. A tip failure at Williamthorpe Colliery, near Chesterfield in March 1966, was also directly related to the collapse of a slurry lagoon bank (National Coal Board, 1968). Also included as minor tip constituents are extraneous materials such as limestone blanketing material, stone dust from the underground roadways, and boiler ash. The latter is always liable to cause accidental combustion.

The older tips with which the present work has been concerned were formed either as distorted conical heaps (mechanical tippler, Fig. 1.1), or as ridge-like aerial ropeway tips (Fig. 1.2) - somewhat analogous to a moving sand-dune (barchan) and seif-dune, respectively. The tippler constructions on occasions reached well over 200 ft. above the original ground level because of economic motivations relating to available land. In England and Wales alone some 20,000 acres of land have been used for tipping (Civic Trust, 1964) and a reasoned estimate by Glover (1967) suggests that by 1966 about 1,600,000,000 tons of spoil could be accounted for in existing heaps. During recent years progressive use of dump trucks, conveyors and earth moving equipment has led to significant changes in constructional methods, such as consolidated and terraced heaps.

Turning now to the question of stability, it was the disastrous Aberfan tip failure of October 21st 1966 which brought to light the lack of expertise and knowledge regarding these 'engineering structures'. Considering South Wales alone, tip failures were numerous prior to the Aberfan disaster. Five land-slide failures in a paper by Knox (1927) are referred to in the Technical Report (Bishop et al., 1969, Appendix 1).

The Abercynon failure is referred to in the latter Report and at a later date a more detailed interpretation is attempted (National Coal Board, 1968). In the National Coal Board's 1968 publication on Spoil Tip Management seven case histories are considered, including Aberfan. At Aberfan itself a major failure took place in 1944 (Tip 4) and intermittent slides affected Tip 7, prior to the disaster. It is also of interest to record that the suggested application of elementary soil mechanics techniques to spoil heap stability had not been completely neglected in pre-Aberfan times (see Nelson, 1955; Watkins, 1959; Nelson and Nelson, 1960).

It is not proposed to discuss Aberfan at length because the details of the Tribunal Technical Reports (1969) are considerable. What is perhaps more important is briefly to describe the geotechnics of the Aberfan situation and to place the present work in the context of the Tribunal findings. Mr. Phillip Wein, Q.C. for the National Coal Board stated that 'the primary causes of the failure of Tip No. 7 were geological in character. There was a coincidence of a set of geological factors, each of which, in itself, was not exceptional but which collectively created a particularly critical geological environment.' The inter-relationships of these factors are adequately explained in a useful summary by Woodland (1968). The present writer however, would suggest that Tip 7 was a 'failed engineering structure' long before the events of October 21st. Briefly, the situation at Aberfan was that Tip 7, which was 150 ft. above natural ground level at the crest (nominally 220 ft. at the toe) had advanced beyond the junction where a tongue of boulder clay infilling a gentle hollow extending up the valley side, thinned out against the Brithdir Sandstone and its superficial cover of post-glacial head deposits. Subsidence effects (pre-1945) resulted in a corridor of residual tensile strain running obliquely across

the area, but this was contained on both sides by compressional zones which therefore gave rise to flanking transmissibility barriers. Hence, a classical situation of enhanced fissure flow in the sandstone aquifer, and potential piezometric-rise in groundwater was created beneath the tip now that the junction with the boulder clay aquiclude had been over-stepped. By 1963 back-sapping in the region where tensile strains were at a maximum was apparent and it was established by most of the technical authorities at the Tribunal that a spring or spring-complex was in existence close to the up-hill junction of the boulder clay and the aquifer. In the latter part of 1963 a slip occurred with a deep surface passing behind the crest of the tip and the implications drawn from the limit equilibrium analysis of Bishop et al., (1969) suggest that a reduction in the angle of internal friction may well have been involved. They concluded (p.32) on the basis of peak internal friction (subsequently obtained from laboratory tests) that for a fresh slip surface to be developed the pore water would have to account for some 60 per cent of the total weight of material above the toe. They concluded that a pore pressure of this magnitude was improbable. Re-activation of this slip was shown to be the 'trigger' for the disastrous events of October 21st 1966. The presence of this failure surface prompts the present writer to adopt the 'failed engineering structure' criterion and this may well apply to other colliery tip failures (e.g. Abercynon; National Coal Board, 1968). The pore-water pressure developed at the base of the Tip 7, Aberfan, following heavy rain, re-activated the pre-existing failure and a flow slide developed due to the presence of a substantial volume of loose, saturated material at the base of the tip and of a large volume of loose, wet material, containing only a small percentage of air in the voids, above it. The shear plane passed down into the boulder

clay, which then ruptured to release an abnormal volume of water. Woodland (1968) quotes a conjectured 18.5 million gallons being drained from the Brithdir Sandstones, which is symptomatic of a considerable excess hydrostatic pressure.

Flow or liquefaction slides usually occur in uniformly graded material in the fine sand range, and among the criteria proposed by Terzaghi and Peck, (1948) for identifying these materials are:

$$D_{10} < 0.1 \text{ mm}$$

and $$D_{60}/D_{10} < 5$$

where: D_{10} is the diameter equivalent to the '10 per cent passing' on a grading curve and D_{60} is the '60 per cent passing' size. The ratio D_{60}/D_{10} is a sorting factor known as the uniformity coefficient. Since Aberfan it is obvious that this range can be extended (Hutchinson, 1967), in that D_{10} for Aberfan is slightly greater than 0.1 mm and the uniformity coefficient is about 10. Hutchinson also shows that the D_{10} size of a liquefaction slide which occurred in P.F.A. at a site in South Wales had a uniformly coefficient of approximately 10 and a D_{10} size of 0.15 mm. Some indication of the state of looseness of recent liquefaction slides can be gained by comparing in situ dry densities (weight of solids/total volume) to maximum dry densities as obtained in the B.S. low standard compaction test (B.S.1377/1967).

	Maximum dry density lb/ft^3	in situ dry density lb/ft^3	% maximum
P.F.A.(Jupille)	73	56	77
" (S. Wales)	62	49	79
Aberfan, Tip 7	121	99	82

Flow-slides occur only in loose cohesionless materials and according to Casagrande (1965) no precise division can yet be drawn between materials which will flow and materials which will not - obviously colliery spoil is included in materials which will. The mechanism involves the transference of the stress, which is initially carried by the metastable solid skeleton (loose particulate materials), to the pore water. Flow slides in which the fluid phase is mainly gas have recently been referred to as 'fluidization' phenomena by Casagrande (1971). The process can be illustrated in terms of Terzaghi's (1936) effective stress principle:

$$\sigma' = \sigma - u$$

where: σ' is the effective pressure carried by the solid particles

σ is the total normal pressure

u is the neutral stress, porewater pressure

A mild shock causes a decrease in volume at an unaltered value of σ. If this decrease takes place below water, it is preceded by a temporary increase in u to a value almost equal to σ, whereupon $\sigma' = \sigma - u$ becomes almost zero and the material flows like a viscous fluid.

One of the most significant pieces of evidence relating to the slope failure of Aberfan was the discovery of a slip surface consisting of fine grained spoil with an angle of internal friction, ϕ', of only 17.5 to 18.5 degrees (compared with a peak ϕ' value of 39.5°). The conclusions of Bishop et al., (1969) were that comminution alone did not produce this low value and that some process of weathering was involved. Similarly, the fact that the older tips at Aberfan remained stable for considerable heights at 33 to 35 degrees (Tribunal Technical Report, p.19) also implied that tip failures could be time-dependent. Certain of the other case histories in

the literature referred to earlier in the text show that failures can occur in old tips. Hence, the present writer has concentrated on the effects of weathering in relationship to the overall stability of colliery spoil.

The possibility that tailings had contributed to the low-strength shear plane material of Aberfan was not entirely ruled-out (Bishop et al, 1969, p.20). A recent failure at Littleton Colliery (SJ 969 131) revealed a slickensided and polished failure plane (Plate 1.1) which has been examined as part of a special project carried out under the writer's direction. Under the microscope the material within 1 to 2 mm of the shear plane consists of clay-grade size material and rounded pseudomorphs of shale and mudstone fragments. Over a further distance of 4.5 mm all the fragments have been rounded in response to shear displacement. In the immediate shear-surface zone the clay minerals have aligned themselves parallel to the shear plane or to the slickenside ridges. The important feature is that the results of shear box tests (see Section 1.3), with the failure plane parallel to and coincident with the split in the box, show that the internal friction angle is again very low (20.5°). Subsequent chemical and mineralogical analyses imply that there is very little difference in these properties between the slip plane sample and those taken from other points in the near-surface zone at Littleton. In other words, it is very unlikely that tailings have contributed significantly to the Littleton shear plane failure mechanics. It will be noted on Plate 1.1 that relatively modern rootlets are present and some of these appeared to be normal to the plane. Here again, there is tentative evidence that this was also a re-activated shear plane.

PLATE 1.1

SLICKENSIDED SPOIL FROM LITTLETON TIP SHEAR PLANE

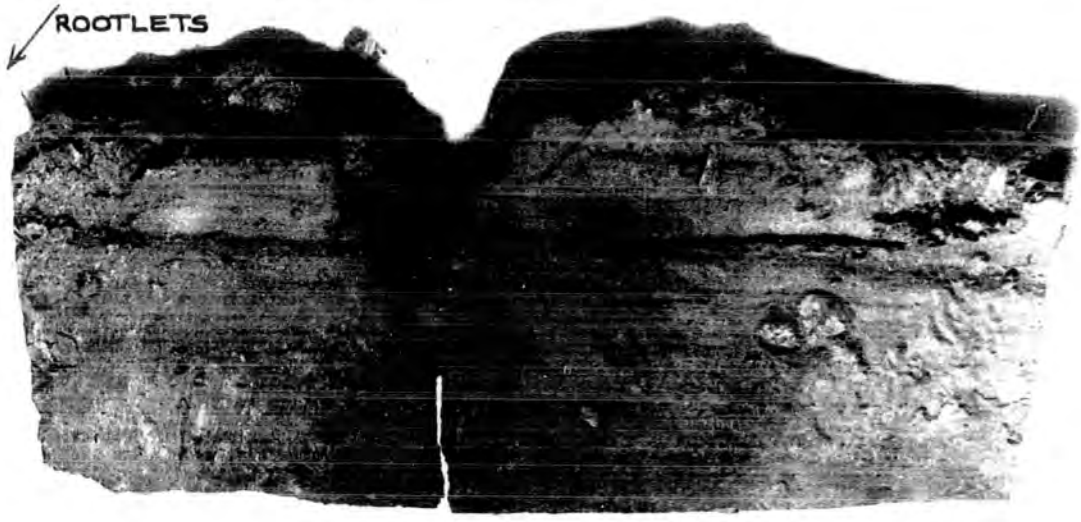

NATURAL SIZE

1.3. Argillaceous rocks associated with colliery discard

The predominance of argillaceous and arenaceous rock types (seatearths, shales, mudstones and siltstones) in colliery tips can be tentatively inferred from the 'cyclothem' concept of Wanless and Weller (1932). The term cyclothem refers to a sequence deposited during a single sedimentary cycle, and the 'ideal' or 'classical' upwards sequence is given by Trueman (1954) as: 1) marine band 2) non-marine shale or mudstone 3) sandstone 4) rootlet bed (underclay or seatearch 5) coal - followed by marine band etc.

This type of sequence is the exception rather than the rule and in the East Pennine Coalfield, for example, the statistical work of Duff and Walton (1962) shows that on a lithological basis the dominant cycle is seatearth - shale - seatearth. Marine bands are very infrequent in the Coal Measures (sensu stricto) but it should be appreciated that many of the coal seams worked in Scotland, and a few of those exploited in North Eastern England are from the lower divisions of the Carboniferous where limestone beds make up a large section of the marine strata. Similarly, both intrusive and volcanic igneous rocks are infrequently found in association with coals. Quantitatively however, the current National Coal Board site investigations of colliery spoil-banks point to limestones and igneous rock-types as being minor contributors. In general therefore the discard most frequently encountered contains seatearth, shale, mudstone, siltstone and minor sandstone fractions.

Classification (particularly on a visual basis) presents considerable difficulties. This is not altogether surprising if the origins and compositions of sediments like seatearths are considered. Huddle and Patterson (1961), Schultz (1958) and Moore (1968) sub-divide this rock into 3 or 4 units:

a) upper plastic clay found immediately beneath the coal, b) carbonaceous unit which in some places is shaly and yet sometimes is unbedded, c) clay-rich unit with siderite ($FeCO_3$) nodules, d) transition zone grading downwards into the underlying rock. These deposits were formed at a stage in delta formation when the fresh or brackish water was shallow and marginal vegetation was beginning to establish itself. First and foremost they are re-worked and leached deposits and consequently some of the above units may be missing, or so confused that divisions cannot be defined. In terms of rock-type they may range from exceedingly strong fine-grained sandstones (ganisters) to kaolinite-rich plastic fireclays. This type of problem is very apparent in Chapters 2 and 3 and can be extended to include shale-mudstone-siltstone.

Insight into the diagenetic history of fine-grained sediments can be gained from recently published field and laboratory studies of Skempton (1970). The term diagenesis is used in the sense designated by Read and Watson (1962) to include, "those changes that take place in a sediment near the earth's surface at low temperature and pressure and without crustal movement being directly involved. It continues the history of the sediment immediately after its deposition and with increasing temperature and pressure it passes into metamorphism". Taylor (1964) compared diagenesis with weathering in that "for the most part diagenetic changes involve increasing lithification (bonding of individual particles together so that an aggregate mass results); weathering is the reverse". In this sense weathering can be regarded as retrograde diagenesis.

In the early stages of diagenesis, argillaceous muds with a porosity*

* Porosity $n = \frac{\text{vol.voids}}{\text{total volume}}$, void ratio, $e = \frac{\text{vol.voids}}{\text{vol.solids}}$

Hence, $n = \frac{e}{1+e}$ and $e = \frac{n}{1-n}$

FIG. 1.3

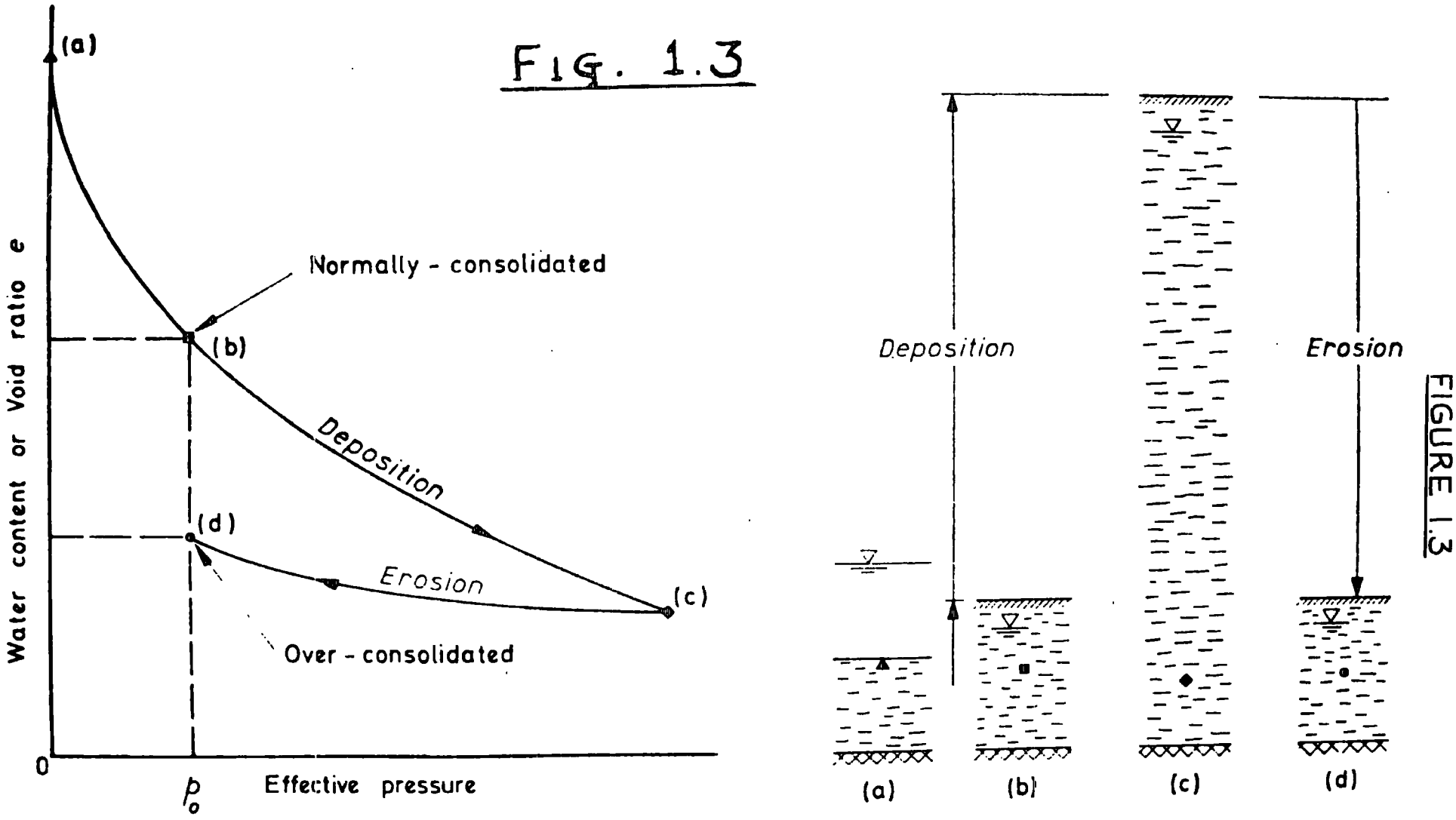

FIGURE 1.3

FIG. 2. Normally- and over-consolidated clay. (SKEMPTON, 1970)

of about 80 per cent undergo marked physical changes during gravitational compaction (expulsion of pore water under increasing weight of overburden). From the laboratory sedimentation compression curve such as that given by Skempton, 1970 (Fig. 1.3) it can be seen that as the effective overburden pressure increases the sediment compacts - points (a) to (b) to (c). In the field situation it is necessary to know the pore pressure in order to calculate the effective overburden pressure, P_o ($P_o = \sigma' = \sigma - u$, as previously). Figure 1.3 establishes the difference between a normally-consolidated sediment and an over-consolidated one - two terms exemplified by behavioural characteristics under shear, which will be mentioned frequently in the following Chapters. A normally-consolidated sediment (Terzaghi, 1941) is one which has never been subjected to a pressure greater than the existing overburden pressure. Point (b) on the curve (a) - (c) could represent this condition. If the existing overburden pressure (simulated by effective normal pressure in the shear box, or confining pressure in the triaxial cell) is less than the maximum effective pressure to which the clay was subjected in the past, the sediment is referred to as being over-consolidated and it would be represented by, say, point (d) on the rebound curve (c) - (d). Implicit in this illustration is the fact that the compaction caused by a given pressure increment on a normally-consolidated clay is much greater than the expansion caused by a numerically equal pressure reduction. Hence the two points (b) and(d) are under the same effective pressure, and the difference in void ratio reflects the consolidation history.

The void ratio versus effective pressure (logarithmic) plot of normally-consolidated sediments is essentially linear to depths in excess of 3000 m Skempton, 1970, Fig. 21). The porosity apertaining to the deepest sediments shown on this diagram is 15 per cent and the highest temperature recorded is

about 75°C. In answer to the present writer Skempton (p.410) stated that the rather fragmentary information available suggested that clays with a high carbonate or organic content behaved in a quantitatively different manner from the sediments he had considered. Hence we have little information relating to the effects of diagenetic minerals (such as carbonates), which must be operative during the early stages of diagenesis and under moderate overburden pressures (Strakhov et al., 1954). Müller (1967) refers to depths in excess of 500 m as the 'deep-burial stage' and considers that by the time a sediment is subjected to this order of overburden pressure a soft clay has already been transformed into an indurated, firm and coherent mudstone (mudstone + fissility = shale) with a porosity of about 30 per cent. Now Müller clearly states that this transformation is brought about by compaction alone and it is probable that the confusion which exists in the nomenclature of argillaceous rocks can be partly attributed to the lack of distinction which is drawn between the younger compacted rocks and the older (more deeply buried) types. The 15 per cent porosity of Skempton (1970) is some 10 per cent higher than that of Coal Measures shales (see for example, Beckett et al., 1958). On the basis of experimental work Lomtadze (1955) showed that diagenesis could be sub-divided into shallow-burial and deep-burial stages, with the initial transformation being a conversion to mudstone (or shale). In the deep burial stage mudstone is converted to an argillite with porosities of around 4 to 5 per cent. The term argillite still implies a non-metamorphosed rock. In the American literature, in particular, mention is rarely made of the fact that Upper Cretaceous shales like the Pierre and Bearpaw are 'compaction shales', which from an engineering point of view have little in common with the indurated, and sometimes highly cemented shales of the British Carboniferous. Similarly, the Tertiary shales of Japan (Nakano, 1967)

have physical properties which are somewhat different from those of the rocks which are considered in this thesis. The differences in engineering behaviour of the younger 'weakly-bonded' shales and the more indurated older types have been clearly recognized by Underwood (1967) in a very comprehensive survey of North American shale-type rocks. He tends to adopt Mead's (1936) classification into two major groups comprising compaction or 'soil-like' shales on the one hand and cemented or 'rock-like' shales on the other hand. With some reservation regarding the degree of cementation the present writer would draw the same divisions. In like manner the term clay-shale has become increasingly nebulous (Johnson, 1969) and this is made very plain by the discussions of Bjerrum and Taylor (in Johnson, 1969). More than fifteen years ago semi-quantitative X-ray work led the National Coal Board's Scientific Department to the conclusion that kaolinite, mica and lesser amounts of chlorite were the main clay minerals in the floors and roof rocks of a wide spectrum of Coal Measures rocks (Pitt and Fletcher, 1955). One of the important features of diagenesis is that the expandable clay mineral, montmorillonite, is transformed into illitic (micaceous types) as the depth of burial increases. Insofar as the behaviour of many of the compaction shales is concerned it is the presence of montmorillonite in these younger rocks which has a marked influence (for example, swelling potential - see Underwood, 1967, p.106).

The data presented by Skempton (1970) show that at depths of around 3000 m temperatures of about 75°C obtain in the Middle Pliocene mudstones of the Po Valley. The geothermal gradient can vary from place to place and in some areas the gradient may well have been considerably lower during the Carboniferous than that pertaining today (Kuyl and Patijn, 1961). The coals associated with the roof and floor measures found in colliery tips have undergone coalification as a result of the same consolidation factors

(more importantly temperature). In the past it was concluded that pressure played an important part in this coalification process because the rank of the coal increases with increasing overburden pressure (Hilt's rule). For the South Wales coalfield Jones (1951) demonstrated that there was a linear relationship between volatile content and depth of cover between the limits 12.5 to 40 per cent volatiles. This increase in rank is related to depth of burial inasmuch as the temperature rises with depth of burial; to this extent Hilt's rule applies (see Teichmüller and Teichmüller, 1967). Very broadly the diagenesis of the coal parallels that of the sediments, and the soft brown coals are associated with 'compaction shales' and sands, whereas the bituminous coals and anthracites of Britain, for example, are associated with more indurated rocks. Although coal is more sensitive to temperature than its host rocks it is interesting to record that Price (1960) obtained an inverse relationship between the uniaxial strength of siltstones and sandstones from the South Wales, Kent, East and West Midland coalfields, and the rank of the associated coal seam.

1.4 Weathering and shear strength characteristics

Weathering is the breakdown and alteration of materials near the earth's surface such that the products are more in equilibrium with newly imposed physico-chemical conditions. The definitions of weathering cited in the literature are numerous but for the present work Polynov's (1937) definition is very apt. His restricted view that weathering is "the change of rocks from the massive to the clastic state" is in line with the view to be presented in this thesis, that most of the detrital minerals (i.e. those transported to the depositional basin) are already in thermodynamic and mechanical equilibrium with the climatic conditions that have prevailed in Britain in post-glacial times. Moreover, the definition in a sense implies the reverse of diagenesis and for present purposes we are

primarily concerned with the reduction of aggregated minerals to fundamental particles. Pertinent to this view of weathering is the comprehensive work of Tourtelot (1962) who studied the geochemistry and mineralogy of the Pierre Shale in the Great Plains region. Under rather more extreme climatic conditions than apply in Britain, hydration, oxidation, ion-exchange reactions and evaporation have had a very modest effect on the detrital mineral fraction (including the clay minerals); it is the non-detrital minerals, which make up a much smaller fraction of the rocks, that have been decomposed.

Breakdown towards fundamental particle sizes has led to the adoption of visual zones based on the degree of weathering. Weathering stages or zones are convenient for physical and mechanical comparisons irrespective of rock type. Hence for igneous rocks (Knill and Jones, 1965), chalk (Ward et al., 1968) and the Keuper Marl (Chandler, 1969), fourfold and fivefold zones have been designated. A zonal scheme that can be applied to many sedimentary rocks is of the type adopted by Chandler (1969), viz.:

Fully weathered -	Zone IVb -	Matrix only
Partially weathered -	Zone IVa -	Matrix with occasional clay-stone pellets, less than 1/8 in. dia. but more usually coarse sand size
Partially weathered -	Zone III -	Matrix with frequent lithorelicts up to 1 in. As weathering progresses lithorelicts become less angular
Partially weathered -	Zone II -	Angular blocks of unweathered marl with virtually no matrix
Unweathered -	Zone I -	Mudstone (often fissured)

In Chapter 3 no formal zonation scheme has been applied because the progressively weathered in situ section of Coal Measures rocks consists of four different rock types. Zones IV and III are well developed in the shale and mudstone horizons (Fig.3.1) and chemical weathering of the non-detrital minerals is restricted to depths generally less than 6 to 8ft below ground level (Zone III equivalent).

An evaluation of slope failures by Bjerrum (1967) showed that about 55 per cent of these failures occurred in weathered over-consolidated clays and shales with strong diagenetic bonds. His proposed theory of progressive failure serves as a useful link with the concept of residual strength. Bjerrum contends that the major effect of disintegration of these rocks or clays is the gradual destruction of diagenetic bonds with the consequent release of locked-in recoverable strain energy. The clay will then expand normal to the surface as no expansion is possible parallel to the surface. The expansion results in an increased moisture content and ultimately a reduced shear strength. Progressive failure is initiated by stress concentrations at the toe of a slope in response to the relief of the high lateral stresses. Evidence in favour of the relief of high lateral stresses is cited in the literature (see Morgenstern, 1967, p.67), but conflicting views are apparent. Underwood (1967, p.108) refers to the difficulty in distinguishing between swelling by water absorption and relaxation, and the present writer finds it difficult to conceive that a rock which according to Price (1959) is invariably heavily jointed because of its inability to store strain energy can contain sufficient recoverable energy to provoke displacements large enough to fail a material.

The Aberfan tip materials were considered to be essentially granular which in terms of the Coulomb equation (modified for effective stress by Terzaghi) infers that cohesion is insignificant: viz

$$s = c' + (\sigma - u) \tan \phi' = c' + \sigma' \tan \phi'; \text{ or } = \sigma' \tan \phi' \text{ (for spoil)}$$

where:

- s = shear strength
- c' = cohesion
- ϕ' = angle of shearing resistance

) in terms of effective stress

- σ' = effective stress normal to the plane of failure
- σ = total stress normal to the plane of failure
- u = pore pressure

The peak $\emptyset'$ value of the Aberfan spoil was 39.5 degrees, which compares favourably with compacted shale earth dams (Burnhope Dam (1936)-35°; Balderhead Dam (1965) -35.5°). A significant feature of the Aberfan results however, concerns the $\emptyset'$ value of the failure plane material, which was only 17.5 to 18.5 degrees.

Tiedemann (1937) was the first worker to show that if in a drained shear test the sample is strained beyond failure, its strength will decrease and will ultimately reach a certain value (known as the residual), which will remain constant for further straining. However, it was Skempton (1964) who drew attention to the real significance of residual strength. On theoretical grounds there are many objections to the shear box apparatus, shown diagrammatically on Figure 1.4. Also shown on the latter diagram are the results of large strain shear box tests carried out on the weathered Carboniferous mudstone from the failure zone of the major slope failure at Walton's Wood, Staffordshire. In the shear box apparatus (Fig. 1.4a) the sample which is contained in a horizontally split box can be kept under effective stress conditions if the shear force is applied at a rate of strain that is sufficiently low for excess pore pressures to dissipate. In actual practice the sample is continuously in contact with water because the inner split box is itself contained in a water reservoir. The shear stress-displacement curve (Fig. 1.4b) for an effective normal pressure of 22.2 lb/in^2 (Skempton, 1964) demonstrates that the peak shear strength of 10.8 lb/in^2 was reached at a very small displacement, whereas the residual strength of 5.1 lb/in^2 necessitated a displacement of about 1 in. With the equipment used by the present writer the box is self-reversing after reaching full travel; small peaks such as that shown on Figure 1.4 b (dotted section) occur during reversal. By carrying out a number of tests at different values of effective normal pressure both peak and residual

Shear box (diagrammatic), and large strain shear tests (b and c)
from Skempton (1964)

FIG 1.4

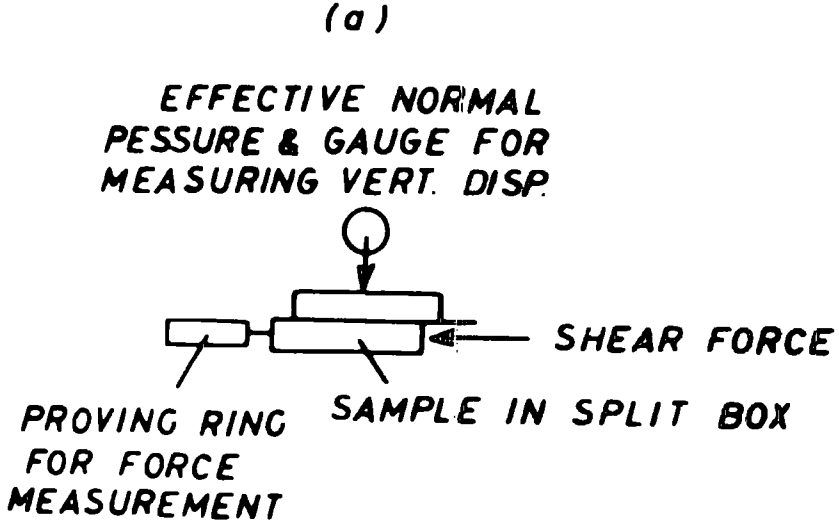

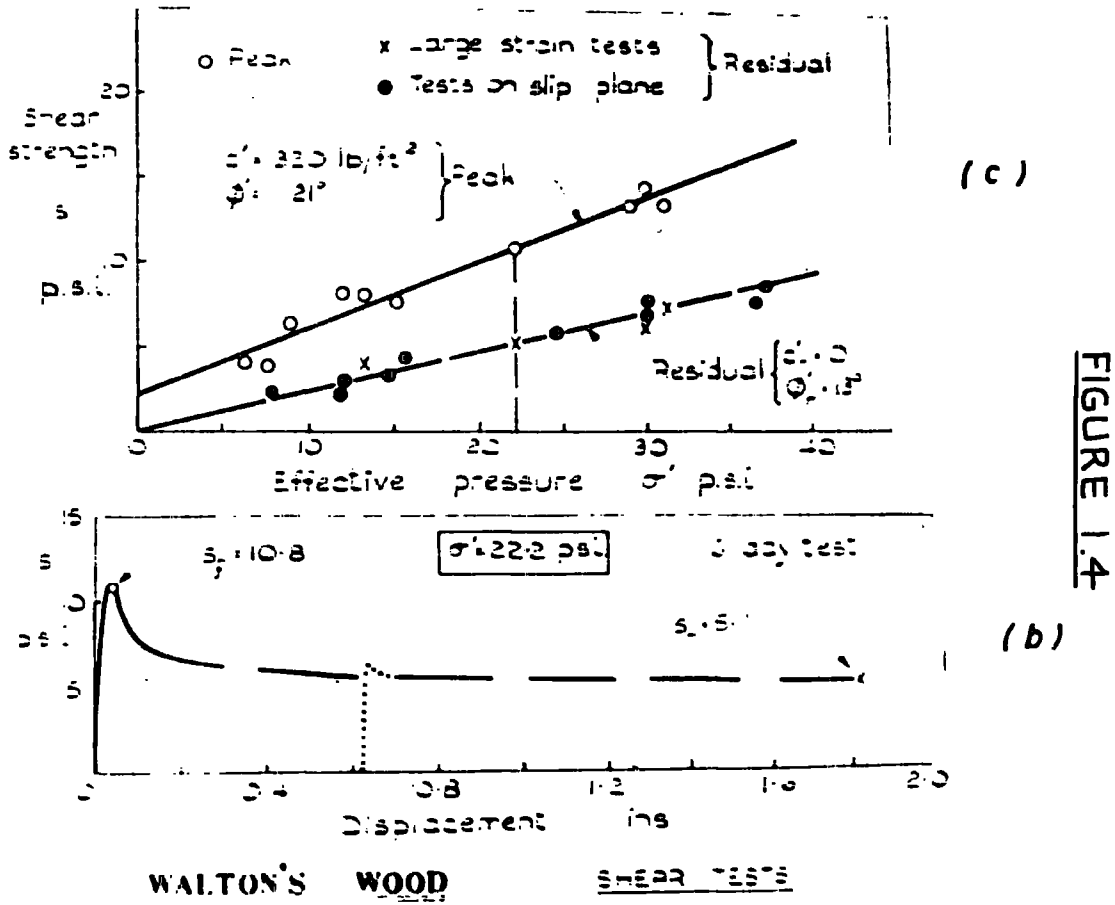

WALTON'S WOOD SHEAR TESTS

FIGURE 1.4

shear strength parameters can be derived (Fig. 1.4c). For the Walton's Wood material the difference is of considerable import (Fig. 1.4c), particularly when applied to actual field conditions. The parity in slip plane values and shear box residual results is notable. A correlation presented by Skempton (1964) showed residual strength decreasing with increasing clay fraction and it has been generally held that the amount of clay in the material is the major factor which governs the magnitude of the residual strength. Inferred from Skempton's results is the criterion that the residual is attained when enough movement has taken place on the shear surface to orientate the component clay mineral particles. Kenney (1967) carried out direct shear tests (using a very simple technique) on a number of naturally occurring shales, soils, pure minerals and mineral mixtures. Shales such as the Bearpaw, Pepper, Pierre and Cucaracha (Panama Canal) with a high proportion of mixed-layer mica-montmorillonite clay minerals and smaller amounts of montmorillonite gave exceedingly low ϕ'_r values (5° to 6°). Quartz, felspar and calcite gave residual values in excess of 30 degrees, whereas hydrous mica and montmorillonite exhibit values of more than 17 degrees and less than 11 degrees, respectively. Although the work raises a number of questions regarding the precise mineralogy of some of his sediments its importance lies in the demonstration that the particular clay mineral species is significant (especially montmorillonite). Kenney (1967) did not obtain any relationship with plasticity but Spencer (1969) showed generally that ϕ'_r falls with increasing liquid limit.* The variation in liquid limit almost certainly implies changing mineralogy and as many of Spencer's liquid limit values are well over 70 with ϕ'_r values of less than 9 degrees it can be concluded that montmorillonite or mixed-layer mica-montmorillonite clay mineral species are present in high proportions.

* Moisture content at which a sediment will flow, determined by standard test (B.S.1377/1967).

The implications of the above results with respect to colliery tips is now apparent. Spoil materials may be subject to weathering and degradation processes. If this is the case then the essentially granular material may be subject to breakdown and become a silt or clay with considerably lower shear strength parameters. In a general review article Smith (1968) concludes that a loosely compacted spoil tends to maintain a fairly constant value of shear strength once its maximum value has been reached, and provided that subsequent movement is not excessive. His limited number of shear tests, carried out on spoil of less than 3/8 in size, showed that under large strains the drop from peak to residual was considerable irrespective of the degree of compaction (ϕ'_p = 42° (compacted), ϕ'_p = 38°(loose), ϕ'_r = 20°). Strain induced comminution processes contribute to the development of failure surfaces like those of Aberfan and Littleton, and knowing that research of recent years has led to the recognition of mixed-layer mica-montmorillonite clay minerals in the British Carboniferous (Wilson 1965a; 1965b; Pearson and Wade, 1967; Trewin 1968; Spears, 1970; Richardson and Francis, 1971) the possibility that weathering may produce a material of exceedingly low shear strength is a live issue.

1.5 Statistical treatment of results

Standard statistical techniques have been used in this work when applicable. For testing the significance of the difference between sample means, and for ensuring that the correlation coefficients have not arisen by chance, Student's t test has been used (Moroney, 1956, p.227, p.311).

The correlation coefficient (more correctly, product moment correlation coefficient) is a measure of association, which cannot exceed +1 or be less than -1 in value.

$$\text{correlation coefficient, } r = \frac{\text{covariance of x and y}}{\sqrt{[\text{variance } (x)][\text{variance}(y)]}}$$

A value of +1 denotes perfect functional relationship between y and x, an increasing x being associated with an increasing y. Similarly, when r is equal to -1, the relationship is again perfectly functional, but this time an increasing x is associated with a decreasing y. When r=o, there is no relation at all between x and y. In terms of the least squares linear regression lines, y on x and x on y (see below), the cosine of the included angle between these two lines is numerically equal to r. For handling large sets of data r and t were obtained from a matrix print-out, using a computer program written in PL/1. When only two variables were involved an Olivetti Programma 101, for which programs can be written and recorded on magnetic card, proved more efficient in that processing time was equivalent to the speed at which the data could be fed into the machine.

The best fit by least squares linear regression is a well established technique for fitting a straight line to data comprising two variables, x and y. Figure 1.5 (after Imbrie, 1956) illustrates the y on x and x on y criteria. In the former case x is the independent variable (for example time) and y is the dependent variable (for example, permeability measured in the constant head permeability test, and which may vary with time). When y is estimated from x the sum of the squares of the deviations measured as A-E on Figure 1.5 are minimized. For the latter case the regression line x on y minimizes the corresponding sum of the deviations measured as D-K on Figure 1.5.

Much of the fragmental material tested triaxially by the writer does not lend itself to simple Mohr circle construction. In other words it is extremely difficult to assess by inspection the limiting tangent from which the shear strength parameters ϕ (intergranular friction) and c (cohestion) are defined (see Chapter 3). It could equally well be argued that because of the variability in materials like colliery spoil the results do not warrant statistical treatment. However, it is considered by the writer that the

FIGURE 1.5

Diagram to show various methods of fitting a line to a scatter of points. A regression y on x minimizes the sum of the squares of the deviations measured as AE. A regression line x on y minimizes the corresponding sum of deviations measured as DK. A major axis minimizes the sum of the squares of the deviations measured as BF. A reduced major axis minimizes the sum of the areas of triangles GCI. (Taken from Imbrie, 1956, The place of biometrics in taxonomy, Bull. Amer. Mus. Nat. Hist. 108:2;211-252).

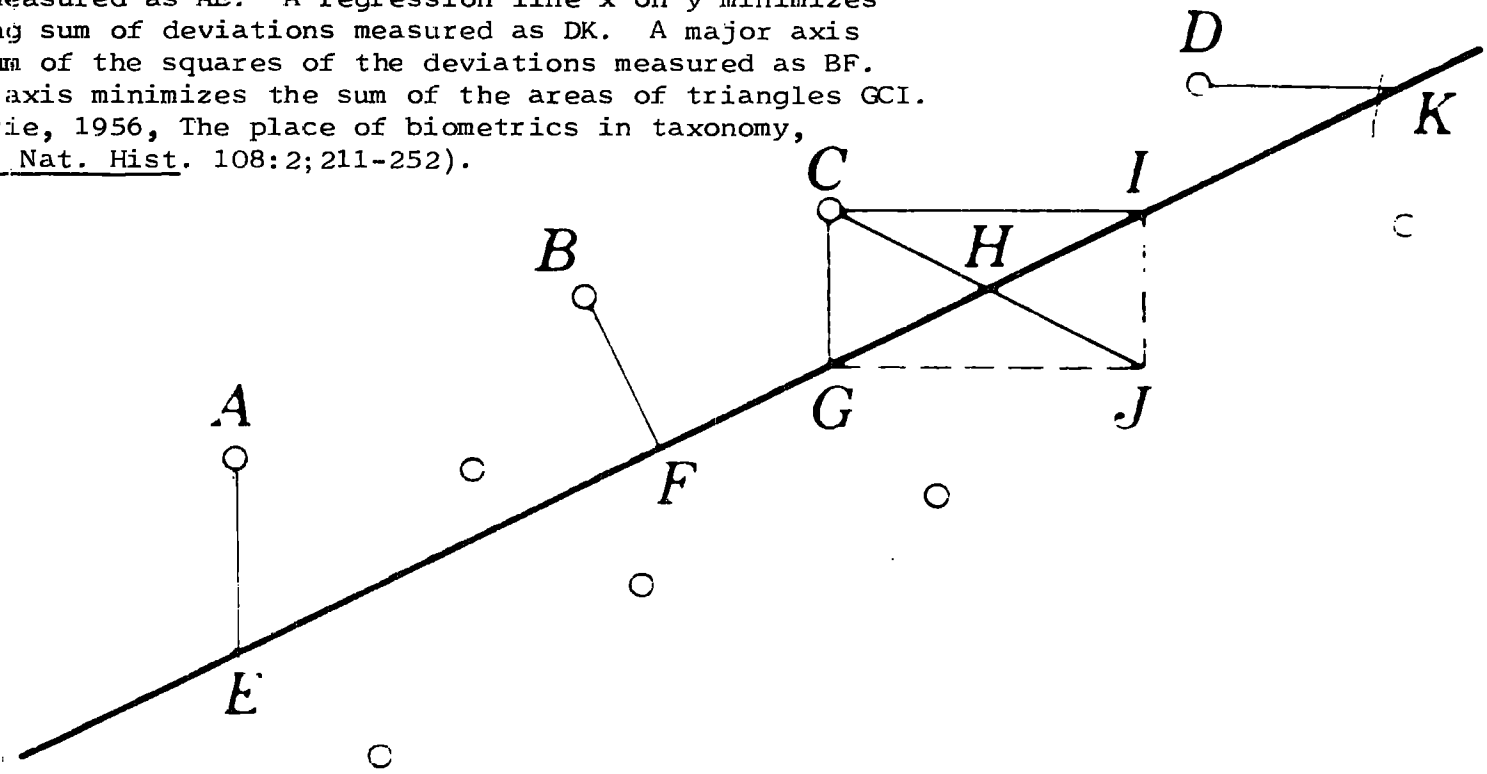

FIG 1.5

FIGURE 1.5

subjective definition of a Mohr envelope can lead to biased results because it is impossible to treat each set of data in exactly the same way - a statistical approach is therefore logical on this basis alone.

The stress-path method of analysis has in recent years been accepted in soil mechanics as a powerful method of analysing shear strength data. The failure envelope is in this case determined indirectly from the 'top points' of the Mohr circles (see Chapter 3, Section 3.12). As far as the writer is aware most authors draw the 'best fit' through the Mohr circle 'top points' by inspection, because implicit in least squares technique is the concept of a dependent and independent variable. However, no such stipulation can be applied to the 'top point' method of presentation. A linear regression method which meets this condition does exist however, and it has proved to be a very significant approach in the field of growth statistics. The line is known as the reduced major axis regression and has now been fully accepted in the geological sciences (see Miller and Kahn, 1962; pp.204-210 for details of the method). In terms of the points shown on Figure 1.5 a reduced major axis minimizes the sum of the areas of the triangles GCI. Another simple regression equation that has been adopted is of the form y=mx, but the justification for using this is dependent on the y - intercept term being statistically little different from zero. Using the format of Miller and Kahn (1962) if the reduced major axis intercept is equal to b , then:

$$b = \bar{y} - \bar{x}\,K$$

and the standard error of the intercept S_b is:

$$S_b = S_y \sqrt{\frac{1-r^2}{n}\left(1 + \frac{\bar{x}^2}{S_x^2}\right)}$$

where: $\bar{x}$ and $\bar{y}$ are the means of the x and y values, respectively

K is the slope of the regression line

S_y is the standard deviation of y

r is the correlation coefficient

and n is the number of pairs of variables

From the definition of the t distribution (Fisher and Yates, 1948, p.1), the significance of b with respect to zero can be checked by looking up the probability of b/S_b in the t tables (e.g. Fisher and Yates, p.32). If the value for n-2 degrees of freedom is greater than the 95 per cent confidence level then b is significantly greater than zero. The difficulty in stipulating that b is not significantly different from zero lies with the fact that the probability threshold is a matter of personal choice. Obviously it would be unwise to place much faith in high probabilities (say, greater than 60 per cent and less than 95 per cent). In general the arbitrary level chosen includes the two lowest probability levels quoted in the t tables (10 per cent to 20 per cent). In this case it is reasonable to conclude that the probability of b being greater than zero is 20 per cent at the maximum.

When a linear regression is used to represent a relationship the question often arises as to whether the relationship holds for two different sets of data. Statistically this question may be answered by testing whether the two sets of observations can be regarded as belonging to the same regression model. A method devised by Chow (1960) tests the equality between sets of coefficients in two linear regressions, by obtaining the squares of the residuals assuming the equality, and the sum of the squares without assuming the equality. The ratio of the difference between these two sums to the latter sum of squares, adjusted for the corresponding degrees of freedom, will be distributed as the variance ratio (F-ratio) under the null hypothesis.

From tables of variance ratio at the 5 per cent level (Fisher and Yates, 1948, p.39) one can determine whether or not there is a statistically significant difference between the two regression coefficients. Here again a useful application of this test is in processing triaxial data in order to verify whether the inter-granular friction values, $\emptyset'$, vary from one tip to another, or from older parts of a specific tip to the younger samples. This test was already on the file of statistical programs at Durham and needed only minor adjustment to make the program loop so that more than two sets of data could be processed at any one time.

1.6 Methods and general comments

All the soil mechanics tests, chemical and mineralogical determinations have been carried out using standard equipment. Imperial units have been used throughout the thesis, primarily because the work was started before SI units were adopted in the field of soil mechanics.

Some of the early conclusions on the question of 'shale' breakdown (Chapter 2) have already been published (Taylor, 1969; Taylor and Spears, 1970). Both the writer's chemical data, together with further results determined in Sheffield (Spears, Taylor and Till, 1971) have been included in the chemical/mineralogical discussion relating to Yorkshire Main tip (Chapter 5). Other papers by the present writer have been referred to in the conventional manner.

CHAPTER 2

THE BREAKDOWN OF EXCAVATED COAL MEASURES ROCKS

2.1 Introduction

The object of this chapter is to discuss the breakdown of excavated Coal Measures rocks, establishing which rocks are prone to breakdown and how this happens. The effects of physical and chemical breakdown are complementary, but in so far as physical breakdown increases the surface area and this accelerates chemical weathering, the physical can be viewed as a control on the chemical. Furthermore, as most of the minerals in Coal Measures rocks have been through at least one previous cycle of weathering, transportation and deposition, that is to say they are detrital in origin, these minerals will have achieved some stability under weathering conditions. There are marked changes in the mineralogy in long-established near-surface profiles developed on Coal Measures rocks, but these have developed over several thousands of years and in many cases can be proved to be Post-glacial (ca. 10,000 yr - see Chapter 3). Little change can therefore be expected to occur under normal weathering conditions in most of the minerals in excavated material over a short period of years. This applies to unburnt material, for there are extensive mineralogical changes in colliery tips which have been on fire; in general this leads to increased stability. However, it is the unburnt material which is the subject of this chapter.

In addition to the detrital minerals there are those minerals which formed within the sediment, in an environment rather different to that encountered during weathering. These non-detrital minerals will therefore break down more readily. Pyrite (FeS_2) is the most important of these minerals in coal and coal-bearing strata because it plays a secondary role

in the initiation of spontaneous combustion (Guney, 1968) on the one hand, and the resultant sulphates formed during low-temperature oxidation of pyrite attack concrete on the other hand. Calcite ($CaCO_3$) is unimportant in the Coal Measures (sensu stricto), the more important carbonate being $FeCO_3$ (siderite). A major potential source of sulphate minerals in colliery tips arises from the presence of pyrite in coal, and ankerite (a mixed Ca Fe Mg carbonate) in the cleat (small-scale joints) of coal. Oxidation of former gives rise to acid attack on the carbonates, and clay minerals to a certain extent, so as to produce sulphates ranging from simple types like gypsum ($CaSO_4.2H_2O$) to the more complex varieties like jarosite ($KFe_3(SO_4)_2(OH)_6$).

The unstable minerals normally constitute only a small fraction of the total, and therefore the average rate of chemical change is slow - much slower than the rate at which physical disintegration can take place. For this reason the emphasis in this chapter is placed on the effects of physical breakdown.

2.2 The role of geological structures in disintegration

In coal measures sequences there is usually an overall upwards increase in grain size between two coal seams. This has led to the establishment of 'classical' cyclothems (Chapter 1) which are exemplified by Table 2.1. Published borehole sections by Meigh (1968, Plate 7) and Taylor (1968, Figs 5, 6, and 8) give some idea of the variations from this 'classical' cyclothem that will be encountered in practice. Statistical work on such variations has been undertaken by Duff and Walton (1962). The work of Elliott (1968) attaches more importance to the lithology, particularly of the siltstone-sandstone units, and deals with the relationships between units and the structures. The relative abundance of different rock types is shown on Table 2.1 after Elliott (1968). Although based on the East Midlands coalfield these values are fairly typical of other British coalfields.

TABLE 2.1

The 'classical' ideal cyclothem upwards sequence*	Relative proportions in East Midlands coalfield+
1. Coal	
5. Seatearth	10-20%
4. Sandstone	5-10% siltstone-sandstone without structures
3. Siltstone	40% siltstone-sandstone with structures
2. Mudstone-shale	30%
1. Coal	2-7%

* Edwards and Stubblefield (1947)
\+ Elliott (1968)

The most common of all sedimentary structures is the bedding or stratification, and this may give rise to a plane of weakness. Table 2.1 shows that stratification is absent in only a small proportion of the siltstone-sandstones (5-10%). The remainder (about 40 per cent of the total sequence) contain both parallel and cross-stratification; ripple structures are typical of the latter. Large-scale cross-stratification is more common in the coarser-grained sandstones, but then such rocks are not very abundant. The bedding is a plane of weakness if it contains a concentration of mica and comminuted plant debris, which is not at all uncommon. A marked change in grain size across the stratification plane has the same effect.

Stratification also occurs in the finer-grained rocks. In some of the mudstones there are thin units of siltstone. In other mudstones stratification on a very small scale may be observed as alternating grey and dark grey units particularly in unweathered borehole material. A study of such varve-like units observed in a core of Mansfield marine shale confirmed that the darker

FIGURE 2.1

NON-MARINE LAMINATED MUDSTONE— SWELLING CHARACTERISTICS IN WATER

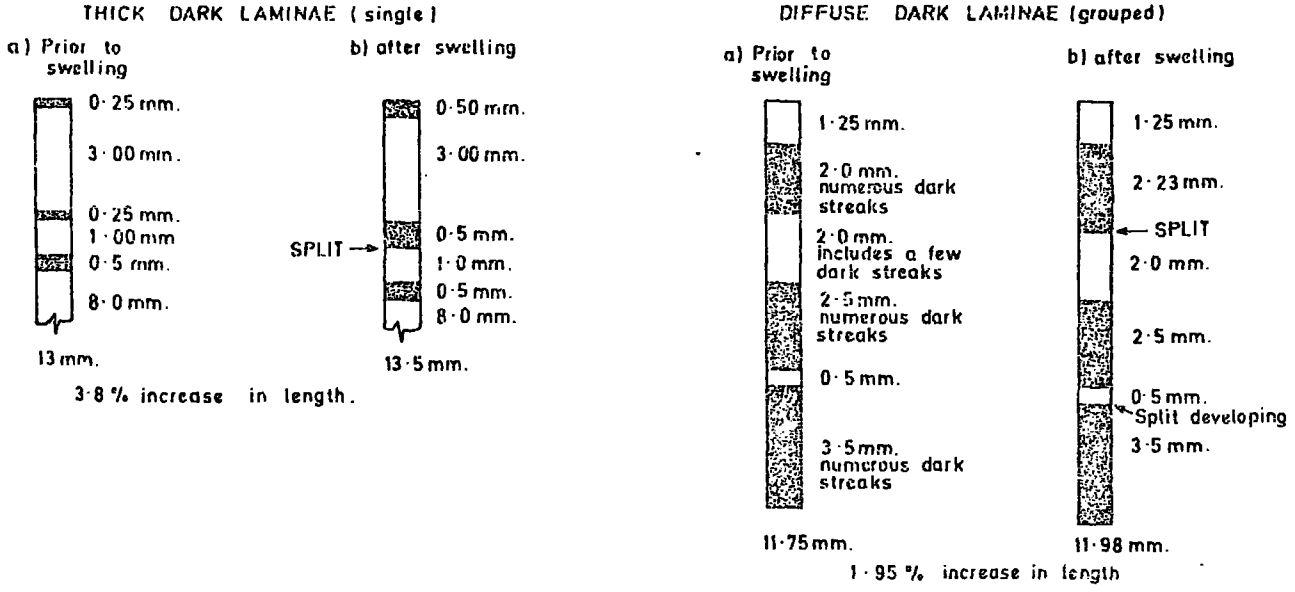

BY TAKING LAMINATIONS SINGLY, (OR BY GROUPING) ONLY THE DARKER BANDS SHOW EXPANSION. BREAKAGE TAKES PLACE ALONG THE INTERFACES BETEEN DARK AND LIGHT LAMINAE.

LUMLEY

HIGH MAIN ROOF MEASURES.

VOLUMETRIC INCREASE ON SOAKING.

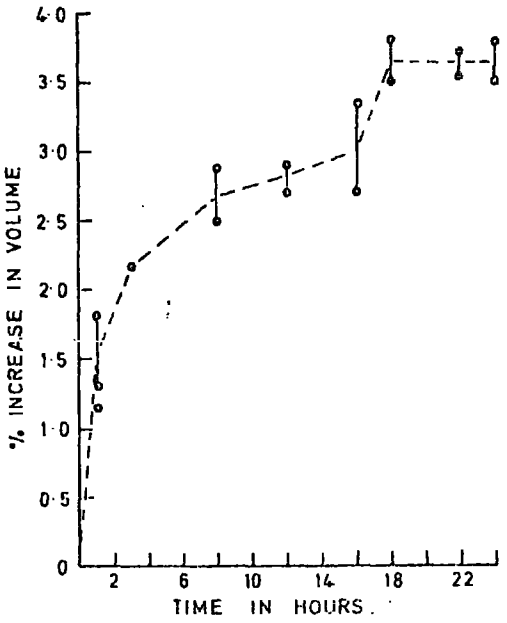

laminae or lenses had the ability to swell in water (Spears, 1969). The swelling was attributed to the uptake of water between grains of the floc-type fabric, rather than to expanding clay minerals. Table 2.2 (K_2O, organic carbon values) demonstrates that the illitic clay mineral fraction and organic content are only marginally higher in the dark laminae than in the light laminae. The former,however, were isotropic under the microscope which points to a floc-type fabric.

In a similar way the laminated silty mudstone roof measures of the Durham High Main seam (Lumley, NZ 314 477) show a volumetric increase in water of nearly 4 per cent (Fig. 2.1).

TABLE 2.2

Chemical composition

a) Mansfield Marine Band Shale, Little Smeaton Borehole

Percentage by weight

	dark laminae (swelling)	dark laminae (sawing)	light laminae (sawing)
SiO_2	55.60	56.0	56.90
Al_2O_3	23.30	24.0	23.60
Fe_2O_3	5.55	5.59	5.61
MgO	2.12	2.13	2.28
CaO	0.33	0.38	0.35
Na_2O	0.97	0.99	0.97
K_2O	4.31	4.23	4.06
TiO_2	0.91	0.91	0.93
P_2O_5	0.15	0.16	0.16
MnO	0.05	0.05	0.06
H_2O^-	-	2.12	1.79
Organic C	1.35	1.32	1.27

b) Chemical composition

Durham High Main Seam Roof Measures, Lumley

Percentage by weight

	dark laminae (sawing)	light laminae (sawing)
SiO_2	63.97	75.45
Al_2O_3	17.54	14.52
Fe_2O_3	5.98	3.40
MgO	1.83	1.25
CaO	0.61	0.38
Na_2O	0.85	1.24
K_2O	3.17	2.02
TiO_2	1.17	0.86
MnO	0.11	0.06
S	0.23	0.10
P_2O_5	0.12	0.09
Organic C	4.42	0.63

By selecting cores with broad laminations it can be seen that once again it is the dark laminae which swell. Furthermore, breakage occurs along the interfaces of the laminations. Chemical analyses (Table 2.2; also Appendix 1), together with thin section observations, revealed a higher quartz and felspar content for the light laminae, whereas the dark laminae are rich in clay and organic matter. In this respect much greater compositional variations occur between laminations of the non-marine rocks than were found in marine shales. Sorting by currents of the more rapidly accumulating non-marine sediments compared with lower sedimentation rates of marine types, almost certainly accounts for these differences.

PLATE 2.1

1

when first exposed

Sample numbers shown, for location and lithology see Fig. 1. Scale: sample R1F = 32 cm in length

2

after 6 months exposure

3

after 24 months exposure

PLATE 2.1 To show the progressive breakdown of a suite of underground samples when exposed out of doors.

FIGURE 2.2

JOINTS AND SLICKENSIDES; MANSFIELD MARINE BAND CYCLOTHEM, TINSLEY PARK, Nr. SHEFFIELD

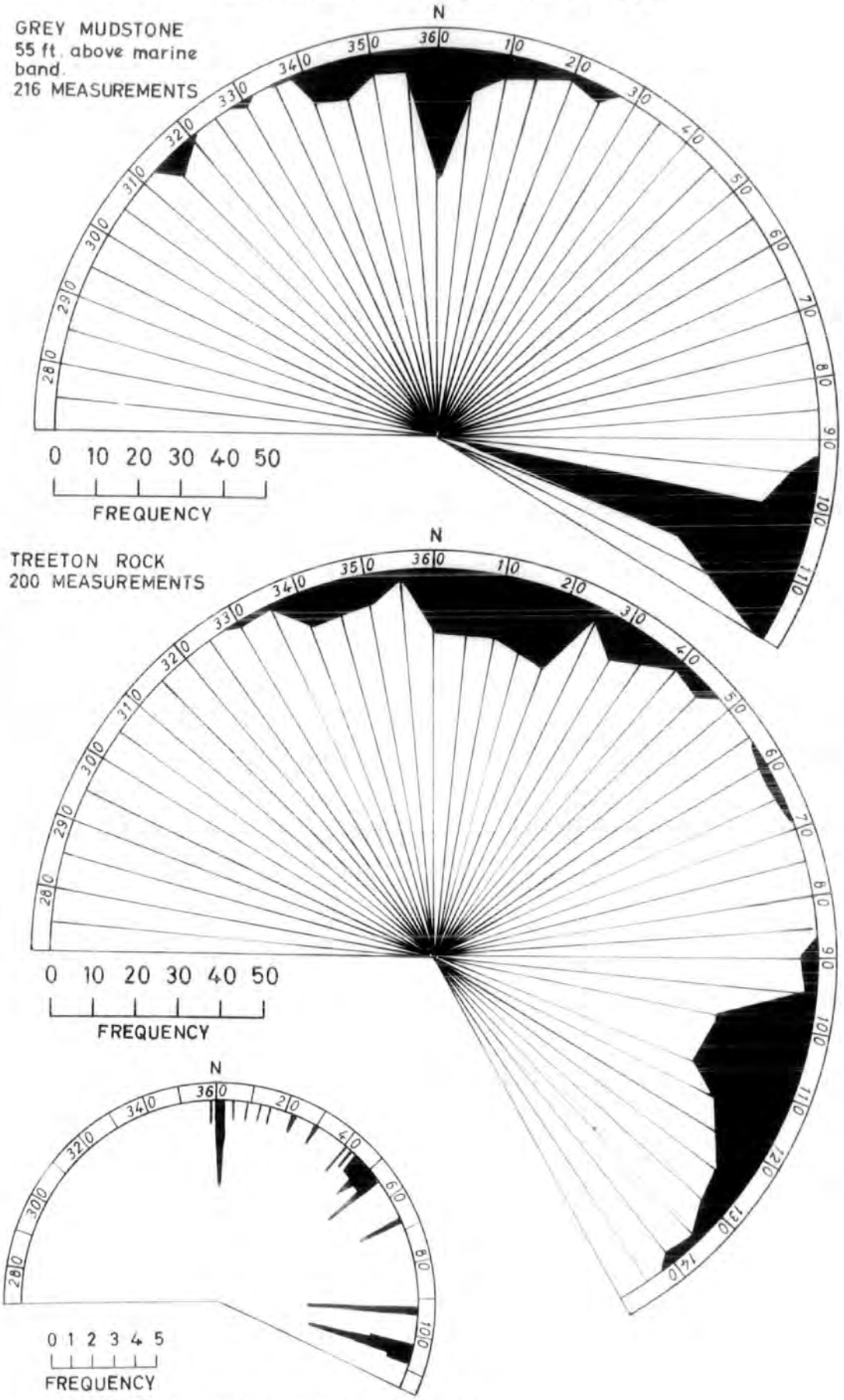

SLICKENSIDES IN SECOND WALES SEATEARTH
50 MICROSCOPIC MEASUREMENTS, PARALLEL TO STRATIFICATION

An increase in grain size, with higher quartz and lower clay contents, signifies a reduction in fissility, and so too does an increase in organic carbon as in the case of carbonaceous mudstones (Plate 2.1 - F1B, F1C). Care should be exercised however, with respect to organic content because some exceptionally fissile marine and non-marine shales may also be rich in organic matter (Pettijohn, 1957, p.352). The resistance to weathering and hardness of carbonaceous mudstones is somewhat unusual and is not readily explicable at the moment.

Specimens F1B, F1C from the floor measures beneath the Barnsley Bed Coal of Yorkshire have very high organic contents but moderate quartz contents (organic carbon 18.56, 18.51; quartz 24.01, 19.85, respectively). The content of mixed-layer clay minerals is no less than in the roof rocks illustrated in Plate 2.1 (R1A to R1F), nor is the chemistry and mineralogy fundamentally different.

Seatearths are to be found below the great majority of coal seams or in association with very thin coals (e.g. SK 476821, Chapter 3). On the other hand the coal may be entirely absent. The original bedding of seatearths has been disturbed by rootlets and because they were initially mechanically weak subsequent movements may have produced numerous small shear planes, with re-orientation of clay minerals in response to stress, often referred to as listric surfaces. As would be expected these are more numerous in the fine-grained seatearths where the decrease in size implies more clay and less quartz. Microscopic measurements of listric surface orientations for the Second Wales seatearth at Tinsley, Yorkshire (Taylor, 1971, Plate 25) infer that these shears are not necessarily random and may well have tectonic affinities (relationship with principal joint directions in the mudstone and underlying sandstone, Fig. 2.2). The NE.- SW. concentrations represent kinking of the North-South set. Small shears also

occur in fine-grained rocks elsewhere in the sequence (see for example Phillips, 1938-1944), particularly above the coal and in dirt bands within coal seams. If shears are present a few cycles of wetting and drying produce considerable disintegration.

Joints (or cleat as they are known in coal) are invariably perpendicular to the bedding and once exposed to the elements after excavation they soon open. Their frequency is a function of the rock's strength, in particular of the amount of strain energy which can be stored (Price, 1959) - the highest frequency is to be found in coal and in the shale-mudstones. With an increase in grain size, macro-quartz and large-sized organic detritus, mudstones grade into siltstones. The joints in these rocks become progressively less frequent.

Whether or not jointing is present a polygonal fracture pattern tends to develop in shale-mudstones perpendicular to the bedding (Plate 2.2 - High Main roof rocks). The attainment of the polygonal pattern depends on the degree of interaction with the joints. It is unlikely that stress relief is important in the formation of these fractures because freshly excavated samples of the High Main roof remained unaltered when immersed and stored under water. A similar conclusion was drawn by Kennard et al., (1967) for the Yoredale shales at Balderhead. The cause of the disintegration was thought to be negative pore pressures following the desiccation of the shale; it was thought that the polygonal pattern develops on the bedding plane because in this direction the rock is isotropic. These fractures are also the main cause of the breakdown (parallel with the bedding as well as perpendicular to it) in more massive mudstones free from laminations and other stratification planes. It is believed from microscopic observations that the orientation of the fractures remains approximately parallel and perpendicular to the bedding because of the sub-normal orientation of the clay

PLATE 2.2

POLYGONAL FRACTURE DEVELOPMENT —
HIGH MAIN ROOF ROCKS
(SAMPLE 18 IN. LONG)

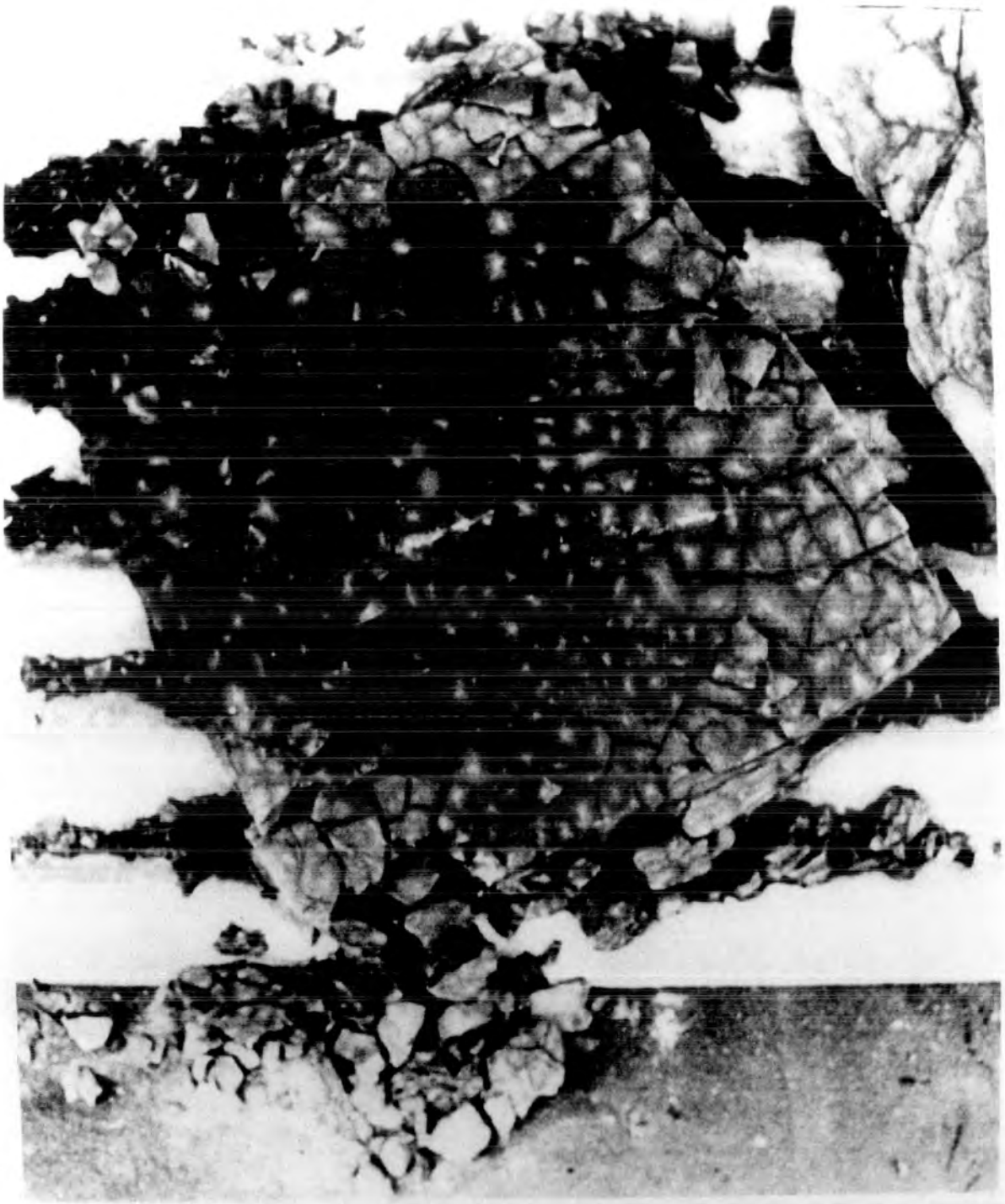

mineral basal planes with the sedimentary overload. The fractures parallel to the bedding are often not in the same plane which gives rise to a blocky or hackly appearance. With increase in silt content and strength of the rock so the frequency decreases. It should be recorded however, that penecontemporaneous 'pseudonodules' are not uncommon in silty strata immediately below Coal Measures sandstones (Taylor, 1971, Plate 24). Stress relief on excavation readily makes these rocks prone to disintegration.

The development of polygonal fractures in conjunction with the jointing and laminations reduces most shale-mudstones to a gravel sized aggregate in a matter of months, the breakdown may be even more rapid depending on fabric and clay mineralogy.

Plate 2.1 is a typical example of progressive breakdown of a suite of fresh rock samples associated with the Barnsley Bed Coal of Yorkshire, when: 1) first exposed, 2) after 6 months in the open, 3) after 24 months exposure. The variations shown illustrate many of the points already discussed and the following key shows the relative positions of the samples:

Downwards sequence	F1A	dark grey mudstone (floor of seam)
	F1B) F1C)	black carbonaceous mudstones - (floor samples from below F1A)
	R1A	dark grey mudstone with coal streaks (immediately above Barnsley Bed coal)
	R1B	Day Bed Coal
Upwards sequence	R1C	dark grey shale
	R1D) R1E)	dark grey shale - mudstone
	R1F	light grey silty mudstone
	R1F (1) - 32 cm in length	

In some samples breakdown is rapid and is controlled by the sedimentary structures, particularly bedding planes (R1A) and laminations (R1C).

Polygonal fractures are best seen in the more poorly bedded samples, and results in fragments of irregular thickness (R1F). The breakdown to a gravel-sized aggregate takes place relatively quickly under test conditions and this should also apply to the Yorkshire Main tip (Chapter 5) provided that the rate of burial is not excessive. The small fragments after a 2-year period were relatively strong so demonstrating that the rate of disintegration towards a fundamental particle size is much slower. As mentioned earlier the carbonaceous mudstones (F1C and F1B) show little change and this is also true of the coal (R1B). Although shales and mudstones from the roof measures break down (samples R1A - R1F, excluding R1B) the nodules of siderite which are present are unaffected, apart from superficial surface oxidation. The presence of unaltered pyrite in sample F1C also demonstrates the theme which this thesis emphasizes, namely, that the rate of chemical alteration is slower than physical breakdown.

2.3 Influence of mineralogy on breakdown

(a) Clay minerals

The reason why chemical weathering is considered to be a secondary process under temperate climatic conditions is because the vast majority of minerals found in shales are stable in a low temperature environment. Certain non-detrital minerals like pyrite undergo irreversible oxidation, but more rapid reversible reactions are associated with certain clay minerals. The latter minerals are expandable types which have the ability to take up water, and other liquids, into interlayer structural sites causing (intraparticle) swelling. Most common amongst these minerals is montmorillonite. With water its expansion mainly depends on the amount of water and nature of the interlayer cation. Mering (1946) and Bradley and Grim (1948) showed that in the presence of large quantities of water sodium-saturated montmorillonite dissociates into platelets which are of the same order of thickness as the unit cell (10Å) - see also Gillott, 1968. With extreme

behaviour, as manifested by the latter case, differentiation between surface adsorption and intramicellar phenomena become somewhat complex. In simple terms both internal and external surfaces are largely one and the same.

Intraparticle expansion was cited by Mielentz and King (1955) as one of the two mechanisms of clay expansion, the other, the enlargement due to capillarity, will be discussed later in the text. The free swell data of Mielentz and King (1955, Table 13) demonstrates the importance of montmorillonite, especially when Na^+ is the interlayer cation.

Montmorillonite has not been recorded as a separate phase in the British Coal Measures, but it does occur as a mixed-layer illite-montmorillonite. The occurrence of mixed-layer illite-montmorillonite in the Harvey seatearth of the Durham coalfield (Pearson and Wade, 1967) was thought to be a prime cause of floor heave in collieries working this seam. The situation is a little enigmatic because recent samples from Fishburn Colliery (type locality) show little in the way of mixed-layering of the 10Å mineral and the exchangeable Na^+ ion values are of a very moderate order (Table 2.3). Probably the most logical conclusion is that this difference in findings is allied to lateral changes in seatearth composition. Mixed-layering usually appears on the X-ray diffraction traces of untreated samples as a tail on the low 2θ side of the 10Å mica peak, but in some cases the peaks are separated. One sample (generally referred to as the Stafford tonstein) has been discovered which consists of mixed-layer mica-montmorillonite which is completely free from a separate 10Å phase (d spacing = 11.0Å). All the other samples examined to date contain varying proportions of kaolinite and illite (including 2M muscovite in places) with subsidiary chlorite; the illite like that of the Mansfield marine shale (Chapter 3) invariably shows some degree of mixed-layering. Treatment with ethylene glycol and cation exchange determinations have helped to confirm the presence of montmorillonite, and although not

recorded as a separate phase, it does occur as a mixed-layer component.

Geographical variations in clay mineralogy have now been ascertained from analysis of 57 tailings samples from all the National Coal Board areas (Fig. 2.3). Reject wet fines from the coal preparation plants consist of some of the inorganic contaminants of the coal and from the associated roof and floor measures. In most cases the preparation plants are dealing with more than one coal seam and hence information can be gained about the likely spectrum of clay minerals which will find their way into colliery tips across the country.

The tailings samples shown on Figure 2.3 were treated with ethylene glycol, the samples having been orientated on sintered glass porous disks (porosity 4). The amount of expanding mixed-layer clay was determined from the difference in areas displayed by treated and untreated 10Å peaks. The combined 7Å and 10Å (untreated) peak were used to express the results as a percentage of the clay fraction. Corrections for variation in peak intensity with composition and crystallinity were not made so the values shown on Figure 2.3 are not entirely accurate although they are reasonable approximations which are good enough to demonstrate the principal clay mineral variations. The 7Å peak is due entirely to kaolinite except in those samples with minor chlorite which also makes a small contribution to the 7Å peak.

Figure 2.3 implies that clay mineral expansion and rock disintegration could well be expected in those samples where the content of expandable clay is high. Other factors affecting breakdown will be the type of interlayer cation and total clay content, (which will mainly be determined by dilution of other minerals and organic matter), and grain size (quartz content). Also shown on Figure 2.3 are four samples which are known to disintegrate rapidly in water. In all of these the expandable clay content is high (Stafford tonstein, Parkgate dirt, Brooch and Park seatearths). It is not

FIGURE 2.3

Showing clay mineral components in 57 tailings samples from all N.C.B. Areas in Britain.

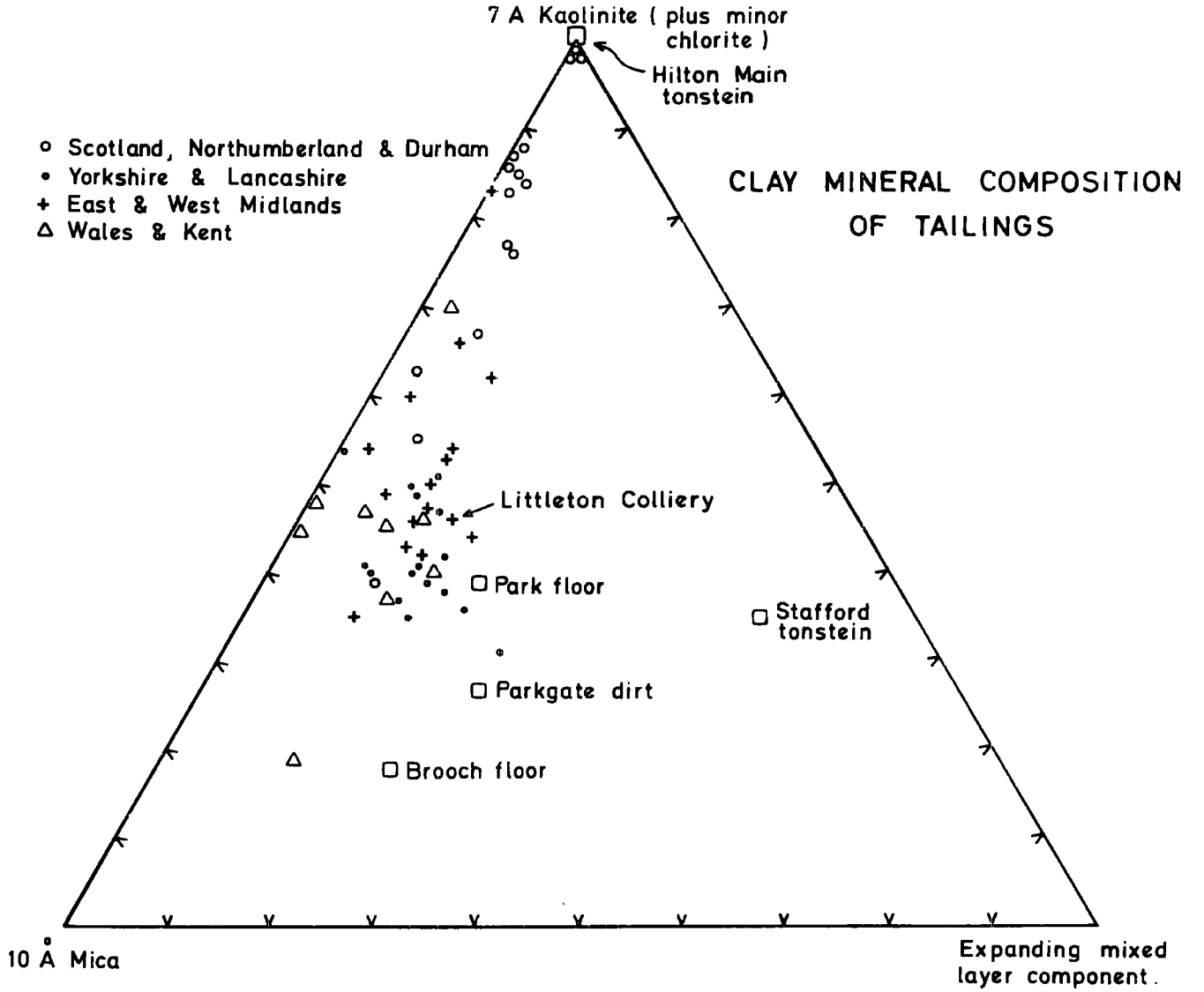

FIGURE 2.3

just the high clay content which is responsible for breakdown because slaking and swelling tests on dominantly monomineralic inert kaolinite-rich rocks (e.g. tonstein from Hilton Main colliery - Fig. 2.3) produce negligible breakdown. The results for these four samples show that in practice interlayer expansion is a contributing factor to shale breakdown.

As a further guide to the importance of interlayer expansion it is noteworthy that kaolinite is the dominant clay mineral in the northern coalfields, to the exclusion of other clay minerals in a few cases. Interlayer swelling should on average be at a minimum. This is borne out in part by behaviour in the coal preparation plants (see Raybould, 1966). South Wales is also cited as an area where shales are relatively stable in the washeries, but this would not have been anticipated from Figure 2.3. The absolute percentage of clay minerals or the nature of the interlayer cations could be responsible, but this remains to be investigated. In a similar manner Warwickshire (W. Midlands) is an area where unstable shales are encountered, but again this is not apparent from the data. Tailings however, represent average values and the contribution from one unstable roof or floor could be masked by stable material from other sources. This is illustrated on Figure 2.3 by Littleton Colliery, where two of the contributing seams are the unstable Brooch and Park which are shown separately on the figure - the plots are somewhat different.

Hence, the clay mineralogy shows firstly a regional variation which makes breakdown due to interlayer expansion much less likely in the northern coalfields of Britain. Secondly, that superimposed on this broad geographical variation there is also a variation in the amount of clay which is a function of the depositional environment (mainly a grain size control). The depositional environment also influences the clay composition (Huddle and Patterson, 1961); this is clearly illustrated in Chapter 3 by the

dominance of well-crystallized mica in the upper part of the Mansfield cyclothem which is in contrast to the mixed-layer and disordered varieties of the marine shales and seatearths, respectively.

Shales that break down rapidly in water are troublesome in the coal preparation plants and for this reason they have been studied by the National Coal Board and associated workers (Badger et al., 1956; Beckett et al., 1958; Berkovitch et al., 1959; Horton et al., 1964). In the work of Badger et al., (1956) the contents of exchangeable Na^+ and K^+ were determined using dilute HCl and a positive correlation was noted between Na^+ content and breakdown, as determined by the standard end-over-end breakdown test. This correlation was thought to be a reflection of interparticle or ionic dispersion (repulsion) due to preferentially adsorbed Na^+ ions in the double-layer. It was therefore concluded that ionic dispersion was a major contributing factor to shale breakdown. Another possibility however, is that the exchangeable cations are in the main derived from the interlayer sites in the montmorillonite component of the mixed-layer clay. This interpretation fits with the previous discussion; it also explains why the contents of exchangeable cations in the unstable shales of Badger et al., (1956) are on the high side. The maximum and minimum values from their work are given in Table 2.3, together with values for samples considered in the current work. The exchangeable cations for these samples were determined using 1N ammonium acetate (Chapman, 1965) as opposed to dilute HCl (see Appendix 1). Because the Stafford tonstein does not contain a separate 10Å phase it is possible to demonstrate accurately that the 70 per cent mixed-layer clay component comprises 65 per cent mica - 35 per cent montmorillonite (see Spears, 1970; Gilkes and Hodson, 1971). The exchangeable cations (particularly Na^+) are too high for either kaolinite or an illite-rich sample (compare with L.S.24), but are of the correct order for the amount of montmorillonite present (e.g. Wyoming bentonite

C.E.C. - Na^+ = 54, Ca^{2+} = 11, Mg^{2+} =15, Total = 89 m-equiv./100g - Carroll and Starkey, 1958). The Na^+ values for the Ryder, Brooch and Park samples also point to an overall high C.E.C., thus indicating the presence of montmorillonite. Badger et al., (1956) noted a variation in the breakdown depending on the electrolyte concentration - again this can be explained by intraparticle, rather than interparticle swelling. It is important to record that the illite-rich Lower Six Feet sample from South Wales (Table 2.3) has low exchangeable Na^+, K^+ and Ca^{2+} values which are similar to the illite-rich Mansfield marine shale (L.S.24[1]). The former shale was shown by Beckett et al., (1958) to have negligible slaking properties. Cation exchange values for the Harvey samples and Littleton tip material imply that they are unlikely to have a significant montmorillonite content which is in line with the X-ray work. The work to date indicates that tip material tends to give higher exchangeable Ca^{2+} values than equivalent fresh shales. This may be a function of cation exchange occurring after emplacement, or possibly contamination by stray cations associated with sulphates (e.g. gypsum). If the former hypothesis is correct then clay mineral stability should ensue and breakdown due to mixed-layer clay should be at a minimum.

Another correlation recorded in the literature is that unstable shales in the coal preparation plants are associated with low-rank coals, Raybould (1966). End-over-end breakdown test results for seatearths mainly from Yorkshire and the East Midlands have been plotted on Figure 2.4. The writer has selected only seatearth values from the National Coal Board's records so as to reduce major lithological variations which obtain in the roof measures. The less than 10μ breakdown versus the rank of the associated coal (which is of course non-linear) demonstrates that the spread of breakdown values does tend to increase as rank decreases. The spread of disintegration values could well

[1] L.S.24 has an enhanced Mg^{2+} C.E.C. value. An increase in exchangeable Mg^{2+} is not uncommon when clay minerals are immersed in sea water (see Müller, 1967).

Figure 2.4

End-over-end breakdown test results for seatearths, plotted against rank of associated coal seam

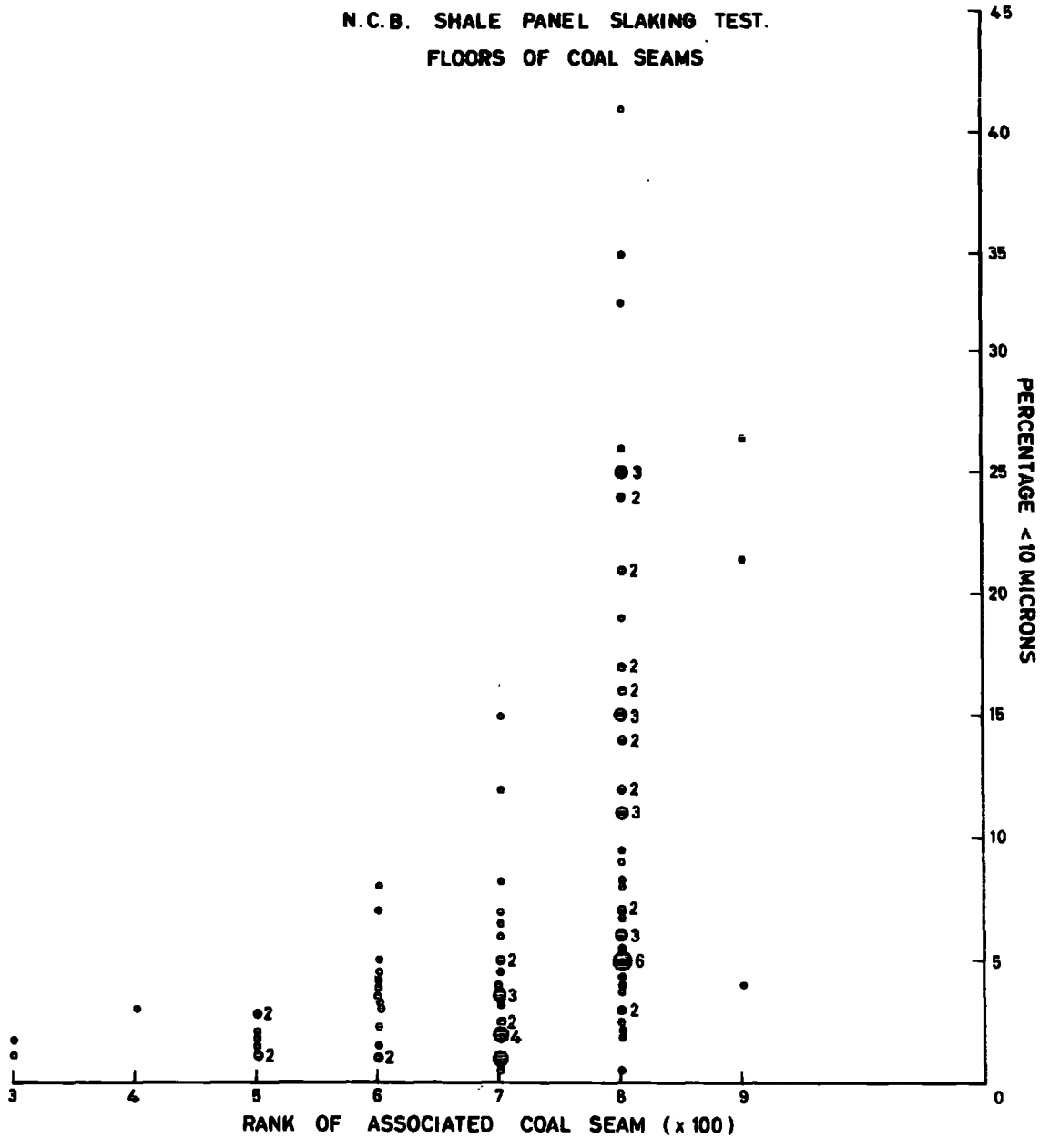

FIGURE 2.4

be a function of original depositional differences as in the Littleton case quoted earlier, and may be influenced by minor structures such as slickensides.

Thus even restricting Figure 2.4 to seatearths has not, so it is thought, eliminated original lithological differences. The work of other authors such as Price (1960) shows that there are other independent reasons for concluding that the concept of an incipient 'rank factor' for the associated measures is not unreasonable. It is possible that the processes leading to high-rank coals could eliminate montmorillonite from the mixed-layer clay (see Grim, 1968, p.551).

(b) Pyrite (non-detrital mineral)

Pyrite oxidation has already been mentioned, but the part it may play in the disintegration of shales deserves further mention. Although quantitatively restricted in Coal Measures rocks it may be concentrated in the coal and associated roof measures, particularly if the latter have marine or brackish affinities (see Chapter 3).

The actual form and details of the low-temperature oxidation process are still a matter of debate; the reaction is probably somewhat similar to that quoted by Winmill (1916), who reported that the consequent volume increase caused the surrounding coal to disintegrate:

$$2FeS_2 + 7O_2 + 8H_2O \rightarrow 2\ Fe\ SO_4 + 2H_2\ SO_4 + 624\ cal.$$

Several foundation failures due to this type of volumetric expansion have been recorded in the literature, although other possible factors such as mineralogy and moisture relationships have tended to be overlooked in the cases described. Little is known about the swelling pressures involved, but the scant laboratory evidence (2 lb/in^2 Anon, 1960) implies that they must be greater in the field if pyrite oxidation is responsible for the overall heave of the shales in question.

TABLE 2.3 Cation exchange values

(m - equiv./100g shale)

	Na	K	Ca	Mg	
Ryder	15.0	5.0	-	-	*
Rushy Park	5.5	4.9	-	-	*
Stafford tonstein	14.2	4.9	6.1	2.5	+
L.S.24 (Mansfield marine shale-Little Smeaton borehole)	1.6	1.1	3.6	12.9	+
Brooch seam - seatearth	10.1	2.3	1.8	2.4	
Park seam - seatearth	12.0	1.8	1.0	2.2	
Lower Six Feet Seam - roof, S.Wales	1.4	1.9	1.6	2.4	
Harvey seam - roof)) Fishburn	4.1	5.1	3.4	1.5	
Harvey seam - floor) Colliery	5.3	2.8	3.9	1.2	
Littleton tip - toe of slip	1.5	2.5	7.9	2.6	
Littleton tip - failure plane	4.4	2.8	6.3	4.0	

* Badger *et al.*, 1956 - dilute H Cl

\+ Spears, 1970 - IN NH_4OAc, pH7.

It can only be concluded that this swelling mechanism may be important locally, and from the presence of pyrite in colliery tips of more than 50 years old it can be expected that oxidation is likely to continue over a protracted period.

(c) Carbonates (non-detrital minerals)

It was concluded by Kennard et al., (1967) that in the shales examined by them solution of the calcite cement was the principal cause of disintegration. The Ca^{2+} values given by Kennard et al., (1967) account for about 2.4 per cent calcite in their unweathered rocks compared with a maximum of about 8.0 per cent siderite in the 'siderite-rich' horizons of the Mansfield marine shale - recomputed CO_2 values, (Chapter 3). Moreover, the computed calcite figure falls to a minimum value of only 0.4 per cent in the slightly weathered Balderhead shales. Although calcite dissolution may be of some importance it is difficult to conceive that this mechanism is a major control, particularly as some of the calcite is probably included in fossil tests, and also within the lattice of clay minerals (Grim, 1968).

In the Coal Measures, however, calcite is relatively rare, the most common carbonate being siderite which occurs most commonly as distinct nodules and bands (especially in the argillaceous strata), and not/as a matrix cement. simply These ironstones were worked as a source of iron, and the relative stability of siderite is shown by the fact that the old method of cleaning the ore was to let it weather in the open for a few years. The stability of siderite was noted in the long-term permeability tests carried out under turbulent and laminar flow conditions (Fig. 2.5). Weathered mudstone fragments rich in siderite (Fe_2O_3% on Table 2.4, dry density (γd) on Fig. 2.5) were subjected to percolation equivalent to the rainfall of 185,000 yr, although at a grossly exaggerated rate (for Co.Durham annual rainfall = 27in, evo-transpiration = 14in, hence percolation = 13in). Table 2.4 shows that there was only a

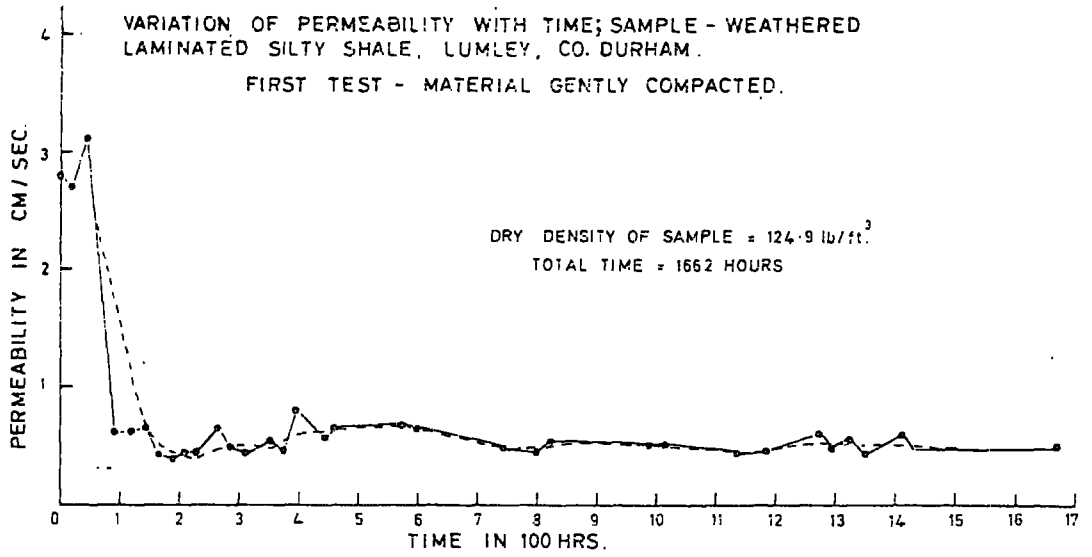
VARIATION OF PERMEABILITY WITH TIME; SAMPLE - WEATHERED LAMINATED SILTY SHALE, LUMLEY, CO. DURHAM.
FIRST TEST - MATERIAL GENTLY COMPACTED.
DRY DENSITY OF SAMPLE = 124·9 lb/ft.³
TOTAL TIME = 1662 HOURS
PERMEABILITY IN CM/SEC.
TIME IN 100 HRS.

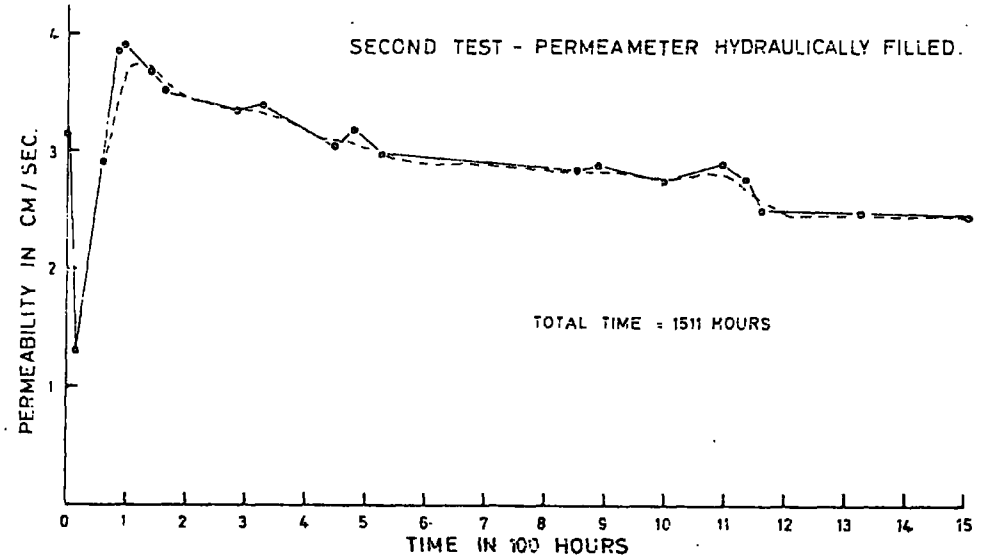
SECOND TEST - PERMEAMETER HYDRAULICALLY FILLED.
TOTAL TIME = 1511 HOURS
PERMEABILITY IN CM/SEC.
TIME IN 100 HOURS

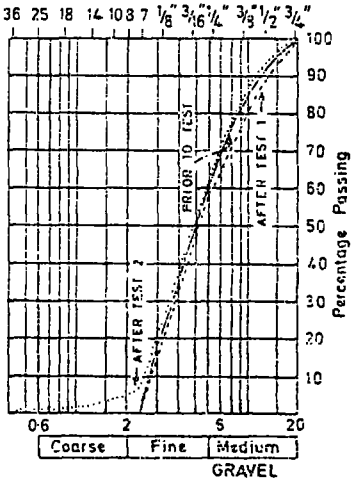
PRIOR TO TEST
AFTER TEST 1
AFTER TEST 2
Percentage Passing
Coarse
Fine
Medium
GRAVEL

FIGURE 2.5

TABLE 2.4 Long-term Permeability - Chemical Changes

	Control sample	After second run
SiO_2	55.59	56.19
Al_2O_3	16.79	18.14
Fe_2O_3	19.79	18.21
MgO	1.46	1.44
CaO	0.62	0.60
Na_2O	0.58	0.53
K_2O	3.20	3.14
TiO_2	1.01	0.97
MnO	0.62	0.56
S	0.11	0.05
P_2O_5	0.24	0.17

LARGE STRAIN DIRECT SHEAR BOX TEST RESULTS

	Control specimens	Ex-permeameter specimens
ϕ'Peak (degrees)	30.0	29.0
c'Peak (lb/in^2)	2.5	3.3
ϕ'Ultimate (degrees)	17.5	17.0
c'Ultimate (lb/in^2)	1.0	1.9

Note: The above results are based on a least-squares linear regression line; c' can logically be regarded as zero.

very small decrease in the Fe_2O_3%. Minor leaching, in particular of the clay minerals, was also noted; this accounts for the small decrease in K_2O, Na_2O, CaO and MgO contents. The other significant features are the very restricted breakdown (Fig.2.5) at the conclusion of the permeameter runs, and the negligible change in mechanical properties determined by large strain direct shearbox tests (Table 2.4).

FIGURE 2.6

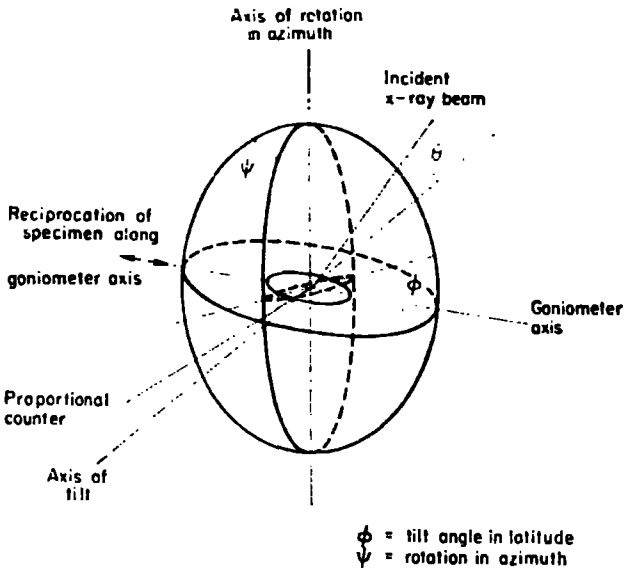

FIG. 2.6. Geometry of the texture-goniometer operating in the reflection mode.

Preferred orientation analyses were performed on a Philips texture-goniometer in conjunction with a 1310 2kW diffractometer and using Ni filtered Cu radiation. The mechanics and diffraction geometry of the system are based on the original Schulz (1949) discussion of his reflection condition whereby the prepared flat surface of an oriented disk specimen (about 25 mm diameter by 3 mm in thickness) is rotated in azimuth about a normal to the surface while being simultaneously tilted through the latitudes about an axis parallel to and within the plane of the surface. This axis also lies within the vertical plane containing the incident and diffracted beams. One complete rotation in azimuth is accompanied by 5° of latitude tilt during a time period of 16 min. Additionally, a mechanical integration facility translates the surface backwards and forwards in its own plane in order to pass a sufficiency of grains through the X-ray beam (see Fig.2.6). The resultant of the first two motions for a particular 2θ setting is an outwardly directed spiral scan of the sphere of projection from zero to about 70 degrees latitude at which point a decrease in counting rate directly attributable to changes in absorption with tilt angle ceases to be wholly offset by concomitant changes in the scattering volume. An analogue record of diffraction intensity in terms of counts per second (for a particular 2θ setting) expressed as a function of azimuth angle and latitude is produced on a chart recorder, the background correction being determined from a diffraction trace carried out immediately after the texture run. The intensity data is also recorded on tape via a direct digital recorder and the tape processed by N.U.M.A.C. 360/67 computer (PL/1 program - Attewell et al., 1969) to give a direct fabric print out (**equal area** stereographic projection) which can then be contoured.

2.4 Textural features

Although sediments undergo changes during diagenesis (Grim, 1968, p.535 et seq.) the imprint of initial sedimentation conditions is still usually recognizable in the lithified rock. The juxtaposition of shales with a highly preferred orientation with more randomly orientated mudstones, confirms that there is no simple systematic correlation between depth of burial and degree of orientation. This will be illustrated in the subsequent discussion on X-ray fabric analysis.

In fine-grained rocks microscopic mineral orientation studies are exceedingly tedious and for this reason an X-ray technique has been adopted to demonstrate certain textural features. Basic details of the method are given on Figure 2.6.

Ultrasonically disaggregated mudstone (with abundant 7Å minerals) from the Mansfield cyclothem at Tinsley Park, Sheffield was first made up into a suspension with distilled water and then allowed to sediment-out into a 50 mm consolidation ring with basal porous plate, the suspension being contained in a 50 mm diameter glass tube. The initial specific gravity of the suspension was 1.015. After 4 days the 47.62×10^{-2} in thick cake of sediment was progressively impregnated with Lakeside 70 dissolved in absolute alcohol, the proportion of Lakeside 70 being gradually increased from 1 in 12 to 1 in 8 by volume. The impregnated cylinder was then rubbed-down to form a texture disc normal to the axis of sedimentation. The resulting fabric (Fig. 2.7a) can be compared with that of the natural unweathered non-marine mudstone (Fig. 2.7b) for which impregnation was not necessary. The quality of preferred orientation decreases as the area covered by the counts per second contour lines (indicative of the volume of clay minerals possessing a particular orientation) increases. A single dot at the centre of the projection would denote perfect orientation of the basal planes of the micaceous minerals ((001) planes) parallel to the anisotropy. Figures 2.7a and b

X-RAY FABRIC DIAGRAMS

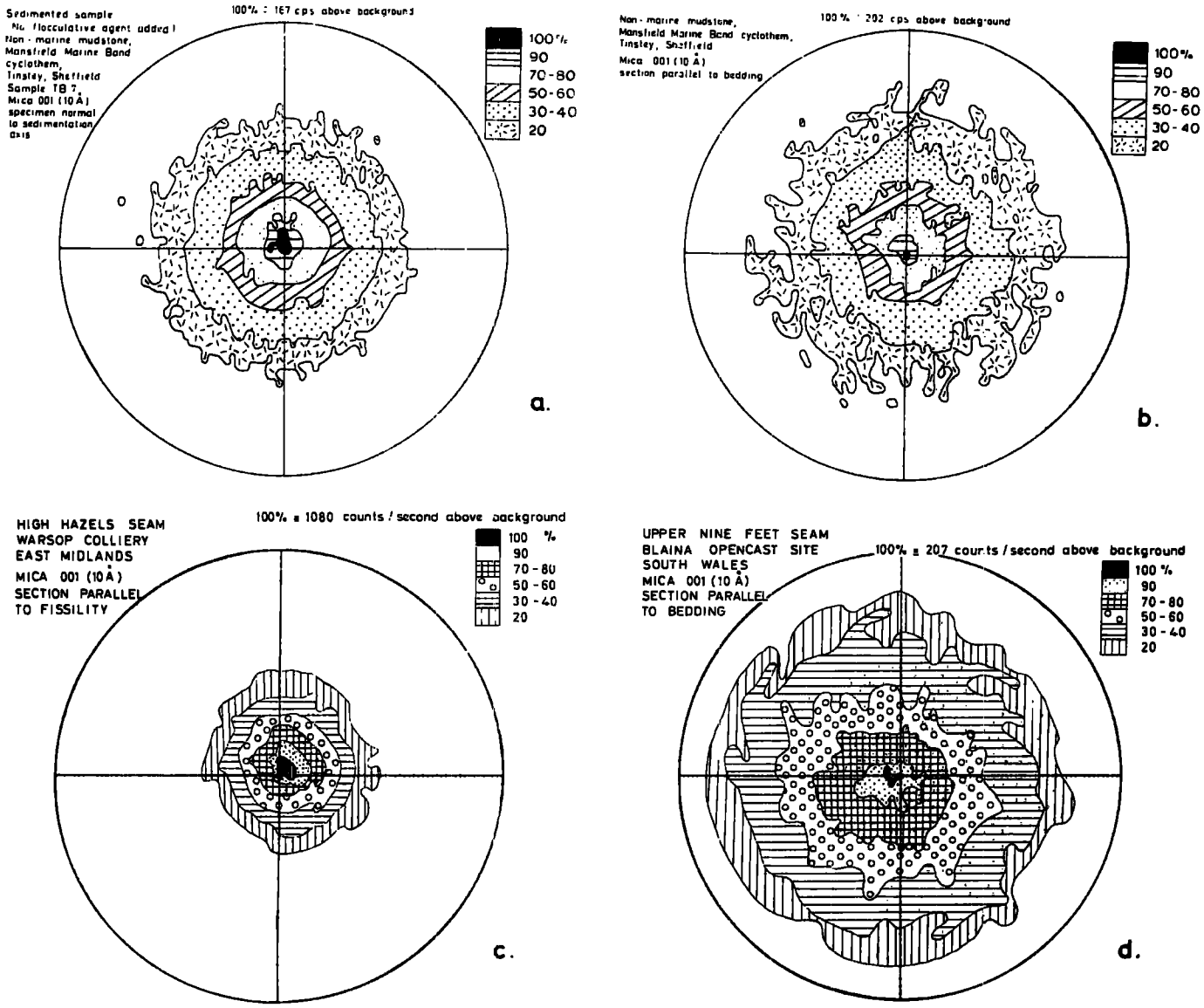

FIGURE 2.7

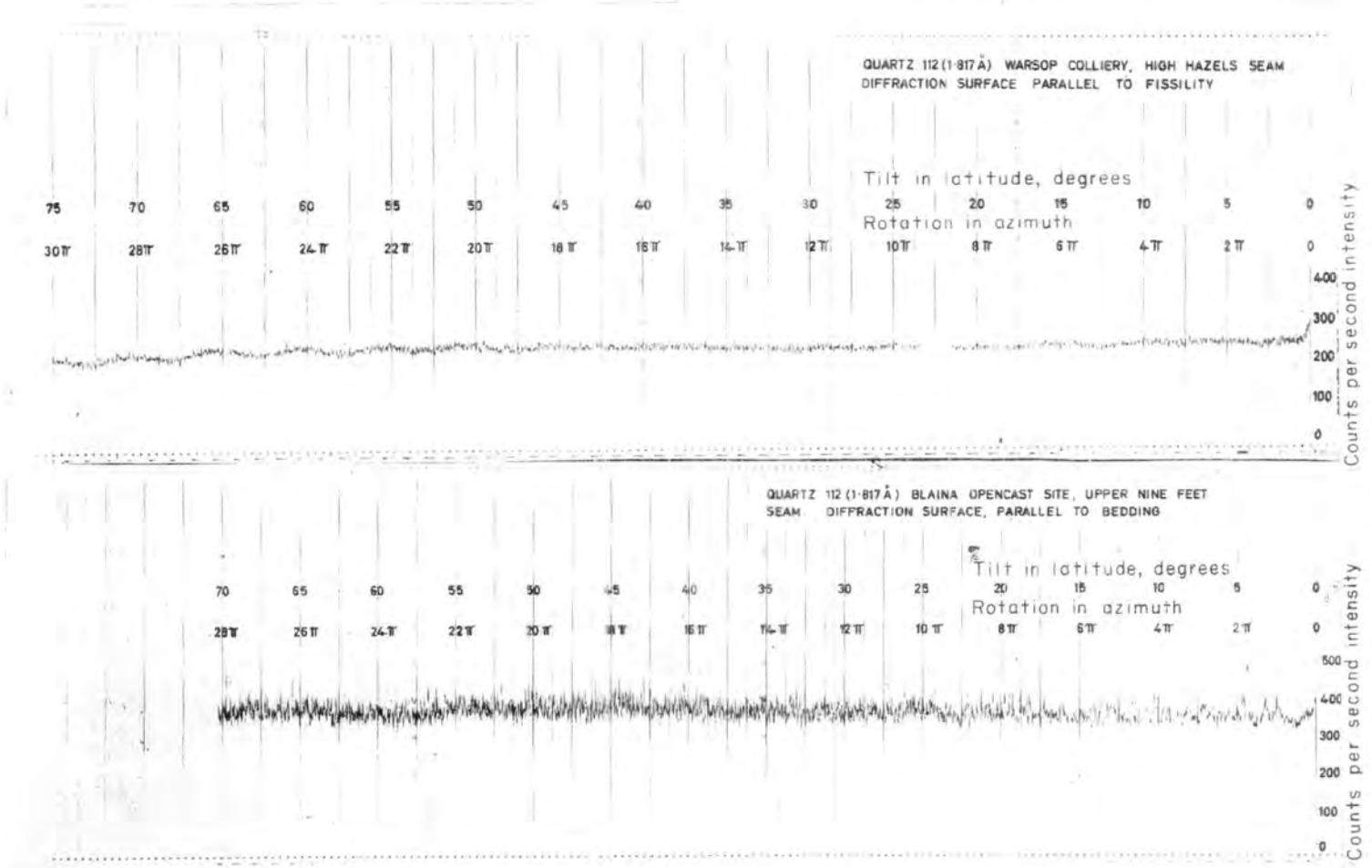

FIGURE 2.8

FIG. 2.8 X-ray texture analogue print-out for quartz (d = 1·817 Å). The diffraction intensities in counts per second are a function of the geometry of the X-ray goniometer system. The horizontal traces are indicative of random orientation and the overall band widths are related to grain size.

demonstrate that the quality of preferred orientation for the dispersed (deflocculated) sediment is not greatly different from that of the natural mudstone which during its geological history has been subjected to a sedimentary overload possibly in the region of 3,000 m, not to mention the concomitant diagenetic processes. The maximum counts per second above background are slightly lower for the laboratory sample, probably because the larger mica laths of higher crystallinity sedimented out initially and were consequently not sampled in the texture specimen. The higher degree of preferred orientation for the lower percentage contours of the laboratory sample, in comparison to the natural one, can also be accounted for by inequality of mineral sizes in the two samples. However, this simple experiment demonstrates the importance of initial depositional conditions. It could well be that the mudstone was initially flocculated in the natural environment, and in the coarser lenses subsequent carbonate ($FeCO_3$) cementation was observed. Alternatively, disorientation of clay mineral laths could arise under low normal pressures (early diagenesis) during the formation of the carbonate from the pore solutions. Whatever the mechanism it is clear that the quality of preferred orientation is not a simple direct function of effective overburden pressure.

The unstable High Hazels (low rank) roof shale from the East Midlands exhibits an exceedingly high degree of orientation concordant with the bedding (Fig. 2.7c). The axial symmetry of the abundant 10Å mica (note high counts per second) is a good example of a dispersed sediment. Like the Tinsley mudstone however, the roof rock of the high-rank Upper Nine Feet seam of South Wales (Fig.2.7d) has a more random textural orientation with respect to the bedding. This latter rock is much coarser grained than the High Hazels shale and under the microscope the clay mineral laths are clearly bent around and displaced by the large equant quartz particles. The conventional analogue

chart records of quartz 112 ($\underline{d}$ = 1.817 Å) are shown on Figure 2.8. The diffraction intensities (counts per second) as a function of the geometry of the goniometer system (azimuth angle and latitude), display horizontal traces indicative of random orientation. The overall band width, which is related to grain size, is in line with the microscopic evidence - quartz appears to have little effect on the High Hazels clay matrix because it is of similar grain size, but this is not so in the coarser-grained Welsh mudstone.

Here again these two latter fabrics demonstrate how original depositional differences exert a considerable influence on the final fabric, to the extent that, in this case, the highest degree of preferred orientation is associated with the coal of lowest rank.

2.5 Water uptake by shales

In highly weathered profiles developed on Coal Measures rocks the seasonal variation in undrained shear strength in the near surface zone may be considerable. At Lumley (N.G.R. NZ/314 477) the upper 12 in of an area 12ft^2 was sampled by Paderes (1967) over the period from December 1966 to June 1967. The regolith (Fig. 2.9 - 75% of the material being of sand, silt and clay grade size) represents the post-glacial breakdown of the laminated silty mudstone above the High Main seam. The highest shear strength (June 20th) is over twice that of the other extreme (January 21st). In terms of ultimate bearing capacity for a footing of unit width (Terzaghi and Peck, 1967, p.221) the summer figure of 7.9 ton/ft^2 is again more than twice the winter value of 3.3 ton/ft^2. Although the particulate matter is by no means of fundamental size (c.f. Fig. 2.15) the density values (Fig. 2.9) show that these large variations in strength are brought about by very small increases in porosity (29.5% to 34% for the two extremes), with concomitant moisture uptake of less than 10 per cent. The meteorological data for the investigation period are: rainfall - 15.2 in; average temperature at 12 in depth - 8.1°C; sunshine - 929.9 hours.

Figure 2.9

Seasonal variation in shear strength parameters for soil horizon developing on breakdown of mudstone at Lumley, Co. Durham.

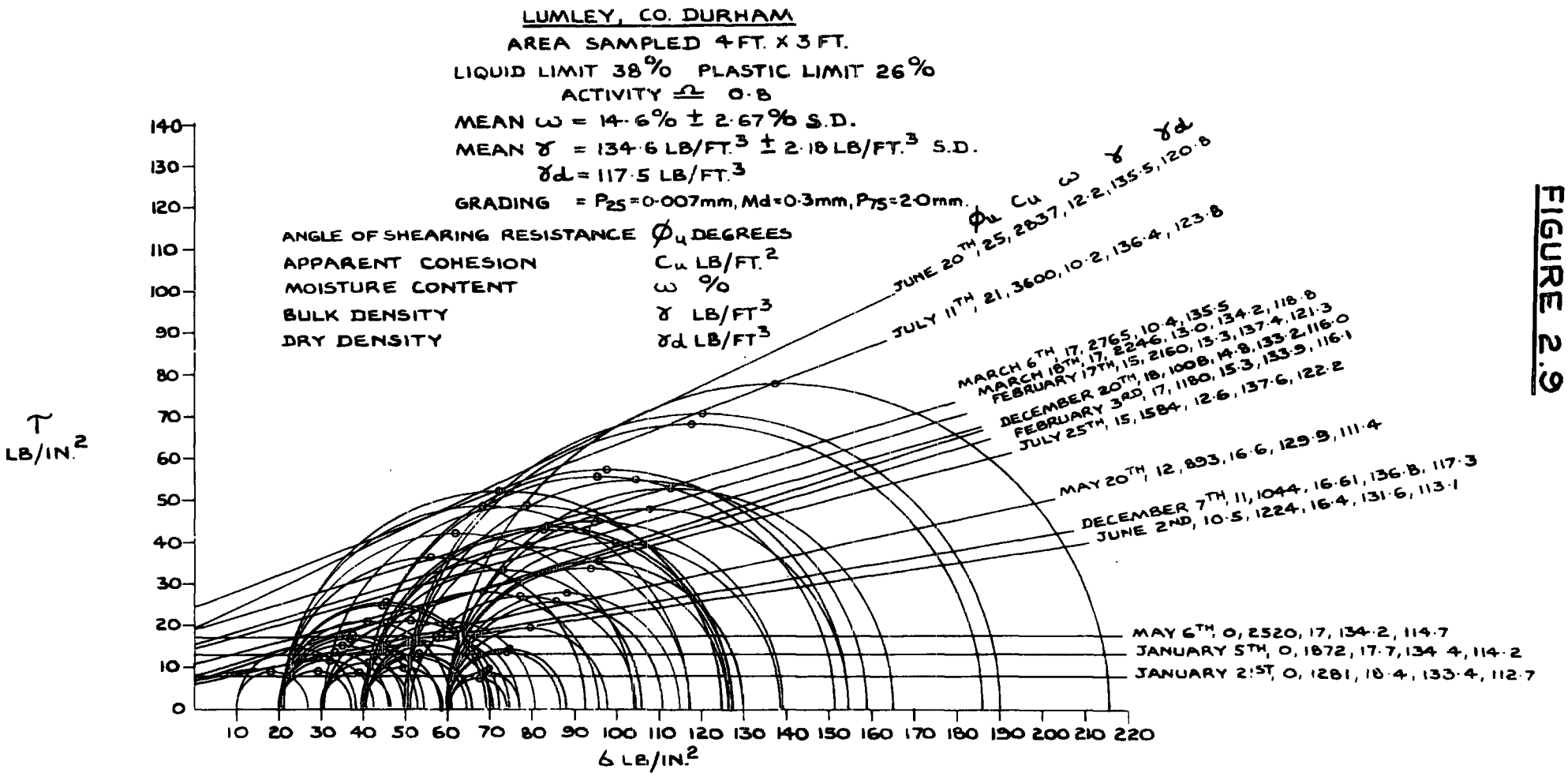

FIGURE 2.9

The consequence of volumetric changes such as the Lumley case raises the question of how diverse rock types, which initially at least will have a skeletal framework, compare with soils in the partly saturated state. Volumetric increases certainly do occur on saturation from room temperature (Section 2.2) but it is important to consider in more detail the precise behaviour during desiccation and saturation.

According to Childs (1969) by far the greatest proportion of water held in granular soils is retained by surface tension around the points of contact of the particles, and in the soil pores and capillaries.

The capillary model which represents the pore space within a soil or rock as a series of connected capillaries of tortuous configuration is a valid model on which to base suction pressure concepts (Aitchison, 1961). The term suction as applied to a soil-water system generally implies the existence of a pressure deficiency or moisture tension in some part of the soil water. Based on the conventional capillary model the pressure deficiency is given by:

$$p'' = -\frac{2T}{r}\cos\alpha$$

where: p'' is the pressure deficiency in the soil water with respect to the pressure in the soil air.
T is the surface tension of water at an air-water interface.
r is the mean effective radius of curvature of the water meniscus.
α is the contact angle between water and soil. (usually taken as zero, although for shales a value of 10 degrees may be applicable (Horsley, 1951-52).

The two pieces of apparatus used in this work to measure 'soil' suction were the suction plate (Croney et al., 1952) and the pressure membrane (Croney et al., 1958). The former (Plate 2.3) measures suctions in the

PLATE 2.3

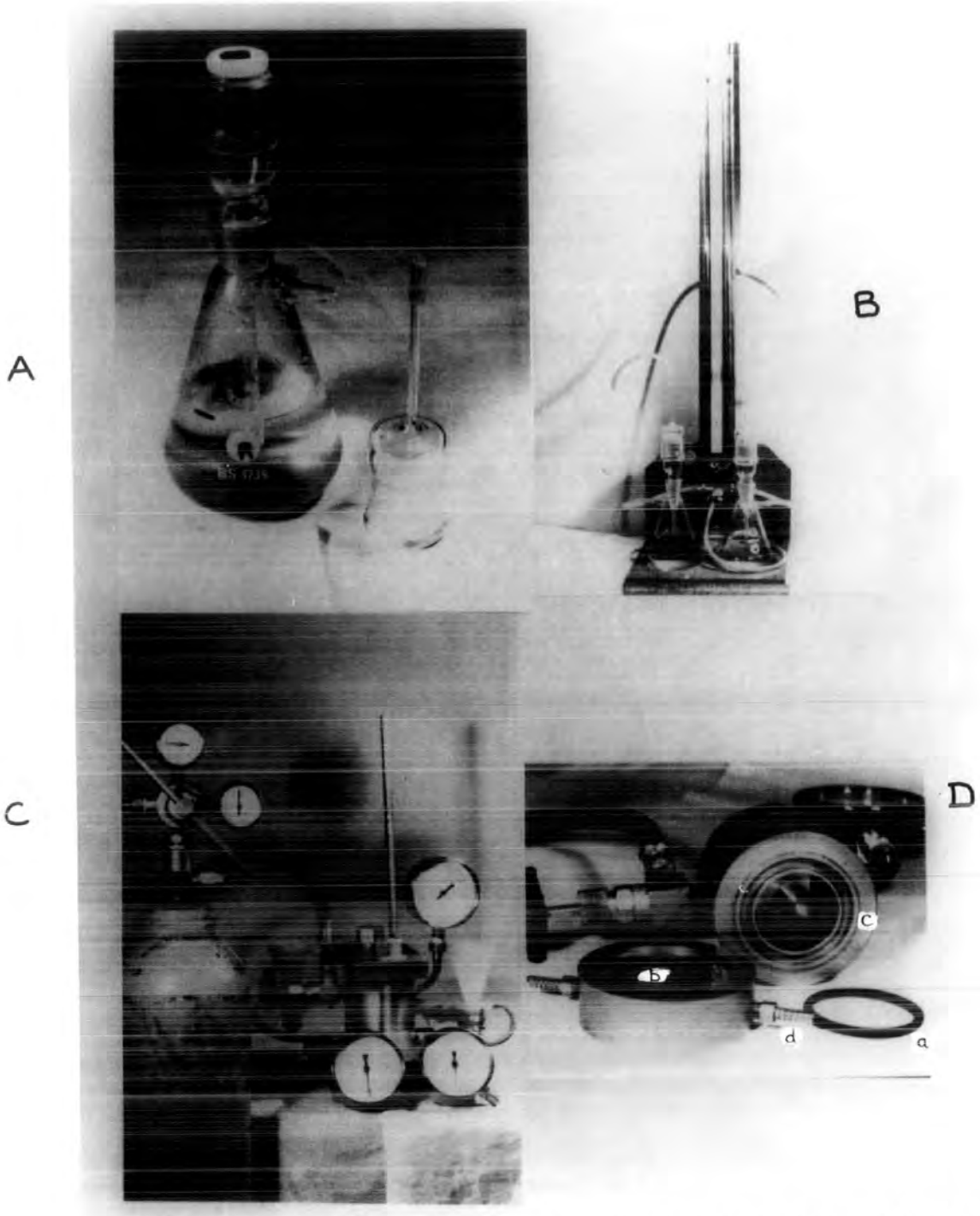

SUCTION PLATE (A AND B); PRESSURE MEMBRANE (B AND C)

A. Demountable chemical glassware of suction plate apparatus, showing sample sitting on sintered-porous-plate which is impermeable to air for pressure difference of up to 1 atmosphere.

B. Suction plate apparatus. Reduced pressure (in line with mercury manometer) applied to plate by evacuating the space above the water level in the filter flasks. After a few seconds the sample is placed on the plate and the glass cap, which is connected to the open end of the manometer, is replaced.

C. Pressure membrane apparatus showing air cylinder for applying pressure, pressure vessel with gauges and water reservoirs.

D. Pressure membrane pressure vessel. (a) 'o' ring for sealing vessel, (b) saturated cellulose membrane, in contact with specimen and supported by sintered bronze disc. Moisture transfer between sample and membrane takes place when air pressure is increased within the chamber (c); connection to water reservoirs (d).

range pF[2] 0 to 3.0. The specimen under test is in close contact with the upper surface of a sintered-glass disk of ~~the~~ fine pore size. Moisture equilibrium is established with water at a known applied suction beneath the disk, the soil being weighed when it has reached equilibrium. The test can be repeated for various fixed suctions to give the relationship between suction and moisture content. The relationship may be determined either by wetting from oven dryness or drying from a saturated condition, the moisture content on a dry weight basis being determined at equilibrium. Using one specimen for each complete set of tests is preferable since this eliminates errors due to variation within the original sample. The writer first considered laminated mudstone and the overlying gradational siltstone from the Mansfield cyclothem at Tinsley, Nr. Sheffield, and this was followed up as part of a student project by Philpott (1970) who investigated amongst others the unstable High Hazels roof shale from Warsop Colliery in the East Midlands, as well as the Stafford tonstein. Slaking was an obvious difficulty and many samples tended to crumble when removed from the plate. A different specimen for each point on the relationship then had to be used. At the Road Research Laboratory (Croney et al., 1952) it has been found that for samples 1 cm high, a day was sufficient for the specimen to reach equilibrium. The time taken for a specimen to reach equilibrium depends on the nature of the material, the height of the specimen, and the closeness of contact between plate and specimen. To help facilitate air expulsion (and reduce slaking) the specimens prepared in all the current work were between 1.5 and 2.5 mm in height after being rubbed down. Samples susceptible

[2]On the pF scale, the logarithm to base ten of the suction expressed in centimetres of water is equivalent to the pF value. Hence 10 cm. of water equals pF1, 1000 cm equals pF3 (approximately atmospheric pressure). Soil in equilibrium with free water has a pF of almost zero, and oven-dried almost pF7.

to slaking were bound around their perimeters with tape. They were left for 24 hours to reach equilibrium because it was convenient to change the pressure once each day. In fact, test runs of moisture content versus time to equilibrium subsequently carried out by Philpott (1970), showed that the majority of specimens could have been changed every 12 hours. The first placings of the specimen, from saturation to approximately pF 1.5, and from oven dryness to pF 4.5, were the only exceptions to the 12 hour period.

The pressure membrane apparatus used (Plate 2.3) was originally developed at the Road Research Laboratory and extends the range of equilibrium suctions in a sample. The suction/moisture content relationship for this equipment is within the pressure range 0.1 to 100 atmospheres (pF2 to pF5). A cellulose membrane on which the soil rests is supported by a sintered bronze disk containing water at atmospheric pressure. The suction produced in the specimen when drainage is complete is equal to the air pressure supplied from a compressed air cylinder (for precise details see Croney et al., 1958). Specimens used were similar in size to those used on the suction plate. As before the equilibrium moisture content after a 24 hour period was found from oven drying at 110°C. The initial and final pressure readings were also taken and the average of these two values used to find the pF value. A drop in pressure of about 2.4 per cent in one 24 hour cycle was common.

2.6 Empirical suction pressure curves for weak rocks

The laminated mudstone and High Hazels roof rock (Figs. 2.10 and 2.11) have suction curves which are characteristic of incompressible materials. Childs (1969, p.123) shows that the sigmoidal shape of the wetting and drying curves for non-shrinking materials can be accounted for by the fact that in general a porous body will not contain pores of uniform size and shape that can be emptied at the same suction. Those with large channels of entry, in which only gentle water/solid interface curvatures can be maintained will empty at

FIGURE 2.10

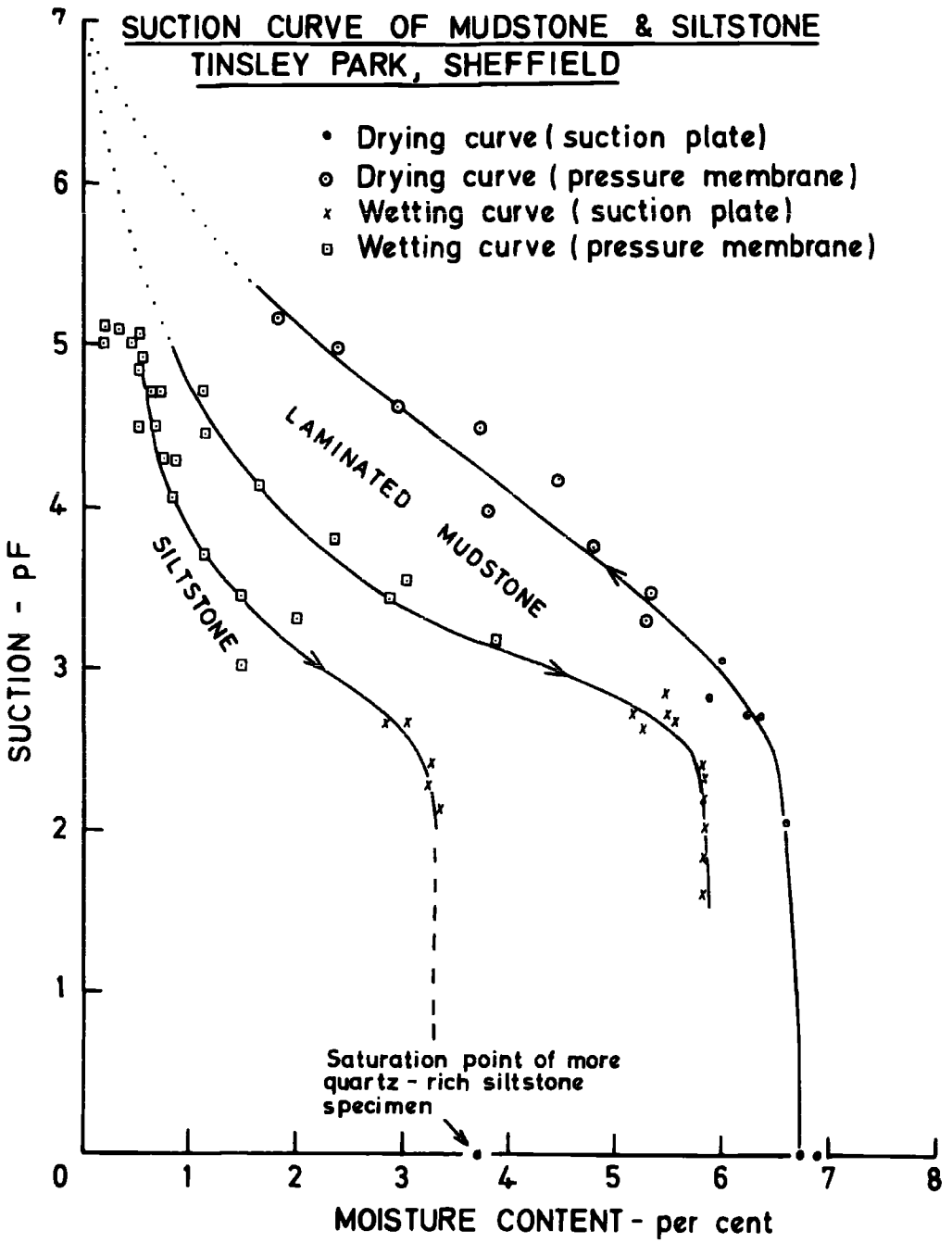
SUCTION CURVE OF MUDSTONE & SILTSTONE
TINSLEY PARK, SHEFFIELD
• Drying curve (suction plate)
⊙ Drying curve (pressure membrane)
x Wetting curve (suction plate)
□ Wetting curve (pressure membrane)
LAMINATED MUDSTONE
SILTSTONE
Saturation point of more quartz - rich siltstone specimen
SUCTION - pF
MOISTURE CONTENT - per cent
0
1
2
3
4
5
6
7
8

FIGURE 2.11

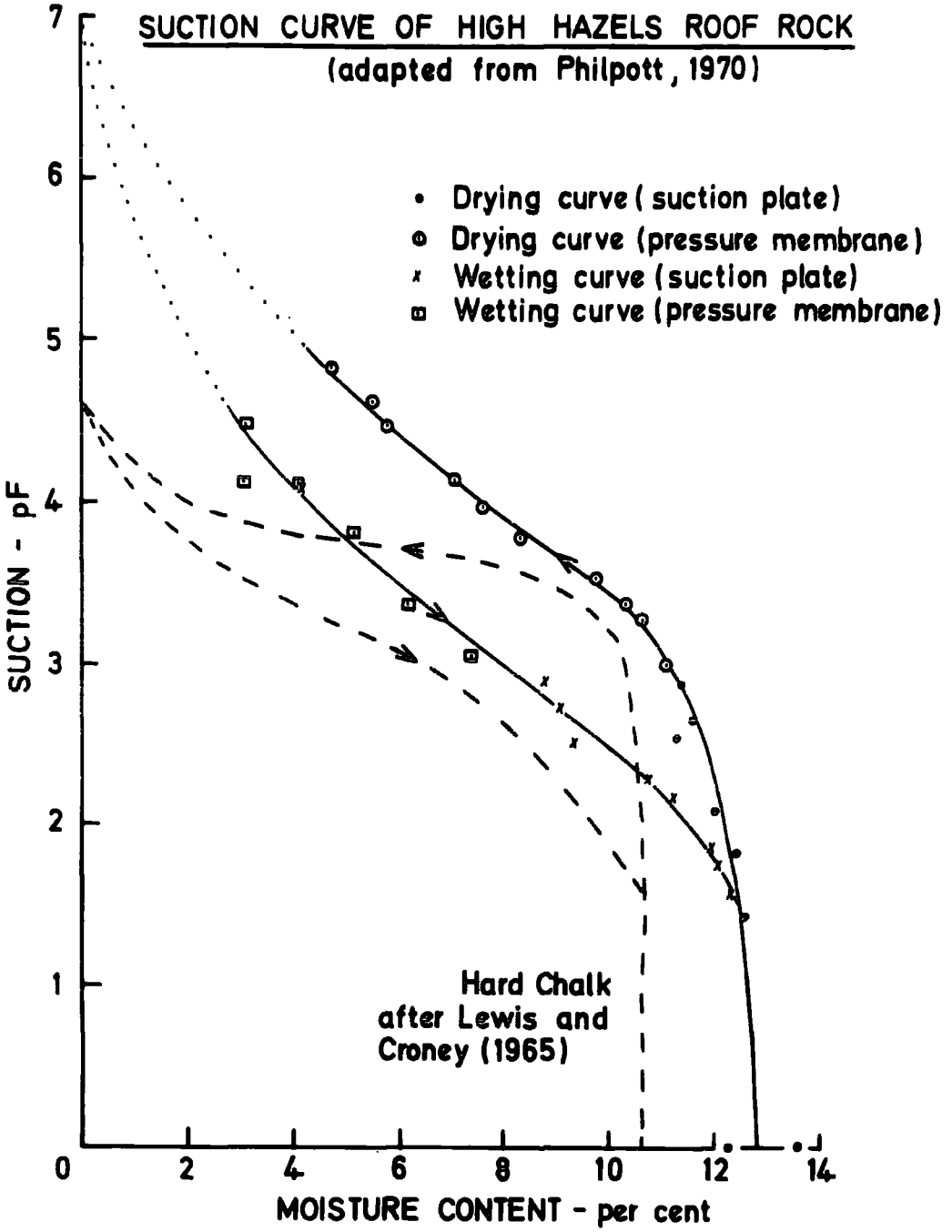
SUCTION CURVE OF HIGH HAZELS ROOF ROCK
(adapted from Philpott, 1970)
• Drying curve (suction plate)
o Drying curve (pressure membrane)
x Wetting curve (suction plate)
□ Wetting curve (pressure membrane)
Hard Chalk
after Lewis and
Croney (1965)
SUCTION - pF
MOISTURE CONTENT - per cent
0
1
2
3
4
5
6
7
2
4
6
8
10
12
14

low suctions, whilst those with narrow channels of entry, supporting interfaces of sharp curvature, will not empty until larger suctions are imposed. The marked hysteresis of the wetting and drying curves depends upon the irregularity in shape of the pore spaces which may be considered as comprising larger voids connected by narrower channels. The greater the disparity between the size of the void and the size of the channel, the more marked is the difference between suctions of emptying and refilling, and hence the hysteresis.

As far as the writer is aware the only other test data in the literature for an indurated rock is for chalk (Lewis and Croney, 1965). Suction curves for a hard (Fig. 2.11) and soft chalk are very similar to the mudstone and roof shale in that they show considerable hysteresis (more so for the soft, less dense chalk), an initially vertical drying curve, and a steep curvature at low moisture contents.

The vertical part of the drying curves show that considerable suctions can be applied to the pore water without change of moisture content, the only effect being a change in the radii of the water menisci in the surface pores. Lewis and Croney (1965) suggest that this is why chalk is invariably saturated. Drainage commences when the air entry suction is reached and is indicated by a change in shape of the curve. This occurs at about pF 2 in the High Hazels shale and at pF 2.3 to pF 2.5 in the Tinsley mudstone and siltstone. Between pF 3 and pF 4.5 all three Coal Measures rocks show a steady decrease of moisture content with increasing suction, but between pF 4.5 and oven dryness the shale and mudstone curves may well steepen again, thus indicating that around pF 6 nearly all the pores spaces have been emptied. The wetting curves show a similar trend to the drying curves in that they begin to show a steep portion at high suctions when there is only a little increase in the moisture content on filling the smallest pore spaces. Similarly, there is

a vertical portion at low suctions. The chalk samples differ from the shales, the former curves having a flatter middle section with zero moisture content being reached at a much lower value (pF 4.5). This demonstrates that once drainage has commenced in the rock it drains very rapidly. The Tinsley siltstone (wetting curve) is of the same general shape as the mudstone, except that around pF 4.8 the curve inflects sharply inferring sudden drainage. The suction curves of the shale/mudstone and the Stafford tonstein (Fig. 2.12) do not have this latter characteristic (which is undoubtedly a function of the pore size distribution), because they have a high clay mineral content. Initially, the shape of these curves is controlled by the amount of air entry, but over most of their length it is controlled by shrinkage of the clay mineral fabric. Air-breakage will be considered later in the text but it is significant to record that Childs (1969, p.126) regards the non-coalescence of wetting and drying curves (for example the laminated mudstone) as being a function of entrapped air.

We have seen that essentially the shale-mudstones are more akin to non-shrinkable than shrinkable materials with respect to negative suction pressures over a large part of their suction curve. The saturation moisture content of the High Hazels shale is not absolute in terms of a perfectly rigid skeleton and even by making the specimens small, slaking has only been reduced and not eliminated. The important point however, is that the behaviour is more in keeping with a rock which has retained the bulk of its diagenetic bonds than one that has not. In contrast the Stafford tonstein (Fig. 2.12) exhibits suction curves which span almost the same range of moisture contents as do those of compacted kaolinite and muscovite. The curves, like those of compressible soils, do not show the vertical sections which are characteristic of incompressible materials, and their shape is the result of air entry and shrinkage over the entire suction range. The

FIGURE 2.12

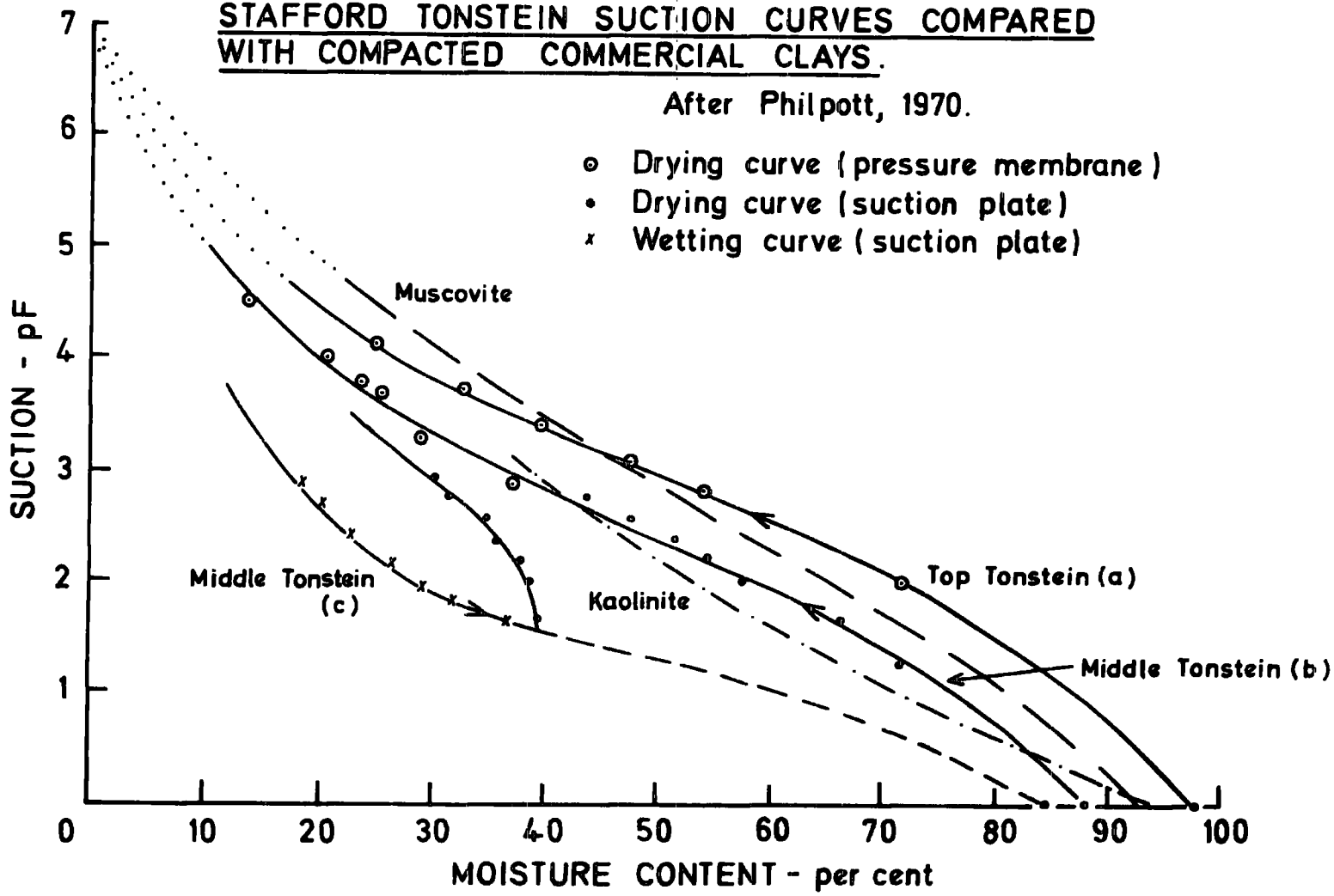

FIGURE 2.12

tonstein curves are sigmoidal in shape and cross those of the kaolinite and illite (Micafine Ltd. material, 82.5% $< 2\mu$, 7% kaolinite impurity, compacted to optimum moisture content - 4% maximum dry density - 74.5 lb/ft^3), between pF 2.8 and pF 4. (Fig. 2.12). The sigmoidal shape is due to the fact that the tonstein is structured and consequently contains pores with a greater range of sizes than the commercial clays. Very similar to the sigmoidal curve of the tonstein are the suction curves of natural clays. They differ, though, because the tonstein with a negligible quartz content has a much higher saturation point than even the Black Cotton Soils which are known to contain montmorillonite. Straight comparisons with other clays and weakly-bonded shales such as the Lias and Kimmeridge are difficult to draw because the suction curves shown in the literature are usually for remoulded, possibly weathered, specimens.

The Stafford tonstein is a banded rock of somewhat variable composition. The tests conducted by Philpott (1970) were on three different specimens - an upper white specimen (a) and two from a lower greyer band (b and c). The lowest value, and the hysteresis effect (Fig. 2.12 c) was obtained for a sample which was first subjected to a wetting test (to about pF 1.6) and then to a drying test. Curve (b) represents the drying curve of another sample with a saturation point of 87-88 per cent. In comparison the drying curve of the sample from the whiter band (curve a) is seen to be of the same shape as the other two, but displaced in the direction of higher moisture content (saturation point, 98%). This difference between the drying curves of the two types of tonstein is a reflection of the mineralogy (as obtained from the X-ray diffraction data). The white band with a greater affinity for water, has a higher mixed-layer mica-montmorillonite component (78%) than the grey band (70-72%).

When we compare the two mudstone-shales with their dominantly well crystallized mica, and the Stafford tonstein of high mixed-layer mica-montmorillonite content, a very important implication emerges. Whereas the shale-mudstones partly retain a skeletal framework (albeit subject to air breakage), the montmorillonitic component of the mixed-layer clay of the tonstein, with its affinity for water, would appear to be almost entirely responsible for breaking diagenetic bonds and reducing the rock to a particulate material with suction characteristics customarily associated with clays rather than rocks.

Although the Stafford tonstein is a true 'clay-rock' with only about 1 per cent quartz it must also be borne in mind that in absolute terms montmorillonite accounts for less than 25 per cent of the total constituents.

2.7 Breakdown of shales and mudstones in water and other liquids

End-over-end breakdown tests (Badger et al., 1956; Franklin, 1970) are by their very nature dynamic experiments and inevitably must involve abrasion of the fragments themselves. It was therefore decided to use a simple slaking test in order to investigate a few, stable and unstable roof and floor rocks (Table 2.5), and at the same time reduce the effects of larger structural discontinuities. Dry aggregate, whose size was visually smaller than the joint or slickenside frequency (passing $\frac{1}{4}$ in and retained on 3/16 in B.S. sieve), was carefully brushed to remove loosely adhering grains. The aggregate was placed on a small No.14 B.S. sieve and immersed in 40 ml of de-aired distilled water. After $\frac{1}{2}$ hr the material on the sieve was carefully washed with a further 10 ml of water and oven-dried. The breakdown was expressed as the percentage retained on the sieve. Similar tests were carried out on samples which had been de-aired for 24 hours, using a closed vacuum system throughout the immersion stage. This was facilitated by first of all de-airing the water in a large dropping funnel,

sealed into a vacuum desiccator. When the material on the sieve had itself been de-aired through a separate desiccator stop-tap the de-aired water was run-in from the closed dropping funnel. The sieve base-tray was so arranged that the aggregate on the sieve was immersed in the water.

Dependent on availability of material it proved possible to check the slaking test behaviour using bulk samples. The Durham High Main material was very stable, showing only minor lamination breakage after months of water immersion with alternate periods of air drying. Similarly, the Barnsley Bed seatearth proved to be more or less intact after 24 months in the open. In contrast, the unstable High Hazels roof shale exhibited major breakdown in 12 minutes (largely controlled by vertical jointing and paper thin laminae), whilst the Stafford tonstein and Brooch seatearth were literally explosive. The Park seatearth disintegrates in less than 30 minutes although it is regarded as being a stable rock in its underground setting. Stability is a matter of degree (and coalfield), and good reasons for its relative behaviour will be discussed later in the text.

The slaking test averages (Table 2.5) show a rather greater breakdown for the low-rank High Hazels roof shale than those of Durham or South Wales (see discussion of Fig. 2.3). The two Staffordshire seatearths have considerably greater disintegration values than any of the other samples, the Brooch seatearth in particular being exceptional.

The in vacuo values (Table 2.5) illustrate that breakdown can be arrested by removal of air, which is obviously a major factor in the disintegration mechanism of the weaker rocks, other factors being equal. It can best be explained in terms of air breakage - during dry periods evaporation from the surfaces of rock fragments promotes high suctions, which in turn result in increased shearing resistance (of individual fragments) by virtue of high contact pressures. With extreme desiccation the bulk of the voids

TABLE 2.5. Slaking Test Results

(Average of 3 tests)

	Rock type	Rank	Slaking in water (% retained No.14 B.S. Sieve)	Slaking in water (% retained No.14 B.S. Sieve) (in vacuo)	Slaking in methyl alcohol (% retained No.14 B.S. Sieve	Slaking in amyl alcohol (% retained No.14 B.S. Sieve)	Slaking in carbon tetrachloride (% retained No.14 B.S. Sieve)	Slaking in benzene (% retained No.14 B.S. Sieve)
Upper Nine Feet, Blaina opencast S. Wales	Dark grey shaly mudstone (roof)	101	96.0	99.0	96.0	98.0	100.0	100.0
Lower Nine Feet Cwmamman opencast S. Wales	Dark grey shaly mudstone (roof)	102	98.0	99.0	99.0	99.0	100.0	100.0
High Main, Lumley opencast Durham	Grey laminated silty mudstone (roof)	502	98.0	100.0	100.0	100.0	100.0	100.0
High Hazels, Warsop Colliery, E. Midlands	Dark grey fissile shale (roof)	802	92.0	98.0	96.0	99.0	100.0	100.0
Barnsley Bed, Yorkshire Main Colliery, Yorkshire	Dark grey carbonaceous mudstone (seatearth)	600	98.0	100.0				
Park, Littleton Colliery, Staffordshire	Grey carbonaceous mudstone (seatearth)	802	79.0	95.0				
Brooch, Littleton Colliery, Staffordshire	dark grey mudstone (seatearth)	802/902	00.0	27.0				
Surface tension (dyn/cm)			76.0	76.0	23.5	26.8	29.4	31.7
Dielectric constant			81.0	81.0	31.0	16.0	2.3	2.3

TABLE 2.6

Fundamental Properties

	Specific Gravity	Mica Shape Factor	Liquid[3] limit	Plastic[4] limit	Effective porosity (%)	Clay size fraction (< 2μ)
Upper Nine Feet (roof)	2.501	0.32	27	18	2.8	53
Lower Nine Feet (roof)	2.574	0.25	26	16	2.1	37
High Main (roof)	2.594	0.15	28	17	5.8	24
High Hazels (roof)	2.506	0.25	28	20	2.9	87
Barnsley Bed (floor)	2.483	0.19	28	16	2.5	33
Park (floor)	2.538	0.74	37	21	5.8	60
Brooch (floor)	2.059	0.97	72	31	-	77

[3]Liquid limit - moisture content at which a sediment passes from the plastic to the liquid state as determined by the standard test (B.S. 1377/1967).

[4]Plastic limit - lower limit of the plastic state, being the moisture content at which a soil begins to crumble when rolled into thin threads.

will be filled with air, which, on rapid immersion in water, becomes pressurized by the capillary pressures developed in the outer pores. Failure of the mineral skeleton along the weakest plane ensues and an increased surface area is then exposed to a further sequence of events. This is much the same mechanism as advocated by Terzaghi and Peck (1967), for slaking of soils.

Restricted breakdown in vacuo was reported by the National Coal Board's Shale Panel scientists and associated workers from the end-over-end breakdown tests (Badger et al., 1956, Berkovitch et al., 1959); air breakage was considered to be an important reason for disintegration. Recently, however, Nakano (1967) has found that although the percentage of smaller grains produced by the slaking of certain Japanese mudstones in vacuo is a little larger, there was no substantial difference between slaking in air and in vacuum. This would be true for the current test material had the montmorillonite content been higher.[5] Nakano attributes breakdown to chemical dissolution, chiefly by hydrogen bonding of originally adsorbed water molecules around clay particles with newly adsorbed ones. The National Coal Board scientists showed that in the end-over-end tests breakdown did not conform to a first-order decay law and this in itself implies that more than one mechanism is involved. They also found that the degree of breakdown was related to initial moisture content and that the percentage breakdown increased as this free moisture was removed by desiccation. The earlier workers attributed the other breakdown mechanism to ionic dispersion, which like Nakano's mechanism in interparticle swelling.

[5] Undoubtedly the Stafford tonstein would behave like Nakano's material. The tonstein is no longer exposed underground and sufficient material was not available for slaking tests to be carried out.

The Japanese mudstones are all montmorillonitic types and hence intraparticle swelling is likely to be the dominant mechanism, largely blanketing any capillarity effects. Similarly their physical properties suggest that they are far less indurated than British Coal Measures mudstones. In other words the Japanese mudstones may be regarded as special cases, the Stafford tonstein and Brooch seatearth in the present work are perhaps our nearest equivalent, but on a much more restricted scale. There is a comparatively minor expandable montmorillonite contribution in terms of total constituents in the British rocks. However, it is reasonable to conclude that intraparticle swelling is the other effective short-term breakdown mechanism in our rocks whilst in the long term interparticle forces are of increasing importance and for this reason will be considered later in the text.

On Table 2.6 are given further details of the samples used in the slaking tests. The range of specific gravities can easily be accounted for in terms of mineralogical composition and organic matter. Consistency limits are very similar for all the roof measures, and prolonged immersion in water of the fine fraction of the High Hazels shale did not reveal any increase in limit values. Ultrasonic disaggregation of the same rock resulted in a small increase in liquid limit (L.L. = 35, P.L. = 21) but it was the Brooch seatearth (L.L. = 72, P.L. = 31) which implied that there may also be compositional differences between the rocks with high breakdown capacities and the more stable types, (see also Stafford tonstein (Table 2.7) for extreme type). It will be recalled that it is the Brooch seatearth that exhibits major breakdown, even when air breakage is eliminated by testing in vacuo (Table 2.5) - it is also the Brooch seatearth which on Figure 2.3 has a high mixed-layer clay content.

Semi-quantitative ratios of quartz to kaolinite-chlorite to mica for the samples used in the slaking tests are also illustrated in Figures 2.13 and 2.14. These were obtained from diffractometer traces of smear mount preparations and are areal ratios of the X-ray reflections 4.26 Å: 7 Å: 10 Å. The quartz to clay ratio vs. 10 Å to 7 Å plots (Fig. 2.13) show that low quartz follows the higher breakdown values of the High Hazels and Brooch rocks, but not the Park seatearth. The two samples from South Wales are rich in both mica and quartz. By plotting clay fraction (size) and the 10 Å mica shape factor against breakdown some interesting and meaningful relationships emerge (Fig. 2.14). The 10 Å mica shape factor takes into account the 'tail' and is thus an indication of the mixed-layer content. First of all it can be readily seen that in general breakdown is accompanied by an increase in inter-layering. The High Hazels mica, however, contains an average amount of mixed-layer clay. In contrast to most of the other samples it is exceptionally fine grained (Table 2.6, Figs. 2.13 and 2.14). Now grain size (clay content) and breakdown show a general trend in that the greatest breakdowns occur in the rocks with the higher clay size fractions. The Staffordshire seatearths, although finer grained than the other rocks, excepting the High Hazels, exhibit a greatly increased breakdown. These seatearths show a higher degree of mixed-layering however, which implies that breakdown due to intraparticle swelling is almost certainly superimposed on air breakage.

In the past rather a lot of significance has been placed on porosities, which fall within relatively narrow limits for the present suite of rocks (Table 2.6).[6] This in itself is not surprising because of the diagenetic

[6] It is believed that the effective porosities, for which small samples similar to those of the suction work were used, are more realistic than water absorption values quoted in the literature, and which may be some 10 per cent higher. Benzene under a vacuum maintained for 7 days was used in conjunction with previously de-aired samples in a closed system. The figures quoted are of the same order as those of Beckett et al., (1958) who used mercury injection at 6,000 lb/in^2.

FIGURES 2.13 & 2.14

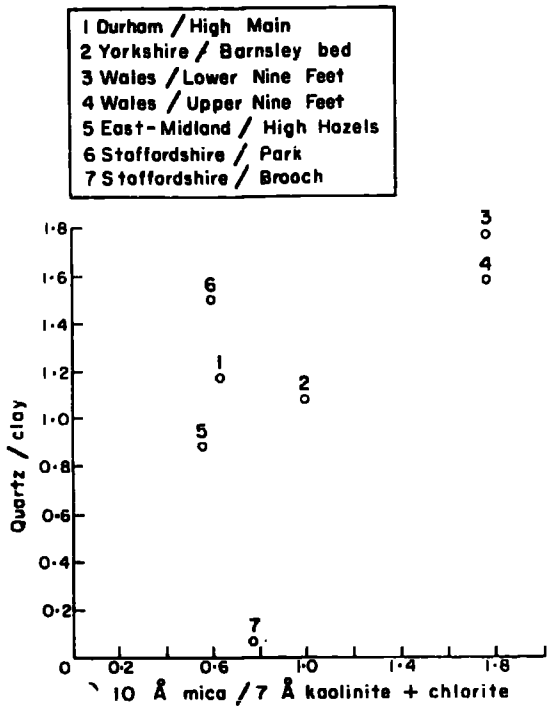

Fig 2·13. Slaking test samples (X-ray data). Ratio of quartz to total clay minerals plotted against ratio of 10 Å mica to 7 Å kaolinite plus minor chlorite.

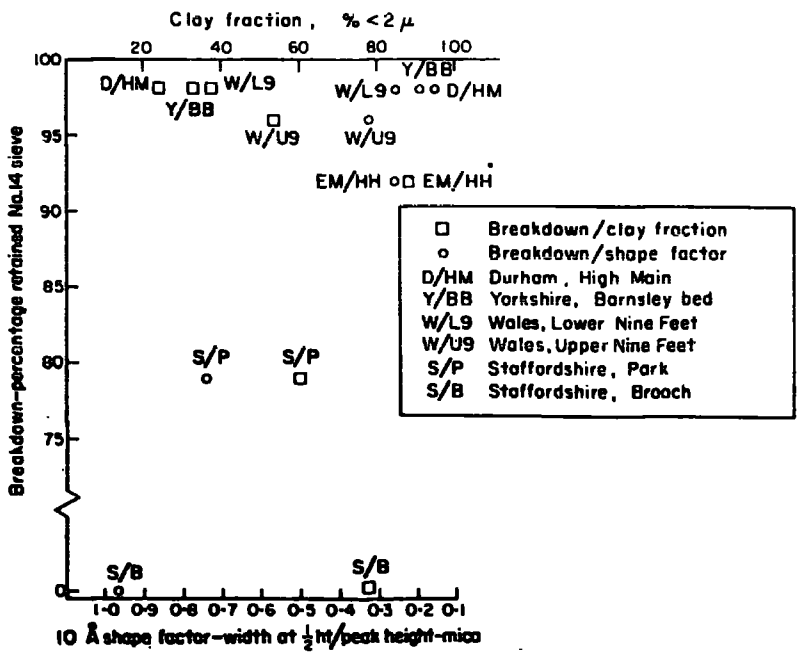

Fig 2·14. Samples considered in the slaking tests. Plot of breakdown vs. clay size fraction and 10 Å 'shape factor' (width at half peak height/peak height).

FIGURE 2.15

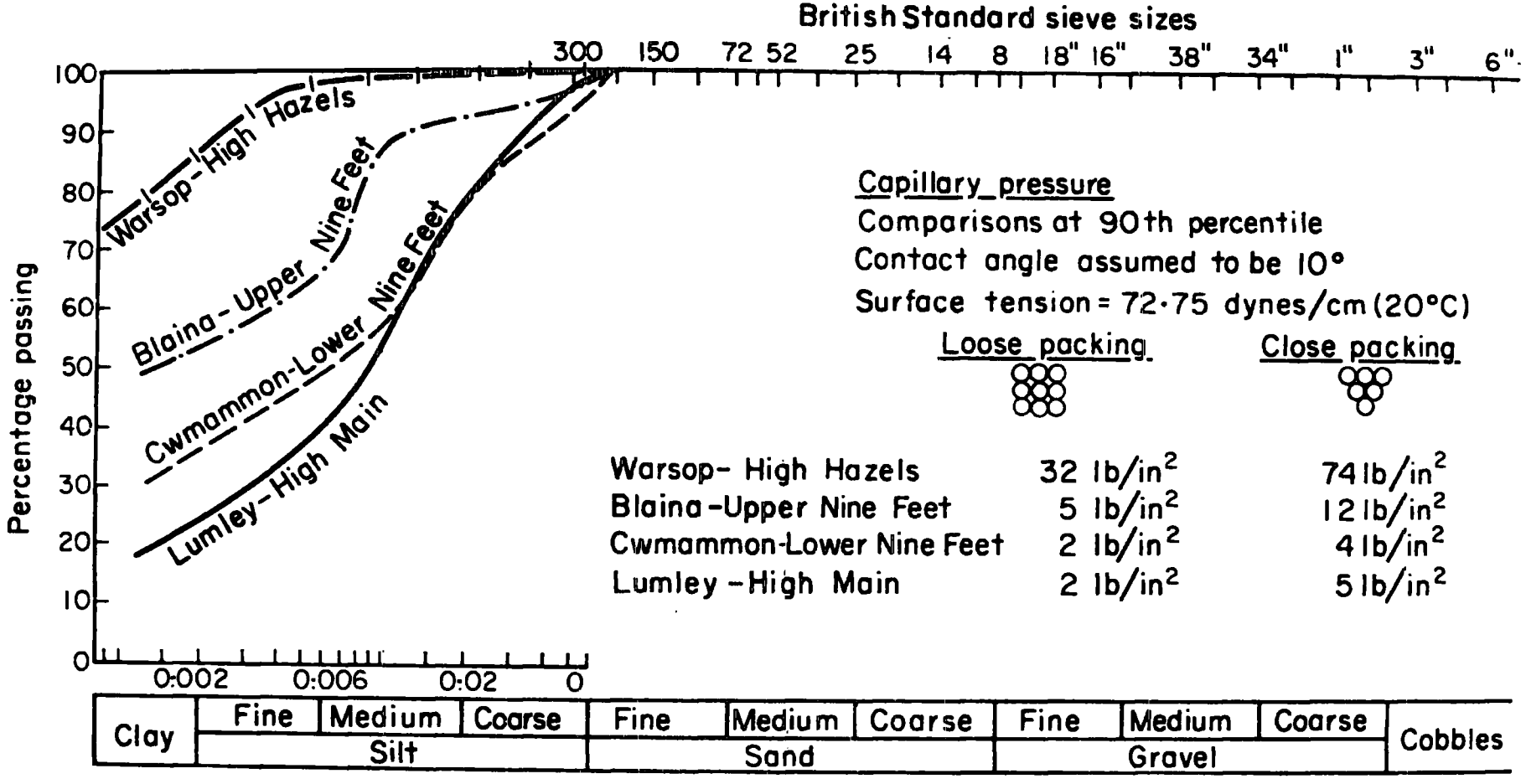

FIGURE 2.15

FIG. 2.15. Simplified illustration of the calculated capillary pressures for the roof rocks referred to. The pore geometry is based on spherical grains at the 90th percentile size.

and tectonic processes to which a sediment may be subjected. The highly preferred orientation of the clay minerals in the High Hazels shale has effectively reduced porosity, but this is matched to varying degrees in the coarser grained rocks by the pore infilling repose of the clay minerals. Porosity is a measure of pore volume, whereas capillarity, which is thought to be a major contributor to the breakdown of Coal Measures shales and mudstones, is governed primarily by pore size (capillary pressure being inversely proportional to pore radius). In other words, the smaller the constituent grains the smaller the intervening voids and hence the greater the capillary pressures. We have already seen that this model is greatly over-simplified as a water uptake illustration, but it serves a useful purpose in demonstrating the points that have been raised. For the roof rocks considered in the thesis, Figure 2.15 gives some idea of the large differences in theoretical capillary pressures that may be involved. That high swelling pressures are involved is relatively easy to prove. The two tonstein-type rocks (Hilton Main and Stafford) were dry cored and then flooded with water in under-size consolidation cells. Free swell measurements were made on one specimen whilst for another specimen swelling was prevented by continuous loading. (i.e. measurement of uplift pressure).

TABLE 2.7

Swelling pressures and free swell data for two air-dried tonsteins

(specimens 25·4 mm diameter)

	Hilton Main tonstein	Stafford tonstein
Air dry moisture content %	1.0	3.9
Clay size fraction,% (ultrasonic disaggregation)	77	84
Liquid Limit	41	106
Plastic Limit	28	48
Free swell, %	0.7	52.8
Swelling pressure, lb/in^2	1.1	1343.0

From the results given on Table 2.7 it is again very clear that for these two rocks of diagenetic origin, with one containing dominantly 'inert' minerals and the other about 25 per cent montmorillonite, it is the latter which generates considerable swelling pressures when exposed to water. The importance of expandable clay minerals in water/clay-rock relationships is clearly demonstrated by this simple experiment.

Capillary pressure is proportional to surface tension so the reduced breakdowns experienced with organic liquids (Table 2.5) could be due to reduced capillarity, because the surface tensions are considerably lower than that of water, rather than to a reduction in ionic dispersion because of lower dielectric constants as previously has been claimed. It is also worth noting that electrolytes have been added in such quantities in the breakdown tests (Badger et al., 1956) that surface tensions are also effected. Nakano's (1967) hydrogen bonding theory is based principally on the behaviour of the Japanese mudstones in organic liquids. His results show that the highest breakdowns occur in organic liquids that are soluble in water. His subsequent geochemical considerations strongly favour hydrogen bonding between the adsorbed water with the respective organic molecules. Unfortunately, no mention is made regarding the nature of the montmorillonite or the inter-layer cations, so once again the possibility of intraparticle reactions cannot totally be ruled out. Nakano's interesting contribution, however, does advance yet another reason for seriously questioning the relevance of dielectric constant in the scheme of inter-particle dispersion.

It is reasonable to suppose that the clay minerals in argillaceous rocks, which may have been excavated from a few thousand feet underground, must once more attain equilibrium in what may be an entirely new chemical environment. Swelling and perhaps re-orientation of minerals can be

attributed to the polarizability of the cations, and a high anion exchange in the new environment may well aid ionic dispersion (or repulsion) of the minerals and help facilitate further breakdown. The evidence up to the present suggests that this is a much slower process in the breakdown reaction than the others already discussed. In the Yorkshire Main Tip (Chapter 5), for example, the material of clay grade size ($< 2\mu$) is only 17 per cent in the 50-year-old unburnt material. This is confirmed under the microscope for there is no apparent increase in the percentage of deformed (plastic) grains with the age of the material. Another point is that in the slaking tests less than 4 per cent of the material in the present series (including the Brooch seatearth) was smaller than fine-to-medium-sized sand. It has not therefore, broken down into individual grains. This is explicable in terms of capillarity and intraparticle swelling but not so readily by interparticle swelling. Evidence, such as content of exchangeable cations, has in the past been interpreted in favour of ionic dispersion, but the earlier discussion shows that clay mineralogy could well be responsible.

The Park seatearth may be used to illustrate the significance of the interlayer mineral and dilution by quartz - a reduction in quartz (Fig.2.13) could well bring this rock into the highly unstable Brooch category. In contrast, ionic dispersion is probably more closely related to chemical weathering as it is dependent on chemical changes in the pore solutions. In this respect it is a mechanism that is controlled indirectly by solution and leaching of minerals and may therefore be a very long-term highly variable process. (see Chapter 3).

Finally, in this context, it would seem reasonable to suggest that the swelling laminae and lenses of both marine and non-marine argillaceous rocks (e.g. Mansfield marine shale and non-marine mudstones) can also be partly

explained as a capillary phenomenon. The randomly orientated floc-type ('open') mineral fabric infers increased permeability. Paradoxically, however, in the rocks so far examined, the clay mineralogy of the laminations may often be basically similar, but invariably it is the finer-grained laminations which swell. Hence, the open voids in these laminae are probably restricted in size. It can also be argued that a floc-type random fabric increases the probability of air filled cul-de-sacs (without involving other cements) and consequently increased capillary pressures are a likely outcome.

2.8 Conclusions

Several broad, and perhaps rather obvious conclusions can be drawn on the behaviour of the different lithological groups present in the Coal Measures. The breakdown of sandstones and siltstones is controlled by geological structures such as joints and stratification planes, the resulting debris after a few months of weathering being dominantly greater than cobble size. Further degradation towards component grains usually takes place at a very slow rate because such changes are in part of a chemical nature. Much of this material was used in the past as a building stone and this alone is a guide to its resistance to weathering.

In general, mudstones, shales and seatearths degrade rapidly to a dominantly gravel-sized aggregate, the geological structures playing an important immediate role. A simple behavioural pattern cannot be readily applied even to these rock types because silty mudstones and carbonaceous mudstones are more akin to sandstones in behaviour. Similarly the upper part of many seatearths are quite plastic when exposed underground in response to long-term dispersive action which is related to the aquifer qualities of the coal. Extreme members of the mudstone-shale group are

literally explosive in water when in a desiccated state and this is considered to be a function of capillarity and clay mineralogy. The importance of montmorillonite as a mixed-layer component has been clearly demonstrated from both the suction characteristics and the slaking and swelling test results. Slaking (air breakage) is an intrinsic feature of the disintegration sequence but the importance of void size rather than void volume should be emphasized with respect to the capillary pressures developed. The overall clay mineral assemblage and dilution by other more equant minerals like quartz restricts the part played by intraparticle swelling of mixed-layer illite in the disintegration of some argillaceous rocks. The term intraparticle is used mainly for convenience and it should be recognized that many colloid chemists would not distinguish between internal and external surfaces of clay minerals. A highly preferred orientation, concordant with the stratification (High Hazels shale) does not necessarily lead to reduced breakdown in argillaceous shales (cf. White, 1961). Ionic dispersion (in the classical sense) or possible chemical dissolution concepts due to hydrogen bonding as proposed by Nakano (1967) are believed to be processes which become progressively more important with time (and after initial breakdown has produced a greatly increased surface area).

The depositional environment is clearly important in that it controls the grain size and hence the composition of the accumulating sediment - it is of course the clay mineral fraction which is of importance in the breakdown process. There is a geographical variation in the clay mineralogy of the British Coal Measures, but a variation with rank, which theoretically could well occur, has not been detected (this may be due to the rather preliminary nature of the X-ray results). The incipient 'rank factor' suggested by the slaking characteristics of the more extreme members may also be partly a function of pore geometry and distribution, in which case a more direct relationship with the rank of the associated coal could emerge.

CHAPTER 3

THE MINERALOGICAL AND DEFORMATIONAL CHARACTERISTICS OF A WEATHERED PROFILE DEVELOPED IN COAL MEASURES ROCKS

3.1 Introduction

Having concluded in the last Chapter that physical processes are more important than chemical processes in the immediate breakdown of Coal Measures rocks it is important to consider the influence of long-term weathering on the compositional and mechanical properties of the strata. The surface of a spoil heap is not an ideal setting in which to study the effects of long-term weathering because the heterogeneity of most spoil heaps makes it very difficult to prove conclusively that changes are due to weathering, rather than being an expression of original variations. Re-grading, compositional and physical changes associated with combustion within the heap, and surface erosion are other objections; the run-off channels on most tips are a familiar sight (for example, Yorkshire Main, Chapter 5). In order to circumvent these difficulties it was decided that the effects of long-term weathering could best be studied on an *in situ* section of rocks. Such a study helps to provide basic information on rock and mineral stability, and also the effect of any changes on the physical and mechanical properties. The behavioural pattern helps not only in the understanding of rock breakdown in colliery tips but also in appreciating likely time effects on embankments constructed from sedimentary rock-fill, or, in the more general field of foundation engineering, where materials may range from the unweathered to the fully weathered state.

The site chosen for the investigation was near the village of Wales (Ref. SK 476 821) in the Sheffield-Rotherham area of the East Pennine coalfield. The site is free from glacial drift and it is reasonable to assume that the

FIGURE 3.1

CROSS SECTION THROUGH BOREHOLES

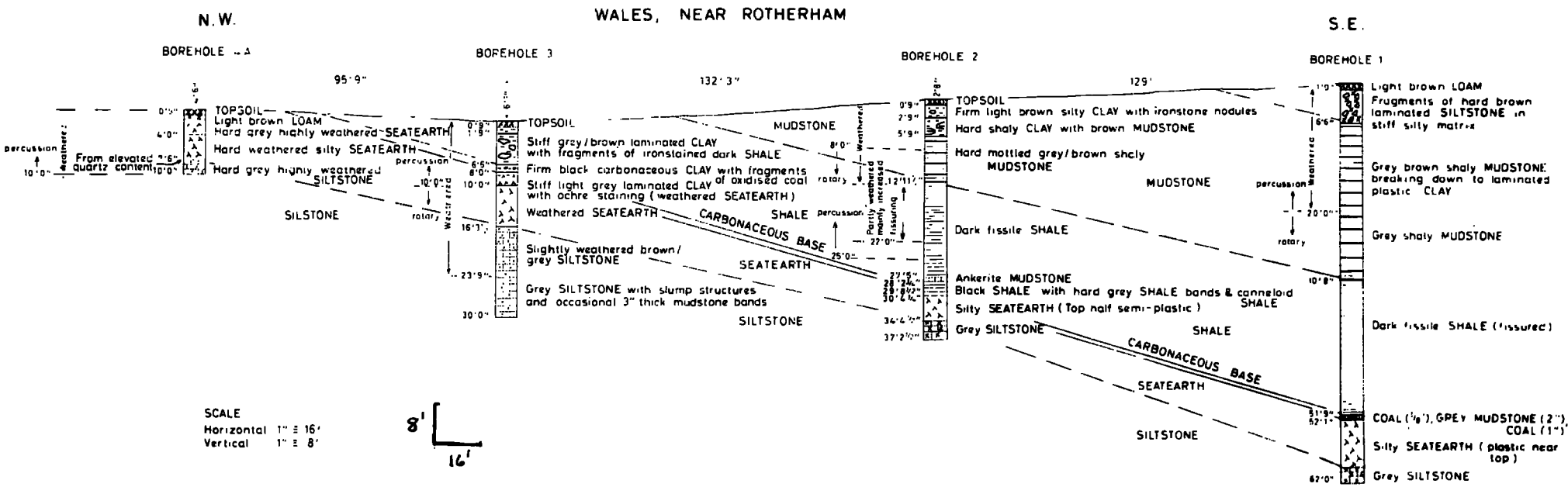

FIGURE 3.1

weathering characteristics have developed in post-glacial times, that is over the last 10,000 years. The rocks exposed at this locality include the Mansfield Marine Band cyclothem for which the mineralogy and geochemistry are known in detail (Curtis, 1967; Spears, 1964; Taylor, 1971). Moreover, the range in lithologies covers a broad spectrum of Coal Measures rocks and includes most of the types encountered in colliery discard.

The samples investigated by the present writer are somewhat limited for mineralogical and geochemical purposes because they comprised specimens subsequently tested in the laboratory. The fragmental nature of the rocks imposed a limitation on the number of such samples. Another sampling scheme was adopted for mineralogical and chemical investigations carried out elsewhere, and brief reference will be made to these latter results when applicable.

The original core descriptions with respect to lithology and degree of weathering has largely been adhered to, the only modification of a minor nature was made when the samples were unsealed in the laboratory.

3.2 Geological sequence and sampling

The succession is exposed in a disused railway cutting (see Edwards and Stubblefield, 1947) and consists of siltstone, seatearth, coal/coaly shale, dark shale, mudstone and siltstone in upwards sequence. Based on the dip and strike of the exposures in the railway cutting four composite boreholes were put down in the adjacent field. The boreholes were drilled in the direction of dip, the relative positions and sequence encountered being shown on Figure 3.1. Siting the boreholes in this way means that the same rock type can be compared at different depths below ground level and therefore at different levels of weathering. Composite boreholes were drilled so as to obtain relatively undisturbed 4 in diameter percussion samples (U4's) of the near surface materials and good quality rotary (air-flush) 3 in diameter cores of the deeper, less weathered, material. Samples were sealed in the field for subsequent physical and mechanical testing, using wax for the U4's and

TABLE 3.1

Modified RQD and Core Recovery

Grey Mudstone			
Bh 2 (8'0 - 12'11½)	RQD = 60	58%	Recovery = 60
Bh 1(20'0 - 30'8)	RQD = 56		Recovery = 98
Dark Shale			
Bh 2 (12'11½ -27'5)	RQD = 43	56%	Recovery = 96
Bh 1 (30'8 - 51'9)	RQD = 69		Recovery = 78
Seatearth			
Bh 3 (10'0 - 16'3½)	RQD = 94	86%	Recovery = 94
Bh 2 (30' 4.3/4 -34'4½)	RQD = 78	76%	Recovery = 78
Bh 1 (52'1 - 59'8)	RQD = 55*		Recovery = 99
Siltstone			
Bh 3 (16'3½ - 30'0)	RQD = 82	89%	Recovery =100
Bh 2 (34'4½ - 37'2½)	RQD = 95	92%	Recovery = 95
Bh 1 (59'8 - 62'0)	RQD =100		Recovery =100

* core jammed in the barrel; mod. RQD too low.

lowerite for the rotary cores.

Boreholes 1 to 3 have been correlated using the thin coal as a datum plane. It must be appreciated that with the exception of the coal junctions, all other boundaries are gradational. Hence there is an upwards passage from siltstone to seatearth, and from shale to mudstone culminating in the upper siltstone.

The rotary core recoveries (Table 3.1) included fragmental material and for this reason a modified 'rock quality designation' (RQD) has been calculated. Intactness, which is implicit in the RQD principle as applied to harder rocks (Deere et al, 1967) is not really applicable to the fissile and fissured shales and mudstones encountered in the investigation. Nevertheless, coherent sticks of core (fissured and/or semi-plastic in parts) were measured on the 4 in (RQD) criterion and expressed as a modified RQD (Table 3.1). On this basis an engineering 'rock quality' sequence emerges which later in the chapter will be shown to be generally in accord with the order of strength:

Lower siltstone > seatearth ≫ mudstone ≥ shale

3.3 Visual weathering

The visual weathering effects seen in the borehole samples are documented on Figure 3.1, and in detail they are as follows:

In borehole 1 below the 1 ft of topsoil there is a silty clay matrix with lithorelicts of original rock down to a depth of 6.5 ft. The underlying 0.75 ft is a laminated plastic silt, identified as the breakdown product of a mudstone. At a depth of 8 ft mudstone is clearly recognizable, although still visually weathered. With depth from this level the degree of weathering decreases, but with fissure development and iron oxidation adjacent to the fissures. Visual weathering is still present to a depth of 20 ft.

Plate 3.1 Selection of weathered and unweathered triaxial specimens after failure.

a) Upper siltstone, borehole 1, 2.75-3.00 feet; fragments in weathered matrix.

b) and c) Partly weathered mudstone, borehole 1, 7.75-8.00 feet

d) Non-weathered dark shale, borehole 2, 22.50-23.00 feet; illustration of fissility - sample coated with promex to retain core for photography.

e) Non-weathered dark shale, borehole 2, 22.00-25.00 feet section; partly broken to show fragmental nature and siderite nodules near top of core.

f) Hard, weathered seatearth, borehole 4, 3.25-3.50 feet; carbonaceous near base.

g) and h) Hard, partly weathered seatearth, gradational with siltstone, borehole 3, 14.50-16.25 feet section; heavily jointed and stratified.

i) and j) Weathered lower silstone, borehole 3, 16.00-23.75 feet section; heavily jointed with slump structures; powdery consistency of more weathered parts seen in core j.

k) and l) Non-weathered lower siltstone, borehole 2, 34.00-37.00 feet specimen 1 showing fissility.

PLATE 3.1

40 lb/in² Confining Pressure a

20 /in² Confining Pressure b

40 lb/in² Confining Pressure c

d

e

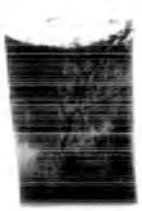

f

g

h

i

j

k

l

FIGURE 3.2

FIGURE 3.2

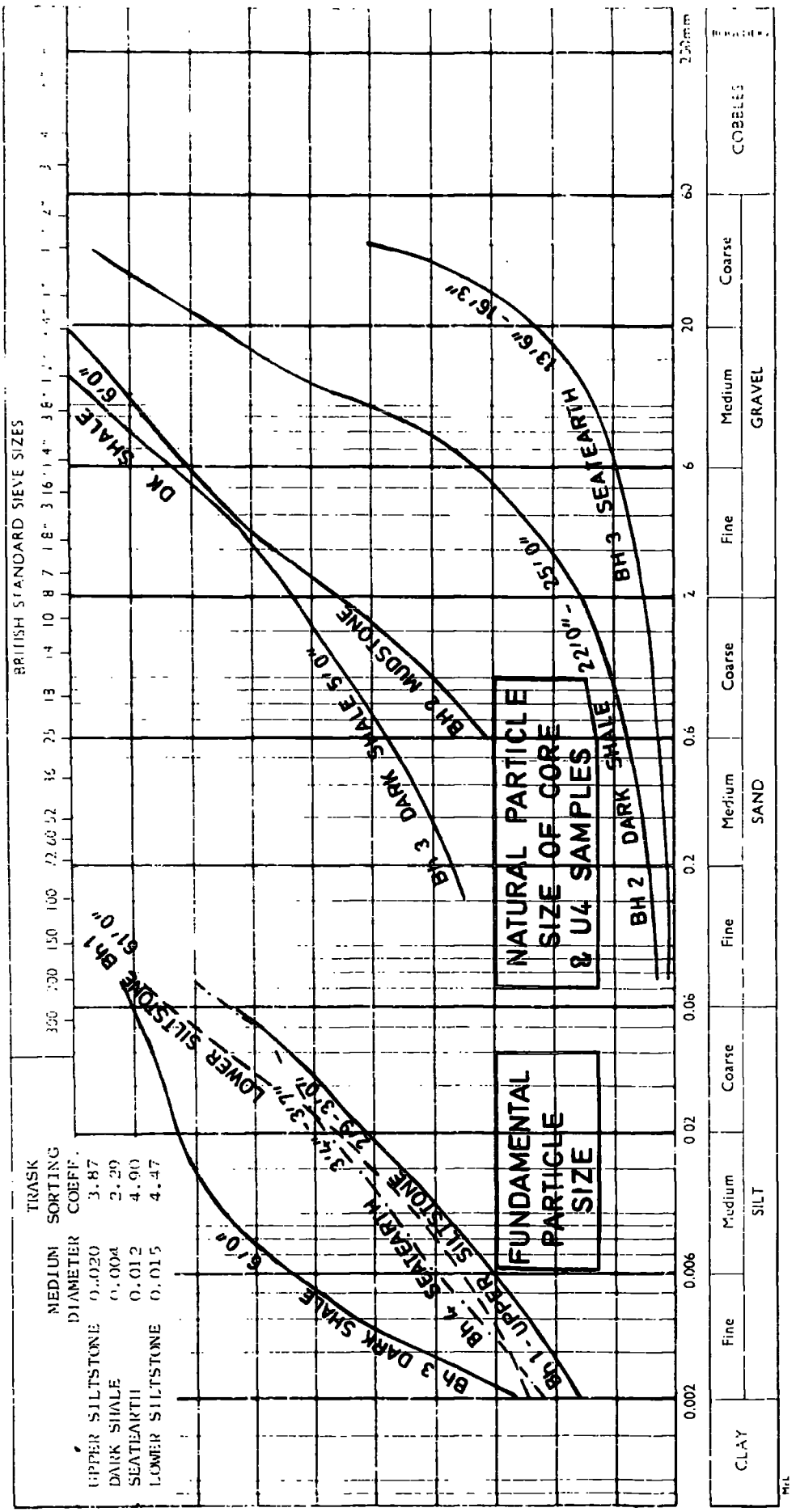

Borehole 2 is very similar to borehole 1, with clayey silt containing rock fragments down to a depth of 5.75 ft. The fragments consist of mudstone and most significantly, ironstone nodules. Mudstone is recognizable below this and down to about 13 ft it is partly converted into fine-grained material. Fissuring and oxidation was recorded to 22 ft below ground level.

In borehole 3 the clayey silt with lithorelicts extends to a depth of 6.5 ft. Based on the presence of ironstained shale fragments the original rock was thought to have been the dark shale horizon. The underlying coal has been partly oxidised to a 1.5 ft thick layer of black carbonaceous clay with small coal fragments. The top of the underlying seatearth is semi-plastic as it is in boreholes 1 and 2. The siltstone shows some evidence of weathering down to a depth of 24 ft. Borehole 4 is again similar in that clay-silt development has taken place to a depth of 7.5 ft. The remainder of this borehole was bored in weathered siltstone. A selection of post-failure triaxial test specimens are shown on Plate 3.1 in order to demonstrate some of points considered above, and also as a general illustration of weathering styles and of small-scale structures present in some rock types.

The general conclusions which can be drawn from this evidence can be enumerated as follows:

1) The rocks have disintegrated to a clay or silt containing fragments down to a depth of just over 6 ft. Certainly, breakdown into fundamental particles is not marked near the base of this zone. The content of fine and medium gravel sizes is appreciable in this material when compared with the fundamental distribution (Fig. 3.2).

2) The fragments present are of original rock and include nodules of siderite. The resistance of near-surface siderite to protracted weathering is an indication that chemical alteration of the minerals may not be an important mechanism in the overall breakdown process.

TABLE 3.2

Quartz and clay minerals

		Quartz	Kaolinite, plus minor chlorite	Illite	Chlorite	Quartz / Clay	7Å / 10Å	10Å Shape factor	7Å shape factor (Boehmite)
ber tstone	Bh.1(1.5-3.0)	37.0	35.5	27.5	5.0	0.62	1.28	0.076	2.3
lstone	Bh.2(6.0-6.25)	17.0	39.5	43.5	5-10	0.23	0.90	0.043	2.3
stone	Bh.1(6.5-8.00)	29.5	38.5	32.0	5.0	0.48	1.21	0.050	2.3
lstone	Bh.1(24.0)	17.5	47.5	35.0	5.0	0.25	1.37	0.073	2.4
Shale	Bh.3(5.0-6.5)	23.5	38.0	38.5	5.0	0.33	0.99	0.179	2.7
"	Bh.3(6.0-6.5)	23.5	38.0	38.5	5.0	0.33	1.00	0.160	2.3
"	Bh.2(22.0-23.0)	15.5	37.0	47.5	1-5.0	0.20	0.78	0.117	2.2
"	Bh.2(23.0-25.0)	19.0	31.5	49.5	1-5.0	0.24	0.64	0.141	2.3
"	Bh.1(32.0-34.0)	15.0	42.0	43.0	5.0	0.21	0.98	0.100	2.7
"	Bh.1(40.0-40.5)	15.0	35.0	50.0	5.0	0.22	0.70	0.111	2.3
"	Bh.1(41.5-42.0)	15.0	34.0	51.0	5.0	0.20	0.67	0.129	2.7
tearth	Bh.4(3.3-3.6)	48.5	30.0	21.5	0	0.94	1.38	0.535	2.0
"	Bh.3(14.5-15.0)	41.0	35.0	24.0	0	0.71	1.43	0.827	2.0
"	Bh.3(15.75-16.25)	40.0	32.0	28.0	0	0.76	1.13	0.666	2.0
"	Bh.2(30.0-34.0)	37.0	40.0	23.0	0	0.60	1.75	0.511	2.7
"	Bh.1(52.0-54.7)	34.0	46.5	19.5	0	0.51	2.38	0.350	3.0
er tstone	Bh.3(16.0-23.75)	52.0	30.0	18.0	0	1.06	1.69	0.391	2.0
	Bh.2(34.3-37.1)	44.0	34.5	21.5	0	0.88	1.60	0.150	2.0
	Bh.1(59.0-62.0)	55.5	32.0	12.5	0	1.14	2.50	0.077	1.8

TABLE 3.3

CHEMICAL ANALYSES

	UPPER SILTSTONE Bh1, 2.75-3.0	MUDSTONE Bh2, 6.0-6.25	MUDSTONE Bh1, 6.5-8.0
QUARTZ	37.0	17.0	29.5
S_iO_2 total	59.01	55.14	55.98
SiO_2 Comb.	22.01	38.14	26.48
Al_2O_3	19.59	21.44	19.63
Fe_2O_3	8.26	6.02	8.78
MgO	1.01	1.71	1.66
CaO	0.21	0.22	0.16
Na_2O	0.50	0.43	0.57
K_2O	2.96	3.70	3.14
TiO_2	1.07	0.96	1.10
MnO	0.15	0.08	0.23
S	0.00	0.00	0.03
P_2O_5	0.10	0.10	0.16
CO_2	0.16	0.45	0.36
C	1.53	1.87	2.82
H_2O+	5.94	7.88	5.96
TOTAL	100.49	100.00	100.58

	MUDSTONE Bh1, 24.0	DK. SHALE Bh3,6.0-6.5	DK.SHALE Bh2,22.0-23.0	DK. SHALE Bh2, 23.0-25.0	DK. SHALE Bh1, 32.0-34.0	DK.SHALE Bh1,40.0-40.5
QUARTZ	17.5	23.5	15.5	19.0	15.0	15.0
SiO_2 total	56.91	54.10	51.13	55.51	49.50	50.19
SiO_2 Comb.	39.41	38.60	35.68	36.51	34.50	35.19
Al_2O_3	23.35	20.77	20.19	22.53	19.55	22.55
Fe_2O_3	6.54	9.35	8.09	5.08	9.41	7.06
MgO	2.08	1.00	1.77	1.58	2.06	1.61
CaO	0.23	0.26	0.33	0.91	0.57	0.18
Na_2O	0.31	0.30	0.20	0.38	0.46	0.39
K_2O	4.00	2.81	3.32	3.75	3.93	3.64
TiO_2	1.05	1.05	0.90	0.86	0.89	0.80
MnO	0.09	0.11	0.15	0.07	0.29	0.11
S	0.06	0.19	2.09	0.24	0.08	4.62
P_2O_5	0.13	0.11	0.12	0.70	0.14	0.08
CO_2	0.49	1.08	2.51	0.41	3.10	0.39
C	2.13	1.67	2.61	2.60	2.40	2.21
H_2O+	3.13	7.20	6.53	6.00	7.63	6.18
TOTAL	100.5	100.00	99.99.	100.62	100.01	100.00

	DK.SHALE Bh1,41.5-42.0	SEATEARTH Bh4,3.3-3.6	SEATEARTH Bh3,14.5-15.0	SEATEARTH Bh3,15.75-16.25	SEATEARTH Bh2,30.0-34.0	SEATEARTH Bh1,52.0-54.7
QUARTZ	15.0	48.5	41.0	40.0	37.0	25.0
SiO_2 total	51.31	61.58	58.44	60.99	63.80	52.33
SiO_2 Comb.	36.31	13.08	17.44	20.99	26.30	27.33
Al_2O_3	18.60	21.03	16.47	17.23	18.17	21.61
Fe_2O_3	8.70	3.68	8.86	8.30	2.52	10.14
MgO	1.87	0.79	0.57	1.00	0.91	1.85
CaO	0.47	0.16	0.89	0.97	0.31	0.36
Na_2O	0.36	0.26	0.29	0.33	0.38	0.44
K_2O	3.29	2.08	1.85	1.97	2.26	3.62
TiO_2	0.86	1.10	0.87	0.91	1.29	0.93
MnO	0.15	0.01	0.06	0.11	0.02	0.16
S	4.66	0.00	0.25	0.03	1.08	0.31
P_2O_5	0.15	0.04	0.66	0.46	0.14	0.15
CO_2	0.72	0.00	0.52	0.89	0.02	0.35
C	2.11	3.07	3.59	3.83	2.00	1.96
H_2O+	7.20	6.20	6.17	4.97	7.21	6.81
TOTAL	100.45	100.00	100.49	100.99	100.11	101.02

	LOWER SILTSTONE Bh3, 16.0-23.75	LOWER SILTSTONE Bh2, 34.3-37.1	LOWER SILTSTONE Bh1,59.0- 62.0
QUARTZ	52.0	44.0	55.0
SiO_2 total	61.14	65.60	65.91
SiO_2 Comb.	19.14	21.60	10.41
Al_2O_3	19.64	21.83	19.74
Fe_2O_3	7.02	2.73	3.32
MgO	0.61	0.77	0.88
CaO	0.16	0.16	0.23
Na_2O	0.29	0.31	0.28
K_2O	2.17	2.00	2.03
TiO_2	1.06	1.05	0.98
MnO	0.07	0.02	0.04
S	0.19	0.04	0.05
P_2O_5	0.10	0.02	0.02
Co_2	0.08	0.01	0.06
C	2.18	2.17	2.43
H_2O+	5.95	3.18	3.94
TOTAL	100.00	99.89	99.91

TABLE 3.4

OXIDE RATIOS AND SELECTED CHEMICAL DATA

	Upper Siltstone Bh1, 2.75-3.0	Mudstone Bh2, 6.0-6.25	Mudstone Bh1, 6.5-8.0
$\frac{Al_2O_3}{Comb.SiO_2}$	0.89	0.56	0.74
$\frac{Fe_2O_3}{Al_2O_3}$	0.42	0.28	0.45
$\frac{MgO}{Al_2O_3}$	0.05	0.08	0.08
$\frac{CaO}{Al_2O_3}$	0.01	0.01	0.01
$\frac{Na_2O}{Al_2O_3}$	0.03	0.02	0.03
$\frac{Na_2O}{K_2O}$	0.12	0.12	0.18
$\frac{K_2O}{Al_2O_3}$	0.15	0.17	0.16
TiO_2	1.07	0.96	1.10
S	0.00	0.00	0.03
C	1.53	1.87	2.82

	MUDSTONE Bh1,24.0	DK.SHALE Bh3, 6.0-6.5	DK.SHALE Bh2,22.0-23.0	DK.SHALE Bh2,23.0-25.0	DK.SHALE Bh1, 32-34	DK.SHALE Bh1, 40-40.5
$\frac{Al_2O_3}{Comb.SiO_2}$	0.59	0.53	0.56	0.61	0.56	0.64
$\frac{Fe_2O_3}{Al_2O_3}$	0.28	0.45	0.40	0.22	0.48	0.31
$\frac{MgO}{Al_2O_3}$	0.08	0.04	0.08	0.07	0.10	0.07
$\frac{CaO}{Al_2O_3}$	0.01	0.01	0.01	0.04	0.02	0.01
$\frac{Na_2O}{Al_2O_3}$	0.01	0.01	0.01	0.01	0.02	0.01
$\frac{Na_2O}{K_2O}$	0.07	0.10	0.06	0.10	0.11	0.10
$\frac{K_2O}{Al_2O_3}$	0.17	0.14	0.16	0.17	0.20	0.20
TiO_2	1.05	1.05	0.90	0.86	0.89	0.80
S	0.06	0.19	2.09	0.24	0.08	4.62
C	2.13	1.67	2.61	2.60	2.40	2.21

	DK. SHALE Bh1, 41.5-42.0	SEATEARTH Bh4, 3.3-3.6	SEATEARTH Bh3, 14.5-15.0	SEATEARTH Bh3, 15.75-16.25	SEATEARTH Bh2, 30.0-34.0	SEATEARTH Bh1, 52-54.7
$\frac{Al_2O_3}{Comb.SiO_2}$	0.51	1.60	0.94	0.82	0.67	0.79
$\frac{Fe_2O_3}{Al_2O_3}$	0.46	0.17	0.53	0.48	0.13	0.46
$\frac{MgO}{Al_2O_3}$	0.10	0.03	0.03	0.06	0.05	0.08
$\frac{CaO}{Al_2O_3}$	0.02	0.01	0.05	0.06	0.01	0.01
$\frac{Na_2O}{Al_2O_3}$	0.01	0.01	0.01	0.01	0.01	0.02
$\frac{Na_2O}{K_2O}$	0.10	0.12	0.15	0.16	0.16	0.12
$\frac{K_2O}{Al_2O_3}$	0.18	0.10	0.11	0.11	0.12	0.17
TiO_2	0.86	1.10	0.87	0.91	1.29	0.93
S	4.66	0.00	0.25	0.03	1.08	0.31
C	2.11	3.07	3.59	3.83	2.00	1.96

	LOWER SILTSTONE Bh3, 16.0-23.75	LOWER SILTSTONE Bh2, 34.3-37.1	LOWER SILTSTONE Bh1, 59.0-62.0
$\frac{Al_2O_3}{\text{Comb. } S_iO_2}$	1.02	1.01	1.89
$\frac{Fe_2O_3}{Al_2O_3}$	0.35	0.12	0.16
$\frac{MgO}{Al_2O_3}$	0.03	0.03	0.04
$\frac{CaO}{Al_2O_3}$	0.01	0.01	0.01
$\frac{Na_2O}{Al_2O_3}$	0.01	0.01	0.01
$\frac{Na_2O}{K_2O}$	0.13	0.15	0.13
$\frac{K_2O}{Al_2O_3}$	0.11	0.09	0.10
TiO_2	1.06	1.05	0.98
S	0.19	0.04	0.05
C	2.18	2.17	2.43

3) Below the 6 ft level and down to a depth of around 20 ft fissuring is intense. These fractures result from the opening of bedding planes and joints. The ironstaining associated with the discontinuities is an indication of water movement (fissure-flow).

3.4 Mineralogy and chemistry

The chemical changes most likely to take place during weathering can be predicted because they will mainly be related to the non-detrital minerals (pyrite and siderite) which grew in the depositional environment. The latter environment was chemically very different from that existing during weathering. The detrital (transported) minerals derived from a land-source during the Carboniferous will have achieved some stability towards weathering. In this context it is likely that the Carboniferous weathering environment was more extreme than the temperate conditions existing today. For the rocks under consideration a complication arises because any weathering changes will be superimposed on the natural chemical and mineralogical variations that can be expected in gradational cyclothemic lithologies. However, it is convenient to consider the minerals under the two groups, namely detrital and non-detrital.

The principal method used for mineral identification was X-ray diffraction (Appendix 2), supplemented by thin section observations under the microscope. Both quartz and clay minerals were determined quantitatively from smear mounts, using boehmite as an internal standard (Griffin, 1954). The quartz determinations for argillaceous strata agree exceedingly well with values obtained by the precise (though protracted) method of Trostel and Wynne (1940) - see Brancepeth tip, Chapter 4. Repeatable kaolinite (6.18Å boehmite to 7Å reflections) were obtained from the empirical standard curves for Cu Kα radiation (Appendix 2). With the mica reflections however, difficulty was experienced because the crystallinity of the mica in the standards (Oligocene

illite from Le Puy-en Velay, France) did not match that of the more highly crystalline mica of the mudstone and upper siltstone units. For this reason mica was determined indirectly using the calculated kaolinite/minor chlorite content and the ratio of the 7Å (kaolinite plus minor chlorite) to the 10Å (mica) peak areas which were measured with a polar planimeter. The quartz to clay mineral ratios are given on Table 3.2 with the individual 7Å and 10Å mineral quantities being normalized so that quartz, kaolinite plus minor chlorite and mica total 100 per cent. The minor chlorite contribution was estimated approximately from the minor chlorite (penninite) which is included in the standards used for quantitative X-ray work.

Major element oxides and sulphur were found by X-ray fluorescence (Philips PW 1212 automatic spectrograph), the results being processed by IBM 360/67 computer (Appendix 1). Carbon dioxide was determined by decomposition with orthophosphoric acid and absorption by Sofnalite; organic carbon by low-grade oxidation (375°C) and H_2O^+ by Penfield tube.

3.5 Detrital minerals

The chemical analyses (Table 3.4 can be rationalized in the light of what is known about this type of sedimentary sequence (see for example Nicholls and Loring, 1960). The total SiO_2 content is apportioned to quartz and to the silicon combined in the silicate minerals. The latter are dominantly clay minerals, although in the lower siltstone, seatearth and upper siltstone units feldspars make up less than about 5 per cent by weight of the total components. Like combined silica, Al_2O_3, Na_2O and K_2O are attributed mainly to the clay minerals, with potassium being a useful measure of mica abundance. Both ferric and ferrous iron, CaO, MgO and MnO are also found in clay minerals. The chlorite for example is an Fe-Mg type, namely penninite (Table 3.6). However, part of the iron

reported as Fe_2O_3 is combined with S to form pyrite (FeS_2). Similarly, part may be attributed to siderite ($FeCO_3$), or secondary iron oxides such as limonite (goethite) or lepidocrocite which are the end products of low temperature oxidation of Fe-rich minerals. Sulphates such as jarosite are formed during weathering so a small amount of iron, potassium and possibly sodium could be combined with S as sulphate. In the Wales strata only one sample exhibited X-ray reflections which may possibly be attributed to sulphates. It is thus reasonable to conclude that sulphates are present in very small amounts indeed. In the dark grey marine shale some FeO, MnO MgO and CaO is present as infrequent bands of the complex carbonate, ankerite (Fig.3.1). TiO_2 is present mainly as rutile needles, although a very small amount may substitute within the clay mineral lattices. The P_2O_5 is mainly present in calcium phosphate but an additional source of P_2O_5 and sulphur may well be organic matter.

In conjunction with the rather complex element apportionment we are also faced with variations in quartz and clay minerals due to lithological changes. For this reason two chemical ratios are a useful measure of clay minerals. A high alumina/combined SiO_2 ratio (Table 3.4) is indicative of abundant kaolinite (mineral ratio 0.833) and a low ratio is symptomatic of abundant mica (ratio 0.291 to 0.298 for muscovite and illite - Brown, 1961, p.231). Most of the potassium is contained by the clay minerals, and by illite in particular. The K_2O/Al_2O_3 ratio is therefore a measure of the illite content, and hence indirectly of the kaolinite content since illite and kaolinite are the two main clay minerals present (Table 3.2). Bearing in mind the above points the detrital and non-detrital minerals can now be considered under their appropriate headings.

Figure 3.3

Showing profile of quartz and clay minerals.

			7/10Å	QUARTZ TO CLAY	Al_2O_3 TO SiO_2	K_2O TO Al_2O_3	10Å SHAPE
SILTSTONE	WEATHERED	BH1 (1·5-3·0)	1·28	0·62	0·89	0·15	0·076
MUDSTONE	WEATHERED	1 (6·5-8·0)	1·21	0·48	0·56	0·17	0·050
MUDSTONE		1 (24·0)	1·37	0·25	0·59	0·17	0·073
MUDSTONE	WEATHERED	2 (6·0-6·25)	0·90	0·23	0·56	0·17	0·043
DK. SHALE		1 (32·0-34·0)	0·98	0·21	0·56	0·20	0·100
DK. SHALE		1 (40·0-40·5)	0·70	0·22	0·64	0·20	0·111
DK. SHALE		1 (41·5-42·0)	0·67	0·20	0·51	0·18	0·129
DK. SHALE		2 (22·0-23·0)	0·78	0·20	0·56	0·16	0·117
DK. SHALE		2 (23·0-25·0)	0·64	0·24	0·61	0·17	0·141
DK. SHALE	WEATHERED	3 (5·0-6·5)	0·99	0·33			0·174
DK. SHALE	WEATHERED	3 (6·0-6·5)	0·99	0·33	0·53	0·14	0·160
SEATEARTH		1 (52·0-54·7)	2·38	0·51	0·79	0·17	0·350
SEATEARTH		2 (30·4-34·0)	1·75	0·60	0·67	0·12	0·511
SEATEARTH	WEATHERED	4 (3·3-3·6)	1·38	0·94	1·60	0·10	0·535
SEATEARTH	WEATHERED	3 (14·5-15·0)	1·43	0·71	0·94	0·11	0·827
SEATEARTH	WEATHERED	3 (15·75-16·25)	1·13	0·76	0·82	0·11	0·666
SILTSTONE		2 (34·3-37·1)	1·60	0·88	1·01	0·09	0·150
SILTSTONE		1 (59·0-62·0)	2·50	1·14	1·89	0·10	0·077
SILTSTONE	WEATHERED	3 (16·0-23·75)	1·69	1·06	1·02	0·11	0·391

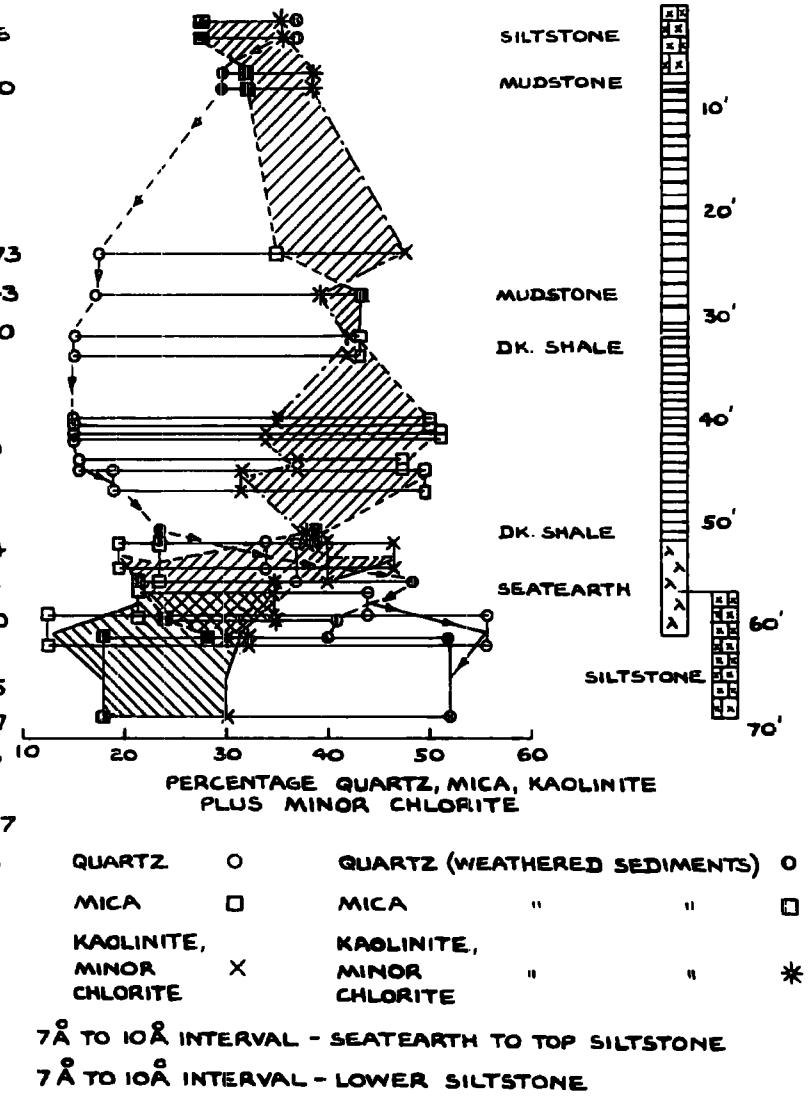

FIGURE 3.3

Using borehole 1 as a control and the coal-coaly shale at the bottom of the marine band as a datum the quartz and clay minerals profiles have been plotted in their stratigraphical positions on Figure 3.3.

The profiles are well defined with the weathered equivalents falling into the overall pattern. In an acid environment ($pH < 5$) it could be expected that the most stable clay mineral (kaolinite) should concentrate relative to the other clay minerals in the weathered zone (Jackson, 1964). In fact the quartz and clay mineral changes appear to be systematic with quartz increasing sharply in the upper part of the mudstone horizon through to the upper siltstone. Quartz increases towards the base of the marine strata showing a steep rise with some fluctuation, through the seatearth and siltstone beds. Dominant mica in the middle part of the marine band is consistent with other Mansfield sections (Taylor 1971) and even the fall in mica in the basal (though weathered) dark shales of Borehole 3 is in line with the previous work (Firth Vickers borehole, Taylor, 1971, Fig. 4). A marked change in the ratio of mica to kaolinite occurs in the seatearth and gradational siltstone beds with the relative mica percentage falling below 28. The somewhat erratic differences between one sample and another are almost certainly due to a) difficulty in placing these samples in an absolute stratigraphical position, and b) sampling incompatibilities with respect to the lithological divisions within seatearths (see Moore, 1968).

The alumina/combined silica ratio (Table 3.4, Fig. 3.3) generally bears out the increase in kaolinite relative to mica in the seatearths and siltstones. The abnormally high values for the rocks with high quartz contents are due to very small errors in free silica determinations. The quantitative curves were designed primarily for colliery spoil of lower quartz content and hence extrapolation of the quartz curve was necessary for quartz values in excess of 30 per cent. Since the distribution of quartz and clay minerals reveals little in the way of weathering evidence it is

pertinent to question whether any conclusions can be drawn from the individual clay mineral groups.

3.6 Micaceous minerals

The term illite has been used as a matter of convenience when describing the wide range of 10Å 'micaceous' minerals which are present in Coal Measures rocks. A selection of basal reflections of minerals included under this heading are shown on Figure 3.4. Some idea of the difficulties involved in quantitative assessment of these minerals and in their nomenclature can be gained from the latter selection. The reference mineral used in the quantitative determinations lies between C and G.

The shape of the 10Å reflection is indicative of the type of illite present and may conveniently be expressed as the ratio of the width at half peak height to peak height (Figs. 3.4, 3.3; Table 3.2). Using the same 1 kW Philips diffractometer (Cu Kα radiation, Ni filtered, 40 kV, 20 mA, 1° per minute scan) it has previously been shown (Taylor, 1971, Fig. 3) that a low ratio is symptomatic of a well-crystallized mica (Miami muscovite ratio, 0.001), whereas illites with a mixed-layer mineral 'tail' on the low angle side of the basal reflection (Fig. 3.4 samples C and D) have ratios. The Morris illite ratio is 0.134.

In all cases in which it was possible to determine the 060 peak the reflection was always close to 1.50Å thus indicating a dioctahedral type. Using the diagnostic reflections given in Brown, 1961 it is concluded that types A, B and in certain samples, G (Fig. 3.4) are 2M polymorphs, whereas type E (Fig. 3.4) appears to be more closely related to the 1Md polymorph described by Yoder and Eugster (1955). The remaining samples are difficult to classify either due to mixed-layering (e.g. sample C, Fig. 3.4) or, because of orientation effects in smear mount preparation. The Stafford tonstein

FIGURE 3.4

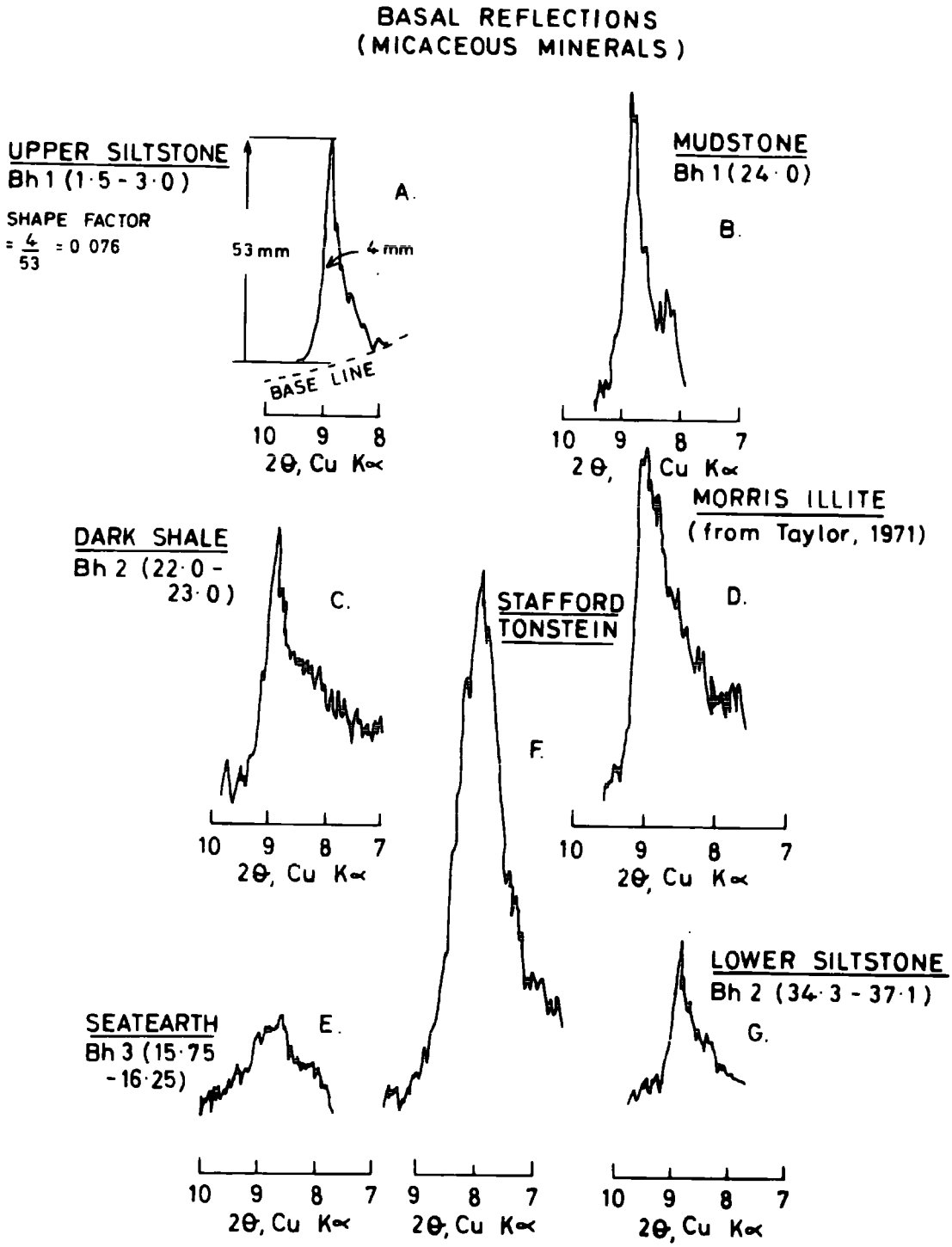
BASAL REFLECTIONS
(MICACEOUS MINERALS)
UPPER SILTSTONE
Bh 1 (1·5 - 3·0)
SHAPE FACTOR
= 4/53 = 0 076
A.
53 mm
4 mm
BASE LINE
10 9 8
2θ, Cu Kα
MUDSTONE
Bh 1 (24·0)
B.
10 9 8 7
2θ, Cu Kα
MORRIS ILLITE
(from Taylor, 1971)
D.
10 9 8 7
2θ, Cu Kα
DARK SHALE
Bh 2 (22·0 - 23·0)
C.
10 9 8 7
2θ, Cu Kα
STAFFORD
TONSTEIN
F.
9 8 7
2θ, Cu Kα
SEATEARTH
Bh 3 (15·75 - 16·25)
E.
10 9 8 7
2θ, Cu Kα
LOWER SILTSTONE
Bh 2 (34·3 - 37·1)
G.
10 9 8 7
2θ, Cu Kα

(sample F, Fig. 3.4) is of course an 11Å mica-montmorillonite. It is interesting to record that some of the seatearth, low amplitude, ragged illite with peak broadening on both the high and low two theta sides, is so disordered that the peak has moved to a lower 2θ position. The micas of the upper siltstone and the mudstones are probably more correctly described as hydromica than muscovite, with that of the marine shales being an illite in the strict sense.

If we now look at these minerals in the light of weathering some very small structural variations can be detected. The shape factors for the 10Å material in the seatearths (Table 3.2, Fig. 3.3) are very high. The K_2O/Al_2O_3 ratio is an expression of the illite content as well as being indicative of leaching of K_2O from the illite lattice during weathering. The ratio (Table 3.4, Fig. 3.3) confirms the semi-quantitative assessment of low illite content in the seatearth and lower siltstone horizons. Moreover, the ratio is marginally lower and the shape factors marginally higher for weathered seatearth samples than for corresponding non-weathered material. From what is known about the genesis of seatearths (Schultz, 1958; Moore, 1968) it is not unreasonable to believe that the illite was originally of poor crystallinity as the shape factors suggest. From the current evidence it is also tentatively suggested that more recent very minor changes have taken place during weathering.

The shape factors for the lower siltstone bed are highly variable and it is more likely that they are representative of inherent variability in coarser grained sediments, rather than being an indicator of mixed-layer mineral breakdown (on a depth basis) during weathering. It is important to note that the average shape factor for the dark shales (0.133) is about four times less than for the seatearths and is very similar to the Morris illite. The increase in crystallinity of the coarser grained mudstones and

upper siltstones is confirmed by a decrease in shape factor. Moreover, although the mica content is falling in the upper measures the K_2O/Al_2O_3 ratio remains relatively high and this again supports the contention of superior crystallinity.

Although the shape factor is relatively higher for the weathered dark shale of borehole 3 and the K_2O/Al_2O_3 ratio is low there is no direct evidence of leaching or variation in crystallinity for the borehole 1 weathered mudstone which is from a similar depth.

3.7 Kaolinite

Kaolinite, which is the most stable of the clay minerals identified is unlikely to exhibit significant changes during weathering. The b/3 disordered form is not uncommon in seatearths according to Mackenzie (1970, p.524), but it is difficult to resolve in multi-component sediments. From the work of Murray and Lyons (1956) the more important differences between disordered and ordered types are:

1) Non-resolution of the 4.12 - 4.17Å doublet in disordered kaolinites.
2) A broad 2.5Å peak replaces the 2.55-2.52-2.49 Å triplet found in ordered forms.
3) A broad 2.3 Å peak replaces the triplet 2.37-2.33-2.28 Å of the ordered form.

In the underclays of South Wales Wilson (1965a) could not resolve the doublet, although the triplets could often be resolved. He concluded that these seatearths were moderately disordered. In the current study the triplets can be resolved in all samples in which the intensities are high enough for resolution. A notable exception is the borehole 1 seatearth (Table 3.2). In certain of the dark shale samples the doublet was not resolved, and again the borehole 1 and 2 seatearth samples are disordered to some degree. Griffin (1954) used the ratio of the width at half peak height (boehmite 6.18 Å) to that of 7Å kaolinite as an order-disorder shape factor.

It was demonstrated that the ratio increased as the degree of disordering increased. Using the 1 kW Philips diffractometer with Cu (nickel filtered) radiation well-ordered reference Cornish kaolinite (English China Clays) gives a shape factor of 2. In the suite of rocks under discussion however, peak broadening does not necessarily indicate disorder because chlorite also contributes to the 7Å reflection. It is of some significance that two non-weathered marine shale samples (borehole 1), and two seatearth samples (boreholes 1 and 2, Table 3.2), all of which from previous evidence show some signs of disorder, have high shape factors. Furthermore, in the seatearth samples, which are all devoid of chlorite, it is of interest to note that a fall-off in the shape factor from 3.0 to 2.0 is mirrored by a decreasing depth of burial (Table 3.2).

Another approach to the order-disorder question was attempted following Hinckley (1963) who compared the $1\bar{1}0$ and $11\bar{1}$ lattice planes for the peak broadening area of the kaolinite diffraction chart. First of all a background base line is drawn on the chart and then another base line is drawn from the low angle 2θ side of the $1\bar{1}0$(4.35Å) reflection to the high 2θ side of the $11\bar{1}$ (4.17Å) reflection.

If:

A is the height of the $1\bar{1}0$ peak above the secondary base line

B is the height of the $11\bar{1}$ peak above the secondary base line

A_t is the height of the $1\bar{1}0$ peak above the primary background base line

the crystallinity factor (CF) = $\frac{A+B}{A_t}$

The resulting crystallinity factor quoted by Hinckley for a well crystallized kaolinite is 1.284, whereas the Cornish kaolinite factor is 24 per cent lower (0.973 - Table 3.5). The borehole 2 siltstone with a shape factor of 2 on the boehmite standard also gives a crystallinity factor which

is almost identical to the Cornish kaolinite. In contrast the borehole 1 seatearth has a lower factor (0.496) but this is much higher than the figure given by Hinckley for a kaolinite of poor crystallinity (Table 3.5).

Taking all the evidence into consideration it is reasonable to conclude that the deeper seatearth samples contain kaolinite that is moderately disordered. It is possible that some kaolinite in the marine shales is also moderately disordered but in the mudstones and siltstones there is no evidence of disorder.

TABLE 3.5

KAOLINITE CRYSTALLINITY FACTORS

	Crystallinity Factor
Well crystallized kaolinite (Hinckley, 1963, p.232)	1.284
Reference kaolinite, Cornwall (SF=2)	0.973
Borehole 2 siltstone (34.3-37.1 ft) (SF=2)	0.974
Kaolinite of poor crystallinity (lowest value given by Hinckley,p.234)	0.25 approx.
Borehole 1 seatearth (52.0-54.7 ft) (SF=3)	0.496

3.8 Chlorite

Although chlorite is a minor component of these rocks it is a sensitive mineral in the scheme of weathering (Loughnan, 1969).

The clean sharp 14Å peak in the Bh1 dark shale (41.5 - 42.0 ft) and its behaviour on heat treatment is characteristic of penninite rather than an Fe-rich variety (Table 3.6). In the weathered shales and mudstones, and to some extent unweathered shale (Bh1, 32.0 - 34.0 ft), the 14Å mineral's characteristics are more problematical. The large sharp peak on the untreated X-ray diffraction traces of the shallow samples would suggest that the mineral is increasing in abundance with weathering, rather than

TABLE 3.6

X-RAY REFLECTIONS - 14Å (SMEAR MOUNTS)

Bh2 Mudstone (6.0 - 6.25 ft)

Untreated - large sharp peak at 14.06Å

Heated to 550°C - very small peak at 14.0Å

small peat at 7.0Å

Untreated - width at ½ peak ht. boehmite, 6.18Å/14.06Å mineral = 0.45

Glycolated - " " " " " " " = 0.28

Saturated with $Mg(NO_3)_2$ - width at ½ peak ht./peak ht. (14.26Å) =0.118

Heated to 610°C - " " " " (14.06Å) =0.545

Bh2 Dk. shale (5.0 - 6.5 ft)

Untreated - sharp peak at 14.06Å

Heated to 550°C - very small peak at 13.87Å

very small peak at 7Å

Bh2 Dk. shale (6.0 - 6.5 ft)

Untreated - broad ragged peak at 14.26Å

Heated to 550°C - very small peak at 13.87Å

very small peak at 7Å

Bh1 Dk. shale (32.0 - 34.0 ft)

Untreated - sharp peak at 14.26Å

Heated to 550°C - broad ragged peak at 14.26Å

sharp peak at 7Å

Bh1 Dk. shale (41.5 - 42.0)

Untreated - sharp peak at 14.26Å

Heated to 550°C - very sharp enhanced peak at 14.26Å

decreasing. Transformation of original chlorite (penninite) to a swelling chlorite or a vermiculite-like mineral can not be ignored. Glycolation of the mudstone sample (Table 3.6) results in peak broadening, but not inter-layer swelling. Although the large 14.06Å peak may at first sight resemble a vermiculite-type mineral the Mg-saturated sample has a peak at 14.26Å and not 14.5Å (see Brown, 1961, p.320). Re-hydration after heat treatment may be rapid with vermiculites but the resulting 14Å d-spacing and the residual 7Å peak is more in keeping with normal chlorite and not a swelling mineral being present in the shallow mudstone sample of borehole 2.

Probably the most logical interpretation of the data is that chlorite is breaking down during weathering; the large 14Å peak of the shallow mudstone sample may well be an orientation effect of small platelets of poor crystallinity which subsequently collapse on glycolation. The important implication however, is that chlorite is still present even after a weathering period of some 10,000 years. It should also be recorded that a 14Å mineral which is believed to be chlorite is preserved in the surface equivalent of the High Main roof rocks at Lumley, Co.Durham (NZ/314 477).

Work currently being carried out by Dr. D.A. Spears (personal communication) on the Wales profile involves some 64 samples for which major element analyses were carried out in Durham using the same standards as the present writer. His work shows that major changes in the detrital minerals are limited to the top and sub-soil zone of less than 2 ft below ground level. These major changes include an increase in the quartz content, an increase in the relative abundance of kaolinite and a decrease in the relative abundance of both chlorite and mixed-layer clay. It is believed that these very near-surface changes are brought about by preferential loss of the finest grain size material. Taking this information into account it is clear that the major structural changes in the clay minerals are restricted to the surface zone.

Very minor changes have been noted within the zone in which the original rock has partly weathered to a silt or clay, but this breakdown does not appear to involve major changes in the detrital minerals.

3.9 Non-detrital minerals

It has already been mentioned that the non-detrital minerals should be more susceptible to weathering than the detrital minerals. These minerals were formed in a restricted environment totally unlike that encountered during weathering; in particular the Eh (redox potential) conditions would be very different.

Siderite and pyrite are the main non-detrital minerals in Coal Measures rocks but variations in abundance due to weathering are not easy to detect because the minerals are non-uniformly distributed in the rocks in which they are found.

From X-ray traces and thin section observations some idea of the relative preservation of non-detrital minerals can be gained. Thus from Table 3.7 it can be seen that siderite is abundant at certain horizons in the dark shales. A marked increase in the shear strength of some of the samples (see Fig. 3.9, sample at 22 ft in borehole 2) is probably due to sporadic ironstone development). Weathered ironstone nodules were also encountered in the near-surface weathered equivalent (Fig. 3.1, borehole 2) and the significance of their stability has already been commented upon. In the weathered horizons original siderite is present in all bar the shallowest borehole 1 sample (Table 3.7), although it is in the process of alteration to limonite. Also recorded on the X-ray diffraction traces of borehole 3 is a sharp reflection with a d-spacing of 6.27Å. This is believed to be lepidocrocite, the secondary iron oxide found in acid mine drainage. The ochre staining of the seatearth/lower siltstones (Fig. 3.1) is attributed to this mineral.

FIGURE 3.5

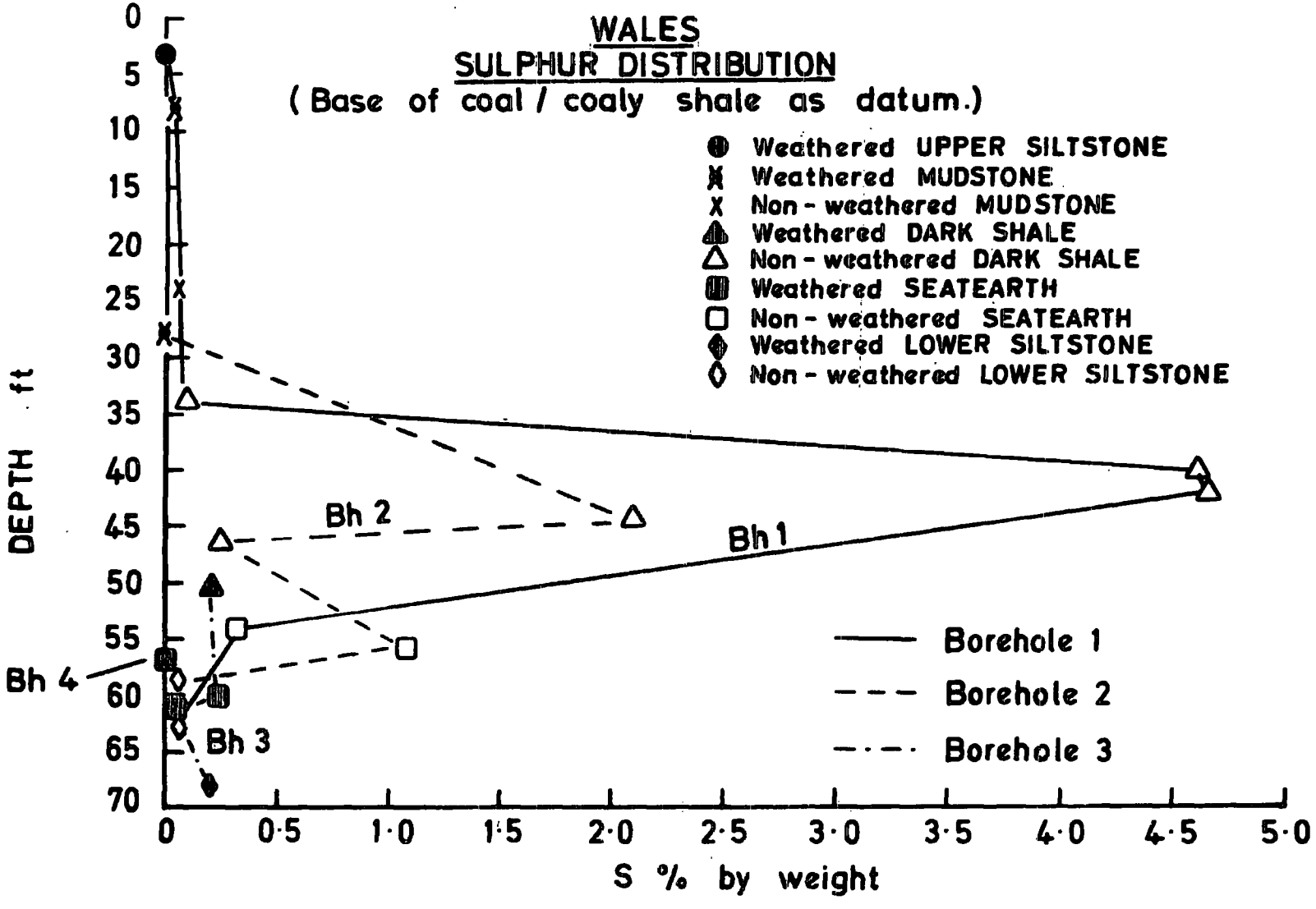

FIGURE 3.5

TABLE 3.7

NON-DETRITAL MINERALS - X-RAY AND THIN SECTION IDENTIFICATION

Borehole 1

1.5 - 3.0 ft, siltstone - LIMONITE

6.5 - 8.0 ft, mudstone - LIMONITE replacing SIDERITE

27.0 ft, mudstone - SIDERITE trace

32.0 -34.0 ft, dk. shale - abundant SIDERITE

40.0 -42.0 ft, dk. shale - abundant PYRITE
trace CARBONATE

Borehole 2

6.0 - 6.25 ft, mudstone - LIMONITE replacing SIDERITE

8.0 ft, mudstone - SIDERITE trace

14.0 ft, dk. shale - PYRITE; trace SIDERITE

22.0 -23.0 ft, dk. shale - abundant PYRITE and SIDERITE

25.5 ft, dk. shale - abundant SIDERITE

30.0 -34.0 ft, seatearth - PYRITE trace

Borehole 3

4.0 - 5.0 ft, shale- LIMONITE replacing SIDERITE

10.0 -11ft, seatearth-LIMONITE and ? LEPIDOCROCITE

Pyrite, like siderite, is not equally distributed between the different rock types. It is mainly restricted to the lower shales and the seatearth. Variations in the pyrite content are shown on Figure 3.5 in terms of sulphur percentages. A small amount of sulphur will occur however, both in organic matter and in sulphates, but where there is a significant increase in the sulphur values this is due to the presence of pyrite. Once again the number of chemically analysed samples is restricted but Figure 3.5 and Table 3.7 provide the key to pyrite stability. The highest pyrite figures are to be found in the dark shale of borehole 1 (8.66 and 8.74 per cent by weight - computed from S values - Table 3.3). Both Figure 3.5 and Table 3.7 give some idea of the variability of pyrite even in the unweathered rocks. A comparison of the borehole 2 profile with that of borehole 1 makes this very clear indeed. The dark shale and seatearth samples of the borehole 3 profile (Fig. 3.5) demonstrate that all the weathered samples are lower in pyrite than equivalent non-weathered material from other boreholes. The same applies of course for the one sample from borehole 4. Inspection of Table 3.7 indicates that pyrite is present at the 14 ft level in borehole 2 but is definitely absent in the 4.0 - 5.0 ft sample from borehole 3. Similarly, it is absent in the 10.0 - 11.0 ft seatearth sample from this borehole, but this is not wholly conclusive because its level in the seatearth samples can drop to about 0.5 per cent by weight which is below the level of X-ray detection. Nevertheless, it can be seen that the mineral is still present within the zone designated as 'partly weathered' (borehole 3), whereas it is absent in the zone which corresponds to a change from rock to clay-with-fragments. Evidence from the literature presented in Chapter 2 indicates that pyrite may contribute to the breakdown of shale and coal. What is abundantly evident is that it is not the prime cause of breakdown. If it were, the

depth of clay-silt development in borehole 3 should be greater than in boreholes 1,2 and 4 where the original content of pyrite was low. Clearly this is not the case.

Like the non-detrital minerals, organic carbon is non-uniformly distributed and hence does not show a systematic decrease in all weathered samples. Another mineral which is claimed to be non-detrital, is apatite (Taylor, 1971). It should be noted that most of the P_2O_5 can be attributed to this mineral. Somewhat elevated P_2O_5 values in two borehole 3 seatearth samples from the weathered zone are matched by elevated CaO/Al_2O_3 ratios (Table 3.4). Phosphates have previously been recorded in the marine strata of the Mansfield cyclothem, but the inferred presence of up to 1.61 per cent mineral phosphate ($hydroxyapatite, Ca_5(PO_4)_3(OH)$) is a little unusual. The amount is small but it is of the same order as the highest marine shale value (1.64%, borehole 2). Phosphatic minerals like apatite have been shown to be very insoluble outside the depositional pH of 7 to 8 (Kardos, 1964). The possibility of acid solution with downwards leaching and re-deposition cannot be entirely ruled out but it is more likely that this minor phosphate development is associated with the coaly fraction of the seatearth. The P_2O_5 percentage falls to the normal level in the immediately underlying siltstones.

3.10 Grain size and consistency limits

From the analysis of representative ultrasonically disaggregated samples (pipette analysis, British Standard 1377/1967) it is clear that the fundamental grain size of the sediments falls dominantly within the silt-grade division of the M.I.T. classification (Fig. 3.2). These findings are in line with previous work (Taylor, 1971) and Pettijohn's (1957) conclusion that most clays and shales contain a very large proportion of silt. The Trask sorting coefficients (So) imply that the three coarser

Figure 3.6

Wales samples shown on Casagrande plasticity chart

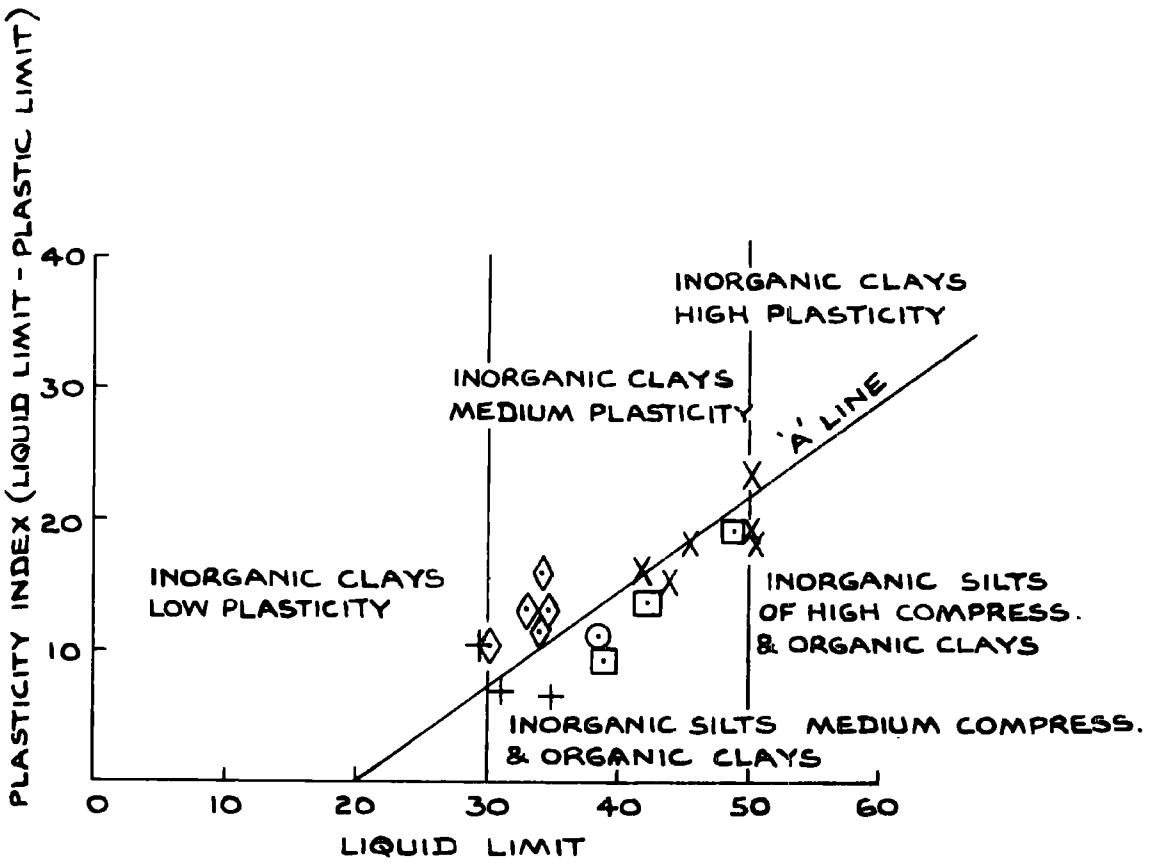

		LIQUID LIMIT	PLASTICITY INDEX
⊙	UPPER SILTSTONE	38·4	10·9
⊡	MUDSTONE	48·7	19·0
	..	38·8	9·2
	..	42·3	13·7
X	DARK SHALE	41·8	16·2
		42·0	16·0
		45·4	18·2
		50·6	18·1
		50·2	19·2
		44·0	15·3
		50·1	23·6
◇	SEATEARTH	34·1	12·8
		33·0	13·2
		34·2	15·9
		34·6	13·3
+	SILTSTONE	35·0	6·6
		29·5	10·6
		31·2	6·9

FIGURE 3.6

sediments of similar grading are statistically 'poorly sorted'. In contrast the dark shale is 'well sorted' according to Trask's original scheme, but more recent work (see Pettijohn, 1957) suggests that his So values for 'well sorted', 'normally sorted' and 'poorly sorted' (2.5, 3.0 and 4.5 respectively) are too high. The shale certainly has a much higher So value than its equivalent near Sheffield (1.75; Taylor, 1971).

The liquid and plastic limits plotted on the Casagrande 'A' line chart (Fig. 3.6) conform with the visual strata descriptions and the concept of 'coarsening upwards' within a cyclothem. The mudstone samples generally bridge the field between the siltstones of low liquid limit and plasticity index and the shales which are of higher liquid limit and increasing plasticity index. A close inspection of the samples in relation to their respective positions in any one unit shows that in some cases the weathered samples have limits which are generally higher than unweathered equivalents whilst in other cases they are lower. In other words, there is no consistent variation in limits with breakdown for the samples studied.

An interesting and possibly more meaningful relationship is that which exists between liquid and plastic limits on the one hand and the quartz content of the rocks on the other hand (Fig. 3.7). The liquid limit is more accurately determined for these materials and hence the relationship is better defined for this parameter. As the quartz content increases within the range 15 - 44 per cent so the limits decrease. Beyond the latter quartz value there is a tendency for the limits to increase again. The increasing abundance of this equant habit angular mineral in these fine grained rocks is apparently precluding the ability of the sediment to flow (liquid limit) as well as subdueing its cohesive properties. The inflexion may well represent the transition from flow to sliding in the context of liquid limit, especially as the two samples with the highest quartz contents

Figure 3.7

Relationship between liquid and plastic limits with quartz

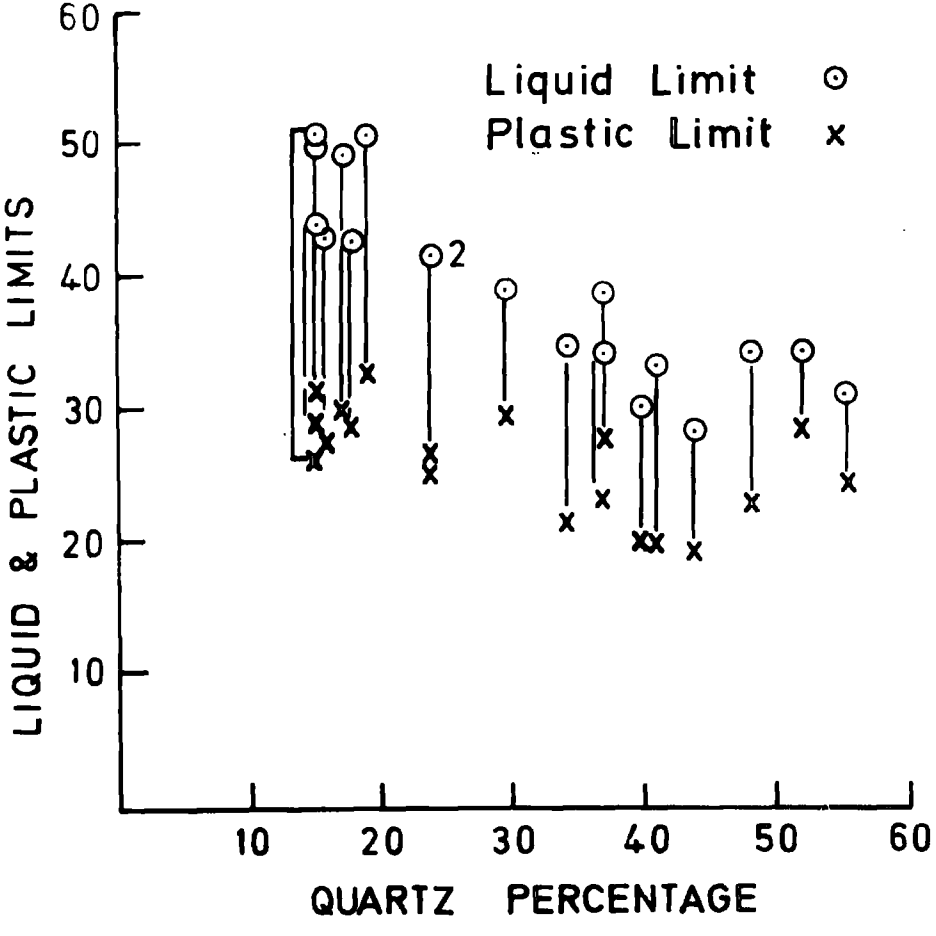

	DEPTH FEET	LIQUID LIMIT	PLASTIC LIMIT	QUARTZ %
UP. SILTSTONE	1·5 - 3·0	38·4	27·5	37·0
MUDSTONE	6·0 - 6·3	48·7	29·7	17·0
..	6·5 - 8·0	38·8	29·6	29·5
..	24·0	42·3	28·6	17·5
DK. SHALE	6·0 - 6·5	41·8	25·6	23·5
..	5·0 - 6·5	42·0	26·0	23·5
..	22·0 - 23·0	45·4	27·2	15·5
..	23·0 - 25·0	50·6	32·5	19·0
..	32·0 - 34·0	50·2	31·0	15·0
..	40·0 - 40·5	44·0	28·7	15·0
..	41·5 - 42·0	50·1	26·5	15·0
SEATEARTH	3·4 - 3·7	34·1	22·5	48·5
..	14·5 - 15·0	33·0	19·8	41·0
..	15·75 - 16·25	30·0	19·6	40·0
..	30·0 - 34·0	34·2	18·3	37·0
..	52·0 - 54·7	34·6	21·3	34·0
LR. SILTSTONE	16·0 - 23·75	35·0	28·4	52·0
..	34·3 - 37·1	29·5	18·9	44·0
..	59·0 - 62·0	31·2	24·3	55·5

FIGURE 3.7

TABLE 3.8

Specific Gravities, Moisture Contents, Densities and Standard Penetration Tests

	Borehole Depth	S.G.	Natural moisture content	Average Bulk Density	Average Dry Density
Upper Siltstone	Bh1 (1.5-3.0)	2.53	10.8	139	125
Mudstone	Bh2 (6.00-6.25)	2.48	5.5	137	130
"	Bh1 (7.75-13.25)	2.49	8.0	142	130
"	Bh1 (24.0)	2.49	8.2	139	128
Dk. Shale	Bh3(5.0-6.5)	2.53	11.2-14.0	141	124
"	Bh3 (6.0-6.5)	2.53			
"	Bh2 (22.0-23.0)	2.57)	9.4	139	127
"	Bh2 (23.0-25.0)	2.57)			
"	Bh1 (32.0-34.0)	2.57	10.4	136	123
"	Bh1 (40.0-40.5)	2.55)	8.8	136	125
"	Bh1 (41.5-42.0)	2.55)			
Seatearth	Bh4 (3.3-3.6)	2.60	11.3	138	124
"	Bh3 (14.5-15.0)	2.65)	10.8	131	118
"	Bh3 (15.75-16.25)	2.60)			
"	Bh2 (30.0-34.0)	2.58			
"	Bh1 (52.0-54.7)	2.62			
Siltstone	Bh3 (16.0-23.75)	2.60	7.2-10.2	136-151	127-137
"	Bh2 (34.3-37.1)	2.63	5.6	157	144
"	Bh1 (59.0-62.0)	2.63	2.7	157	153

Standard Penetration Tests

	Borehole Depth	Blows per foot		Borehole Depth	Blows per foot
Mudstone	Bh1 (11.0-12.0)	39	Dk. Shale	Bh2 (16.0-17.0)	21
"	Bh1 (16.0-17.0)	45	"	Bh2 (20.0-21.0)	21
"	Bh2 (9.0-10.0)	16	"	Bh2 (26.0-27.0)	24
Dk. Shale	Bh2 (13.0-14.0)	14			

are siltstones with 'granular' plasticity characteristics. Granular characteristics could also be expected in the case of surface material when there is a marked increase in the quartz to clay minerals ratio.

3.11 Specific gravity, density, and Standard Penetration Tests

The mean specific gravity (G_s) values (Table 3.8) increase from shale, through mudstone and seatearth to siltstone (2.49, 2.55, 2.61 and 2.62, respectively). They also exhibit a statistically significant linear positive relationship with quartz (correlation coefficient, r=0.653; Student t = 3.552). From Table 3.8 it can be seen that there is a very general tendency for weathered equivalents to have lower G_s values, but this to a large extent is purely a reflection of quartz variation.

Density has been considered to be a property which is moderately sensitive to depth of burial and weathering (see for example Iliev, 1966). The average dry densities have been computed from the bulk densities of the laboratory samples and natural moisture contents shown on Table 3.8. For the horizons sampled there is little evidence of density changes with the degree of disintegration or weathering. The lower siltstone bed does reveal an increase in density with depth of cover, but this may well be a reflection of specimen discontinuities and may not be truly representative of the *in situ* state because there was disparity in sample sizes between the upper samples of lower siltstone, and the deeper ones. It is important to note that the detailed *in situ* measurements made by Kennard *et al.*, (1968) in Carboniferous shales at the Balderhead site showed uniformity in density below 2 ft and the maximum depth of measurements, namely 8ft. Certainly in argillaceous Carboniferous strata it should not be assumed that an increase in depth of cover is matched by an increase in density.

Seven Standard Penetration Tests (S.P.T.'s- B.S. 1377: 1967, p.189) were carried out during boring operations in the upper parts of boreholes 1 and 2.

Although the variations in penetration values (Table 3.8 - particularly borehole 1 mudstone) do not mirror the uniformity in bulk densities of the mudstone/shale beds they are consistent with the strata classification and structural characteristics of the rocks. Penetration values in rocks of less than 100 are usually considered to be symptomatic of weak weathered strata. The chemistry and mineralogy of the dark shale horizons tested reveal no evidence of weathering at depth, although the SPT values at the 26 to 27 ft level are as low as 24 blows per foot. These rocks are extremely fissile (since they are shales rather than mudstones) and this accounts for the low values. This fissility has been found to be one of the important structural controls on breakdown when the rocks are exposed at surface (see Taylor and Spears, 1970, Fig. 1). The penetration values of the borehole 1 mudstone are representative of the higher more silty part of the bed whereas the borehole 2 values represent gradational shaly material at the bottom of the bed. In the context of weathering it is pertinent to note that the dark shale of borehole 2, which was visually designated as partly weathered from its fragmental nature (Fig. 3.1), is only marginally different on a penetration basis from the non-weathered rock.

3.12 Shear strength measurements and treatment of results

Two basic testing methods were adopted for shear strength investigations a) triaxial*, b) shear box (direct-shear). All the 2 in long by 1 in diameter siltstone specimens (Table 3.9) were dry-cored from the original material. For these triaxial tests a Wykeham Farrance steel cell (T 103) was used in conjunction with a Clockhouse 10 ton compression testing machine.

* Most of the triaxial tests were carried out by Jones (1970) under the writer's supervision. However, the raw test data has been completely re-processed and supplemented when necessary.

TABLE 3.9

Triaxial and shear box tests

BOREHOLE	DEPTH (Feet)	TEST & SAMPLE SIZE (in)	SATURATED/NON-SATURATED	EFFECTIVE CONFINING OR NORMAL PRESSURE (lb/in²)	DEVIATOR STRESS OR PEAK STRESS (lb/in²)	RESIDUAL STRESS (lb/in²)	PEAK DISPLACEMENT (in)	RESIDUAL DISPLACEMENT (in)	ϕ/ϕ_p^1 (degrees)	c/c_p^1 (lb/in²)	CORRELATION COEFF.	STUDENT t	SIGNIFICANCE LEVEL (p)	TANGENT MODULUS (E_t) (lb/in²)	SECANT MODULUS (E_s) (lb/in²)	VOLUMETRIC STRAIN AT FAILURE β	ϕ_r^1 (degrees)	c_r^1 (lb/in²)	CORRELATION COEFF.	STUDENT t	SIGNIFICANCE LEVEL (p)	BULK DENSITY lb/ft³
										UPPER SILTSTONE											
a) 1*	2.75	TRI-	NON-	10	143.5				43.5	23.25	0.9982	16.44	>0.01	7.2×10^3	7.2×10^3	-0.36					138
	to	AXIAL	SAT.	20	209.6									7.2×10^4	7.5×10^3	-0.75					140
	3.00	3x1.5 dia.		40	275.2									1.4×10^4	1.4×10^4	-0.81					140
										MUDSTONE											
b) 2*	6.00	TRI-	NON-	10	46.2									2.6×10^3	1.8×10^3	-1.90					135
	to	AXIAL	SAT.	20	72.3									2.4×10^3	2.0×10^3	-0.59					139
	6.25	3x1.5 dia.		40	73.4									5.7×10^3	4.9×10^3	-0.29					138
c) 1*	7.75	TRI-	NON-	10	139.9									8.0×10^3	7.8×10^3	-0.64					141
	to	AXIAL	SAT.	20	249.8									1.2×10^4	1.2×10^4	-0.64					145
	8.00	3x1.5 dia.		40	265.6									1.4×10^4	1.3×10^4	-0.52					142
	13.00			10	214.9									8.0×10^3	8.5×10^3	-0.62					144
	to			20	243.3									4.4×10^3	1.1×10^4	-0.65					137
	13.25																				
d) 1	20.70	SHEAR	NON-	15	10.9		0.24		39.0	0	0.9658	3.72	<0.05								100
	to	BOX	SAT.	20	18.1		0.22			(-0.01)											100
	30.70		AGGRS-GATE	30	23.7		0.10														100
e) 1	24.00	SHEAR	SAT.	7.9	8.2		0.42		36.5	2.21	0.9996	35.44	>0.02								99
	to	BOX		15.9	13.9		0.35														99
	25.00			23.7	20.0		0.12														101

BOREHOLE	DEPTH (Feet)	TEST & SAMPLE SIZE (in)	SATURATED/NON-SATURATED	EFFECTIVE CONFINING OR NORMAL PRESSURE (lb/in²)	DEVIATOR STRESS OR PEAK STRESS (lb/in²)	RESIDUAL STRESS (lb/in²)	PEAK DISPLACEMENT (in)	RESIDUAL DISPLACEMENT (in)	ϕ/ϕ^1_p (degrees)	σ^1/σ^1_p (lb/in²)	CORRELATION COEFF.	STUDENT t	SIGNIFICANCE LEVEL (p)	TANGENT MODULUS (E_1) (lb/in²)	SECANT MODULUS (E_s) (lb/in²)	VOLUMETRIC STRAIN AT FAILURE %	ϕ^1_r (degrees)	σ^1_r (lb/in²)	CORRELATION COEFF.	STUDENT t	SIGNIFICANCE LEVEL (p)	BULK DENSITY lb/ft³
f) 3*	5.00 to 6.50	TRI-AXIAL 3x1.5 dia.	NON-SAT.	8.8	17.3									1.5×10^3	1.7×10^3	-8.75						144
				18.5	27.8									1.5×10^3	1.3×10^3	-7.67						143
				27.5	37.7									4.3×10^3	3.9×10^3	-10.00						136
				46.8	78.7									4.7×10^3	4.7×10^3	-6.90						141
g) 2	22.00 to 25.00	TRI-AXIAL 6x3 dia.	NON-SAT.	10	130.0									2.2×10^3	2.6×10^3	-1.60						142
				20	362.6									2.0×10^3	3.3×10^3	-1.85						140
				40	326.0									3.8×10^3	4.3×10^3	-2.70						134
h) 1	32.00 to 34.00	TRI-AXIAL 6x3 dia.	SAT. (WATER INGRESS)	20	22.3									2.5×10^3	1.3×10^3	-3.20						133
	40.00 to 40.50	"	"	40	70.8									2.5×10^3	3.7×10^3	-3.10						138
	41.50 to 42.00	"	"	60	182.0									8.6×10^3	6.0×10^3	-2.50						135
	46.00 to 46.5	"	NON-SAT.	40	154.7									7.9×10^3	7.1×10^3	-0.81						138
i) 1	30.70 to 51.75	SHEAR BOX PRE-SPLIT	SAT.	10																		
				20																		
				30																		
			DARK SHALE		26.0	0 (0.09)	0.9963	16.33	0.001								14.5	0.530	0.9997	32.23	0.001	

BOREHOLE	DEPTH (Feet)	TEST & SAMPLE SIZE (in)	SATURATED/NON-SATURATED	EFFECTIVE CONFINING OR NORMAL PRESSURE (lb/in²)	DEVIATOR STRESS OR PEAK STRESS (lb/in²)	RESIDUAL STRESS (lb/in²)	PEAK DISPLACEMENT (in)	RESIDUAL DISPLACEMENT (in)	ϕ/ϕ_p^1 (degrees)	c^1/c_p^1 (lb/in²)	CORRELATION COEFF.	STUDENT t	SIGNIFICANCE LEVEL (p)	TANGENT MODULUS (E_i) (lb/in²)	SECANT MODULUS (E_s) (lb/in²)	VOLUMETRIC STRAIN AT FAILURE %	ϕ_r^1 (degrees)	c_r^1 (lb/in²)	CORRELATION COEFF.	STUDENT t	SIGNIFICANCE LEVEL (p)	BULK DENSITY lb/ft³
											SEATEARTH											
j) 4°	3.25 to 3.50	TRI-AXIAL 3x1.5 dia.	NON-SAT.	10	145.0				39.0	25.17	0.9526	6.26	>0.01	4.8×10^3	4.8×10^3	-0.23						135
				20	156.5									6.2×10^3	6.2×10^3	-0.69						133
				10	216.7									2.4×10^3	1.5×10^4	-0.30						133
	5.25 to 5.50			10	161.0									4.7×10^3	4.7×10^3	-0.23						143
				20	227.9									5.0×10^3	7.5×10^3	+0.24						143
				40	218.6									5.3×10^3	4.8×10^3	-0.53						144
k) 3°	5.50 to 6.00	SHEAR BOX	SAT.	5	6.6	3.5	0.10	1.95	31.0	3.56	1.0000	-	0.001				17.5	1.79	0.9969	12.67	>0.05	
				15	12.5	6.1	0.11	2.53														
				27.5	20.0	10.5	0.15	2.56														
l) 3°	10.00 to 13.00	TRI-AXIAL 6x3 dia.	SAT. WATER INGRESS	20	169.9				36.0	18.78	0.9501	3.05	<0.05	6.5×10^3	6.5×10^3	-0.67						
				40	151.4									3.1×10^3	7.0×10^3	-0.47						
				60	244.7									4.4×10^3	5.8×10^3	-						
n) 3°	13.50 to 14.00	TRI-AXIAL 6 x3 dia.	NON-SAT.	10	365.4									1.4×10^4	1.8×10^4	-0.42						132
	14.50 to 15.00			20	612.8									1.2×10^4	1.7×10^4	-0.25						125
	15.75 to 16.25			40	589.3									1.8×10^4	2.0×10^4	-0.63						135

BOREHOLE	DEPTH (Feet)	TEST & SAMPLE SIZE (in)	SATURATED/NON-SATURATED	EFFECTIVE CONFINING OR NORMAL PRESSURE (lb/in²)	DEVIATOR STRESS OR PEAK STRESS (lb/in²)	RESIDUAL STRESS (lb/in²)	PEAK DISPLACEMENT (in)	RESIDUAL DISPLACEMENT (in)	ϕ'/ϕ'_p (degrees)	c'/c'_p (lb/in²)	CORRELATION COEFF.	STUDENT t	SIGNIFICANCE LEVEL (p)	TANGENT MODULUS (E_t) (lb/in²)	SECANT MODULUS (E_s) (lb/in²)	VOLUMETRIC STRAIN AT FAILURE %	ϕ'_r (degrees)	c'_r (lb/in²)	CORRELATION COEFF.	STUDENT t	SIGNIFICANCE LEVEL (p)	BULK DENSITY lb/ft³
n) 2	32.00 to 34.00	SHEAR BOX	SAT.	10	6.7	4.4	0.25	1.54	32.0	0	0.9940	9.08	<0.05				17.0	1.40	0.9995	31.63	>0.05	
				20	11.8	7.6	0.29	2.05														
				30	19.3	10.5	0.25	1.98														
o) 1	52.00 to 54.70	SHEAR BOX	SAT.	10	7.0		0.13		36.5	0.82	0.9814	10.22	0.001									
				20	16.7		0.22															
				30	23.8		0.22															
				10	9.7		0.11															
				20	14.0		0.19															
				30	22.5		0.21															
									LOWER SILTSTONE													
p) 3*	16.25 to 23.75	TRI-AXIAL 6x3 dia.	NON-SAT.	10	371.0				67.5	7.12	0.9999	66.05	>0.01	1.1×10^4	1.5×10^4	-0.50						139
				20	471.0									1.1×10^4	1.5×10^4	-0.30						136
				40	1032.0									3.4×10^4	4.0×10^4	-0.35						151
q) 3	23.75 to 30.00	TRI-AXIAL 2x1 dia.	NON-SAT.	20	4810.0				72.5	219.27	0.9922	11.25	>0.01	1.6×10^5	2.1×10^3							157
				40	5000.0									7.5×10^5	1.5×10^5							157
				60	4400.0									1.3×10^5	1.8×10^5							157
				80	5300.0									1.5×10^5	2.1×10^5							157
r) 2	34.00 to 37.00	TRI-AXIAL 2x1 dia.	NON-SAT.	20	3125.0		(inc.tensile value)		68.0	48.48	0.9998	85.61	0.001	1.9×10^5	2.3×10^5							157
				40	4500.0		(low range compress.)		74.0	147.5	10.9999	130.93	0.001	2.4×10^5	2.4×10^5							157
				60	4650.0		(conventional Mohr)		34.0	2050				1.7×10^5	2.4×10^5							157
				80	6175.0									2.3×10^5	2.8×10^5							157
				500	9179.3																	155
				1000	10767.0																	159
				2000	12993.9																	155
				4000	11128.9																	157

BOREHOLE	DEPTH (Feet)	TEST & SAMPLE SIZE (in)	SATURATED/NON SATURATED	EFFECTIVE CONFINING OR NORMAL PRESSURE (lb/in^2)	DEVIATOR STRESS OR PEAK STRESS (lb/in^2)	RESIDUAL STRESS (lb/in^2)	PEAK DISPLACEMENT (in)	RESIDUAL DISPLACEMENT (in)	ϕ_p^1 (degrees)	c_p^1 (lb/in^2)	CORRELATION COEFF.	STUDENT t	SIGNIFICANCE LEVEL (p)	TANGENT MODULUS (E_i) (lb/in^2)	SECANT MODULUS (E_s) (lb/in^2)	VOLUMETRIC STRAIN AT FAILURE %	ϕ_r^1 (degrees)	c_r^1 (lb/in^2)	CORRELATION COEFF.	STUDENT t	SIGNIFICANCE LEVEL (p)	BULK DENSITY lb/ft^3
		TENSILE 2x1 dia.	FISSURED	0	151.5																	156
				0	64.5																	151
s) 2	34.00 to 37.00	SHEAR BOX PRE-SPLIT	SAT.	10	5.4												28.0 (0.2)	0	0.9995	31.63	>0.05	
				20	11.0																	
				30	16.0																	
t) 2	34.00 to 37.00	SHEAR BOX PRE-SPLIT	NON-SAT.	10	6.6												35.0 (-0.47)	0	0.9999	70.91	>0.01	
				20	13.4																	
				30	20.6																	
u) 1	59.00 to 62.00	TRIAXIAL 2x1 dia.	NON-SAT.	20	4925.0				79.0	5.31	0.9989	30.12	>0.01	1.7×10^5	2.6×10^5							157
				40	5525.0									2.1×10^5	3.1×10^5							157
				60	7175.0									2.3×10^5	2.7×10^5							157
				80	5200.0									2.3×10^5	2.7×10^5							157

Significance levels: 0.05 - probably significant
0.01 - significant
0.001- highly significant

Rates of strain Triaxial 0.00024 to 0.00048 in/min.
Shear box 0.000043 in/min.

Instrumentation with L.V.D.T. transducers linked to a Bryan X-Y auto-plotter facilitated direct recording of the principal stress difference and strain. In order to explore the Mohr envelope of the unweathered siltstone at higher confining pressures four specimens were also tested to failure in a Wykeham Farrance high pressure (10,000 lb/in^2 confining pressure) balanced-ram cell with the appropriate pressure controller 397/SP/1b). The tensile values were determined from 'direct pull' using a Hounsfield tensometer with the 1 in diameter specimens araldited into steel platens. The visually unweathered siltstone values are of course on a total stress basis. It is probably reasonable to compare these results with the other consolidated-drained tests because the moisture content of the siltstone specimens was low and pore pressures may well be low in comparison with the skeletal strength of the rock fabric.

All the remaining tests were conducted on an effective stress basis, the small cylinders (3 in long by $1\frac{1}{2}$ in diameter) being extruded or partly cored from the U4 tubes. The highly fractured 3 in diameter material from the rotary borehole cores was particularly difficult to prepare and porous end pieces (3:1 coarse sharp sand/plaster of paris mix) were cast onto the specimens to preclude imperfections adjacent to the platens. In no case did the end-pieces fail prior to the rock material. Normal soils cells were adopted for the consolidated-drained tests with manual pore pressure monitoring and twin burettes (Bishop and Henkel, 1962, p.71) for volume change measurements.

Due to the fissured and fragmental nature of some of the specimens the sheaths punctured when the confining pressure was applied (Bh 1 shale specimens, 32 - 42ft; borehole 3 seatearth, 10 - 15 ft). A certain amount of slaking was observed in these specimens and in others that were purposely back-saturated (Bishop et al., 1960) in order to make up sets of saturated

27 JAN 1972

specimens which were subsequently tested under fully-drained conditions (Appendix 3).

The stress levels at failure for these samples (Figs. 3.8, 3.12) are on the whole, lower than equivalent non-saturated types and consequently the saturated results are treated with reservation. This experience led to the adoption of two sheaths per specimen with the appropriate membrane corrections (B.S.1377/1967, p.204).

The shear box tests were carried out on both saturated specimens (parallel to the stratification) and in one case specimens at natural moisture content. So that disturbance could be kept to a minimum a 3 in diameter circular box was used rather than a conventional square box. The entire testing programme was limited by the suitability of samples so the results must in the main be considered in terms of broad lithological divisions rather than as specific levels within a division.

The confining pressures bracket the range of low normal stresses that are applicable to the profile under investigation. Moreover, high pressure cells of sufficient size to take the 3 in diameter specimens are not customarily available, and in any case, rock fragments readily punctured the sheaths, even at low confining pressures.

Triaxial tests carried out on rocks are invariably conducted on small intact specimens over a wide range of normal pressures. From such tests the shear strength parameters (cohesion, c, and intergranular friction, $\emptyset$) can be scaled from the Mohr envelopes, which generally show some curvature.

The innumerable discontinuities and variable nature of the material (Plate 3.1) raised the usual problems in defining the Mohr envelope. An endeavour has therefore been made to reduce the subjective interpretations by employing a statistical reduced major axis regression computation to determine the shear strength parameters from the triaxial tests. The top points of the Mohr circles $\left[\frac{1}{2}(\sigma_1 + \sigma_3)\right.$ vs. $\left.\frac{1}{2}(\sigma_1 - \sigma_3)\right]$ are plotted

and the regression equation (with no assumption of dependent and independent variable) is computed, together with product moment correlation coefficient, r, and the Student t value. The slope of the regression line ($\tan \alpha$) and the y intercept, (a), are from the geometry of the Mohr construction transformed into shear strength parameters as follows:

$$\tan \alpha = \sin \phi; \quad c = a/\cos \phi$$

For the direct-shear tests a conventional least squares linear regression (y on x) was computed, the slope of which is equivalent to $\tan \phi$ and the y intercept represents the cohesion, c.

3.13 Deviator stresses

The composite plot of all the triaxial test results [$\frac{1}{2} (\sigma_1 + \sigma_3)$ vs. $\frac{1}{2} (\sigma_1 - \sigma_3)$ - Fig. 3.8] reveals a statistically highly significant linear relationship. Lower siltstone specimens tested at high confining pressures were excluded from these computations because they define the curved rather than linear portion of the respective Mohr envelope. The logarithmic presentation subdues minor variations but it will be observed that the trend of shallow depth shale and mudstone specimens is less steeply inclined ($\phi' = 28.5°$, $c' = 1.39$ lb/in^2) than the upper samples (near origin $\phi = 81°$, with a high negative y intercept). The latter ϕ angle emphasizes the steepness of the composite Mohr envelope adjacent to the origin and implies a high compressive to tensile strength ratio which is verified by the lower siltstone parameters for which tensile values are available (Table 3.9, Fig. 3.10). It should however, be appreciated that the method of interpretation can exaggerate the steepness of the envelope which may not always be strictly linear (Fig. 3.9) even at low confining pressures. On Figure 3.9 are included non-saturated specimens of upper siltstone, mudstone from greater than 7.75 ft in depth, the deeper dark shales, and the seatearth specimens. Siderite-rich shale specimens (22 ft - 25 ft) and the deeper

FIGURE 3.8

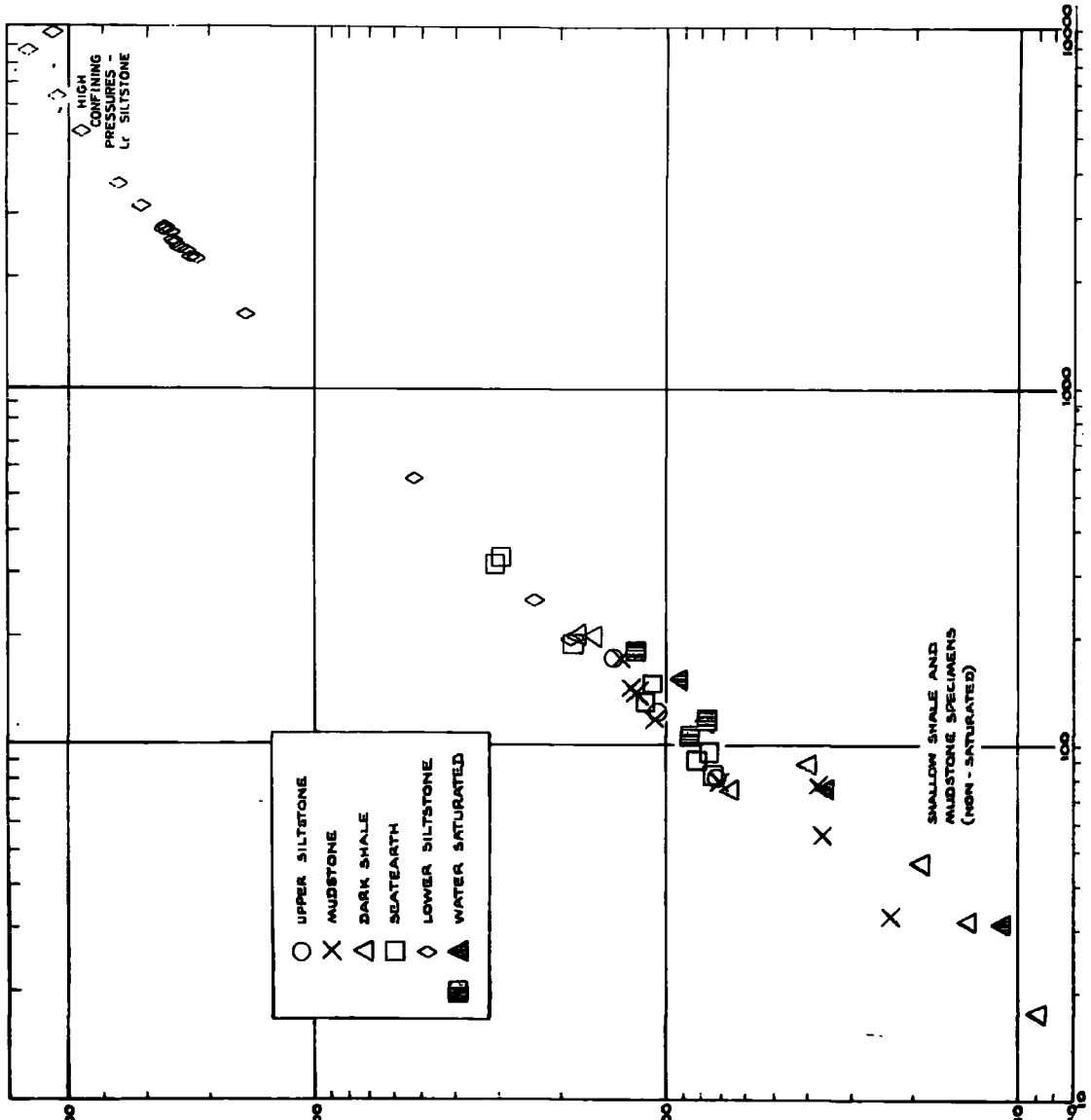

Figure 3.8

Mohr circle 'top point' plot for all triaxial specimens

Figure 3.9

Shale, mudstone, seatearth, upper siltstone specimens (excluding shale and mudstone from less than 6.5ft) - Mohr circles.

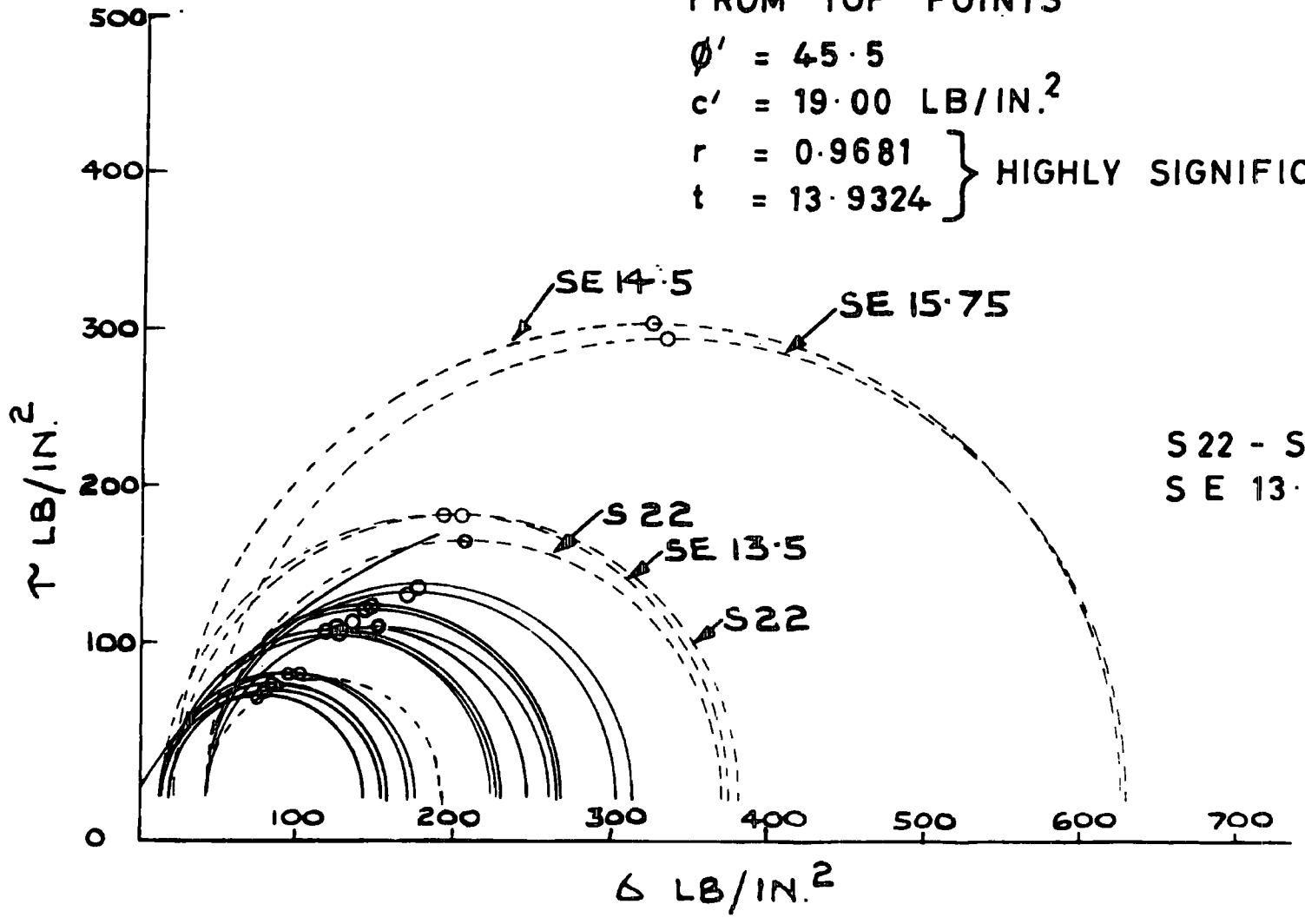

S 22 - SHALE SPECIMEN 22 FT.
S E 13·5 - SEATEARTH 13·5 FT.

FIGURE 3.9

seatearth specimens have 'top points' which are off-set towards the origin. The conventional Mohr construction suggests that the remaining specimens comprise a family of circles with a $\emptyset$ value (curved envelope) perhaps some 5 degrees lower than the statistical one given on Figure 3.9. In line with the steeply rising Mohr envelope of the composite plot it is not unreasonable as a first approach to treat the principal stress difference at failure for the lowest confining pressures (minimal specimen support) as though they are uniaxial compressive strength results. Table 3.10 lists the values (all non-saturated tests) which are also expressed as a percentage of the non-weathered siltstone mean. There is a natural break-down into four groups (a,b,c and d). By comparing the weathered dark shale (group a) with its non-weathered equivalent (group b) and the weathered siltstone (group c) with the non-weathered value (group d), the drop in strength from non-weathered to weathered for these two rock types is 91 per cent and 86 per cent, respectively. The other significant feature of Table 3.10 is that although group b types comprise a wide range of rock types the difference between the maximum and minimum values is very small indeed. This observation is indirectly a reflection of the composite Mohr construction (Fig. 3.9 and footnote).

The gradational nature of the borehole 3 seatearth-weathered siltstone bed is emphasized by group c and confirmed by the composite shear strength parameters (Table 3.11). Basing the strength criterion on this initial approach it is of interest to note that Meigh's (1968) approximate compressive strength range for the upper weathered zone developed on Coal Measures rocks is from 2 - 5 ton/ft^2 (31 - 78 lb/in^2). The 'group a' shale-mudstones of the current work conform to the range but not so the 'group b' types. The

* By taking mean stress difference at failure similar groupings are obtained. The group b order of increasing strength is: seatearth, upper siltstone, mudstone and dark shale, the difference between minimum and maximum values being 102 lb/in^2.

minimum value of the latter group (Table 3.10) is nearly twice as high and the lowest mean deviator stress (see footnote) is more than twice as high as Meigh's compressive strength maximum.

TABLE 3.10

Principal stress difference at failure for the lowest confining pressure.

Borehole	Rock type	Depth ft	Deviator stress lb/in^2	Percentage of mean Lower siltstone value	Group
3	Dark shale*	5.00-6.50	17.8	0.4	a
2	Mudstone*	6.00-6.25	46.2	1.1	
2	Dark shale	22.00-25.00	130.0	3.0	
1	Upper siltstone*	2.75-3.00	143.5	3.3	
4	Seatearth*	3.25-3.50	145.0	3.4	b
4	Seatearth*	5.25-5.50	161.0	3.8	
1	Mudstone*	7.75-8.00	177.4	4.1	
3	Seatearth*	13.50-14.00	365.4	8.5	c
3	Siltstone*	16.25-23.75	371.0	8.6	
1,2,3	Lower siltstone	20 lb/in^2 confining pressure	4286.7	100.0	d

* visually weathered

TABLE 3.11

Comparative shear strength parameters - Triaxial tests

Bh	Rock type	Depth ft	ϕ'/ϕ degrees	c'/c lb/in^2	
1	*up.siltstone	2.75 - 3.00	43.5	23.25	
3	*dk. shale	5.00 - 6.50	26.0	0	
4	*seatearth	3.25 - 3.50) 5.25 - 5.50)	39.0	25.77	
3	*seatearth	10.00 -13.00	36.0	18.78	(saturated specimens)
3	*siltstone	16.25 -23.75	67.5	7.12	(near origin, apparent)
3	siltstone	23.75 -30.00)	77.5	58.58	(near origin, apparent)
2	siltstone	34.00 -37.00)			
1	siltstone	59.00 -62.00)	r = 0.9992, t = 79.1159		
		)	p = 0.001		
2	siltstone	34.00 -37.00)	34.0	2050	(from Mohr construction)

For comparison calculated unconfined compressive strength, borehole 2 (apparent ϕ = 74.0°, c = 147.51 lb/in^2) = 2,100 lb/in^2
compressive: tensile strength = 13.8:1

Composite samples - Triaxial tests

3	*dk. shale	5.00 - 6.50)	28.5	1.39
2	*mudstone	6.00 - 6.25)	r = 0.9164, t = 5.1188	
			p > 0.01	
3	*seatearth	13.50 -16.25	66.5	6.11 (near origin, apparent)
3	*siltstone	16.25 -23.75	r = 0.9982, t =33.1363	
			p = 0.001	

Comparative shear strength parameters - Shear Box

Bh1	mudstone	20.70 -30.70	ϕ'_p=39.0°, c'_p = 0 lb/in^2 (non-saturated aggregate)
Bh1	mudstone	24.00 -25.00	ϕ'_p=36.5°, c'_p = 2.21 lb/in^2 (saturated)
Bh1	dark shale	30.70 -51.75	ϕ'_r=14.5°, c'_r = 0.53 lb/in^2(saturated-pre-split)
Bh4*	seatearth	5.50 -6.00	ϕ'_p=31.0°, c'_p = 3.56 lb/in^2(saturated)
			ϕ'_r=17.5°, c'_r = 1.79 lb/in^2(saturated)
Bh2	seatearth	32.00 -34.00	ϕ'_p=32.0°, c'_p = 0 lb/in^2 (saturated)
			ϕ'_r=17.0°, c'_r = 1.40 lb/in^2(saturated)
Bh1	seatearth	52.00 -54.70	ϕ'_p=36.5°, c'_p = 0.82 lb/in^2(saturated)
Bh2	lower siltstone	34.00 -37.00	ϕ'_r=28.0° (saturated ϕ'_r=35.0° (non-saturated } pre-split

* visually weathered horizons

3.14 Shear strength parameters

Apart from the shallowest borehole 3 specimens of dark shale the triaxial test results (Table 3.9 show that failure took place at very low volumetric strains. It is important to record however, that at failure all specimens were dilating. The shear strength parameters (Table 3.11) generally bear out the principal stress difference groupings. The results for the near surface samples of dark shale (borehole 3, $\phi' = 26.0°$, $c' = 0$ lb/in^2; negative volumetric strains up to 10%) suggest that this horizon, and possibly the mudstone nearest to ground level in borehole 2 (composite results - Table 3.11), are the only horizons in which over-consolidation characteristics have been largely eliminated during weathering. Particle size distributions (Fig. 3.2) confirm that these latter samples have a high sand content on the M.I.T. scale - medium diameters of borehole 2 mudstone, borehole 3 shale are 1.0 mm and 0.7 mm, respectively. (c.f. with 10 mm for borehole 2 dark shale, 22 ft - 25 ft, Fig. 3.2). Even so the dark shale peak ϕ' is some 11.5 degrees higher than the residual ϕ' value for the intact non-weathered rock. In contrast to the shallowest mudstone-shale horizons the equivalent upper siltstone and seatearth triaxial parameters are conspicuous by their high cohesions. Using the Figure 3.9 parameters as a very rough guide the drop in strength from weathered rock to 'soil' (low value shale-mudstones) may entail a fall-off in ϕ' of about 37 per cent accompanied by a large drop in cohesion of over 93 per cent. Similarly, on the assumption that the 'near origin' (apparent) c/ϕ values are proportional to the 'conventional' extended Mohr envelope values it can be demonstrated from Table 3.9 that the change from unweathered to weathered quartz-rich lower siltstone could involve a drop in cohesion of between 85 and 95 per cent, whereas ϕ only falls by about 10 per cent ($c = 99$ to 301 lb/in^2, $\phi = 30.5$ to 34° - calculated conventional parameters,

weathered siltstone, borehole 3).

The shear box results introduce the problem of anisotropy in these thinly-bedded and laminated rocks*. In certain instances failure took place along stratification planes and in other instances the material undoubtedly behaved as an aggregate; cohesion values are negligible (Tables 3.9 and 3.11) in comparison with the triaxial tests. Similarly, the peak $\emptyset'$ values are lower than non-saturated triaxial suites, but in the case of weathered seatearths the saturated peak $\emptyset'$ is not greatly different from the unweathered shear box results. Based on shear box tests alone there is apparently little difference in strength between weathered and unweathered seatearth.

An argument in favour of considering higher strength rocks (in this case quartz-rich lower siltstones and non-plastic gradational seatearths) in terms of an extended Mohr envelope is borne out by the compatibility in $\emptyset'$ peak (Mohr envelope Fig. 3.10)and $\emptyset'$ residual (pre-split non-saturated results Tables 3.9 and 3.11). An unexpected feature of the lower siltstone specimens however, is the statistically highly significant response to low confining pressures. Although it would normally be expected that a rock of this type would not be sensitive to such low cell pressures the composite plot of Mohr circle 'top points' implies that for these high compressive to tensile strength rocks the envelope is both linear and exceedingly steep adjacent to the origin.

An elevated quartz content (see Fig. 3.7) and the presence of non-uniformly distributed carbonates both influence the peak strengths of these unweathered-weathered lithologies. Another mineralogical relationship that is emerging concerns the effect of quartz on residual strength. The results

* Stratification by thin silty layers is a feature of the seatearth and some of the aforementioned difficulties in elucidating mineralogical variations in this horizon are due to this textural feature.

FIGURE 3.10

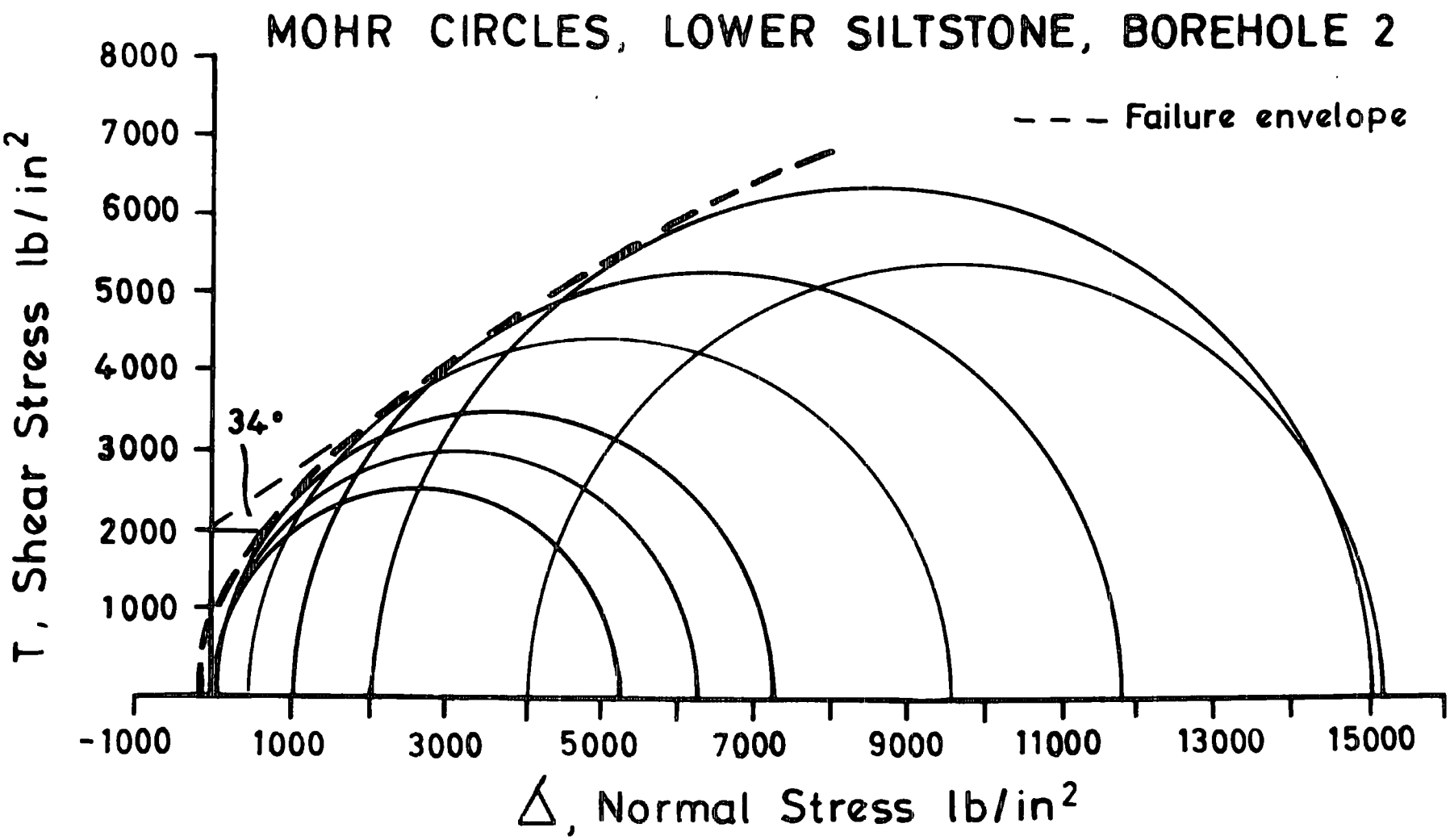

FIGURE 3.10

Figure 3.11

Relationship between ϕ'_r (c'=0) and quartz to clay minerals ratio

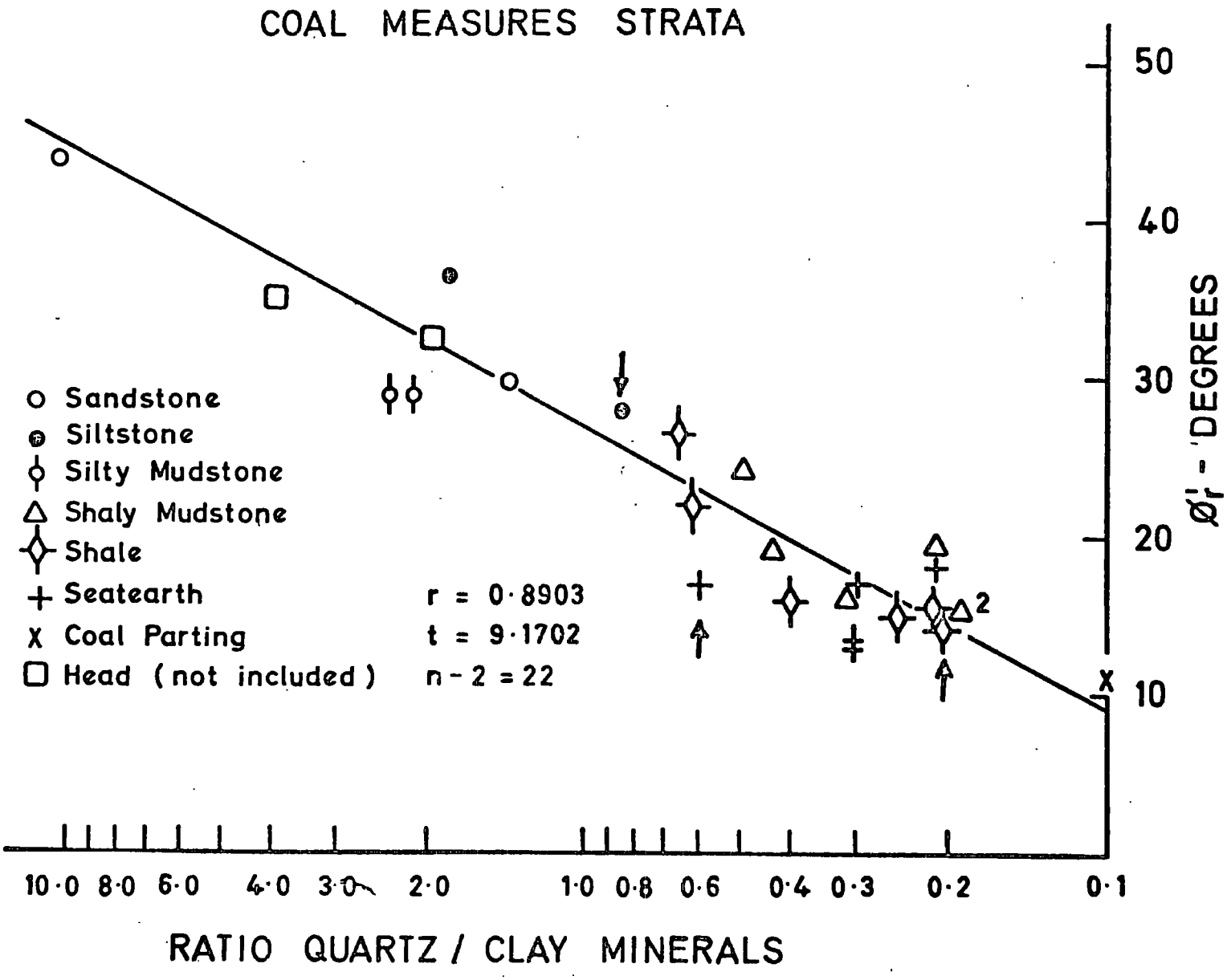

FIGURE 3.11

to date (Fig. 3.11) show a very marked covariance between ϕ'_r (c' assumed zero) and the logarithm of the quartz to clay minerals ratio. On Fig. 3.11 three samples from the current profile are depicted by arrows, together with other samples mainly from the East Pennine coalfield, and in various stages of weathering.

The specimens originated from a) Neepsend, Sheffield - 6, b) measures underlying Markham tip, Derbyshire - 6, c) Chesterfield, Derbyshire - 8 (including Head) d) Lumley, Hett and Finings opencast site, Co.Durham (coal parting) - 3.

The quartz to clay ratio was determined from smear mounts using the integrated areas of the 4.26 Å quartz reflection and the 7 Å plus 10 Å clay minerals reflections. Because the degree of crystallinity of the clay minerals in the samples varied no attempt was made to apply a truly quantitative technique.

Skempton (1964) showed that the residual strength was attained when movement along the shear surface was sufficient to orientate component clay (sized) particles along the failure surface. His results showed that ϕ'_r decreased with increasing clay content. It is believed from this initial work that as the content of resistant equant habit minerals (dominantly quartz) increase so the attainment of preferred orientation is impaired. The recent work of Kenney (1968) implies that ϕ'_r is a function of both clay content and more importantly the specific mineralogy of the samples. From this latter work it is very clear that there are considerable inherent difficulties involved, and in these Coal Measures rocks more detailed mineralogical and orientation studies are necessary before the full implications are realized, particularly when dealing with progressively weathered lithologies and aggregated sediments (for example Chandler, 1969).

3.15 Deformation modulii

Two modulii were determined from the stress/strain curves, the tangent modulus, E_i, and the secant modulus at half failure stress, E_s (Table 3.9). Apart from the lower siltstones, and to a lesser extent the seatearths, both E_i and E_s values show a general increase with confining pressure. This increase is in agreement with Price's (1958) findings for Coal Measures rocks subjected to much higher confining pressures. The shallowest horizon of a particular rock type tends to have E_i values which are greater than corresponding E_s values, whereas for the deeper horizons E_s values are greater than E_i. These relationships are purely a function of the shape of the stress/strain curve and using Hendron's (1968) terminology E_s is greater than E_i for 'plastic-elastic' stress/strain curves and E_i is the greater for 'elastic-plastic' types.

The most striking features of the deformation modulii are, a) the order of the values determined and b) their apparent sensitivity to weathering. In comparison with collected values for Coal Measures strata such as those given by Price et al. (1969) for intact, dominantly small specimens, all the current values fall below their minimum of 1.2×10^6 lb/in^2, which was for a Nottinghamshire Coal Measures mudstone. On the other hand the current tests are much more compatible with Meigh's (1968) conclusions which were based on Plate Loading Tests and are therefore probably more typical of the rocks en masse. With the exception of the unweathered shale-mudstones, and remembering the gradational nature and terminology of different authors, the general order of agreement for the other rock types is reasonably good (Table 3.12).

TABLE 3.12

Comparison of Deformation Modulii

Rock Type	Rounded Means (E_s, lb/in^2)	Rounded Values Meigh, 1968 P.L.T. lb/in^2
Unweathered sandstone		1.9×10^5
Unweathered Lr. siltstone (high quartz)	2.4×10^5	
Unweathered shale-mudstone	4.3×10^3	2.8×10^4
Weathered sandstone		2.2×10^4
Weathered Lr. siltstone	2.3×10^4	
Weathered shale-mudstone		3.1×10^3
Weathered mudstone and upper siltstone	1.0×10^4	
Decomposed products		1.5×10^3
Shallow shale-mudstones	2.9×10^3	

The secant modulus has been plotted against the principal stress ratio at failure on Figure 3.12. The two extremes (non-weathered siltstones and soil-like shale-mudstones) span some two orders of magnitude, and the drop from unweathered to weathered siltstone/seatearths is more than one order of magnitude. The low E_s values of the unweathered dark shale are probably a function of fissility and small-scale jointing discussed in the earlier part of the thesis. In contrast the less fissile coarser-grained weathered mudstone, upper siltstone and typical seatearth specimens have very similar mean E_s values.

FIGURE 3.12

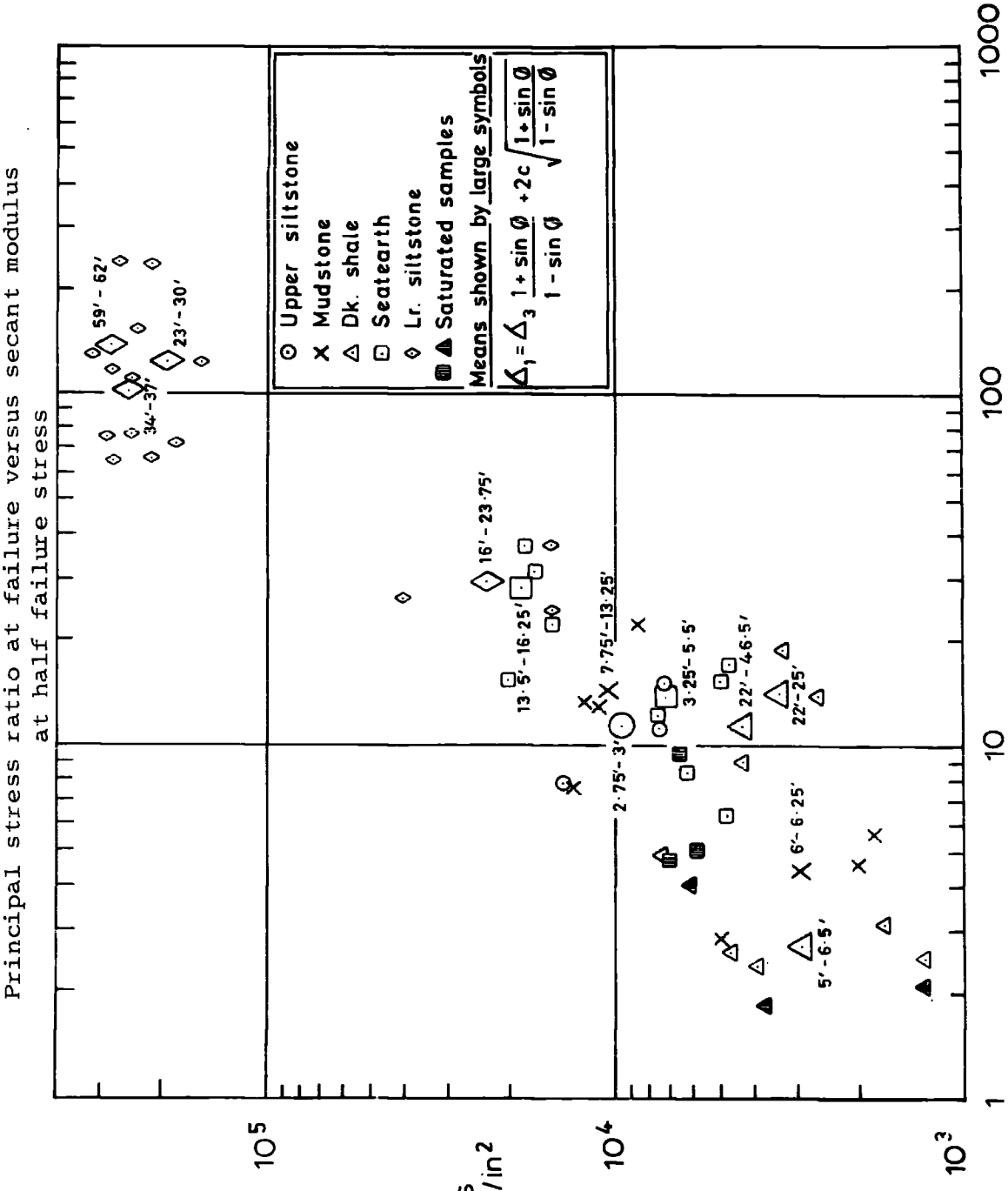
Figure 3.12
Principal stress ratio at failure versus secant modulus at half failure stress
Upper siltstone
Mudstone
Dk. shale
Seatearth
Lr. siltstone
Saturated samples
Means shown by large symbols
$\Delta_1 = \Delta_3 \frac{1+\sin\phi}{1-\sin\phi} + 2c\sqrt{\frac{1+\sin\phi}{1-\sin\phi}}$
59' - 62'
34' - 37'
23' - 30'
16' - 23·75'
13·5' - 16·25'
7·75' - 13·25'
2·75' - 3'
3·25' - 5·5'
22' - 46·5'
22' - 25'
6' - 6·25'
5' - 6·5'
E_s lb/in^2
10^5
10^4
10^3
1
10
100
1000
$\frac{\Delta 1}{\Delta 3}$

3.16 Conclusions

Although based on a limited number of samples the evidence presented shows that structural changes due to weathering of the detrital mineral complement are very limited indeed below the sub-soil level. Chlorite is partly decomposed within the zone characterized by silty-clay with lithorelicts (about 6 ft from the surface). Very small weathering effects have been detected in the 10 Å minerals but these are so minor that they are almost completely masked by the natural variations which occur within the profile.

Unlike the detrital minerals the two principal non-detrital types (pyrite and siderite) are at least partly decomposed within the lithorelicts zone. Even so siderite is relatively stable, as anticipated, below 3 ft in depth. Oxidation of pyrite in particular could well aid rock breakdown but it is certainly not a primary control. If it were, the depth of clay-silt development should be greater in the boreholes where the original content of pyrite was high; this is not the case. In fact the depth to which bedding planes and joints have separated to produce intense fissuring is between 20 and 24 ft, irrespective of rock type. Within this zone and below 6 to 8 ft pyrite is still present.

The Casagrande classification based on the liquid and plastic limits bears out the visual rock descriptions; the values for samples from the zone of clayey silt with lithorelicts conform with mineralogical stability of the dominant detrital fraction in that they show no consistent variations that can be attributed to weathering. Both the limits and specific gravities are influenced by quartz content, the mean specific gravity values increasing from shale through mudstone and seatearth to siltstone. In contrast, the only density variations which might be ascribed to weathering are for the lower siltstone and even these variations are more readily interpreted in

terms of the frequency of discontinuities due to disparity in sample size, and possibly small changes in quartz content. Standard Penetration Tests carried out in both weathered and unweathered (though fissured) shales are very low for unweathered rock. These values are undoubtedly a reflection of fissility and as the shales pass upwards into weathered mudstones, the S.P.T. values do increase as the fissility decreases. The mudstones also have a higher quartz content and a more isotropic texture.

Because the samples were extracted from depths not exceeding 62 ft below ground level low confining and normal pressures were used for the consolidated-drained and undrained triaxial tests and shear box tests, respectively. The ranges used which bracket the low in situ stresses are more applicable to the near surface zone than the extended pressures customarily used for laboratory tests on rocks. If the principal stress difference at failure for the lowest confining pressures (minimal specimen support) are considered as uniaxial values it is evident that the most highly weathered equivalents of both lower siltstone and dark shale show a strength decrease of around 90 per cent when compared with the unweathered parental rocks.

The derived values of cohesion c, and internal friction ϕ, from the reduced major axis regression fit to the Mohr circle 'top points' demonstrate that the envelope is exceedingly steep adjacent to the origin (enhanced ϕ values), particularly for the more brittle lower siltstones and gradational seatearths of high compressive to tensile strength. Limited conclusions can again be drawn regarding weathered/non-weathered strengths. The upper siltstone, fragmental mudstone from 7.75 ft to 13.25 ft in depth and the more typical seatearth specimens (3.25 to 13.00 ft below ground level) give individual and composite shear strength parameters within the range ϕ'=36 to 45.5 degrees, c'=19 to 26 lb/in^2. In other words the cohesion values approach those usually quoted for very soft rocks, the intergranular friction values

being in line with those jointed shales and siltstones (Hoek, 1970). Based on the above results the shear strength parameters for the shallowest fissile mudstones and shale samples (albeit from the clayey silt with lithorelicts zone) show a fall in $\emptyset$ of up to 37 per cent and a drop in cohesion of around 93 per cent. Non-weathered to weathered quartz-rich lower siltstones show a similar large fall-off in cohesion, whereas $\emptyset$ only changes by about 10 per cent. In general only the shaly specimens have shear strength parameters which are characteristic of soil development. It is also important to record that the rounded means of the secant modulii (E_s) are not greatly different for the unweathered/weathered shales, whereas siltstone equivalents are an order of magnitude apart.

The seatearth is somewhat enigmatic because it is gradational with the lower siltstone and also because the shear box results are greatly influenced by silty stratification development. The cohesion values obtained from these latter tests are very small indeed. However, the residual angle of internal friction is little more than 50 per cent of the peak value.

It should be emphasized that for all the specimens tested in the laboratory the overall chemical and mineralogical changes are small so in situ physical breakdown is the dominant feature. With respect to colliery tips these shear strength parameters of in situ weathered strata do raise certain implications. The peak internal friction value, $\emptyset'$, of the shallow shale specimens is only 26 degrees ($c' = o$). It could be argued that this again is approaching twice the residual value. The residual value, however, was determined on pre-split non-weathered intact shale specimens which mineralogically under the microscope show a high degree of preferred orientation parallel to the fissility. Moreover, the initial work on Coal Measures rocks infers that the low residual angle of internal friction of this parental rock is influenced by the low quartz to clay minerals ratio (Fig. 3.11). Breakdown during weathering of the parental

rock will produce a new set of conditions in that the clay minerals in the particulate material produced will have to re-orientate once again in order to attain residual conditions. The Aberfan shear plane material (Bishop et al., p.58) demonstrates that this may well happen in colliery tips under large strains. What is perhaps more pertinent to the present results is that the peak ϕ' value of the degraded fissile shale is considerably lower than the peak values of 34.5 to 35 degrees which have already been reported for compacted shale fill used in the Burnhope and Balderhead dams (Chapter 1). The fissile shaly rocks of the Wales profile have been exposed to weathering conditions for about 10,000 years. Can weathering of highly fissile roof rocks (or initially plastic seatearths) within the body of a spoil-bank produce such low values during a relatively short time interval? The following investigations of colliery spoil (Chapters 4 and 5) resolves this question.

CHAPTER 4

THE CHEMICAL, MINERALOGICAL AND GEOTECHNICAL CHARACTERISTICS OF AN ANCIENT COLLIERY TIP

4.1 Introduction

The colliery spoil of Tip 7, Aberfan, was of recent age, much of it being less than 8 years old (Bishop et al., 1969, p.21). Long-term weathering effects in ancient colliery tips will be superimposed on comminution due to regrading, and possibly upon the effects of spontaneous combustion. However, it is important to consider discard which may well have reached an ultimate stage of degradation; the 100-year-old Brancepeth tip at Willington, Co.Durham provided such an opportunity. This conical heap (Plate 4.1) contained the discard from six seams (Table 4.1), and was emplaced on the northern flank of the buried channel of the River Browney on top of fluvio-glacial laminated deposits (probably similar in nature to sample 8, Table 4.2), the topographical gradient being about 1 in 18.4 from north to south.

4.2 History of the heap

The evolution of the heap can in part be resolved from ordnance sheets dated 1898, 1924 and 1938 (Fig. 4.1), together with the aerial survey taken just prior to reclamation in 1967 (Fig. 4.2). By 1938 the heap would appear to have reached almost its full areal extent of 24 acres and the National Coal Board's records point to the later development taking place across a regraded profile of the older section. Observations using stereo-pairs (Plate 4.1, aerial photographs dated May 1968) show that the northern edge of the tip was at that time impinging on what appear to be old tailings lagoons (marked by arrows on Plate 4.1). Similarly, along the south eastern margin of the heap, an older plateau is clearly visible (Plate 4.1). Outlined in black on Plate 4.1 is a loose superficial mass of spoil which

Plate 4.1

Brancepeth tip (Aerial photograph, 1948)
arrows-probable tailings ponds; probable failed spoil outlined in black

PLATE 4.1

FIGURE 4.1

O.S. 2nd EDITION OF 6" 1898

O.S. EDITION OF 6" 1924

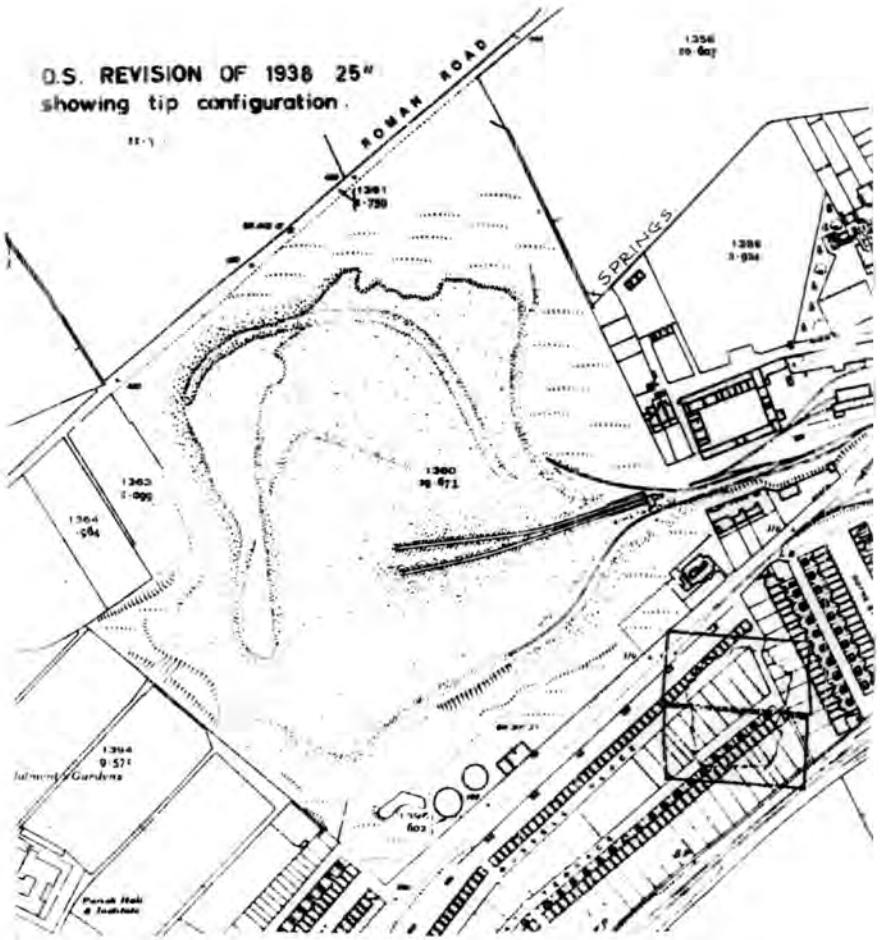

FIGURE 4.1

FIGURE 4.2

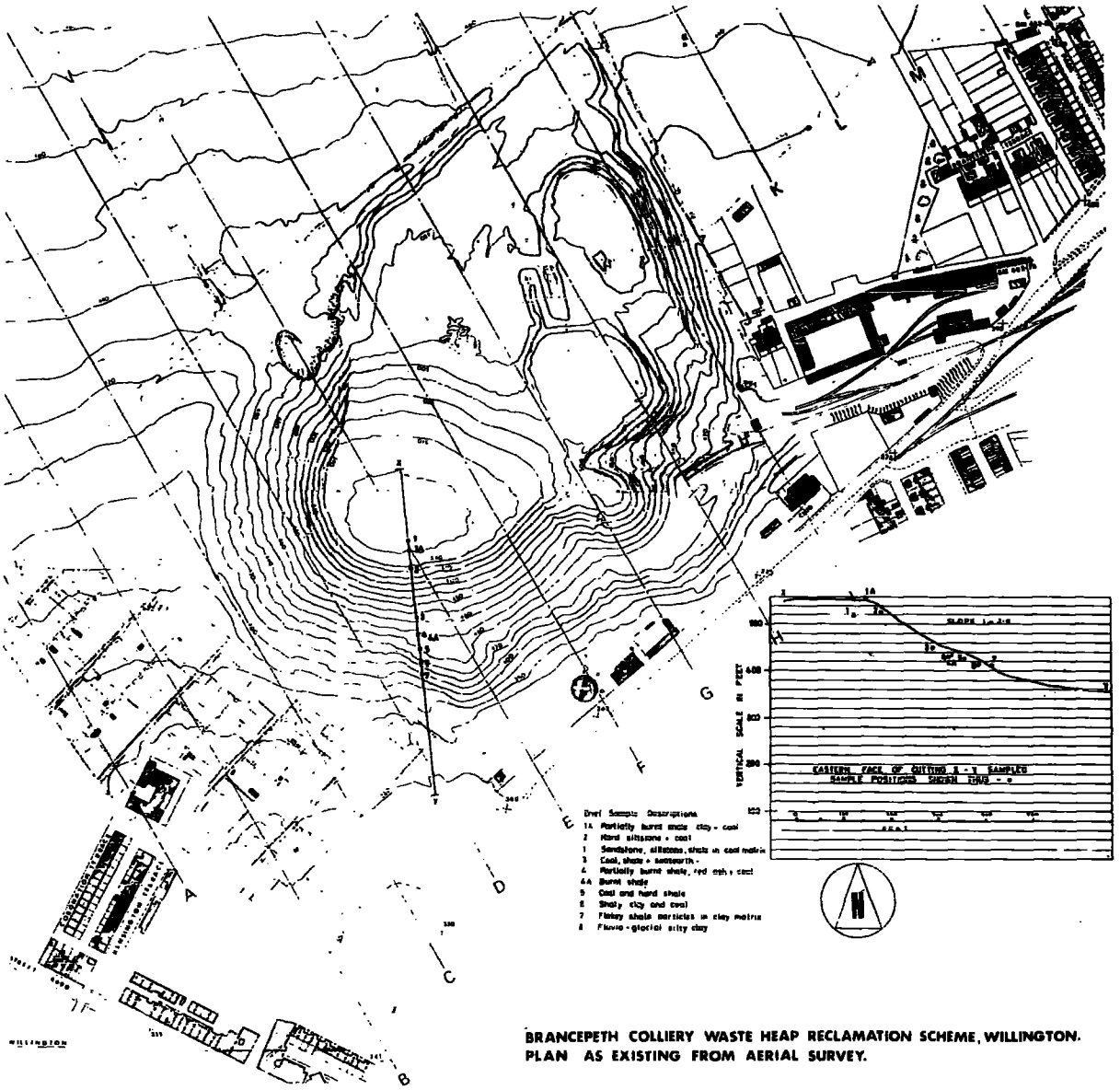

BRANCEPETH COLLIERY WASTE HEAP RECLAMATION SCHEME, WILLINGTON.
PLAN AS EXISTING FROM AERIAL SURVEY.

is thought to be the debris from a superficial failure which was causing concern at that time. According to the National Coal Board's records the apex of the heap was 640 ft A.O.D. in early 1949, but aerial photograph measurements by the author (parallax bar) suggest a discrepancy of 10 to 15 ft (see Fig. 4.13). In all probability this discrepancy is a function of ground slope which may have been ignored by the Board in their height measurements of spoil (sensu stricto).

In 1949 the quantity of spoil was 3 million tons and because of minor instability 30,000 yd^3 of material was removed from the crest and deposited at a lower level. Further regrading took place in 1961 and a further 40,000 yd^3 of spoil was re-distributed. Tipping ceased in the late nineteen fifties when the colliery closed; the shape of the heap and disposition of spoil was as shown on Figure 4.2 when the County Planning Authority commenced reclamation in December 1967.

4.3 Sampling

Undisturbed 4in diameter sample tubes (U4's) were driven at suitable points along the eastern face of a deep cutting which was driven through the heap along the line X-Y shown on Figure 4.2. The gradient of the base of the cutting was about 1 in 5, so exposing a face about 40 ft high in the middle of the heap. It can be seen from Table 4.2 that secondary minerals and combustion products are very common in this material which is representative of a superficial zone of up to 17 ft in thickness. At the location from which the samples were taken (Figs. 4.2 and 4.13) no direct evidence of 'bedding' was recorded, nor was there any indication of instability. In vertical succession samples 3 to 6 had certainly not been disturbed in the recent past but a lateral auger hole in the vicinity of sample 7 encountered more highly degraded spoil (similar to sample 6) at a depth of 5.5 ft. The former sample was probably derived from a higher level.

TABLE 4.1

National Coal Board records relating to seams which have contributed to Brancepeth tip

	SEAM	RANK	EARLIEST RECORDED WORKINGS	NATURE OF WASTE MATERIAL
LOWER COAL MEASURES	HARVEY (N)	401	1909/13	Roof - Mainly shale; some sandstone
	TILLEY (P)	401	1916/17	Roof - Mainly shale; some sandstone
	TOP BUSTY (Q1)	301/401	Ancient	Floor - Seggar (seatearth) and sandstone
	BOTTOM BUSTY (Q2)	301/401	1931/32	Roof and Floor - shale and seatearth
	THREE QUARTER (R)	301/401	1925	Floor - Shale and seatearth
	BROCKWELL (S)	301/401	Ancient	Roof and Floor - Sandstone, shale and seatearth

TABLE 4.2

Sample descriptions

Sample 1A (Surface skin since 1961; previously within body of heap)

Angular fragments of partly burnt hard grey fissile SHALE in a matrix of grey shaly CLAY and fine COAL.

Sample 2.(14 ft below top of heap)

Angular to sub-angular fragments of pale grey finely laminated SILTSTONE and COAL. Traces of powdery white and brown decomposition products.

Sample 1 (17 ft below top of heap)

Angular fragments of very hard fine grained SANDSTONE, SILTSTONE and black SHALE in a matrix of powdery COAL.

Sample 3 (14 ft from exterior of heap)

Grey and black fissile SHALE, COAL fragments, SEATEARTH and a powdery white decomposition product.

Sample 4 (Sample 4A is a red shale development; 14 ft from exterior of heap)

Medium hard angular fragments of partly burnt dark SHALE in a matrix of powdery red ASH, fine COAL and a white decomposition product.

Sample 5 (14 ft from exterior of heap)

Very hard fissile angular black SHALE, bituminous COAL with high concentrations of white and pale brown decomposition products.

Sample 6 (14 ft from exterior of heap)

Mainly grey laminated shaly CLAY, fine COAL and slightly burnt grey SHALE. Traces of white and brown decomposition products.

Sample 7 (Surface skin; probably more recent in age than other lower samples)

Flakey discoidal fragments of fissile black and grey SHALE in a grey CLAY matrix.

Sample 8 (Fluvio-glacial subgrade)

Firm brown laminated sandy clayey SILT with some fine rounded and sub-rounded gravel.

Sample 9 - Water sample.

No water table was encountered in the heap during regrading but along the southern margin of field 1358 (Fig. 4.2, 1938 sheet) a preliminary investigation revealed a number of small springs for which combative drainage measures were designed for the Planning Authority. The origin of the springs was not clear although a 10 ft fault crosses the area some 200 ft to the south and rock-head contours infer that the drift cover may be less than 20 ft thick in the vicinity of the springs (private communication - Mr. G. Richardson, Institute of Geological Sciences). The possibility that a water table existed in the heap immediately prior to reclamation cannot be entirely ruled out and this question will be considered again, later in the text. The level of the conjectural phreatic surface shown on Figure 4.13 conforms with the level of the springs.

4.4 Mineralogy of equivalent strata

Because Brancepeth Colliery had closed more than a decade previously it was not possible to draw straight comparisons between the mineralogy of the tip debris and equivalent underground strata. The N.C.B. Scientific Department collected roof and floor samples from neighbouring South Durham collieries and from these it is possible to draw limited conclusions about the original composition of the tip debris. First of all however, it is very obvious from the X-ray diffraction studies that the lithologies vary considerably. Hence, at Whitworth Park (Table 4.3) the Harvey roof contains a high proportion of mixed-layer clay, whilst at Langley Park kaolinite is abundant. At the former colliery ankerite is the common carbonate, whereas siderite is the dominant species at Langley Park. The Top and Bottom Busty seams have little in common. At Whitworth Park and Esh Winning quartz is abundant in both roof and floor material with muscovite as the principal 10Å species. In contrast, quartz is virtually absent in the Bottom Busty floor of Esh Winning which contains mixed-layer clay, moderately disordered kaolinite and no chlorite.

TABLE 4.3

Mineralogy of equivalent measures represented in the Brancepeth tip (samples from neighbouring collieries)

Seam	Roof	Floor	Colliery	Quartz	Kaolinite	Illite	Chlorite	Carbonate	Pyrite
Harvey	Fossiliferous shale	-	Whitworth Park	X	X	XHI	X	Ankerite (A)	X
Harvey	Shale	-	Langley Park	X	XA	X	-	Siderite	XT
Tilley	Shaly mudstone	-	Bearpark	X	XA	XI	XT	-	-
Top Busty	Shale	-	Whitworth Park	XA	X	XM	X	ND	ND
Top Busty	-	Carbonaceous seatearth	Esh Winning	XA	XA	XM	X	ND	ND
Bottom Busty	Mudstone with plants	-	Esh Winning	X	X	XI	XT	ND	ND
Bottom Busty	-	Carbonaceous seatearth	Esh Winning	XT	XMD	XI	-	ND	ND
Three Quarter	- No information -								
Brockwell	-	Highly carbonaceous seatearth	Esh Winning	XA	X	X	-	ND	ND

HI - High concentration; mixed-layer clay
I - Mixed-layer clay present
M - Muscovite present
MD - Moderately disordered

A - Abundant
T - Trace amount
ND - Not detected

NOTE: The Bottom Busty seatearth from Esh Winning was contaminated with stone dust- gypsum present.

Despite these lateral variations which are common in deltaic sediments like the Coal Measures, the following broad generalizations can be tentatively drawn from Table 4.3:

1) Quartz should be present in about the same proportions as kaolinite and illite.

*ii) Kaolinite is generally well-ordered and may be quantitatively slightly in excess of illite (which is commonly of the mixed-layer variety).

*iii) Chlorite is insignificant.

Quantitative estimates relating to the proportions of roof and floor measures in the tip were not possible and indeed the record of workings is incomplete (Table 4.1). Similarly, sample descriptions (Table 4.2) do not bear out the abandonment records (Table 4.1), particularly with respect to sandstone (c.f. Tables 4.1 and 4.2). It is highly probable that the earliest workings were in the Top Busty and Brockwell seams of the Durham Lower Coal Measures, but all information relating to workings prior to the beginning of the present century are highly speculative (see Taylor, 1968).

4.5 Mineralogy and chemistry of the tip materials

The principal analytical methods used in the Brancepeth work comprise:

a) X-ray diffraction for mineral identification (Table 4.4) and quantitative estimates of quartz and the clay minerals (Table 4.6 Appendix 2), supplemented by thin section observations under the microscope.

b) PW1212 automatic X-ray fluorescence spectrograph for major element oxide determinations on a carbon and water free basis. The results were processed using the computerised matrix correction procedure of Holland and Brindle (1966) - Appendix 1.

* These findings pre-date the X-ray work on tailings samples from British coalfields (Chapter 2). Both lines of research lead to the same conclusions.

c) Carbon train (Groves, 1951) for carbon dioxide and organic carbon determinations; Penfield tube for H_2O^+ and oven drying at 105°C for H_2O^- determinations.

d) Spectrophotometer (Shapiro, 1960) for ferrous iron determinations. This method is suitable for sediments rich in organic matter. The ferrous iron determined excludes that combined with sulphur to form pyrite (FeS_2). Fe_2O_3 (X.R.F.) is adjusted for FeO.

The totals were then normalised to 100 per cent by weight (Table 4.5).

From Table 4.4 it can readily be seen that the mineralogical suite is very different from that of the in situ rocks (Chapter 3), particularly with respect to secondary sulphates and ferric oxides. It is proposed to discuss the mineralogy and chemistry in terms of detrital and non-detrital minerals (including secondary minerals). The discussion on sulphates will not be limited to Brancepeth alone and will include all the work carried out to date, including background information on effects due to spontaneous combustion.

4.6 Detrital minerals

a) Quartz

One of the most significant features of the mineralogy (Table 4.6) concerns the free silica (quartz) values which are much lower than can reasonably be expected in marine and non-marine strata (e.g. Table 3.2; also Taylor, 1971). The most likely explanation is that quartz is being removed, although it cannot be entirely ruled out that the original detritus had a low quartz content. Quartz is virtually absent in the Bottom Busty floor (Table 4.3), but it is most unlikely that this material was a universal diluent, particularly as the first extractions of the seam were in the 1931-1932 period.

The solubility of silica is little affected by pH within the range of 0-9 and Krauskopf (1967) states that ordinarily the silica concentration in

TABLE 4.4

Minerals identified by X-ray diffraction in the Brancepeth tip

Sample	Quartz	Feldspar	Kaolinite	Mica	Chlorite	Calcite	Ankerite	Siderite	Pyrite	Goethite	Hematite	Gypsum	Hemihydrate	Jarosite	Aluminite
1A	X	X	X	X	X	-	-	-	?	-	X	X	-	XT	-
2	X	XA	X	X	-	-	-	X	-	XT	-	-	X	-	-
1	X	XT	X	X	X	X	X	X	-	-	XT	X	-	-	-
3	X	XT	X	X	XT	-	XA	-	XT	-	-	XT	-	-	-
4	X	XT	X	X	-	-	-	-	-	-	X	XA	-	X	-
4A	X	-	-	X	-	-	-	-	-	X	XA	-	X	XA	-
5	X	-	X	X	XT	-	-	-	XT	X	X	-	X	-	-
6	X	-	X	X	?	-	?	-	-	-	XT	XA	-	X	?
7	X	-	X	X	XT	-	-	?	-	XT	-	XA	-	XT	-
8	XA	X	X	X	-	-	-	-	-	-	-	-	-	-	-

TABLE 4.5

Normalized chemistry

Sample	Total SiO_2	Free SiO_2	Combined SiO_2	Al_2O_3	Fe_2O_3	FeO	MnO	MgO	CaO	Na_2O	K_2O	TiO_2	S	P_2O_5	Organic Carbon	CO_2	H_2O^+
1A	37.19	9.01	28.18	20.06	2.47	2.78	0.02	0.65	0.33	0.43	2.34	1.02	1.43	0.15	22.76	0.00	8.37
2	43.09	9.02	34.07	22.26	2.46	2.25	0.03	0.83	0.36	0.24	3.56	1.12	1.13	0.09	15.09	0.14	7.35
1	28.49	3.74	24.75	15.89	5.10	1.68	0.08	0.58	0.88	0.27	2.00	0.72	3.43	0.12	32.88	2.64	5.26
3	27.90	2.47	25.43	16.79	3.85	3.17	0.18	0.98	3.93	0.20	1.88	0.72	3.67	0.01	26.47	1.38	8.83
4	32.84	4.13	28.71	20.61	4.92	2.25	0.03	0.35	1.95	0.21	1.99	0.80	2.52	0.04	23.41	0.12	7.96
4A	38.83	6.63	32.20	24.34	11.92	1.02	0.77	0.92	7.18	0.28	2.47	1.09	8.19	0.01	0.97	0.00	2.00
5	34.51	3.29	31.22	20.14	3.78	3.16	0.14	0.85	2.92	0.19	2.02	0.94	3.26	0.03	20.45	0.10	7.50
6	30.74	5.33	25.41	18.88	3.64	1.83	0.01	0.48	1.60	0.33	2.41	0.88	3.27	0.09	25.61	2.47	7.76
7	38.00	5.36	32.64	21.00	7.85	2.75	0.02	0.69	2.06	0.24	2.78	0.97	4.44	0.03	11.58	0.00	7.57
Mean	34.62	5.44	29.18	20.00	5.11	2.32	0.14	0.70	2.36	0.27	2.38	0.92	3.48	0.06	19.91	0.76	6.96
Standard Deviation	4.81	2.24	3.31	2.45	2.86	0.68	0.23	0.20	2.03	0.07	0.50	0.14	1.94	0.05	8.92	1.04	1.98
%	66.33	51.15	15.18	14.67	6.62	0.47	0.07	0.79	0.30	1.22	1.84	0.84	0.22	0.02	1.13	0.00	5.46

TABLE 4.5

Oxide/alumina ratios*

Comb. SiO_2/ alumina (Al_2O_3)	Fe_2O_3/ alumina	FeO/ alumina	MgO/ alumina	CaO/ alumina	Na_2O/ alumina	K_2O alumina
1.405	0.123	0.139	0.032	0.016	0.021	0.117
1.531	0.111	0.101	0.037	0.016	0.011	0.160
1.558	0.321	0.106	0.037	0.055	0.017	0.126
1.515	0.229	0.189	0.058	0.234	0.012	0.112
1.393	0.239	0.158	0.017	0.095	0.010	0.097
1.323	0.500	0.042	0.032	0.295	0.012	0.101
1.550	0.188	0.157	0.042	0.145	0.009	0.100
1.346	0.193	0.097	0.025	0.085	0.017	0.128
1.554	0.374	0.131	0.033	0.098	0.011	0.132

*Samples 1A to 7 in same order as p.125.

TABLE 4.6

Clay minerals, mica shape factor, free silica (quartz), sulphate content, adsorbed moisture, hydrogen ion concentration

Sample	Mica wt.%	Kaolinite wt. %	Chlorite wt.%	Mica shape factor	Free silica chemical (1)	Free silica (quartz) X-ray (2)	SO_3 % or ppm (3)	H_2O^- wt%	pH
1A	46.0	18.5	1.5	0.966	9.01	9.2	1.32	0.99	3.5
2	57.5	20.5	0.0	0.313	9.02	8.5	0.83	1.09	3.8
1	31.0	12.5	1.0	0.605	3.74	3.2	0.20	0.54	7.4
3	35.5	10.0	1.0	0.700	2.47	2.8	0.55	0.74	6.6
4	42.5	13.0	0.0	0.571	4.13	4.0	5.73	1.07	4.0
4A	73.5	0.0	0.0	0.321	6.63	6.3	4.24	0.93	4.3
5	54.5	16.0	0.3	0.757	3.29	3.2	1.94	0.48	6.2
6	51.5	14.5	0.4	0.780	5.33	4.6	1.22	0.39	2.8
7	62.5	16.0	1.5	0.525	5.36	4.9	4.51	1.80	2.7
subgrade 8	-	-	-	-	-	-	0.03	-	5.0
water 9	-	-	-	-	-	-	651.7 ppm	-	4.4

(1) Method of Trostel and Wynne (1940)

(2) Quantitative X.R.D. curves - Mr. R.G. Hardy

(3) Samples from in situ density material, not U4's

Figure 4.3

Silica (quartz) solubility data superimposed on solubility/pH stability fields of other oxides (adapted from Loughnan, 1962)

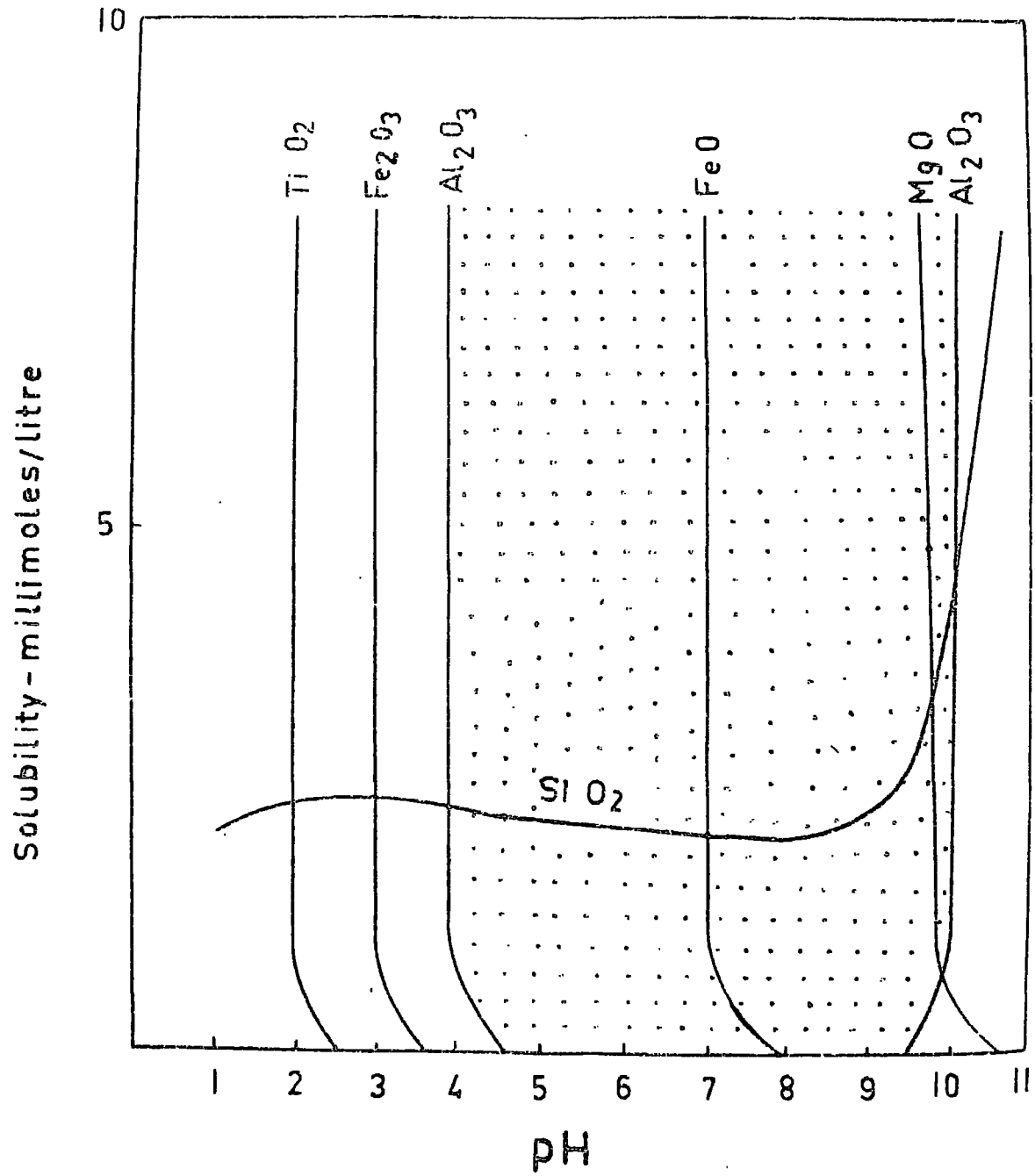

stream water and groundwater lies between 10 and 60 ppm SiO_2, which is well below the equilibrium solubility of amorphous silica (120 ppm). Loughnan (1962) superimposes the silica data of Krauskopf (1959) upon solubility curves of Bardossy (1959) - Figure 4.3. In relation to pH this composite curve shows that in natural environments (pH4 to 10) titania, ferric oxide and alumina cannot be mobilized. Silica maintains a low but constant solubility whereas ferrous oxide is precipitated at values above neutrality. Magnesia is mobile almost to the limit of normal alkaline environments while the alkalies and lime are soluble throughout the complete range. In the present discussion we are mainly concerned with the relative solubilities of silica and alumina (e.g. solubility of clay minerals as well as free silica). Livingstone's (1963) data shows that the solubility of alumina in river and sea water is less than 1 ppm and the highest value recorded by Durum and Hafty (1963) for North American rivers is just over 9 ppm. The assumption that alumina does not change appreciably during weathering is a pre-requisite of weathering calculations (e.g. Krauskopf, 1967, p.103). At Brancepeth five out of nine samples had a pH of 4 or over (Table 4.6). Leached spoil pH values (BS 1377/1967) are only an indication of recent conditions but it is of interest that water issuing from the base of the tip (Table 4.6, sample 9) had a pH of 4.4. This figure is probably more indicative of the pH of the water percolating through the tip. Hence it is probable that on balance the pH of the tip favoured solution of silica relative to alumina.

Hydrogen ion concentration is by no means conclusive, especially as pH values of less than 4 were recorded, and the probability that an aluminium sulphate is present in the oldest sample (Table 4.4) also favours some mobility of alumina. Loughnan (1962) regards leaching by water as the most important single factor controlling mineral breakdown under weathering conditions. Based on the ionic potential concept of Cartledge (1928) it was Goldschmidt (1937),

followed by Gordon and Tracey (1952), who showed that ions can be arranged into three groups according to their valencies and ionic radii: soluble cations, soluble complex anions and insoluble compounds, termed hydrolysates. Importantly, Si^{4+} falls within the soluble cation group which includes Na^{+}, K^{+}, Ca^{2+}, Mg^{2+} and Fe^{2+}, whereas Al^{3+}, Fe^{3+} and Ti^{4+} are hydrolysates which are independent of the leaching potential.

One very important factor controlling mineral degradation at Brancepeth is of course temperature. The burnt shale (sample 4A, Table 4.4) is devoid of kaolinite which would normally imply 'hot spots' with temperatures in the region of 500 - 600°C occurring at some stage in the tip's history. The latter temperatures may well be on the high side however, because De Keyser (1939) found that kaolinite can be completely dehydrated at temperatures as low as 350°C over more protracted time intervals than are customarily involved in short term differential thermal experiments. The present writer considers that the analogy with tropical weathering conditions may not be wholly out of place. In line with Krauskopf (1967) the most reasonable hypothesis is that tropical weathering does not differ essentially from temperate weathering - it simply goes farther towards completion. The clay minerals are not true end products but metastable intermediate alumino-silicates. All reactions of weathering go faster in the tropics because of the higher temperature*, and where conditions of rainfall and topography are particularly favourable for leaching, the reactions go beyond the clay mineral stage. Tropical temperatures are commonly only of the order of 30°C, compared with temperatures of over 70°C (see Section 4.8) at Brancepeth.

It is of interest to note that the effect of temperature on silica (quartz) solubility is dramatic. The collected data of Siever (1962) shows

* A 10°C rise in temperature customarily involves a two or three-fold increase in the rate of chemical reactions.

that a rise in temperature from 25°C to 200°C is mirrored by a solubility increase from 10 ppm to just over 600 ppm. Extrapolating his data to 350°C gives a solubility figure of about 1000 ppm, and at 500°C the solubility is approximately 2,400 ppm.

Taylor (1971) showed that in marine and non-marine shales and mudstones some 40 to 50 per cent of the quartz fraction is of less than 2 microns in size. It will be shown later in the text that it is the smaller particle sizes that are being removed from the Brancepeth heap. There is thus good reason for believing that quartz is being removed preferentially, unless dilution by spoil which is deficient in quartz is responsible. This latter proposition has already been shown to be unlikely and recent ecological work carried out in Durham (Dr. B.A. Whitton, personal communication) lends considerable weight to the opinion that silica may be preferentially removed from colliery tips. Between the months of May to July 1971 the silica concentration in a stream adjacent to Brandon Pit House tip reached over 80 ppm, which is far in excess of Krauskopf's (1967) upper limit of 60 ppm.

b) Feldspars

Feldspars are commonly used as weathering indicators (e.g. Millot, 1970, p.63) but it would be unwise to draw the conclusion from Table 4.4 that they have been decomposed in the lower (older) strata in response to weathering. It is more likely that they were never a component of the original spoil. The only sample with strong X-ray reflections symptomatic of possibly 5 per cent feldspar is sample 2 (Table 4.4), which contains fragments of siltstone.

c) Clay minerals

Difficulty was experienced with both qualitative and quantitative X-ray studies, since peak enhancement due to high coal content occurred in the 3.35Å to 3.40Å region of the diffraction chart. On glycolation,

all samples with a high organic content showed background intensification from the main quartz reflection to about 4.45Å. Similarly, spurious peaks at 20Å or more are thought to be a function of coal content (see also Van Krevelen, 1961, p.326).

Because potassium is also present in jarosite (Table 4.4) the K_2O/Al_2O_3 ratios (Table 4.5) are not solely due to clay mineral variation. Alumina (corrected for organic matter) and combined silica/alumina ratios infer that the total clay mineral content of the samples is reasonably uniform. This does not appear to conform with the quantitative analyses, however (Table 4.6). It is therefore relevant to question the reliability of the latter analyses. One way in which the analyses can be partially verified is by re-calculating the other mineral constituents. Hence, P_2O_5 can be apportioned to hydroxy-apatite, sulphur to acid soluble sulphate and pyrite, CO_2 to siderite (see Nicholls, 1962). Quartz, organic carbon and H_2O^- are already known. Summation of all the mineral species ranged from 95 to 107 per cent, which is acceptable for quantitative clay mineral studies. Reeves (1971) using standards from the writer's collection obtained a range of 95 to 105 per cent for a much larger group of 49 seatearths which did not involve the complication of enhanced coal content. The low ratio of kaolinite to illite in all samples would not have been expected from the mineralogy of the equivalent roof and floor measures and it is therefore very clear that this mineral is subject to temperature and time-dependent oxidation processes (development of combustion 'hot spots' - N.C.B. Technical Handbook, 1970).

Grim and Bradley (1940) showed that illite loses hydroxyl water from the lattice between 200°C and 600°C, whilst still retaining its essential micaceous character. The H_2O^+ value of sample 4A (Table 4.5) confirms that this sample is in accord with these findings, whereas the more normal H_2O^+ values for the other samples infer that they were subjected to generally lower temperatures, which is borne out by other evidence presented later in

the text. The illite shape factors are high and the 10Å reflections exhibited the broad low-amplitude ragged 'two-tailed' peaks, very similar in character to the disordered mica of the insitu seatearths (Fig. 3.3). Another feature of disordered illite is the development of a tail-like extension on the high 2θ side of the 4.5 Å peak. Because of background enhancement (mentioned previously) this feature could not be resolved. Disordered micas commonly adsorb potassium and are consequently re-constituted (Grim, 1968, p.220). The two oldest samples (5 and 6) were immersed in 2N KCl for 17 days and the 10Å peaks compared with the original material. Re-constitution of the 10Å peak was not apparent but a series of small peaks developed with the following d- spacings: 8.78-9.34Å, 9.97-10.37Å, 10.7Å .

Just as in the Wales profile so in the Brancepeth samples chlorite is still present in trace amounts (Tables 4.4 and 4.5). With respect to temperature, residual chlorite is not altogether unexpected because heat treatment at 550°C to 600°C is used to differentiate between chlorite and kaolinite (kaolinite decomposes). However, chlorite is susceptible to acid attack (Brown, 1961, p.85) so it can only be presumed that the original grains were large enough to preclude complete dissolution. Both Taylor (1971) and Reeves (1971) observed that apart from muscovite, chlorite (penninite) was the largest clay mineral present in a wide spectrum of Carboniferous rocks.

4.7 Non-detrital and secondary minerals (excluding sulphates)

a) Pyrite

Pyrite may be present in the coal, or in marine and brackish roof measures (Table 4.3). Oxidation commences immediately the mineral is exposed to the atmosphere (for example Bray, 1951) and it will be recalled that it was the one principal non-detrital mineral which had been completely decomposed in the in situ rocks (Chapter 3). The two Brancepeth samples

in which pyrite was diagnosed with confidence (samples 3 and 5, Table 4.4) contained large coal fragments (see similar organic carbon distributions, Fig. 4.4). It is therefore probably reasonable to conclude that the large coal fragments enabled it to escape oxidation. Its presence in two (possibly three) samples points to temperatures at these horizons being well below 395°C.

b) Carbonates

The calcite in sample 1 (Table 4.4) is unexpected because of its solubility in an acid environment. One possible explanation is that limestone blanketing has been used to combat combustion; this was a common mining practice, particularly during the last war. In contrast the identification of ankerite demonstrates that this mineral, which commonly originates as cleat waste, is able to survive for periods well in excess of 50 years (see Chapter 5). The high CO_2 value of the oldest sample (sample 6, Table 4.5) is a little difficult to account for. The coal in this sample was in an advanced state of oxidation and it is believed that the CO_2 may have originated from this source. Carbonates were certainly well below the detection limit (about 1 per cent) in all the sample 6 smear mounts that were subjected to X-ray diffraction.

The identification of siderite in two (possibly three) tip samples (Table 4.4) is further proof of the stability of ferrous carbonate which can survive in the near-surface zone of weathering for periods approaching 10,000 years (Chapter 3).

c) Iron oxides

Goethite (limonite) is the commonly occurring weathering product of ferrous minerals like siderite and pyrite. Under low temperature conditions it is the normal ferric oxide to be expected. Hematite (hydrated αFe_2O_3) can be formed under low temperature conditions, but in a temperate environment it

is very unlikely to be the dominant oxide. The Brancepeth samples have been subject to temperature fluctuations, and above approximately 250°C goethite begins to decompose, being transformed into hematite under oxidising conditions. Appreciable line broadening is common on X-ray films of hematite derived in this manner but the inequalities are usually eliminated by 600°C (Francombe and Rooksby, 1959).

The comparatively sharp peaks exhibited by sample 4A are in line with a perfected hematite structure and this is further evidence that this horizon has been subject to elevated temperatures. In contrast, the hematite peaks of the other samples are similar to those of samples of tropical red soils.

4.8 Spontaneous combustion and sulphates in colliery tips

The available evidence implies that during this century combustion of colliery tips has been the rule rather than the exception (Carr, 1947).

Tipping of hot ashes (see Chapter 5) may on occasions accidentally ignite spoil, but the principal cause of burning spoil heaps is spontaneous combustion. For burning to occur with visible flame it is normally necessary for the material to be combustible, to reach its specific ignition temperature, and for sufficient oxygen to be available. Oxidation of coal proceeds very slowly at ambient temperatures but increases rapidly as the temperature rises. In essence spontaneous combustion can be regarded as an atmospheric oxidation (exothermic) process in which self heating occurs. This leads to ignition of the coal and other carbonaceous materials, at which point normal burning takes place. Neither oxidation, spontaneous combustion or burning will take place in the absence of air.

In general the lower rank coals are more susceptible to combustion and their higher free moisture content increases the rate of heating at lower temperatures. As early as 1864 it was appreciated that the oxidation of pyrite was not the prime cause of combustion (Lewes, 1912), but the strongly exothermic reaction of this mineral at normal temperatures (for example,

FIGURE 4.4

DISTRIBUTION OF ORGANIC CARBON, BRANCEPETH

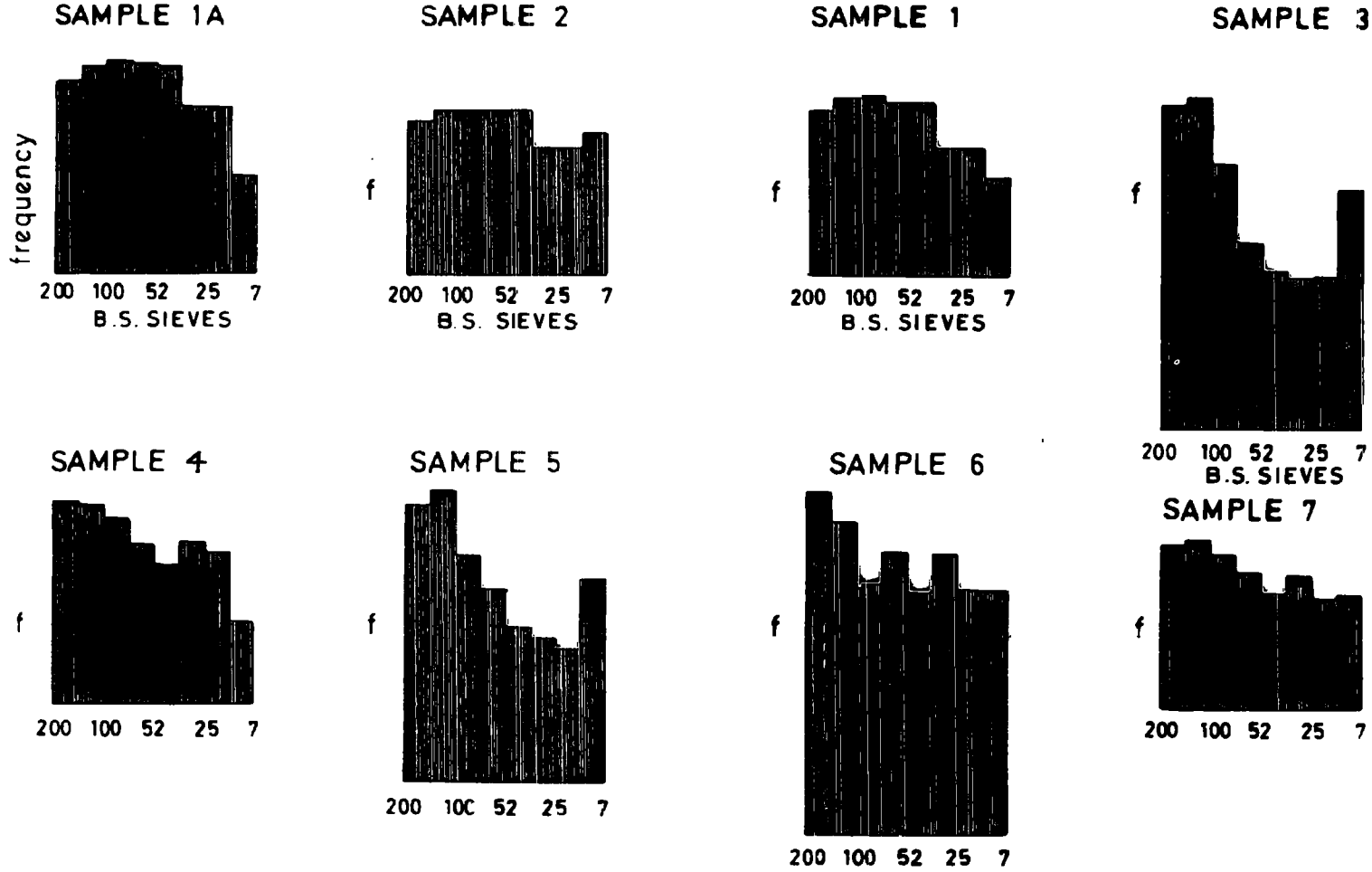

ORGANIC CARBON DETERMINATIONS AT 375°C
(RESULTS SHOWN AS RELATIVE FREQUENCIES)
ALL HISTOGRAMS TO SAME SCALE

FIGURE 4.4

Mr. G.H. Gale, personal communication, Table 4.8, No.2) increases the tendency towards combustion in spoil heaps.

As pointed out in the National Coal Board Technical Handbook (1970, p.65) void size (indirectly particle size and packing) are important controls. With large size material and voids, the movement of air is usually sufficient to carry away any heat generated. It is the intermediate gradings and voids which lead to spontaneous heating and 'hot spots', which eventually break into flame. These zones may be very restricted (as small as 1 to 2 ft in diameter at Brancepeth), and the boundary between burnt and unburnt spoil is usually very sharp indeed. Sample 4, Brancepeth, was driven at such a junction, the sudden change in organic carbon content (Table 4.5) is very marked indeed. The rate of oxidation generally increases as the specific surface increases (i.e. as particle size decreases). It is relevant to note that in the very coaly spoil of Brancepeth (mean organic carbon content, 19.91%) organic carbon tends to concentrate in the finer sieve sizes (Fig. 4.4). Low grade oxidation was used for organic carbon determinations (see Keeling, 1962) because of the protracted time interval involved in the carbon train method. The results are shown as relative frequencies because, although repeatable, the method can lead to inaccuracies of up to 10 per cent absolute.

Once combustion has started the temperature may commonly rise to many hundreds of degrees centigrade, the highest measured temperature reported to the writer being 1350°C (Messrs Blakemore, Kellet and Williams, Darlington, -private communication). The fused, vitreous cores which on occasions are excavated (for example, Fig. 2.1, N.C.B. Technical Handbook, 1970) are undoubtedly the result of such elevated temperatures.

It has already been mentioned that temperature may well be the main control on the ultimate mineralogy (and stability) of spoil. Temperature apparently plays an important role with respect to sulphate species as well.

TABLE 4.7

X-ray confirmation of unusual sulphates in Brancepeth spoil

Brancepeth		Brown (1961)	
d-spacing Å	Relative Intensity	d-spacing Å	Relative Intensity
6.00	10	6.07	10
3.47	8	3.50	9
2.998	10	3.02	10
2.80	9	2.818	10
2.725	3	2.728	5
2.355	4	2.352	5
2.275	4	2.284	4
2.135	5	2.140	8
		1.997	4
1.981	5	1.920	5
1.845	6	1.855	9
1.740		1.735	5
1.706	3	1.700	6

HEMIHYDRATE

Brancepeth		A.S.T.M. Card 10 - 443	
d-spacing Å	Relative Intensity	d-spacing Å	Relative Intensity
5.93	5*	5.94	3
5.70	3	5.71	2
5.09	7	5.09	4
3.675	2	3.66	1
3.52	4	3.52	4
3.10	3	3.11	6
3.078	10	3.08	10
2.960	2	2.97	1
2.855	2	2.87	2
2.55	3	2.55	2
2.275	4	2.29	5
1.98	*	1.98	5
1.94	2	1.94	2
1.903	2	1.91	1
1.831	3	1.82	5
1.54	2	1.54	3

JAROSITE

* Interference from hemihydrate

TABLE 4.8

Sulphate species from in situ and colliery tip materials

(1) MELANTERITE $FeSO_4.7H_2O$	Hambleton Quarry, nr. Bolton Abbey	Quartz-kaolinite in situ shale (Purton and Youell, 1969)
(2) ROZENITE $FeSO_4.4H_2O$	Terra Nova Mine Newfoundland (Mr. G.H. Gale, personal comm.)	Incrustation on massive pyrite (Generation of heat and noxious gases underground. No organic matter associated with the massive sulphide ore body)
(3) JAROSITE and GYPSUM	Tinsley Park Sheffield	In situ weathering of Mansfield Marine Band shale
(4) JAROSITE and kaolinite	Chester South (*) Moor tip	Jarosite growing on bedding planes of dark shale fragments (surface of heap)
(5) JAROSITE and kaolinite	Yorkshire Main tip	Jarosite growing on bedding planes of dark shale fragments (surface of heap)
(6) JAROSITE, GYPSUM, HEMI-HYDRATE ? ALUMINITE	Brancepeth tip	Sulphate species identified by X-ray diffraction
(7) GYPSUM, MAGNESIUM SULPHATE ($MgSO_4.6H_2O$)	Brancepeth spoil in distilled water	Crystals growing on side of beaker after a few days desiccation at room temperature
(8) GYPSUM	Yorkshire Main	X-ray and microscopic examination of spoil from below 10 ft in depth below surface
(9) ANHYDRITE	Creswell tip Derbyshire	White-yellow sublimation zone around cone of burning tip
(10) GYPSUM, ankerite calcite, kaolinite	Yorkshire Main Colliery	Cleat minerals identified in Barnsley Bed coal

(*) Scrapings X-rayed:
a) Surface layer - jarosite and kaolinite
b) partly decomposed - jarosite, kaolinite, 10Å peak
c) unweathered - kaolinite, 10Å peak (including mixed-layer clay)

The highest temperature measured at Brancepeth in the near-surface zone was 20°C (Table 4.11). This temperature is some 5 degrees lower than that of the unburnt section of Yorkshire Main tip (measured at depth over a period of a year), and is obviously lower than the average temperature within the body of the tip. The presence of metastable hemihydrate (Table 4.7) in three samples is interesting because this form of calcium sulphate ($CaSO_4.\frac{1}{2}H_2O$) is produced when gypsum is slowly heated in air at around 70°C. Considering that all samples were from less than 17 ft below the free surface of the heap it is probable that hemihydrate is more stable than is generally thought. However, the important point is that 'background' temperatures of around 70°C can be established.

The other sulphate species identified in the Brancepeth spoil is jarosite (Tables 4.4 and 4.7). This soluble low temperature sulphate has also been identified from in situ exposures and surface tip materials (Table 4.8). Jarosite forms an incomplete isomorphous series between jarosite (sensu stricto), $KFe_3(SO_4)_2(OH)_6$, natrojarosite in which sodium proxies for potassium, and hydronium jarosite $(H_3O)Fe_3(SO_4)_2(OH)_6$ - see Cosgrove and Hodson (1963). According to Millot (1970) the sodium species is rare and all the types considered by the present writer are in keeping with a potassium variety.

Recent work by Sherwood and Ryley (1970) on five Durham tips also points to calcium sulphate being the dominant sulphate in colliery tips. It is therefore appropriate to consider the source of this mineral which is uniformly distributed through the Brancepeth and Yorkshire Main* tips. Generally, it is considered that the sulphuric acid of pyrite oxidation reacts with calcium from the clay mineral lattices, or, with calcite ($CaCO_3$) that is present as fossil debris or as a component mineral (for example, Glover, 1967). From Table 4.8 (Nos. 1 and 2) it is clear that ferrous sulphate (oxidation product of pyrite) is relatively stable and may be the end product if Ca^{2+} or K^+ ions are not available. In nature jarosite may be formed by

*Large enhedral grains of up to 100 microns can be observed under the microscope. These grains are free from corrosion and greatly different from the small grains and aggregates observed in the Brancepeth material.

leaching of potassium from illitic clay minerals (Hartley, 1957) and initial work (Table 4.8, No.4) suggests that the potassium may be derived from the mixed-layer clay component. The clay mineral kaolinite would also appear to be an end-product.

We can establish from Table 4.8 the likely source of gypsum in tips as follows:

a) Pyrite in the coal waste oxidises within the tip and the sulphuric acid reacts with available Ca^{2+} ions.

b) Limestone blanketing material may be a source of Ca^{2+} ions for reaction with a).

c) Stone dust from underground provides Ca^{2+} ions, and some gypsum is also introduced into the tip from this source (e.g. Table 4.3).

d) In the underground environment the sulphuric acid of pyrite oxidation (pyrite from the coal) reacts with secondary carbonates which infill the coal cleat (Table 4.8, No.10).

Sources a), b) and c) are unlikely to result in gypsum being the dominant species and the very convincing evidence from Yorkshire Main suggests that in unburnt tips in particular the mineral is introduced into tips as a waste product. The sequence gypsum, hemihydrate, anhydrite can be explained as purely a function of temperature fluctuation (e.g. Brancepeth and Cresswell tips). Magnesium sulphate which is more soluble than gypsum was also found by Sherwood and Ryley (1970) to be second in importance to calcium sulphate in colliery tips. Its presence as a minor constituent of the Brancepeth material is undoubtedly being masked (compare Table 4.4 and Table 4.8, No.7). The possible occurrence of aluminite ($Al_2O_3 . SO_3 . 9H_2O$) in the oldest Brancepeth sample is in line with Glover's (1967) proposition that an aluminium sulphate is the ultimate species.

The chemistry of the fully burnt shales of Sherwood and Ryley (1970) is cast in a rather different format so for comparisons with the Brancepeth

TABLE 4.9

Chemistry of the burnt shales from Co.Durham (Sherwood and Ryley, 1970) compared with Brancepeth

	Brancepeth sample 4A	Tanfield Lea	Ouston E	Wheatley Hill	Ravensworth Ann	Chester Moor	Trimdon Grange
Total SiO_2/Al_2O_3	1.596	1.840	1.807	2.840	2.098	2.421	2.112
Fe_2O_3/Al_2O_3	0.537	0.123	0.139	0.379	0.172	0.264	0.622
CaO/Al_2O_3	0.295	0.012	0.033	0.021	0.006	0.021	0.293
MgO/Al_2O_3	0.032	0.029	0.026	0.048	0.055	0.042	0.134
Na_2O/Al_2O_3	0.012	0.007	0.006	0.023	0.009	0.019	0.030
K_2O/Al_2O_3	0.101	0.080	0.066	0.156	0.130	0.113	0.129
Acid soluble SO_3 (wt.%)	4.24	0.10	1.39	0.89	1.86	2.82	4.66

FIGURE 4.5

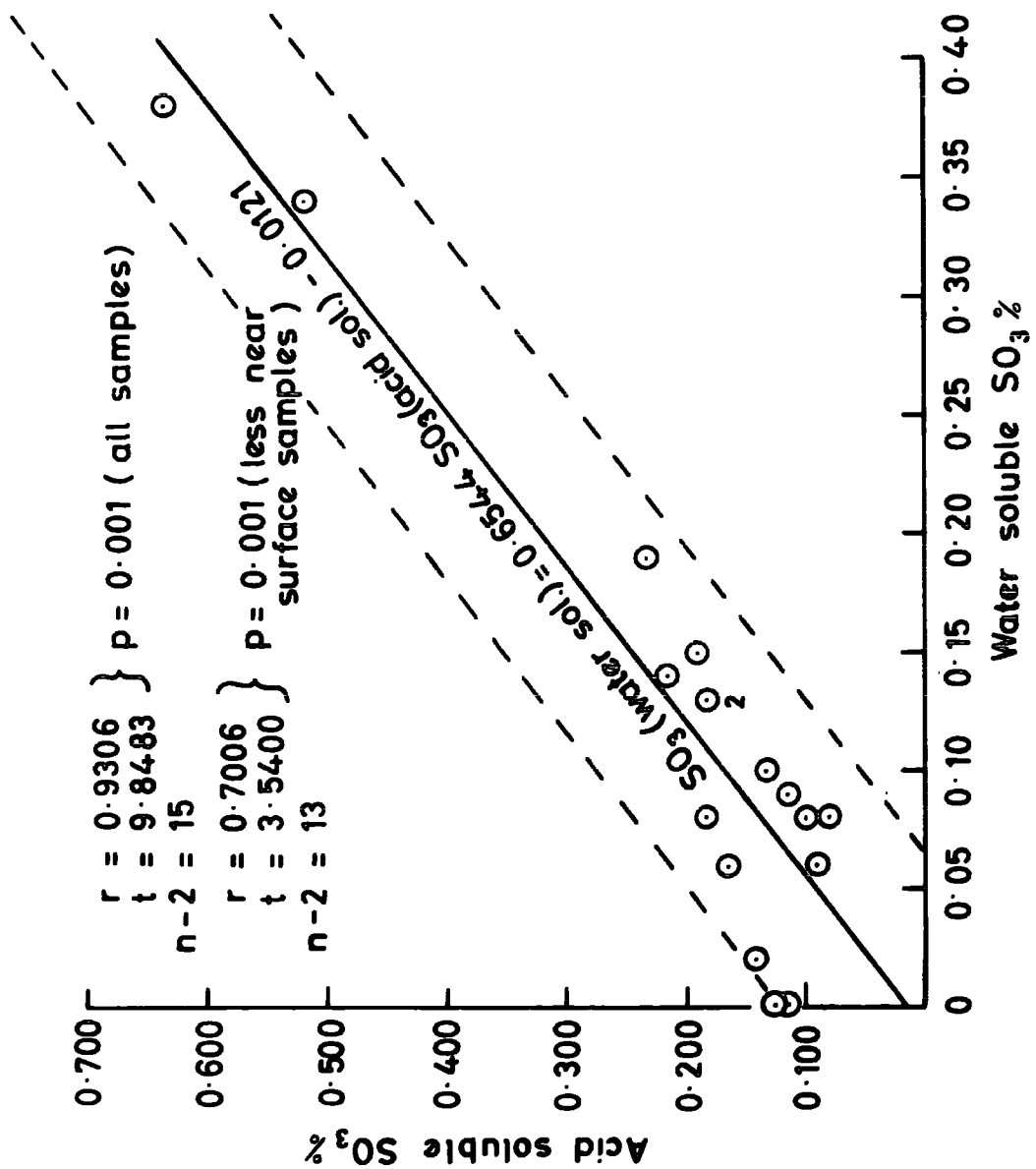

FIGURE 4.5

burnt shale their results are expressed as ratios (Table 4.9). The total silica/alumina ratio of Brancepeth is lower than that of the other shales but it is significant that three of the other Brancepeth samples have higher ratios than Ouston E tip. Similarly, the other oxide ratios for the Brancepeth burnt shale are bracketed by those of Sherwood and Ryley's Durham tips. In other words, the Brancepeth chemistry is unlikely to be greatly different from that of other ancient partly burnt tips in the County.

The high acid soluble sulphate (SO_3) figures for Brancepeth are matched only by Trimdon Grange. If the SO_3 content of Brancepeth, sample 4 is attributed to gypsum a figure of 12.3 per cent results, which is no mean contribution. The acid soluble contents represent all the sulphate that is present and that could, in theory, be leached out by water over a long time interval. This amount of sulphate is unlikely to be removed in practice and the Brancepeth groundwater content (651.7 ppm) is only 54 per cent of the theoretical maximum figure. Six out of the nine Brancepeth samples have a total sulphate content of more than 1 per cent and are therefore unsuitable for cement stabilization (Ministry of Transport Specification, 1969; Sherwood and Ryley, 1970). Similarly, the Brancepeth water sample falls within class 2 of the B.R.S. classification (see Akroyd, 1957, p.55) which means that limited precautions would be necessary if concrete were to be exposed to this water. On the other hand only the two near-surface samples from the unburnt Yorkshire Main tip (Fig. 4.5) have a water soluble SO_3 content in excess of 0.2 per cent which is designated in the B.R.S. classification (also Sherwood and Ryley, 1970) as the lower limit at which sulphates will adversely affect cemented materials. It is of interest to record that acid soluble and water soluble sulphates show a very strong positive association in the Yorkshire Main material (Fig. 4.5), the relationship being of the form:

$$\%\ SO_3 \text{(water soluble)} = 0.6544 \text{ acid soluble } \% - 0.0121$$

The pH of the Brancepeth spoil (Table 4.6) is considerably lower than that of the unburnt Yorkshire Main material (Table 5.6) which is more in line with the earlier N.C.B. reports. It was not appreciated until the post-Aberfan period that low pH values were so common in burnt tips.

4.9 Chemical-mineralogical correlations

Although limited in number it is relevant to consider statistical inter-relationships which should be a reflection of combustion effects. It could be argued that organic carbon should be excluded as the coal simply acts as a diluent. In tips however, (especially partly burnt types) the coal plays an active part and hence it has been included (organic carbon) in the correlation matrix (Table 4.10). The results can be interpreted as follows:

a) In the first place the clay mineral oxides, combined silica, Al_2O_3, K_2O and TiO_2 correlate positively. The correlation of TiO_2 and free silica (quartz) may well be a reflection of their indirect detrital association (Taylor, 1971).

b) Total clay correlates positively with the oxides associated with clay minerals, and hence negatively with the major diluent, organic carbon (coal).

c) MnO follows Fe_2O_3 as in normal sediments (i.e. pyrite). However, the positive correlation of Fe_2O_3 with CaO (which correlates positively at a very high level with S) is a reflection of their sulphate affinities.

d) The negative correlation between the kaolinite/illite ratio and the elements combined as sulphates shows that with oxidation and sulphate development, the kaolinite content decreases. The positive correlation of H_2O^+ with FeO and the negative correlation of H_2O^+ with Fe_2O_3 is yet another pointer towards oxidation processes. The positive correlation of the kaolinite/illite ratio with organic matter and negative association with S implies that kaolinite and coal decrease as oxidation proceeds.

e) CO_2 is apparently following coal, possibly as a constituent of the minerals in the coal cleat.

TABLE 4.10

Correlation matrix - chemistry/mineralogy

	Free silica	Combined silica	Al_2O_3	Fe_2O_3	FeO	MnO	MgO	CaO	Na_2O	K_2O	TiO_2	S	P_2O_5	Organic C	CO_2	H_2O^+	Kaolinite/Illite	Total clay
Free silica										+95	+99							
Combined silica			+99							+95	+99			-99	-99			+99
Al_2O_3											+99			-99	-95			+99
Fe_2O_3						+99		+95				+99		-95		-99	-99	
FeO																+99		
MnO								+99				+99		-95		-99	-99	
MgO																		
CaO												+99	-95				-99	
Na_2O													+95					
K_2O														-95				
TiO_2																		+99
S																-95	-99	
P_2O_5																	+95	
Organic C															+95		+95	-95
CO_2																		
H_2O^+																	+95	

+ and - 95% confidence level, r= 0.6664
+ and - 99% " " , r= 0.7977

f) The positive association of Na with P_2O_5 (which correlates negatively with Ca) is unusual. Possibly, sulphuric acid from pyrite oxidation is breaking down hydroxypatite and the P_2O_5 is reacting with Na^+ from the clay minerals. Sodium phosphate 'beads', originally used in analytical chemistry are very insoluble.

It is an interesting feature of this correlation matrix that MgO plays no part at all.

4.10 Fundamental properties

All the determinations were carried out in accordance with BS 1377/1967. In recent years the National Coal Board has evaluated test results from some 20 laboratories (including Durham) and it has become apparent that modifications to BS 1377 are necessary with respect to colliery spoil. A publication on this subject is now available (N.C.B. Joint working party on soil mechanics testing, 1969), but the current work pre-dates the trial tests. For the sake of consistency the writer has adhered to BS 1377 throughout this thesis.

a) In situ density

In situ densities determined by the sand replacement method, adjacent to the positions where U4's were driven (Fig. 4.2), together with moisture contents and calculated dry densities are given in Table. 4.11.

The dry densities of the material forming the central section of the slope range from 84 to 98 lb/ft^3. It will be seen that these relatively near-surface densities are substantially lower than those from the body of the undisturbed Yorkshire Main tip (Chapter 5, Table 5.7). Brancepeth sample 1A had been compacted by site traffic and it is of interest to compare its density with that of the other surface sample (No.7 - 66 lb/ft^3). It has previously been mentioned that this latter sample was probably derived from a higher level in the slope.

TABLE 4.11

Physical properties

Sample	Air temperature °C	U4 temperature °C	In situ bulk density lb/ft^3	Moisture Content %	Dry density (in situ samples) lb/ft^3	Specific Gravity
1A	8	20	117	11.9	105	2.10
2	-	-	97	5.3	92	2.06
1	-	-	89	6.5	84	1.81
3	8	8.5	103	8.7	95	1.88
4	8	8	97	7.6	98	2.04
4A	-	-	-	-	-	2.54
5	7.5	7.5	106	10.8	96	1.87
6	8	10	102	17.7	87	1.89
7	-	-	79	19.9	66	2.18

The moisture content of the lower samples are significantly higher than the remainder (Table 4.11). Using the applicable specific gravities it can readily be demonstrated that the degree of saturation of samples 5 and 6 are in excess of 95 per cent and it was for this reason that a possible water table was fixed at the level shown on Fig. 4.13. The fluvio-glacial subgrade to the north of the tip is certainly fully saturated, having a moisture content of 30 per cent.

b) Specific gravity (G_s)

The low specific gravity values (Table 4.11) are a function of the high coal content of this tip. It will be demonstrated (Table 4.17) that statistically there is a highly significant negative correlation between G_s and organic carbon. For coarse discard the range of specific gravities collated by the Board (N.C.B. Technical Handbook, 1970) is from less than 1.8 to 2.7. The burnt shale figure of 2.54 is lower than the average value usually attributed to 'soils' (2.65).

4.11 Classification

a) Liquid and plastic limits

The liquid limit, plastic limit, and plasticity index in conjunction with the Casagrande classification system may provide a rough guide to the engineering properties of a material as well as being a more specific means of classification (for example, the cyclothemic rocks of Chapter 3). Limits are determined on the fraction which passes a No.36 B.S. sieve and therefore in many colliery spoils the results may not be particularly significant when this fraction of fine material is low. Some difficulty was experienced with the Brancepeth material in obtaining repeatable plastic limits.

The results (Table 4.12, Fig. 5.6) do however, demonstrate an important feature which will be referred to again when shear strength characteristics are considered. Compared with Yorkshire Main (Fig. 5.6) the Brancepeth spoil is more granular and in fact three points lie below the N.C.B. collation

line. Very generally these latter samples could well be designated as 'non-plastic'.

b) Particle size distribution

With weathered and friable soils such as colliery spoil, it may often prove difficult to obtain a realistic grading curve. Aggregation of particles suppresses the fine fraction during dry sieving whilst water may cause exaggerated breakdown during wet sieving.

In the present study both dry and wet analysis (silt fraction by pipette analysis) are presented - Figures 4.6 and 4.7. From these distributions (M.I.T. system) the conclusion is drawn that suppression of the fine fraction by dry sieving greatly exceeds the effects of water. Samples with a visible silt fraction like 1A and 6 (Plate 4.2) are devoid of fines on the dry sieve basis. The Trask sorting coefficient (So) shows that the 'aggregated' dry sieved spoil is better sorted than the wet analysed material. Hazen's (1892) uniformity coefficient (P_{60}/P_{10} - Table 4.12) which is the grading parameter commonly used in soil mechanics implies that the wet analysed spoil is 'very non-uniform' (Hazen's coeff: < 5 - very uniform, 5-15 medium uniformity, > 15 very non-uniform).

A common practice in geology when studying abraded sediments is to plot cumulative frequency on a probability scale and size on a logarithmic scale (log-probability paper). Log-normal distributions produce a linear plot. Crámer (1946, p.220) attributes the origin of log-normality as being due to removal of random increments from materials of finite size. The size of the abraded material must be appreciably affected by the abrasion process, and this material must be included in the final distribution measurements. However, Kittleman (1964) showed statistically that the distributions of mechanically produced detritus are better elucidated in terms of the Rosin-Rammler law of crushing. He showed that natural materials exhibited a far better linear distribution on Rosin's-law probability scale than on the perhaps more conventional log-probability scale.

FIGURE 4.6

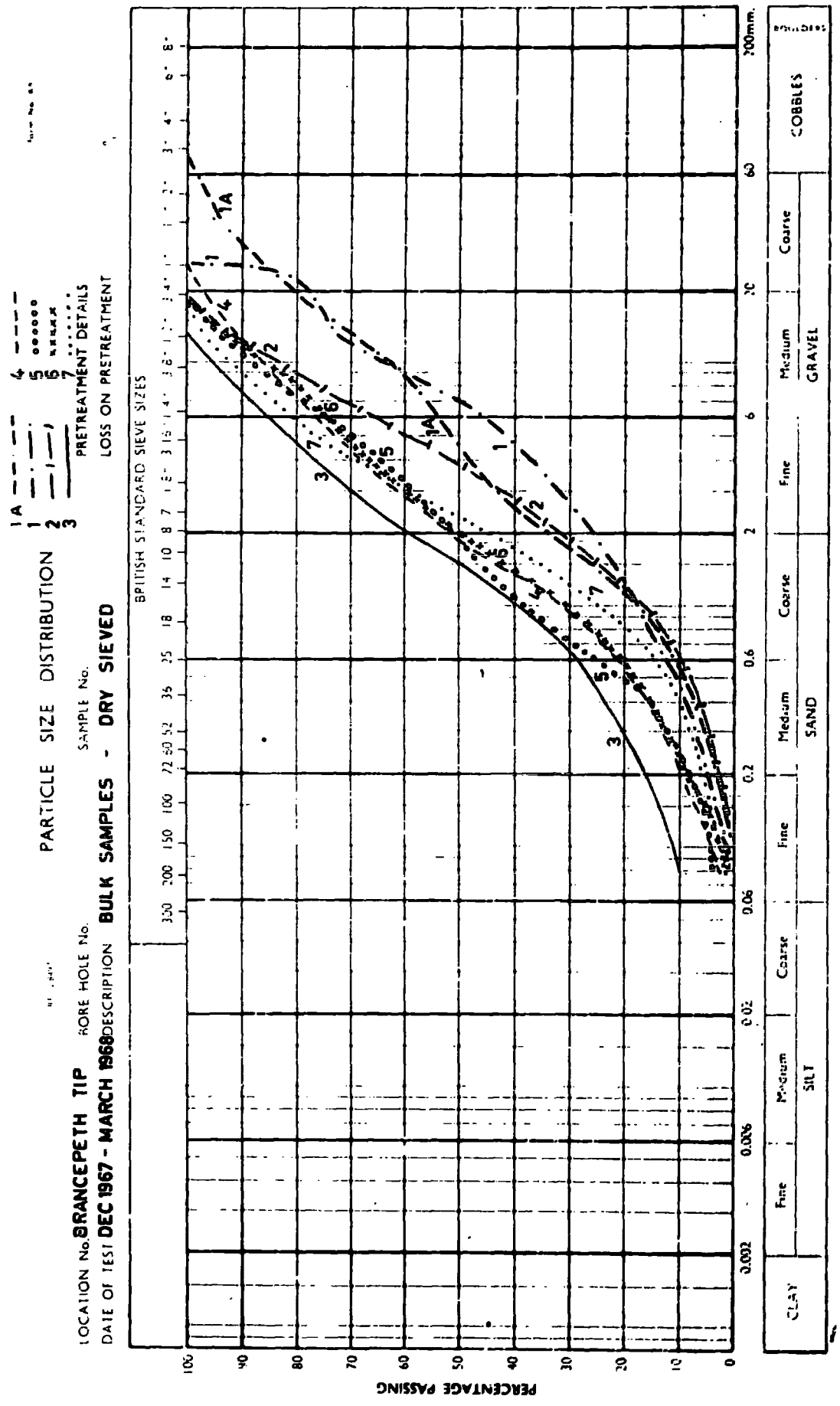

FIGURE 4.6

FIGURE 4.7

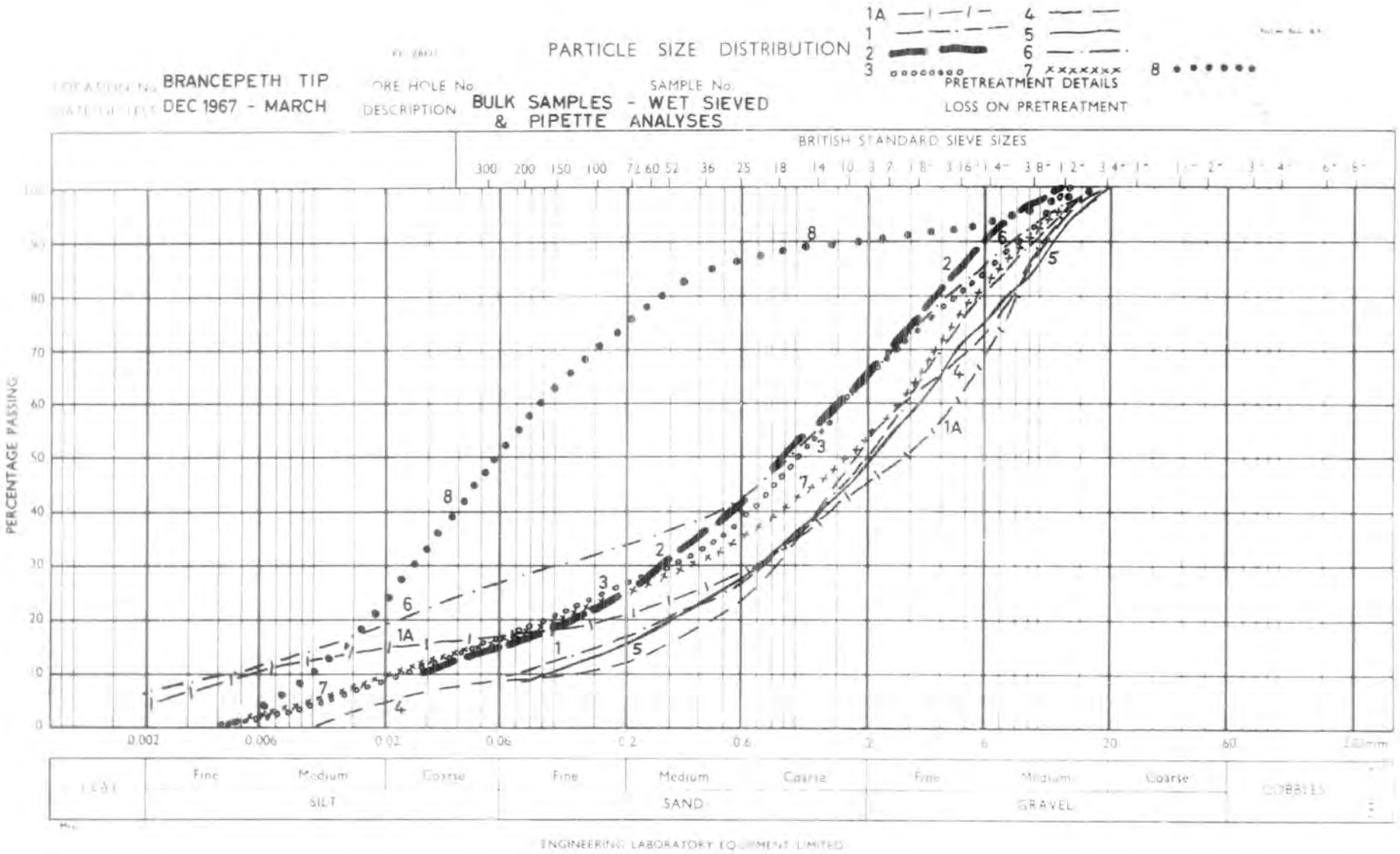

FIGURE 4.7

PLATE 4.2

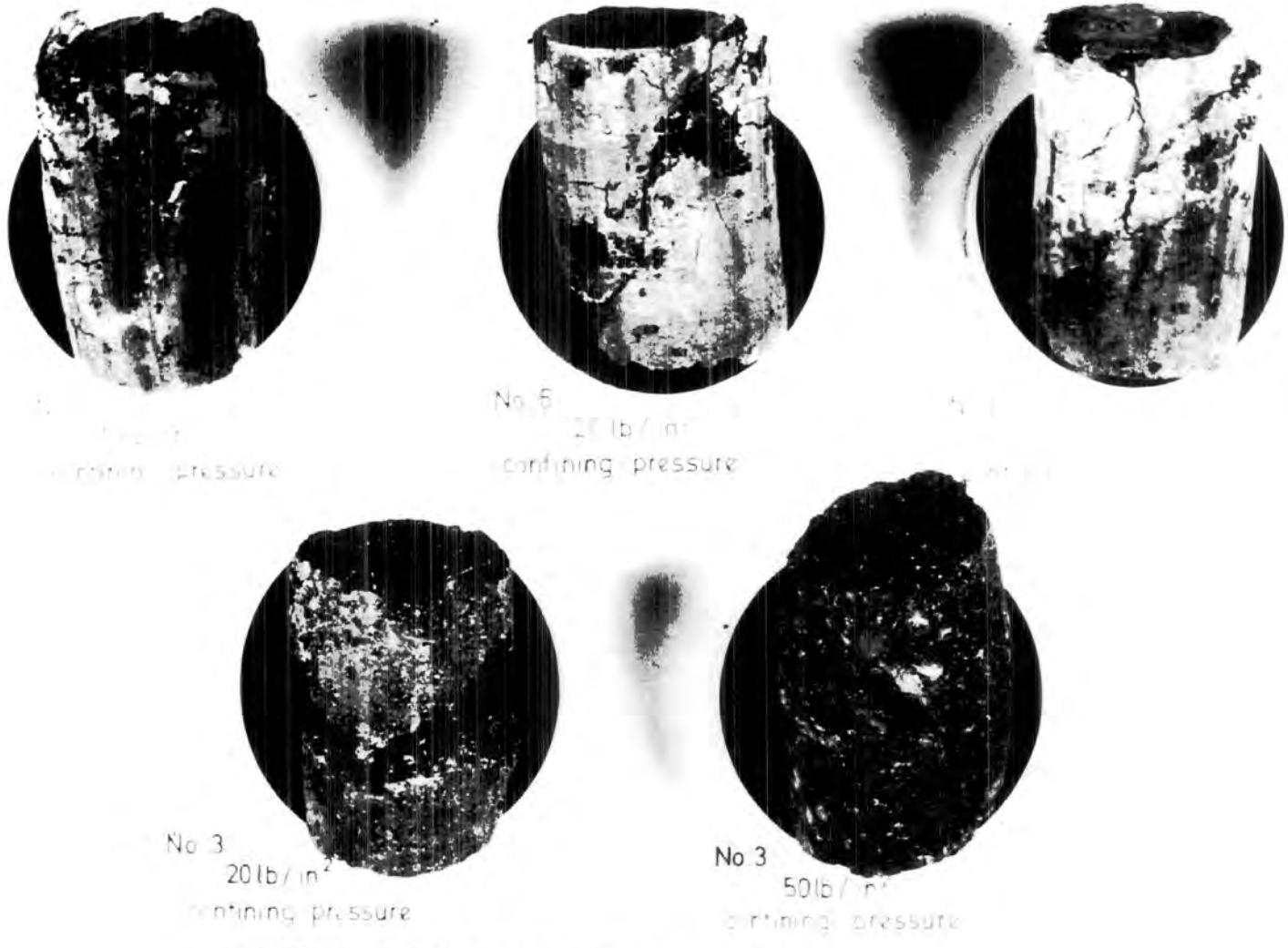

TRIAXIAL SPECIMENS AFTER FAILURE

BRANCEPETH TIP

PLATE 4.2

Figure 4.8

Particle size distribtuions, Brancepeth, dry sieving - Rosin's-Law probability scale.

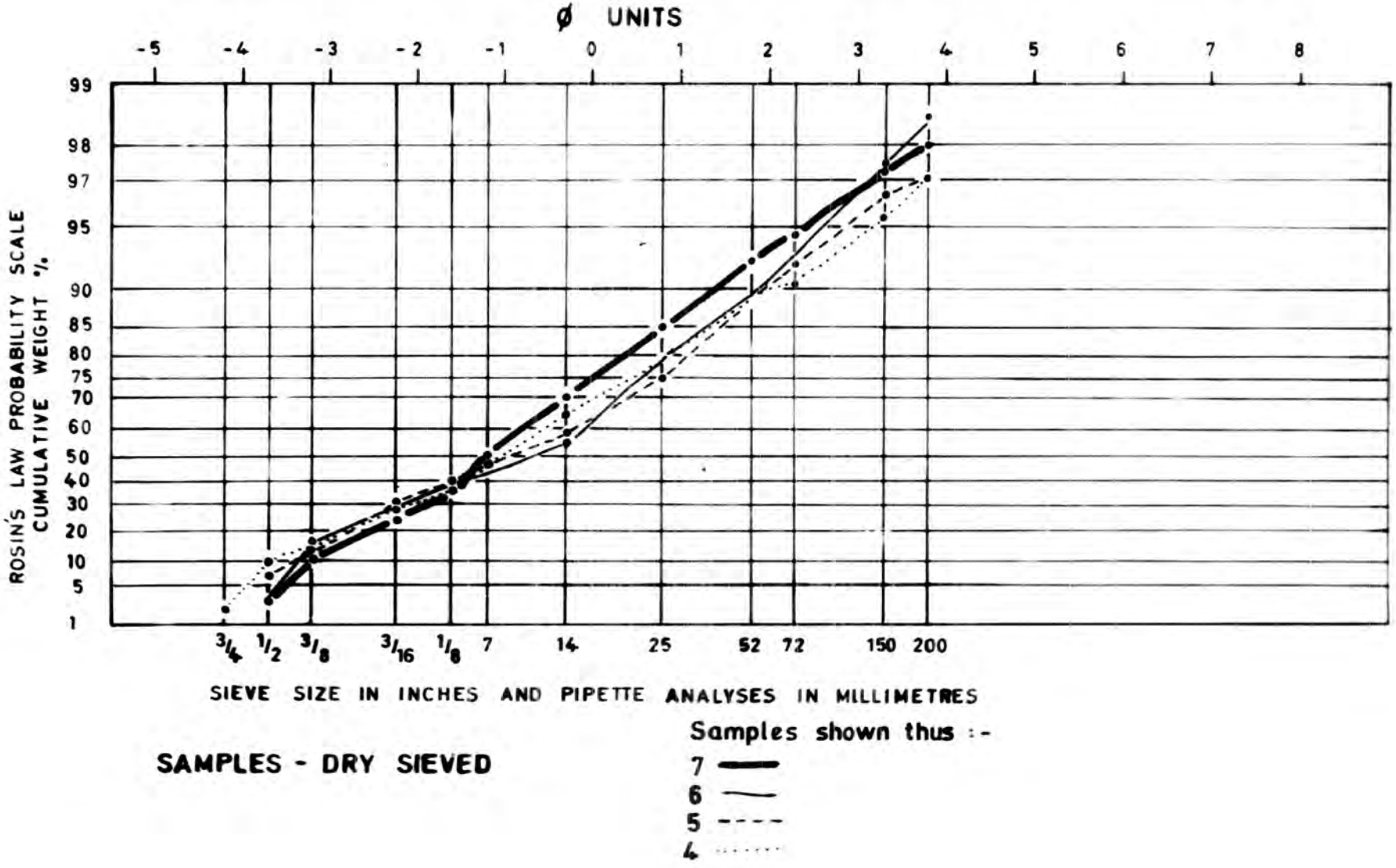

FIGURE 4.8

Figure 4.9

Particle size distributions, Brancepeth, wet analyses - Rosin's-Law probability scale

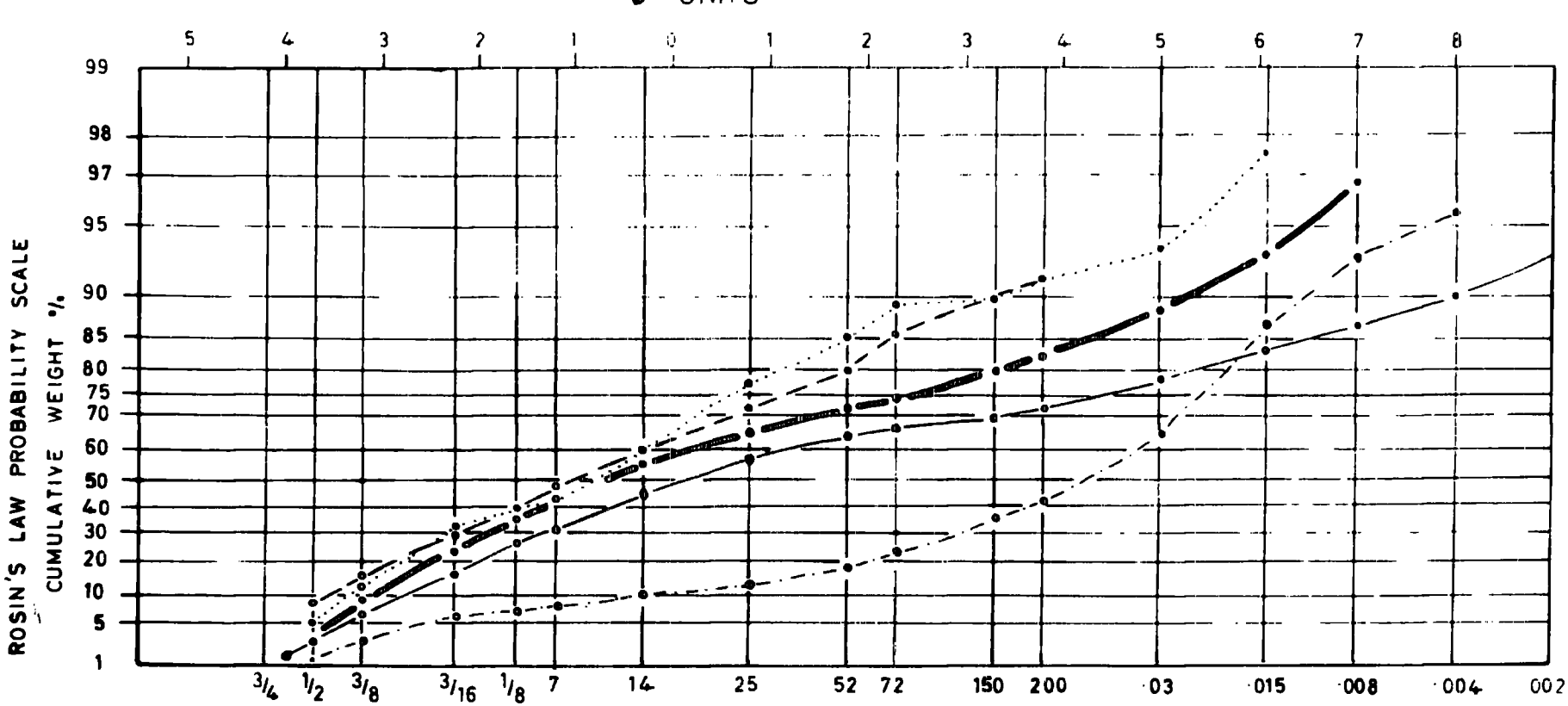

FIGURE 4.9

TABLE 4.12

Consistency limits and grading parameters

Sample	Liquid Limit	Plastic Limit	Plasticity Index	Dry sieving: Trask Sorting coeff. (So) $\sqrt{P_{75}/P_{25}}$	Dry sieving: Uniformity coeff. P_{60}/P_{10}	Dry sieving: Correlation coeff.(r) with respect to Rosin distribution	Wet analyses: Trask Sorting coeff. (So)	Wet analyses: Uniformity coeff.	Wet analyses: Correlation coeff. with respect to Rosin distribution
1A	32	24	8	3.43	15.7	0.9828	4.63	750	0.9470
2	29	21	8	2.24	8.5	0.9583	4.08	73	0.9759
1	29	25	4	2.99	19.1	0.9540	3.00	43	0.9919
3	23	20	3	2.94	25.0	0.9786	4.54	75	0.9883
4	30	27	3	2.70	13.8	0.9843	3.16	30	0.9763
4A	41	37	4	-	-	-	-	-	-
5	36	26	10	3.16	128	0.9858	3.65	33	0.9851
6	41	38	3	2.83	12.5	0.9855	9.08	375	0.9823
7	42	35	7	2.17	7.8	0.9673	4.18	127	0.9745

Consequently the present writer considered the possibility that the Rosin's-law probability plot of dry and wet colliery spoils might bring to light differences that could be attributed to the two very different methods of analysis. By considering the sections of the curves that are common to both methods of analysis (Figs. 4.8 and 4.9, Table 4.12) it is clear that there is no perceptible difference in linearity; half the wet analysed samples have correlation coefficients which are higher than the dry sieved equivalents, whilst half have correlation coefficients which are lower.

What this method of presentation does show however, is probably of more import to the Brancepeth work. It will be noted from Figure 4.9 that the silt fraction of the natural subgrade sediments (sample 8) shows a non-linear swing in a negatively skewed direction. From Kittleman's (1964) work this may well imply that the fine fraction is of ultimate or fundamental grain size and is thus not compatible with the Rosin distribution. A similar swing exhibited by the tip materials may well infer that these are also lacking in clay-grade sizes. It can readily be seen from Figure 4.7 that the highest clay content (sample 6) is in fact 8 per cent. When the results were originally obtained little data existed with which to compare the curves but it was fairly obvious that the Brancepeth gradings were generally different from those of non-burnt tips under investigation. The point can be satisfactorily explained as one of fundamental grain size in that a further sample of ultrasonically disaggregated silt sized spoil (sample 6) passing a 2oo B.S. sieve yielded only 7 per cent clay size material. The conclusion can therefore be drawn that in this partly burnt tip the time-dependent temperature reactions are resulting in a loss of fines (including the fine quartz).

4.12 Shear strength

a) Triaxial tests

The tests were carried out on an effective stress basis at a rate of

strain of 0.00012 in/minute. Saturation under a back-pressure of 50 lb/in^2 (Appendix 3) resulted in all samples bar sample 2 (σ_3' = 10 lb/in^2) attaining at least 90 per cent saturation. Fifty per cent of the specimens reached a saturation in excess of 95 per cent. Blockage of the drainage connections occurred on three occasions and these specimens were subsequently sheared under undrained conditions with pore pressure measurement (Table 4.13 - specimens with $\bar{A}_f$ values).

The basic test data are given in Table 4.13 from which it can be seen that only one specimen (sample 4, σ_3' = 10.0 lb/in^2) shows a positive volumetric strain at failure. Dilation implies over-consolidation which has not been detected by the present writer in any of the hundred or so triaxial results that have been processed. The pore water parameter $\bar{A}$ is defined as follows:

$$\bar{A} = \frac{U_d}{\Delta p}$$

where: U_d is the pore pressure produced by the stress difference Δ_p. $\bar{A}_f$ (Table 4.13) refers to failure conditions.

For normally consolidated materials the $\bar{A}$ parameter at failure approaches 0.5 (see Terzaghi and Peck, 1967, Fig. 15.5). Two of the undrained tests conform with accepted practice but again it is a sample 4 test which gives a low value for this parameter. Now it will be recalled that this sample was driven at the junction with the burnt shale. Probably the most logical conclusion is that over-consolidation (or over-compaction) occurred because the U4 tube was abutting against a more indurated material.

Turning now to the shear strength parameters (Table 4.14) computed from the reduced major axis straight line to the Mohr circle 'top points' (Fig. 6.1), a limitation of statistical treatment is immediately obvious. Both sets of composite results show a small negative cohesion, and more importantly so

TABLE 4.13

Triaxial and Shear Box results

(basic test data)

Sample	Effective minimum principal stress (lb/in^2) at failure	Stress difference lb/in^2	$\bar{A}_f$ parameter	Volumetric strain %	Sample dry density lb/ft^3
	3.6(1)	13.5	0.47	-	104.9
1A	20.0	52.3		-2.16	90.5
	28.5	60.9		-0.87	96.2
	47.5	89.4		-2.31	94.8
	6.5	15.8		-0.30	89.8
2	10.0	37.7		-0.27	92.4
	19.3	64.6		-1.73	92.5
	49.9	153.5		-2.91	89.4
	8.5	38.3		-0.25	90.6
1	20.0	60.7		-0.30	87.8
	27.0	86.2		-0.42	90.0
	50.2(2)	98.0		-1.61	90.5
	4.0(1)	11.5	0.52	-	82.3
3	19.0	65.3		-2.85	85.3
	32.3	96.1		-3.00	86.4
	48.9	136.8		-4.66	87.3

Sample	Effec tive minimum principal stress (lb/in^2) at failure	Stress difference lb/in^2	$\bar{A}_f$ parameter	Volumetric strain %	Sample dry density lb/ft^3
4	10.0	43.9	0.11	+0.21	98.5
	18.3	68.0		-1.20	97.7
	19.0(1)	57.0		-	99.8
	25.0	89.8		-4.00	95.4
4A	9.6	48.8		-1.69	99.2
	19.9	95.5		-1.80	101.5
	29.9	109.7		-3.10	98.6
	40.0	145.5		-5.00	99.7
5	10.0	20.0		-0.37	99.7
	19.1	35.1		-0.59	100.8
	34.9	48.8		-1.32	101.0
	45.0	90.0		-1.97	93.6
6	9.9	33.8		-1.52	83.0
	16.5	32.2		-1.72	78.1
	29.0	57.4		-3.90	83.2
	46.8	100.8		-3.10	88.3
7	9.5	27.4		-2.00	89.0
	18.0	54.6		-3.30	86.7
	30.0	73.2		-3.10	88.0
	47.5	121.9		-3.25	88.1

Sample	Effective minimum principal stress (lb/in^2) at failure	Stress difference lb/in^2	$\bar{A}_f$ parameter	Volumetric strain%	Sample dry density lb/ft^3
	7.7	27.9		-0.02	110.5
8	19.9	41.1		-1.49	110.7
	29.5	63.3		-2.01	108.4
	43.6	103.5		-2.70	108.6

(1) Tested under undrained conditions with pore pressure measurement

(2) Not included for computation of individual c' Ø' values

Shear box tests

Sample	Effective normal pressure (lb/in^2)	Peak shear stress (lb/in^2)	Residual shear stress (lb/in^2)	Ø' peak (degrees)	$Ø'_r$ (degrees)	c' peak (lb/in^2)	c' residual (lb/in^2)
	5	5.2	3.5				
6	15	10.6	7.3	29	21	2.5	1.5
	25	13.9	11.0				

TABLE 4.14

TRIAXIAL SHEAR STRENGTH PARAMETERS - STATISTICS

BRANCEPETH

Sample	N-2	ϕ^1 (c^1=0)	ϕ^1 degrees	c^1 lb/in^2	r*	t*	Significance* level	U	Significance with respect to	c^1=0
All data	34	35.5	36	-0.33	a) 0.9733 b) 0.9933	24.7039 50.0944	= 99.9% = 99.9%	0.1784	P = 0.9-0.8	10-20%
35 points	33	35.5	36	-0.28	a) 0.9740 b) 0.9940	24.6934 51.9870	= 99.9% = 99.9%	0.2777	P = 0.8-0.7	20-30%
1A	2	30.5	27.5	3.40	a) 0.9964 b) 0.9980	16.5814 22.3779	> 99.0% > 99.0%	2.5691	P = 0.2-0.1	80-90%
2	2	37.5	37.5	0.53	a) 0.9995 b) 0.9998	42.6367 66.6582	= 99.9% = 99.9%	0.6008	P = 0.7-0.6	30-40%
1	1	37.5	35.0	2.39	a) 0.9885 b) 0.9985	6.5312 18.4490	> 90.0% + > 95.0%	0.7556		
3	2	36.5	35.5	1.38	a) 0.9990 b) 0.9996	31.3948 53.3198	= 99.9% = 99.9%	1.1367	P = 0.4-0.3	60-70%
4	2	40.0	38.5	1.21	a) 0.9896 b) 0.9993	9.7478 37.7843	> 98.0% = 99.9%	0.4069	P = 0.8-0.7	20-30%
4A	2	41.5	37.5	5.66	a) 0.9973 b) 0.9992	19.0810 35.8217	> 99.0% = 99.9%	2.4985	P = 0.2-0.1	80-90%
5	2	28.5	29.5	-1.50	a) 0.9860 b) 0.9968	8.3731 17.5573	> 98.0% > 99.0%	0.5439	P = 0.7-0.6	30-40%
6	2	31.0	30.0	1.47	a) 0.9939 b) 0.9986	12.7083 26.4581	> 99.0% > 99.0%	0.7658	P = 0.6-0.5	40-50%
7	2	34.5	33.5	1.51	a) 0.9988 b) 0.9996	28.2934 52.1533	= 99.9% = 99.9%	1.3464	P = 0.4-0.3	60-70%
8	2	32.5	31.5	1.00	a) 0.9953 b) 0.9990	14.5160 31.8110	> 99.0% = 99.9%	0.5460	P = 0.7-0.6	30-40%

TABLE 4.14.

TRIAXIAL SHEAR STRENGTH PARAMETERS - STATISTICS

BRANCEPETH

Sample	N-2	ϕ^1 (c^1=0)	ϕ^1 degrees	c^1 lb/in^2		r*	t*	Significance level	U	Significance with respect to	c^1 = 0
1A+2+1+3	13	35.5	35.0	0.63	a)	0.9890	24.0749	= 99.9%	0.3542	P = 0.8-0.7	20-30%
					b)	0.9969	45.3311	= 99.9%			
5+6+7	10	31.5	32.5	-0.73	a)	0.9825	16.6942	= 99.9%	0.3437	P = 0.8-0.7	20-30%
					b)	0.9962	36.0019	= 99.9%			
1A+2+1	9	35.0	35.0	0.63	a)	0.9837	16.4349	= 99.9%	0.2705	P = 0.8-0.7	20-30%
					b)	0.9954	31.1801	= 99.9%			
3+5+6+7	14	33.0	34.5	-1.35	a)	0.9829	20.0000	= 99.9%	0.6528	P = 0.6-0.5	40-50%
					b)	0.9958	40.4763	= 99.9%			
2+1	5	37.5	37.0	0.78	a)	0.9982	37.4388	= 99.9%	0.7320	P = 0.5-0.4	40-60%
					b)	0.9994	65.6869	= 99.9%			
4+4A	6	41.0	39.5	1.59	a)	0.9942	22.6813	= 99.9%	0.7465	P = 0.5-0.4	50-60%
					b)	0.9991	59.2873	= 99.9%			

* a) for reduced major axis regression, c^1, ϕ^1

b) for y = mx

\+ below 95% (probably significant) level

95% probably significant; 99% significant; 99.9% highly significant

TABLE 4.15

Variance Ratio (F-test) on differences between regression lines

(Mohr circle top points)

Samples	F-value	Degrees of freedom	Variance ratio significance at 5% level
a) 1A + 2 + 1 + 3 vs. 5 + 6 + 7	4.522	2,23	Significantly different
b) 1A + 2 + 1 vs. 3 + 5 + 6 + 7	0.940	2,23	Not significantly different
c) 1A + 2 + 1 vs. 5 + 6 + 7	2.516	2,19	Not significantly different

TABLE 4.16

TRIAXIAL SHEAR STRENGTH PARAMETERS - STATISTICS

ABERFAN

Sample	N-2	ϕ^1 (c^1=0)	ϕ^1 degrees	c^1 lb/in^2		r*	t*	Significance* level	U	Significance with respect to	c^1=0	ϕ^1 (Bishop et al)
P.59 Tip 7 4" consol-drained	10	38.5	36.5	1.83	a) b)	0.9930 0.9990	26.5964 69.6098	= 99.9% = 99.9%	1.3185	P = 0.3-0.2	70-80%	39.5
P.60 Tip 7 4" consol-undrained with pp. measurement	3	40.0	37.5	1.27	a) b)	0.9986 0.9996	32.2809 63.6369	= 99.9% = 99.9%	2.4684	P = 0.1-0.05	90-95%	41.5
P.59 Tip 4 4" consol-drained	1	38.0 (37.8)	36.5	2.02	a) b)	0.9997 0.9998	42.3185 48.9371	> 98.0% > 98.0%	2.8544	P = 0.3-0.2	70-80%	37.7
P.57 Tailings 1½R T-CP(pre-cut)	1	34.0	33.5	0.53	a) b)	1.0000 1.0000	203.6210 171.5972	= 99.0% = 99.0%	4.4639	P = 0.2-0.1	80-90%	33.5
P.57 Tailings 1½R T-CS	1	33.0	33.0	0.75	a) b)	0.9994 0.9999	28.0105 57.8677	> 95.0% > 98.0%	0.9348	P = 0.6-0.5	40-50%	32.5

* a) for reduced major axis regression, c^1, ϕ^1

b) for y = mx

95% probably significant; 99% significant; 99.9% highly significant

does sample 5. The composite results present no problem because the y-intercept value of the regression divided by its standard error, (U), results in a significance with respect to c' (effective cohesion) being greater than zero of only 30 per cent at the maximum. A composite value of 35.5° for the angle of friction (Ø') is therefore justifiable (c'=o). For sample 5 a mean value of Ø' = 29.0° (c'=o) would certainly involve little error, and in any case it is more realistic to compare the upper (younger) slope samples with the lower (older) slope samples on a composite basis. Excluding the high Ø' burnt horizon (samples 4 and 4A) from the scheme it is important to record that the variance ratio (F-test) approach of Chow (1960) shows that composite samples 1A, 2 and 1 belong to the same regression model as composite samples 5,6 and 7 (Table 4.15). Sample 3 substantially alters the statistical reasoning (Table 4.15) but this sample is closer in level to the lower group than it is to the upper group (Fig.4.13), so for any consideration of possible degradation of spoil with age it is logical to exclude it. Hence, from a statistical view point the 10 per cent drop in strength of the lower slope samples is not necessarily a function of degradation with the age of material.

Cohesion values are low, apart from the burnt shale and it could well be that this latter value may represent a 'secondary cohesion' (incipient fusion). What is very striking about the Table 4.14 values is the fact that not one of the probabilities (from t-distribution) can really justify the acceptance of c' being greater than zero. The two statistically valid regression lines with high cohesion values (samples 1A and 4A) have confidence levels of <u>less</u> than 95 per cent (with respect to $c' > 0$). We can begin to accept as quite feasible the argument that the Brancepeth spoil is in general, granular, rather than cohesive. On Table 4.16 are shown selected Aberfan data which have been processed by the writer to conform with the statistical propositions, set out in Chapter 1. Based on the assumption that C'=0,

the $\emptyset'$ values of Bishop et al., (1969) are reasonably compatible with the present writer's processing methods. However, for the tip samples the probability that c' is greater than zero is generally higher than for Brancepeth.

An important aspect of the selected Aberfan data concerns the high coal content tailings samples (Table 4.16) whose $\emptyset'$ values are of the same order as the Brancepeth lower slope samples. The influence of coal on the Brancepeth results could on balance be dependent on the actual size of the coal fragments. Fine coal apparently does affect $\emptyset'$ (Table 4.16) and for this reason a series of large strain shear box tests were carried out on fresh samples of the Day Bed Coal from Yorkshire Main Colliery (Fig. 4.10). The $\emptyset'$ angle of this coal is slightly lower than that of tailings but the results show that $\emptyset'$ does not change with appreciable strains. It is therefore unlikely that had tailings been present in the Aberfan shear plane material, the coal content at least would not have contributed to the low residual $\emptyset'$ that was actually measured.

b) Deformation modulii

Figure 4.11 shows that there is a statistical association between the tangent modulus (E_i) and the secant modulus at half the failure strain (E_s) - the E_s value being about 0.6 E_i. In general the scatter or deviation from the best fit regression line increases with increasing cell pressure.

Of greater interest with respect to the behaviour of the Brancepeth spoil is the good agreement with Scheidig's (1931) findings. He showed that for loose sands a linear relationship existed between E_i and effective confining pressure (σ'_3). The form of the relationship is:

$$E_i = C\,\sigma'_3$$, where C is approximately 100 for loose sand.

For Brancepeth C = 95.4 (r = 0.7269, t = 5.8939, N-2 = 31 - highly significant), which is further evidence in favour of granularity.

FIGURE 4.10

YORKSHIRE MAIN
BARNSLEY DAY BED COAL
60 x 60 mm SHEAR BOX

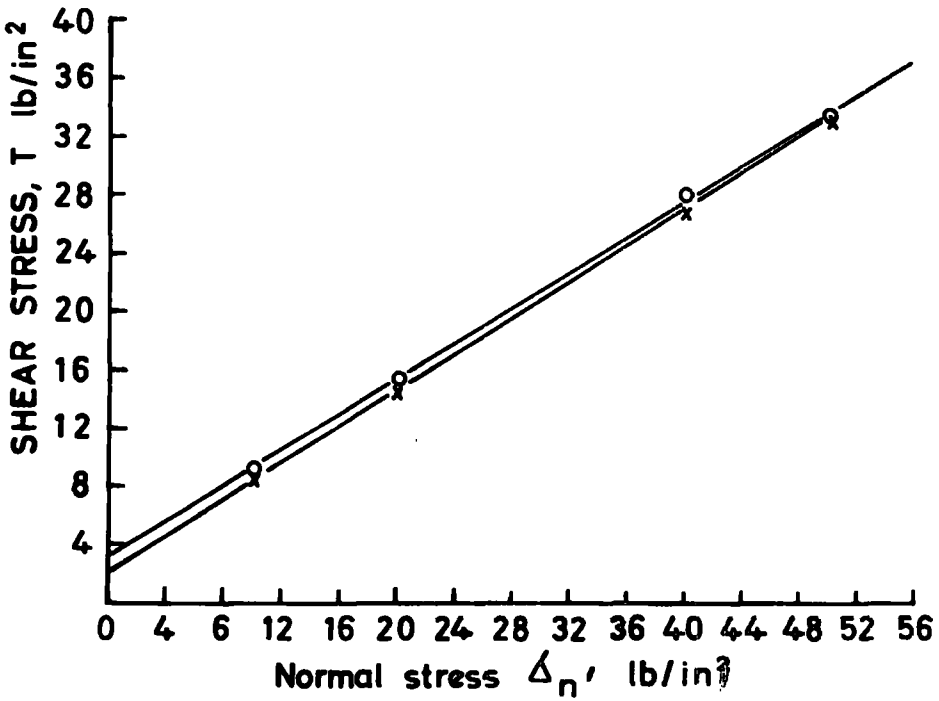

$\phi' = 31 \cdot 5°$, $c' = 2 \cdot 29$ lb/in² } r = 0·9980, t = 22·33, p = 0·01

$\phi' = 31 \cdot 5°$, $c' = 3 \cdot 17$ lb/in² } r = 0·9997, t = 57·94, p = 0·001

$\Delta n'$ lb/in²	10	20	40	50
Peak stress, lb/in²	9·25	15·4	28·1	33·6
Strain %	11·00	9·00	10·70	7·40
Final peak lb/in²	8·60	14·6	25·8	33·6
Final strain %	56·00	77·00	99·4	77·40
Reversals	3	4	5	4

Dry density prior to test = 50 lb/ft³
Material passing B.S.100 sieve, retained on 200

FIGURE 4.10

Figure 4.11

Relationship between deformation modulii, E_i and E_s.

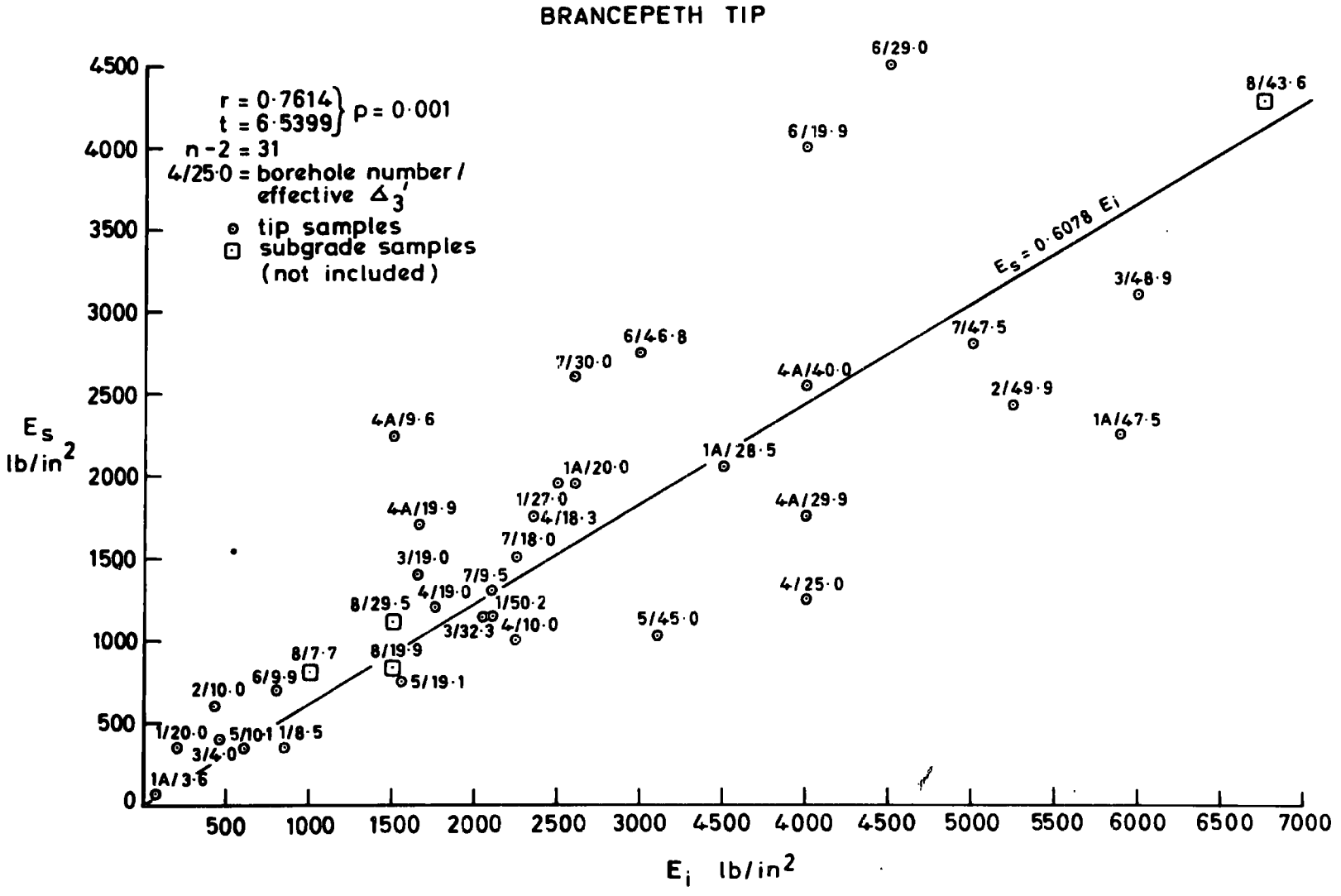

FIGURE 4.11

c) Large strain shear box tests

Three specially selected 3in diameter specimens were taken from a U4 tube which was driven through a particularly fine grained portion of horizon number 6. These specimens were dominantly of less than coarse sand size. At a rate of strain of 0.00048 in/minute the specimens were sheared in a small reversing shear box until a constant shear stress was attained (i.e. residual conditions).

The shear-displacement (strain) curves (Fig. 4.12) demonstrate that the decrease in strength is very gradual and is symptomatic of comminution processes. It will be recalled that Bishop et al., (1969, p.20) suggested that communition alone was insufficient to attain residual conditions and that weathering (possibly accelerated in a generally acid environment), or hydration of clay minerals in the shale was necessary. Clay mineral hydration may play a major role in shale breakdown (Chapter 2), but Kenney's (1967) tests imply that clay minerals which might be expandable (his hydromicas) have a higher residual $\emptyset'$ than kaolinite. In the context of Aberfan however, it is not clear how the mineralogical composition of the freshly ground shale used in shear box simulations (p.20) compared with the actual material on the shear plane. The importance of quartz to clay minerals ratio alone has already been demonstrated (Fig. 3.11, Chapter 3) and it is this writer's opinion that a high ratio may well have been partly responsible for the elevated $\emptyset_r'$ value obtained by Bishop et al., (1969) on freshly ground shale. Before considering the Brancepeth residual it can be seen from Figure 4.12 (peak failure envelope) that a marked change in slope occurs between normal pressures of 15 lb/in^2 and 25 lb/in^2. Messrs. George Wimpey and Company have recorded marked curvature of both shear box and triaxial failure envelopes at low normal pressures and confining pressures (Mr. S. Rodin, personal communication). In the current work saturation under a back pressure has been used primarily to try and eliminate this type of problem. In shear

FIGURE 4.12

SHEAR BOX TESTS

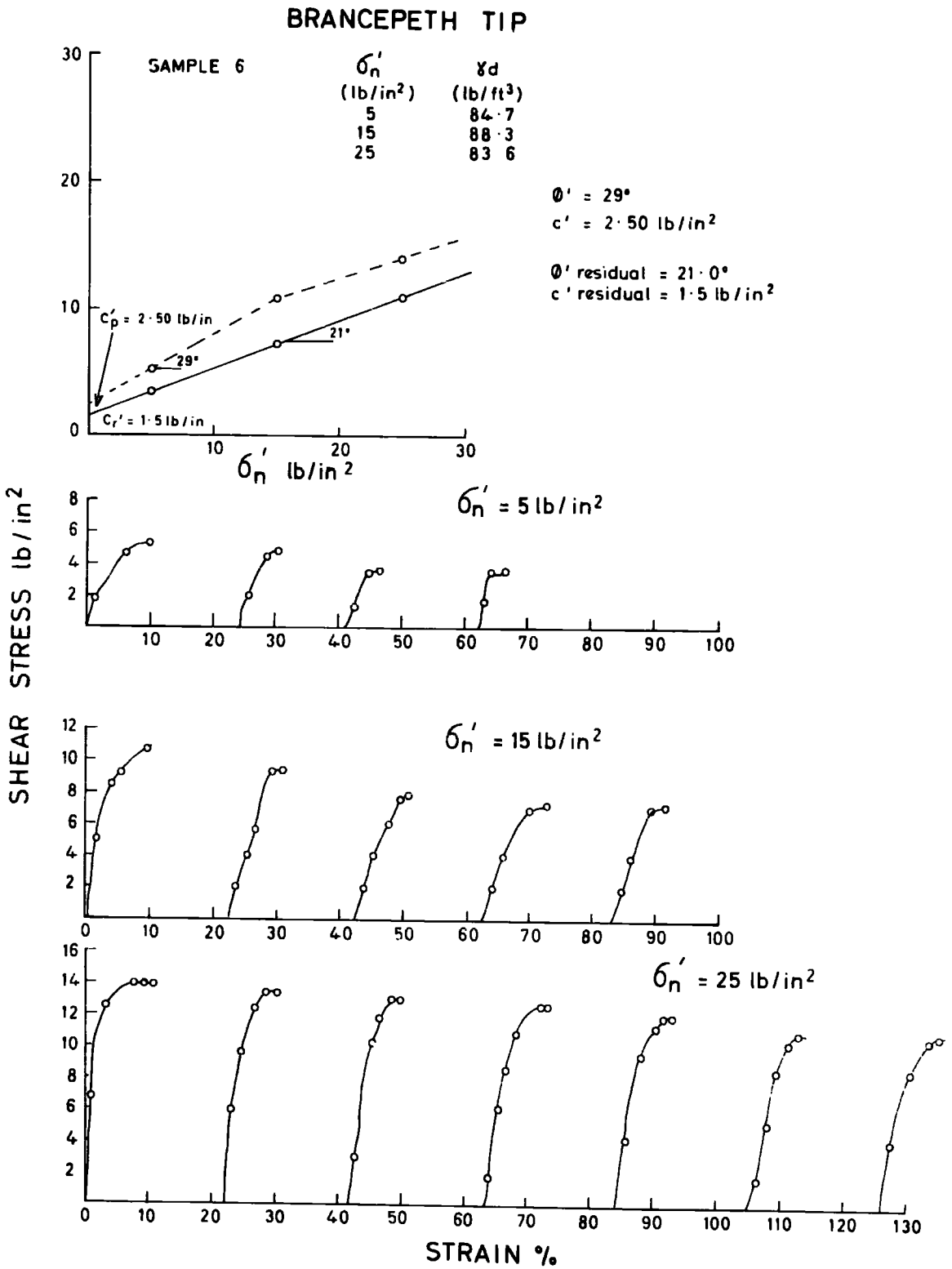

box tests sudden flooding with water is more than likely to cause slaking and comminution when high normal loads are applied (prior to the shearing stage). The initial slope (ϕ' = 29°) is not greatly different from the triaxial values for the lower slope samples. The residual is higher than Aberfan but of the same order. Moreover, it is very similar to Littleton (Chapter 1) and to Smith's (1968) results for loose spoil (ϕ_r' = 20°).

Accepting a minimum peak value of 29 degrees means that a further reduction in the ϕ' parameter alone of at least 8 degrees is necessary before the spoil is at residual strength. Returning to the questions posed at the end of Chapter 3 it is very clear that the lowest peak ϕ' value of this grossly altered spoil is at least 3 degrees higher than the most weathered in situ rocks. What is more important, the minimum Brancepeth ϕ' value is some 27 per cent higher than the residual for this tip.

4.13 Correlation matrix; physical data versus mineralogy and chemistry

Having determined and discussed the physical and mechanical properties, it is now possible to consider briefly the statistical inter-relationships between these properties and the mineralogy and chemistry of Tables 4.5 and 4.6.

The resulting correlations are listed on Table 4.17 and can be explained as follows:

1) Specific gravity is dominated by organic carbon (strong negative association) and probably the clay minerals. The highly significant positive correlation of G_s and Al_2O_3 and the positive correlation with illite at a lower level help confirmthe latter proposition. The positive illite correlation is probably an expression of the effect of combustion on the clay minerals. With combustion kaolinite decreases and illite increases (i.e. negative correlation between G_s and 7/10Å clay minerals ratio). The positive correlation between G_s and Fe_2O_3 and MnO are probably another reflection of oxidation processes. The effect of lattice water on G_s may be yet another oxidation relationship.

TABLE 4.17

Correlation data - physical, mechanical, chemical and mineralogical data

Note: Chemical and mineralogical inter-relationships have already been considered (Table 4.10). The relationships shown below are from a correlation matrix consisting of the following chemical oxides and elements, together with the mineralogy:

Combined SiO_2, free SiO_2, Al_2O_3, Fe_2O_3, FeO, MnO, CaO, Na_2O, K_2O, TiO_2, S, P, CO_2, H_2O^+, H_2O^-, organic C, kaolinite, illite and chlorite.

The physical mechanical data comprise:

ϕ' (c'=o), ϕ', c' (reduced major axis), specific gravity (G_s), mean triaxial sample dry densities (γ_{d_2}), liquid limit (LL), plastic limit (PL) and plasticity indices (PI).

+ 95% level (r = 0.6664)	+ 99% level (r = 0.7977)	-95% level (r = -0.7977)	-99% level (r = -0.7977)
G_s correlates with illite	ϕ' (c'=o) correlates with ϕ' (r.m.a.)	G_s correlates with c'	G_s correlates with org. C
G_s " " Fe_2O_3	PL correlates with LL	G_s " " H_2O^+	
G_s " " MnO	G_s " " Al_2O_3	C' " " H_2O^+	
		G_s " " 7Å/10Å	
LL " " illite		C' " " FeO	
γ_{d_2} " " CO_2			

2) The negative association between effective cohesion (c') and FeO could possibly imply the onset of a secondary cohesion in the form of fusion. With temperature rise FeO will be reduced; H_2O^+ correlates with FeO at a high confidence level (Table 4.10) so giving rise to the negative correlation with c'. Hence, the possibility of incipient fusion being superimposed on a spoil which is behaving like a granular material must not be ignored. The rather unusual positive correlation between c' and G_s is possibly a reflection of oxidation (note positive relationship of G_s and Fe_2O_3 mentioned under 1)).

3) Plastic limit follows liquid limit. Why this should be is not clear and it is difficult to speculate about consistency limits because they are a function of a relatively small fraction of the total particle size distribution. The positive correlation of liquid limit and illite has also been recorded by the writer for a much wider selection of colliery spoils not considered in this thesis.

4) The negative correlation of the triaxial sample dry densities with CO_2 is indirectly a function of obvious dependencies, organic carbon (coal) and specific gravity. The specific gravity determinations were carried out on a representative sample from the U4 tube and not simply on the triaxial specimens. However, G_s and organic carbon do correlate positively and negatively, respectively, with the triaxial specimen dry densities. The correlation coefficients however, are just below the acceptable 95 per cent confidence limits.

5) That ϕ' (c'=o) and ϕ' (reduced major axis) should correlate positively at a high significance level is not unexpected, particularly as the cohesion intercepts are low.

4.14 Stability analyses

Using the computer program developed by the writer as a student project specifically for colliery tips (see Appendix 4), it is feasible to consider

FIGURE 4.13

BRANCEPETH COLLIERY TIP
WILLINGTON, CO. DURHAM.

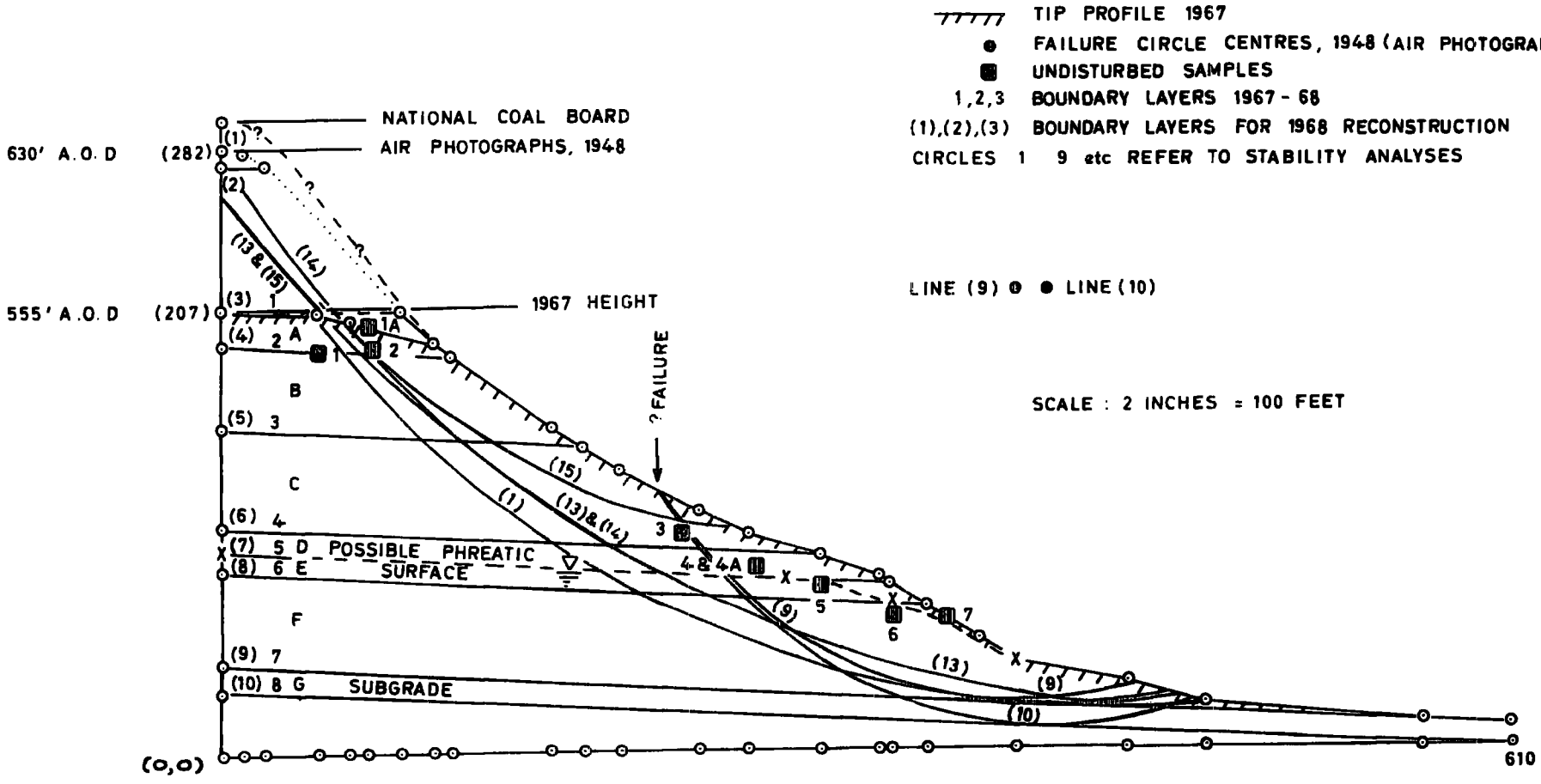

FIGURE 4.13

the overall stability of this colliery tip at the pre-reclamation stage (1957), and during the period when the tip reached its maximum height (1948). Limit equilibrium methods (in this case the Bishop Method of Slices) are based on simplifying assumptions, which at Brancepeth includes some highly speculative conditions, particularly with respect to the water table. By its very nature end-tipped loose granular material resting at its angle of repose will have a factor of safety only marginally greater than unity. However, with a deeper surface of sliding the factor of safety will be greater (e.g. planar slide analytical methods such as Haefeli, 1948). The Bishop (1955) method considers a failure surface which is the arc of a circle, but it has stood the test of time and is remarkably accurate even for non-circular simulations.

a) 1957-58 reclamation period

The slope profile (Fig. 4.13) has been constructed along the line X-Y, Figure 4.2. From the latter Figure it can be seen that the slope has been divided up into layers (A to G) and assigned in situ density values and effective shear strength parameters in accordance with samples 2,1,3,4 plus 4A, 5,6 and 8. In a number of analyses the possible water table mentioned earlier in the chapter has been included (Figure 4.13, Table 4.18). For clarity only certain critical and selected failure circles are shown on Figure 4.13.

If we assign c' and $\emptyset'$ shear strength parameters to the individual layers in the first instance it can be seen (Table 4.18, circles 1-4) that the resulting factors of safety are high for the simple condition, which excludes a water table, and is still greater than unity (incipient failure) when water is included. On assigning the composite $\emptyset'$ value of 35.5° to all layers the factor of safety is even higher for the simple condition, but failure ensues when a water table is established. At first sight there is an apparent paradox, but this can be explained. The shearing resistance of the spoil around the failure surface is governed by the modified Coulomb equation, viz:

TABLE 4.18

Slope stability analyses

Circle	Tangential to line no.	Shear strength parameters	Water table	Factor of safety	
(1)	7	c' ø'	No	1.600 (Minimum)	For 1967-68 period
(2)	8	c' ø'	No	1.620 "	
(3)	7	c' ø'	Yes	1.140 "	
(4)	8	c' ø'	Yes	1.157 "	
(5)	7	ø' tip composite	No	1.628 "	
(6)	8	ø' tip composite	No	1.759 "	
(7)	7	ø' tip composite	Yes	< 1.000	
(8)	8	ø' tip composite	Yes	< 1.000	
(9)	(9)	ø' tip composite	No	1.987 centre co-ords	Fig.4.13
(10)	(10)	ø' tip composite	No	2.096 " " "	
(11)	(9)	ø' tip composite	Yes	1.026 " " "	For 1948 period
(12)	(10)	ø' tip composite	Yes	1.083 " " "	
(13)	(9)	ø' tip composite	No	1.396 trial circle	
(14)	(9)	ø' tip composite	Yes	1.035 trial circle	
(15)	(6)	ø' tip composite	No	1.043 trial circle	

$$S = c' + (\sigma - u) \tan \phi'$$

where S = shear strength

c' = cohesion) effective stress conditions

ϕ' = angle of shearing resistance)

σ = total stress normal to the failure plane

u = pore water pressure

The pore pressure term has a greater effect on the factor of safety (F) for circles 7 and 8 than it does for circles 3 and 4 because there is no cohesion in the first case, and it is this term which is independent of pore pressure. It is relevant to record that for all these conditions it is the toe circle (line 7) which is the more critical.

b) 1948 period - Reconstruction from aerial photographs

On the stereo-pairs the upper margin of the loose spoil can be delimited (Fig. 4.13). Unless this material was an extremely superficial veneer it could be postulated that it failed along an arc that is tangential to either line (9) or line (10) of the reconstructed profile. Centres for these two circles (Fig. 4.13) can be fixed with reasonable accuracy. For the analysis of the reconstructed slope it is possibly more logical to use the composite ϕ' value of 35.5° with a mean density (taken from the known tip samples) for the upper section (horizons (1) to (3)).

The lowest factor of safety computed is once again for a toe circle (No. (9) tangential to line (9)). However, the factor of safety is well above the acceptable value for populated areas (F = 1.5), and it is clear that without an established water table, failure is very unlikely. Even when a water table condition is considered (circle (11)) the factor of safety is marginally greater than unity. Although the number of imponderables in the reconstruction case have increased it could be argued that this latter factor of safety is close to unity so one should draw a parallel with the 1967-68 conditions, which can be elucidated with more certainty. During the reclamation period no signs of instability were apparent even though a deep cutting was driven into the spoil-bank. Minimum values for the factor

of safety were 1.140 (circle (3)) and $\leq$ 1.000 (circle (7)), respectively. From a practical point of view it would appear that these values of F are unlikely. In other words, a water table within the tip is unlikely, and this logic can be applied equally well to the 1948 period. What is most interesting is that for failure conditions along circle (9) a ϕ' angle of only 19.8° is required (assuming no water table). This value is not greatly different from ϕ'_r .

The convexity in the slope in the loose spoil region (probably including sample 7) can be clearly seen on Figure 4.13. For failure to take place in this region, however, requires a somewhat different hypothesis, exemplified by trial circles (13) and (15) - the water table condition of circle (14) is probably unnecessary. Circle (13) shows that a more deep seated failure circle affecting the complete slope still gives rise to a factor of safety well above unity. On the other hand a more restricted failure which is limited to the upper, more steeply inclined section of the heap is rapidly approaching unity. It must be recognized that a post-mortem analysis of this kind is by its nature an academic exercise, but the balance of evidence implies that the material derived from a relatively superficial failure of the upper slope (probably shallower than circle (15)), would be readily removed by erosion to a lower level. The small plateau of the older tip in the vicinity of sample 6 could well 'contain' this material (e.g. sample 7). Trial circle (15) demonstrates that the factor of safety would be compatible with such a proposition. Hence, we can draw a tentative conclusion that the 1949 regrading operation was an adjunct of a small failure (as the records suggest), and that it is unlikely that a permanent water table was established in the Brancepeth tip.

4.15 Compaction

At the end of April 1968 when the major part of the reclamation scheme had been completed, comparisons were drawn between the re-graded spoil and

the original field densities and moisture contents of the tip itself. Four in situ density determinations (A, B, C and D) were carried out at widely spaced intervals on the ground.

In order to relate the densities and moisture contents to an accepted civil engineering standard, both high and low standard compaction tests were carried out (B.S.1377/1967). The results set out in Table 4.19 show that the average field dry density of the reclaimed waste is only 1 lb/ft^3 higher than the average density of the tip material itself. At the end of April however, the average moisture content was only 8.3 per cent, compared with 11.5 per cent for the tip material in December 1967 to January 1968.

The tandem scrapers with an approximate working load per tyre of $9\frac{1}{4}$ tons could have achieved a higher degree of compaction if the average moisture content during the drier period had been closer to the December/January value. The degree of compaction achieved can be tabulated as follows:

i) Compared with average density of tip - 101.1%

ii) Compared with high standard compaction test - 83.9%

iii) As ii) but based on moisture content of April 26th - 86.3%

iv) Compared with low standard compaction test - 91.5%

v) As iv) but based on moisture content of April 26th - 95.7%

The usual civil engineering compaction standard is 95 per cent of the optimum value achieved in the low standard B.S. test. Generally speaking the standard achieved during regrading operations at Brancepeth was satisfactory, but the implications in relation to compaction of colliery tips should be considered. First of all it should be appreciated that density is proportional to specific gravity. The high coal content of Brancepeth thus means that the spoil densities fall well below the modal range for spoils of England and Scotland (N.C.B. Technical Handbook, 1970, Fig. 5.9). In terms of optimum (B.S. low standard) however, the existing

TABLE 4.19

Compaction and field density data

Equipment: Tandem scraper 19 tons. Laden - 37 tons
Effective tyre width - 1 ft 11 in
Working load per tyre - 9¼ tons (approx.)

In situ densities and moisture contents, April 26th, 1968

Location	In situ density lb/ft³	Moisture content	December 1967 - January 1968 Mean tip density lb/ft³	Mean tip moisture content %
A	94	8.4		
B	86	9.1		
C	89	7.2	90.4	11.1
Access Road D	97	8.5		
Mean	91.5	8.3		

B.S. Compaction tests

	Maximum dry density lb/ft³	Optimum Moisture content%
10lb rammer (high)	109	12
*5½lb rammer (low)	100	14

*Usual civil engineering standard.

degree of compaction of this relatively superficial zone of spoil is just over 90 per cent. It can reasonably be argued that compaction of existing colliery tips by civil engineering plant is unlikely to result in greatly improved stability. Certainly the plant used during the reclamation phase at Brancepeth was working under less restrictive conditions than usually apply to the plateau area of a colliery tip. However, the standard of compaction achieved was little more than had previously been attained under gravity with periodic redistribution of unstable material. The 90 per cent maximum compaction of this 100 year-old tip must be set against the low Aberfan value of 83 per cent (Bishop et al., 1969, p.18), which is less likely to apply to mature tips (for example, Yorkshire Main, Chapter 6).

4.16 Conclusions

A relatively superficial 17 ft thick zone of the 100-year-old Brancepeth tip in Co. Durham has been studied in detail.

Combustion has had a marked effect on the spoil constituents. Fully burnt shale, now devoid of kaolinite, has been subject to temperatures in excess of 350°C and possibly as high as 600°C. The partially hydrated calcium sulphate mineral, hemihydrate was identified and this is symptomatic of temperatures of around 70°C which may well have been the general 'background' temperature to which most of the spoil was subjected over the years. Mineralogical comparisons with equivalent Lower Coal Measures strata from neighbouring collieries imply that the clay mineral balance has been changed with illite becoming the dominant clay mineral species. The content of soluble sulphates in this very coaly spoil is also high and there is very clear evidence that free silica has been removed, probably with the clay sized matrix which is quantitatively very low indeed.

Trace chlorite is still present but the illite is disordered and in the burnt shale, deficient in lattice water, almost certainly in response to the intense oxidation to which it has been subjected. Statistical

treatment of the chemical and mineralogical components confirms that the expected oxides are combined in the clay minerals and that these minerals increase as the coal content decreases. Similarly, the decrease in kaolinite with increase in sulphate content (i.e. oxidation) has statistical validity. An evaluation of sulphates identified in natural strata and tip materials suggests that most of the gypsum may well be tipped directly as a waste product in association with other secondary minerals found in the cleat of coal. Sulphate species do form within the tip environment but this contribution is believed to be quantitatively a much smaller fraction.

The in situ densities are low because of the high coal content. On the other hand the degree of compaction of the Brancepeth spoil is far higher than that of Aberfan; field compaction studies at Brancepeth imply that it is unlikely that a higher standard can be attained artificially than already exists under normal mechanical tippler emplacement.

The liquid and plastic limits, deformation modulus (E_i) and statistical treatment of the failure envelopes demonstrates that the Brancepeth spoil is essentially granular in mechanical behaviour. Limited evidence to date suggests that the small cohesion values may in any case be more in the nature of secondary bonds (incipient fusion), rather than cohesion of the type usually associated with soils.

The composite angle of shearing resistance is compatible with the compacted shales of the Burnhope and Balderhead dams; it is some 3° to 4° lower than the younger spoil of Tip 7, Aberfan. Comparison of the upper (younger) samples with lower (older) samples shows that $\emptyset'$ falls by some 10 per cent (with age). This could be attributed to weathering (degradation with age) but there are statistical reasons for suggesting that the difference can be accommodated within the experimental boundaries. Importantly, the minimum $\emptyset'$ value is some 8° higher than the residual value for this spoil.

Limit equilibrium stability analyses carried out for various slope conditions show that unless a water table was present in the past, the failure which occurred in 1949 probably involved a superficial mass of spoil rather than a deep-seated zone.

CHAPTER 5

THE MINERALOGY AND GEOTECHNICAL PROPERTIES OF UNBURNT SPOIL - YORKSHIRE MAIN COLLIERY

5.1 Introduction

In the last chapter the overall mechanical stability of the Brancepeth spoil has been shown to be remarkably unaffected by its long history of weathering, combustion and regrading. Progressive breakdown of fresh underground material from Yorkshire Main Colliery during a period of 2 years (Chapter 2, Plate 2.1) infers that most of the discard in the equivalent single seam Barnsley Bed tip probably reached its level of degradation relatively quickly. The roof measures and certain beds from the floor of the seam disintegrated rapidly, but even so the small fragments were relatively strong after their two year exposure period, and had not reached fundamental grain size. The possibility of further breakdown occurring in the body of the tip is therefore pertinent, especially as the unburnt degraded material may have somewhat different mechanical characteristics than the Brancepeth material.

It was therefore decided to investigate the Barnsley Bed tip at Yorkshire Main Colliery (Grid Ref. SK 554 992 - Plate 5.1, view of south face), particularly as it had a number of seemingly uncomplicated features which are usually absent in tips:

a) The aerial ropeway tip consists of discard from a single seam.

b) The equivalent strata could still be sampled underground.

c) A large section of the tip (free from regrading) was unburnt.

d) The spoil was sufficiently old for any significant time-dependent changes to be apparent. Tipping commenced between 1918 to 1920, was terminated in 1954, with samples being taken in 1968.

Most of the tip consists of washery discard, estimated at not less than 70 per cent, the remainder being run-of-mine dirt. It is a pocket of the

Plate 5.1

View of southern face of Yorkshire Main tip

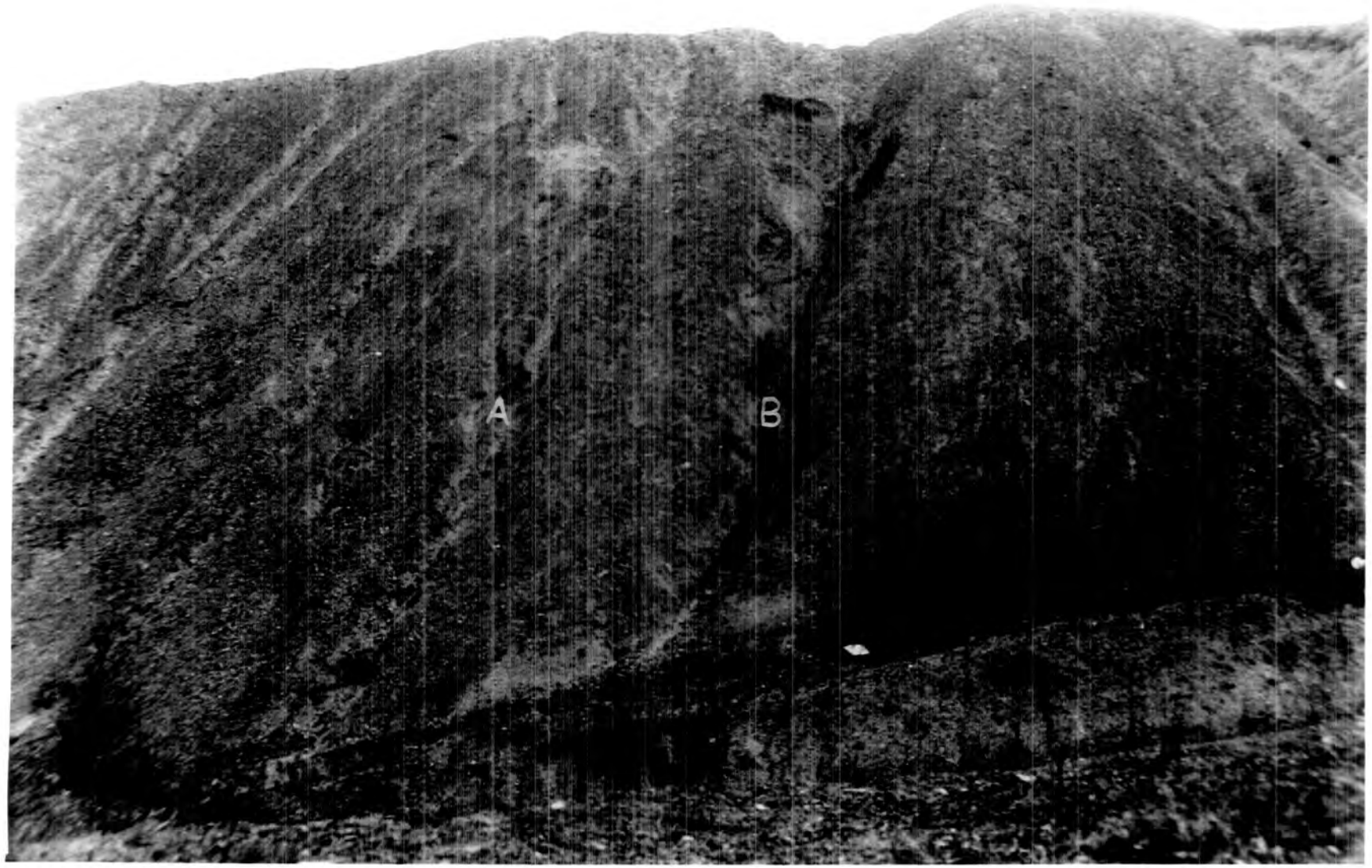

PLATE 5.1

TABLE 5.1

Sampling and testing scheme

Depth	U4	SPT	Thin section	XRF	XRD identification	XRD semi-quantitative	Bh.1 Density Moisture Cont.	Bh.2 dry density	Gs, limits org.carb. Bh.1 & 2	Particle size Bh. 2	Triaxial Bh.1	Triaxial Bh.2	Permeability[3] Bh.2	Compaction Bh.1 & 2
2.5-4.0	A			X	X	X	X	X	X	X	X		X	0-4.5ft[4]
4.5 -6.0		Y1	X	X	X									
7.5 -9.0	X													
9.5 -11.0		Y2		X	X	X								
12.5 -14.0	B			X	X		X	X	X	X	X		X	
14.5 -16.0		Y3		X	X	X								
17.5 -19.0	X													
19.5 -21.0		Y4	X	X	X	X								
22.5 -24.0	C			X	X		X	X	X	X	X		X	
24.5 -26.0		Y5		X	X	X								
27.5 -29.0	X													
29.5 -31.0		Y6		X	X	X								
32.5 -34.0	D			X	X		X	X	X	X	X		X	
34.5 -36.0		Y7	X	X	X	X								
37,5 -39.0	X													
39.5 -41.0		Y8		X	X	X								
42.5 -44.0	E			X	X		X	X	X	X[1]	X[2]	X[2]		
44.5 -46.0		Y9		X	X	X								
47.5 -49.0	X													X[5]

49.5 -51.0		Y10		X	X	X								
52.5 -54.0	F			X	X		X	X	X	X	X		X	
54.5 -56.0		Y11		X	X	X								
57.5 -59.0	X													X^{5}
59.5 -61.0		Y12	X	X	X	X								
62.5 -64.0	G			X	X		X	X	X	X	X		X	
64.5 -66.0		Y13		X	X	X								
67.5 -69.0	X													X^{6}
69.5 -71.0		Y14		X	X	X								
72.5 -74.0	H			X	X		X	X	X	X	X		X	
74.5 -76.0		Y15		X	X	X								
77.5 -79.0	X													$X^{6,7}$
79.5 -81.0		Y16		X	X	X								
82.5 -84.0	I			X	X		X	X	X	X	X		X	
84.5 -86.0		Y17		X	X	X								
87.5 -89.0	X													X^{7}
89.5 -91.0		Y18		X	X	X								
92.5 -94.0	J			X	X		X	X	X	X^{1}	X^{2}	X^{2}		
94.5 -96.0		Y19		X	X	X								
97.5 -99.0	X													X^{8}
99.5 -101.0		Y20		X	X	X								
102.5 -104.0	K			X	X		X	X	X	X	X		X	
104.5 -106.0		Y21	X	X	X	X								
107.5 -109.0	X													X^{8}
109.5 -111.0		Y22		X	X	X								
112.5 -114.0	L			X	X		X	X	X	X^{1}	X^{2}	X^{2}		
114.5 -116.0		Y23	X	X	X	X								

117.5 -119.0	M		X	X		X	X	X	X	X	X
119.5 -121.0		Y24	X	X	X						
125		(bag)Y25	X	X	X						
130.0 -131.5	X		X			X		X		X	

1. Including ex-triaxial samples
2. 8in long x 4 in diameter triaxial specimens
3. Remaining material after particle size analysis. Re-compacted to dry density value.
4. N.C.B. bulk sample

5,6,7,8. Composite samples utilising all U4 material

latter very coarse material (Fig. 5.8) which is believed to have fired around 1925.

In order to detect time-dependent changes in the spoil two boreholes were put down from the plateau area on top of the tip. The boreholes, which were within a few feet of each other (along the strike) were on the same traverse as the gulley marked A on Plate 5.1. The function of the second hole was to provide sufficient duplicate samples for physical and mechanical tests. In practice alternating U4 and Standard Penetration Test samples were taken, the sampling and testing scheme being shown on Table 5.1. The relationship between depth and age of the spoil will not be exact (i.e. linear) for the situation is analogous to that in any sedimentary sequence where the rate of deposition is irregular.

5.2 Underground samples

These samples were collected in order to determine the nature of the material prior to emplacement on the heap (Chapter 2, Plate 2.1), and also to enable fabricated specimens to be made up for shear strength comparisons with the tip materials (Section 5.14). Sampling was undertaken by Mr. J.E. Johnson of the National Coal Board at two main localities. The sections and sampling plan are shown on Figure 5.1. The main lateral variation in the strata is the eastwards split of the Day Bed rider seam off the Barnsley Coal. The sections are thought to be typical of the two districts (eastern and western) with approximately two thirds of the output coming from the area west of the Day Bed split.

All horizons shown on Figure 5.1 will have contributed to the heap but it is not possible to estimate in what proportions, or how the proportions have varied with time. In addition to the waste derived from the working faces, there is also the contribution from both new and old roadways; material has also been back-ripped from old roadways to counteract closure. The situation is further complicated because material was left underground

Figure 5.1

Roof and floor measures Yorkshire Main Colliery

FIGURE 5.1

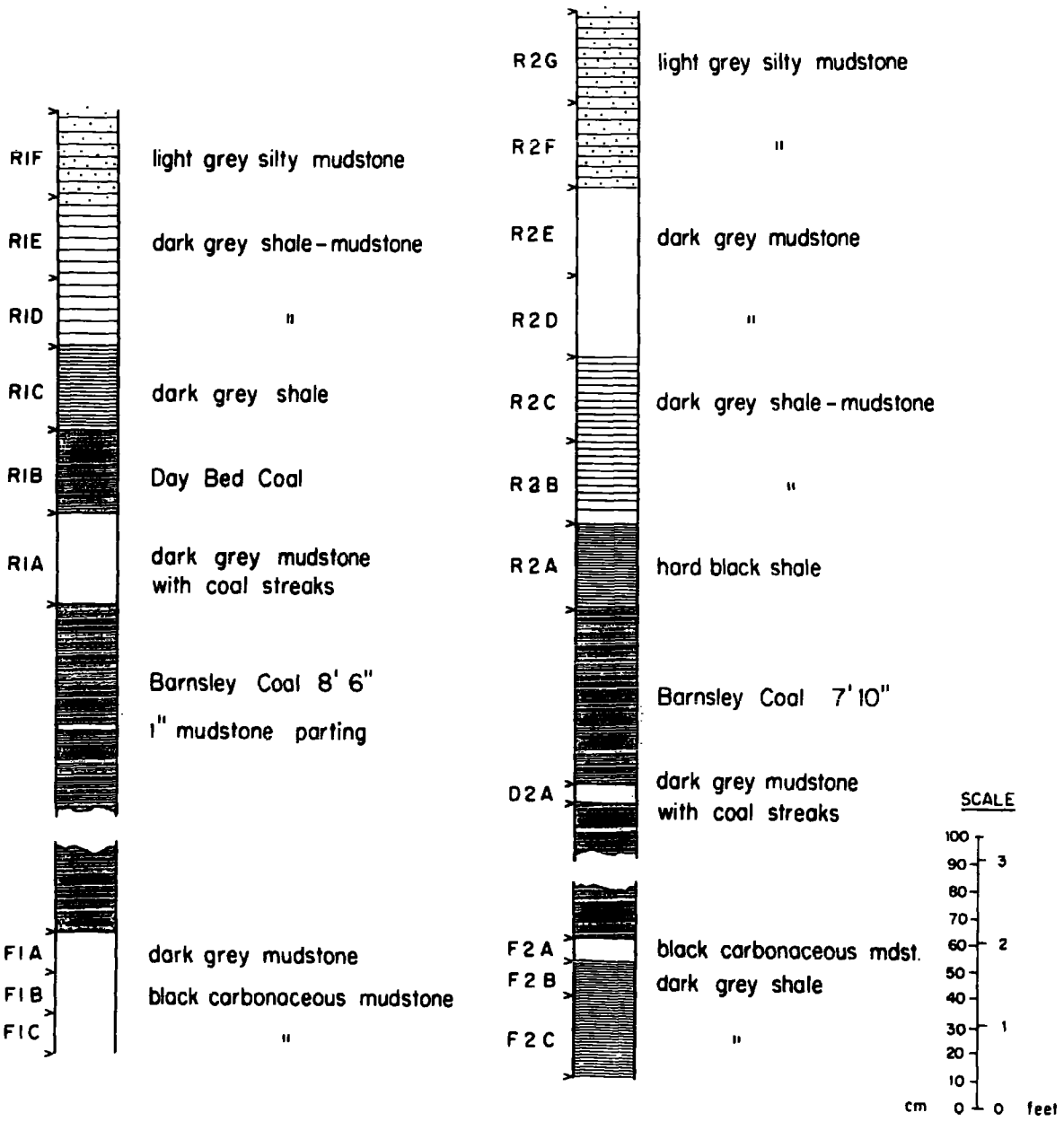

whenever possible. A seemingly simple single seam working is thus complicated by variation in stratigraphy, mining methods and washery practice. The approach adopted in the work has therefore been to look for variations within the spoil heap, and then to eliminate if possible the effects of original variations in the material. On the other hand, the lack of variation in any mineral, element or material property is convincing evidence that the material is not changing with time.

5.3 Hand specimens and thin sections

The material examined visually from borehole samples (Table 5.1) consisted of unburnt shale, mudstone and coaly fragments in a clay matrix. There was no apparent variation with depth and hard fragments of mudstone and shale were as abundant at the base of the tip as at the top. Siderite nodules were encountered, and in line with evidence already presented in this thesis, oxidation was only superficial.

Thin sections were prepared of some of the S.P.T. samples (Y1, Y4, Y7, Y12, Y21 and Y23; depths given in Table 5.1). Their most striking feature was the high proportion of mudstone, shale and coal fragments, the coal in particular, being extremely angular. On Table 5.2 is shown the approximate proportions of the major constituents based on point counts of all the above sections. The proportion of matrix (material too small to be resolved under the microscope) to rock or mineral fragments lies between 1 to 3 and 1 to 4. The matrix is quantitatively less important than the appearance of the hand specimens suggests. Deformed grains are present but do not increase in abundance downwards. Grains of carbonate are scattered through all the sections, and comprise aggregates of either small or unusually large crystals. Gypsum* is also present and its appearance suggests that it did not grow within the heap (see Chapter 4, Section 4.8). The lack of corrosion and its uniform distribution suggests that there has been little leaching of this soluble mineral.

* Hemihydrate was proved by X-ray diffraction at 10 ft and 50 ft. Adjacent U4's contained some boiler ash which presumably had been tipped when still hot.

In thin section no variation with depth was noted in the proportion of matrix to fragments and the particle size distribution data (Table 5.7) shows that the various grain sizes do not change systematically with depth. Taking all the findings together (including the breakdown evidence (Plate 2.1 and discussion) it can be suggested that most of the spoil was reduced to small fragments by physical breakdown (controlled by sedimentary structures), and that this took place relatively quickly.

TABLE 5.2

Average modal composition from thin sections, (percentage)

Mudstone/ shale	Siltstone	Coal and other organic matter	Deformed fragments	Carbonates	Quartz	Matrix
35	4	21	12	5	2	21 (RKT)
33	2	25	14	3	1	22 (DAS)

5.4 Chemistry and mineralogy

The samples used for chemical determinations comprised post-failure triaxial specimens and a much wider array of S.P.T. split-spoon samples (plus one bag-sample) numbered Y1 to Y25 (see Table 5.1).

The following elements and oxides were determined in Durham by X-ray fluorescence, and processed after Holland and Brindle (1966): SiO_2, Al_2O_3, Fe_2O_3, MnO, MgO, CaO, Na_2O, K_2O, S and P_2O_5. The X.R.F. analyses are summed to 100 per cent and exclude organic matter, CO_2 and water. Further analysis of free silica (quartz) FeO, acid-soluble sulphate and H_2O^+ were carried out in Sheffield by Dr. D.A. Spears on the S.P.T. samples, so that the largest group of samples could be considered on a whole rock analytical basis. The X.R.F. analyses are given in Table 5.3 and the chemical composition of the spoil (25 S.P.T. samples) is given in Table 5.4 (after Spears, Taylor and Till, 1971). The clay mineralogy of the S.P.T. samples was also determined in Sheffield and is shown on Figure 5.2, together with

TABLE 5.3

Chemistry of S.P.T. and U4 samples (X.R.F., summed to 100 per cent)

a) S.P.T. samples

Sample	SiO_2	Al_2O_3	Fe_2O_3	MgO	CaO	Na_2O	K_2O	TiO_2	MnO	S	P_2O_5
Y1	50.50	21.14	9.81	2.45	6.12	0.69	4.31	1.13	0.26	3.47	0.12
Y2	40.32	20.06	14.59	1.53	2.18	0.49	3.97	0.96	0.07	15.75	0.09
Y3	52.00	22.91	9.17	2.10	3.14	0.85	4.42	1.54	0.14	3.56	0.19
Y4	55.60	22.96	8.25	1.80	2.81	0.62	4.53	1.18	0.14	1.97	0.15
Y5	54.15	22.83	8.38	1.94	2.99	0.31	4.75	1.19	0.12	3.13	0.21
Y6	55.03	21.99	8.42	1.91	3.25	0.80	4.50	1.19	0.13	2.65	0.12
Y7	55.84	23.29	7.59	1.89	2.83	0.56	4.64	1.16	0.13	1.93	0.15
Y8	58.35	22.14	7.33	1.78	2.53	0.88	4.06	1.14	0.12	1.53	0.14
Y9	52.96	23.14	8.40	1.99	4.91	0.83	4.42	1.10	0.18	1.96	0.14
Y10	56.03	22.56	7.76	1.81	3.11	0.99	4.34	1.12	0.13	1.06	0.16
Y11	55.26	23.05	7.78	2.01	3.80	0.71	4.37	1.12	0.15	1.62	0.13
Y12	53.94	23.03	8.77	1.94	3.59	0.54	4.48	1.14	0.16	2.28	0.15
Y13	54.44	24.27	7.22	1.90	3.69	0.59	4.51	1.18	0.14	1.94	0.12
Y14	56.45	23.42	7.23	1.91	3.16	0.70	4.17	1.12	0.14	1.60	0.11
Y15	52.05	21.99	9.57	2.17	5.56	0.53	4.22	1.12	0.22	2.44	0.13
Y16	51.38	24.09	8.64	2.00	4.29	0.63	4.57	1.17	0.15	2.98	0.09
Y17	51.87	24.41	9.08	1.67	1.54	0.75	4.49	1.18	0.09	4.82	0.09
Y18	53.42	26.92	7.06	1.66	1.52	0.15	5.01	1.31	0.08	2.77	0.11
Y19	54.61	25.29	7.58	1.68	1.75	0.80	4.47	1.18	0.09	2.44	0.10

Sample	SiO_2	Al_2O_3	Fe_2O_3	MgO	CaO	Na_2O	K_2O	TiO_2	MnO	S	P_2O_5
Y20	57.49	25.68	5.96	1.76	1.26	0.86	4.29	1.17	0.07	1.36	0.09
Y21	55.30	24.48	7.70	1.69	2.52	0.66	4.25	1.15	0.12	2.04	0.13
Y22	45.48	22.02	13.02	1.42	1.25	0.69	3.95	1.06	0.07	10.95	0.10
Y23	51.72	25.22	9.37	1.85	3.00	0.63	4.43	1.17	0.15	2.06	0.41
Y24	54.60	23.80	8.30	1.69	2.10	0.82	4.26	1.15	0.10	3.02	0.16
Y25	56.43	24.30	7.05	1.80	1.68	0.87	4.65	1.22	0.09	1.80	0.11
b) U4 samples											
A	51.35	29.09	6.35	1.77	3.41	0.59	4.38	0.91	0.18	1.84	0.14
B	38.52	29.17	12.82	1.70	3.13	0.61	5.70	1.20	0.18	5.86	0.56
C	47.47	27.51	8.39	2.04	4.64	0.64	4.53	0.98	0.21	3.48	0.12
D	40.92	25.78	14.35	1.50	2.34	0.68	4.21	0.90	0.11	8.78	0.43
E	55.44	27.97	6.13	1.48	0.96	0.70	4.60	1.07	0.07	1.48	0.08
F	55.85	25.27	6.94	1.61	2.20	0.58	4.03	0.96	0.13	2.30	0.12
G	45.81	26.82	9.87	1.99	4.57	0.81	4.74	1.03	0.23	3.89	0.23
H	50.72	26.29	7.80	1.90	3.50	0.82	4.57	1.13	0.19	2.94	0.13
I	52.28	26.90	7.55	1.76	2.45	0.82	4.40	1.00	0.15	2.53	0.14
J	52.28	27.98	6.70	1.74	2.47	0.70	4.60	1.11	0.14	2.15	0.10
K	50.31	27.15	7.39	1.80	3.79	0.53	4.63	1.08	0.16	3.05	0.13
L	50.48	26.70	7.86	1.51	2.65	0.95	4.54	1.20	0.11	3.89	0.11
M	53.33	27.53	7.46	1.60	1.38	0.78	4.50	1.17	0.10	2.02	0.11

TABLE 5.4

Chemical composition of Yorkshire Main Spoil Heap*

(based on 25 samples)

% total oxides	Mean	Standard Deviation	Minimum	Maximum
free SiO_2(quartz)	15.84	3.22	10.65	21.86
combined				
SiO_2	37.74	3.48	29.75	46.53
TiO_2	1.17	0.10	0.96	1.54
Al_2O_3	23.48	1.51	20.10	26.98
Fe_2O_3	4.86	2.35	1.59	12.72
FeO	3.36	0.86	1.70	5.21
MnO	0.13	0.05	0.07	0.26
MgO	1.86	0.21	1.41	2.46
CaO	2.99	1.28	1.25	6.15
Na_2O	0.68	0.19	0.15	1.00
K_2O	4.42	0.24	3.96	5.02
SO_4 acid soluble	0.23	0.15	0.10	0.76
S in FeS_2	3.06	3.13	1.09	15.16
P_2O_5	0.14	0.06	0.09	0.41
	99.96			
% dry wt.				
Organic carbon	23.97			
H_2O^+	6.77			

*from: Spears, Taylor and Till (1971)

Figure 5.2

Relative proportions of clay minerals

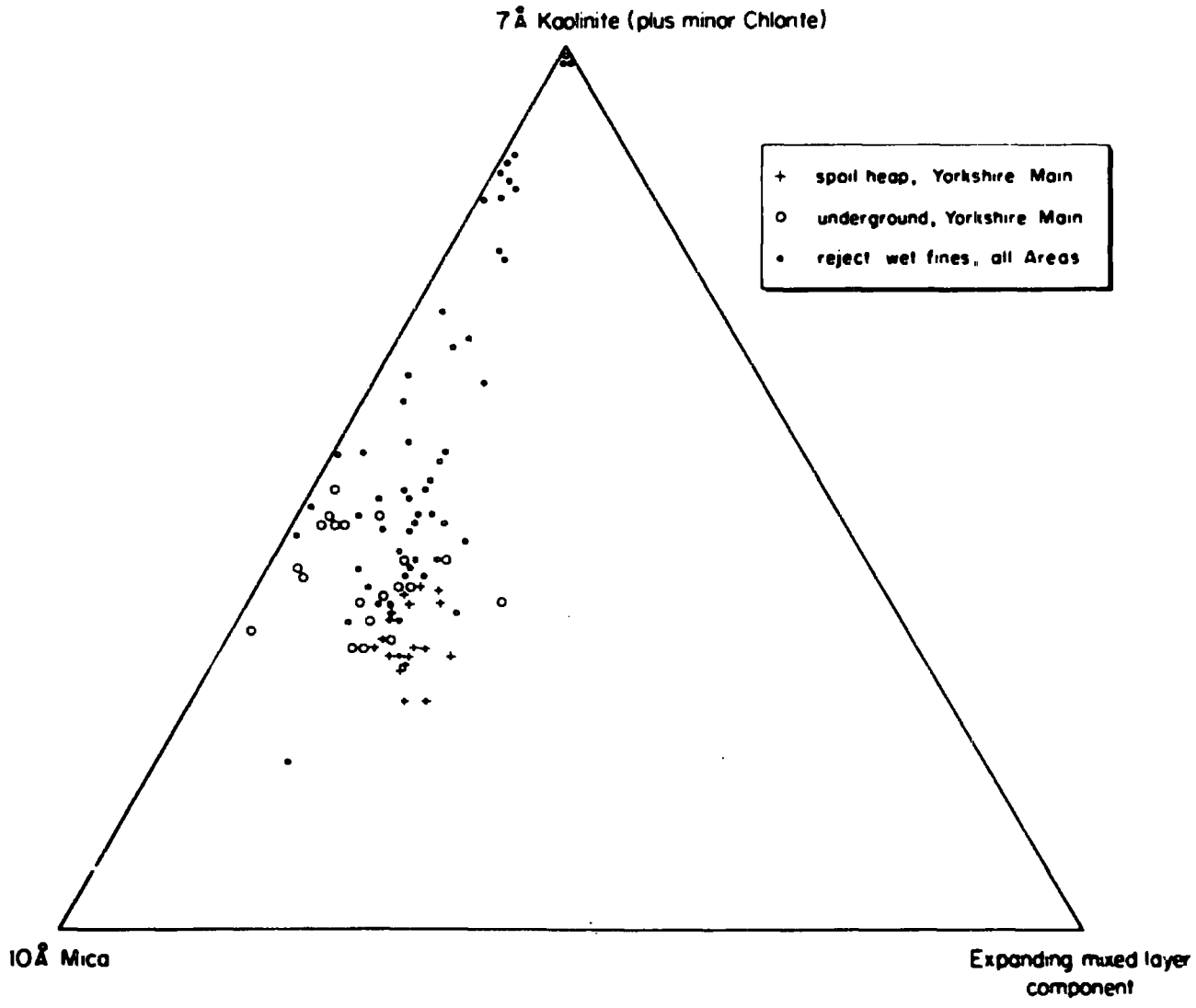

FIGURE 5.2

that of the underground samples (Fig. 5.1). These results are superimposed on the clay mineralogy of the tailings samples discussed in Chapter 2.

The writer has used the S.P.T. chemical analyses for the discussion of tip chemistry and mineralogy because it is likely that these samples are dominantly matrix material which is more susceptible to weathering; the larger resistant fragments are pushed aside during the driving of the small split-spoon sampler. In Section 5.15 it will be demonstrated that there are differences in the mineralogy and chemistry of the two sample sizes.

From Figure 5.2 it is evident that kaolinite and illite are present in about equal proportions, with smaller amounts of mixed-layer clay and subsidiary chlorite. Feldspars were detected only in the Permian marl beneath the tip. As mentioned earlier in the text hemihydrate was proved in two samples, whilst the presence of gypsum was confirmed. The carbonates proved to consist of calcite, siderite and ankerite (given in order of increasing abundance). It is important to record that pyrite was also identified in 28 out of the 38 samples. The value of microscopic and X-ray identifications lies in the interpretation of the chemistry.

From the correlation matrix (Table 5.5) the positive correlation between Al_2O_3 and K_2O reflects variations in total clay abundance. This may also be true for correlations between both these oxides and TiO_2. The positive correlation between free silica (quartz) and Al_2O_3 implies that the variation in quartz is similar to that of the clay minerals. At the 95 per cent confidence limit MnO, MgO and CaO show a negative correlation with depth. All of these oxides and FeO, show positive inter-relationships, which are due to variations in the total carbonate content in the spoil. This is different from Brancepeth where secondary sulphates and not carbonates played a leading role in mineralogical considerations. It will also be

TABLE 5.5

Correlation matrix for elements and oxides in the Yorkshire Main tip

depth																
free silica						Correlations of the Type A/B vs. B are excluded										
combined silica						±95% confidence limit, r=0.4227										
TiO_2						±99% confidence limit, r=0.5368										
Al_2O_3	+99	+95		+95												
Fe_2O_3		-95	-99		-99											
FeO			+99			-99										
MnO	-95						+99									
MgO	-95					-95	+99									
CaO	-95				-95		+99	+99	+99							
Na_2O			+95													
K_2O				+99	+99					-95						
SO_4, acid sol.	-99	-95			-99	+99										
S, in pyrite		-95	-99	-95	-99	+99	-99	-95	-99		-95	+95				
P_2O_5																
H_2O^+										-99						
Organic carbon			-99			+99				-99			+99			
combined SiO_2/Al_2O_3	-95	+95					+99		+95	+95	+95					
K_2O/Al_2O_3	-99							+95	+95	+95		+95				
Na_2O/Al_2O_3											-99				-99	-95
MgO/Al_2O_3	-99						+95	+99		+99		+99				
CaO/Al_2O_3	-99						+99	+99	+99			+95				

Depth
free silica
comb. silica
TiO_2
Al_2O_3
Fe_2O_3
FeO
MnO
MgO
CaO
Na_2O
K_2O
SO_4, acid sol.
S, in pyrite
P_2O_5
H_2O^+
Organic C

recalled that oxide/alumina ratios did not prove particularly useful in Brancepeth interpretations because of the masking effect of sulphates. In the Yorkshire Main mineral suite some proportion of the carbonate oxides are contained in the clay minerals but this is not apparent from Table 5.5. These oxide/alumina ratios show a change in the proportion of carbonate to clay minerals and hence the negative MgO/Al_2O_3 and CaO/Al_2O_3 correlations with depth. However, jarosite is only present in the very near-surface material so the negative K_2O/Al_2O_3, correlation with depth signifies that illite is decreasing as the age of the material increases.

The profiles of element variation through the Yorkshire Main tip are instructive (for example, CaO, MgO and FeO, Fig. 5.3). First of all it will be noted that a sharp decrease occurs between samples Y16 and Y17 (85 and 90 ft). This is due partly to a change in carbonate content. Ankerite and calcite have been recorded in the underground samples in intimate association with the coal so it could be claimed that the carbonates in the older spoil have broken down more. However, there are good reasons for believing that the changes are original, viz:

1) The change is sharp; if due to weathering a more gradual change would be expected.

2) If due to weathering, calcite would be preferentially removed, but calcite and ankerite are both involved in this change.

3) The carbonate is present on the cleat faces in the coal and is thus susceptible to changes in the coal preparation practice, which has taken place according to the N.C.B. records.

It must be emphasized that in any case these changes are small, amounting to no more than a few per cent of the total composition. Certainly they have not had an adverse effect on physical properties, especially shear strength (Table. 5.9).

Figure 5.3

Variation in CaO, MgO, FeO and MnO through Yorkshire Main tip.

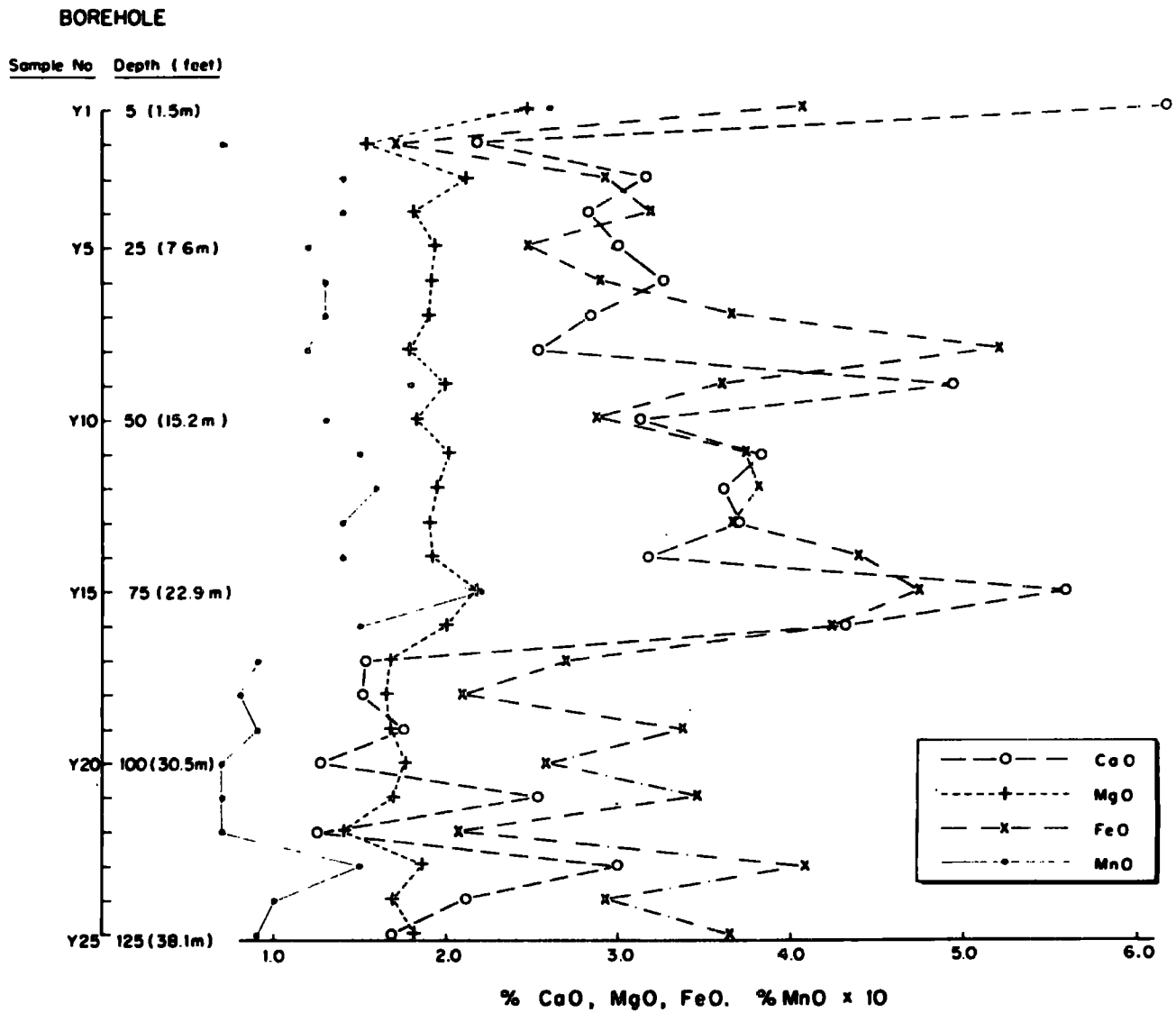

FIGURE 5.3

FIGURE 5.4

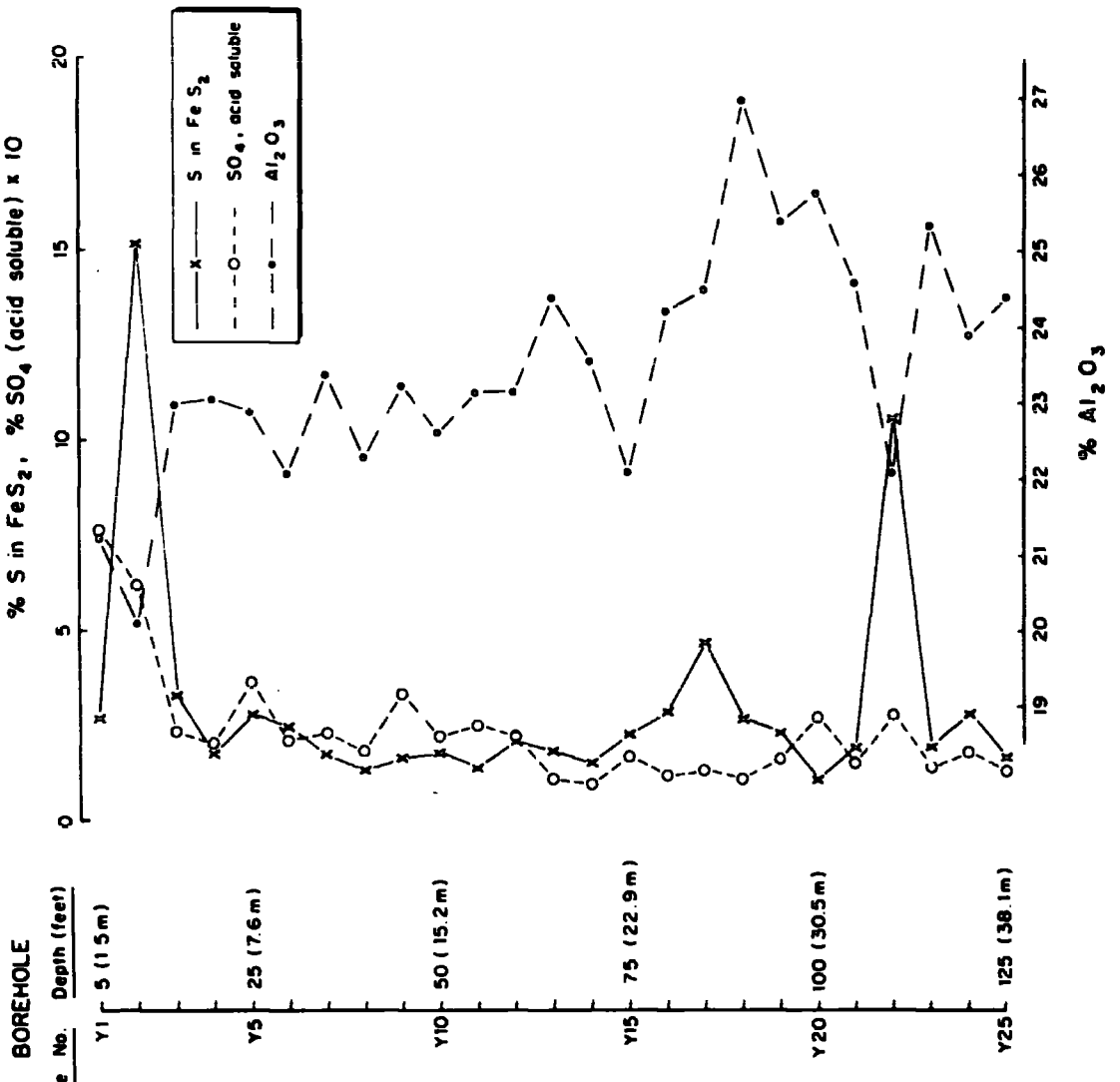

Figure 5.4

Variation in acid-soluble sulphate, sulphur in pyrite and Al_2O_3 through Yorkshire Main tip.

The acid soluble sulphate percentage (Fig. 5.4) is a measure of gypsum content. The relationship with depth (Table 5.5) is due primarily to the top two samples (Y1 and Y2). If these two samples are excluded the acid soluble sulphate (gypsum) distribution is similar in some respects to the carbonates (i.e. similar origin - cleat faces of the coal). The two highest sulphates (both in position and percentage) probably result from pyrite breakdown within the superficial zone and it is of interest that the vertical depth of the erosion channels (Plate 5.1, channel marked B) is 10 ft (c.f. sample Y2). The survival of pyrite in the Yorkshire Main tip is yet another indication that once the unburnt spoil is tipped and buried it changes little. The amount of pyrite now present is probably at its original level, there being no evidence from the acid soluble sulphate that pyrite decomposition has occurred in the body of the tip. Jarosite was identified to depths of about 2.5 ft below the surface, but this low temperature sulphate has not been recorded at depth. The high level of acid soluble sulphate in samples Y1 and Y2 may be related to surface weathering but it is probably more a measure of shallow percolation and precipatation. Once again the shear strength parameters in the upper near-surface zone are not markedly affected (Table 5.9).

The detrital fraction (including the clay minerals) are relatively stable under weathering conditions (Chapter 3). Extensive structural breakdown of the clay minerals in the spoil-bank is therefore unlikely. If we now consider the Al_2O_3 profile and correlation with depth (Fig. 5.4, Table 5.5) a systematic increase is apparent. This of course could reflect a change in total clay abundance, but if this were so both K_2O and combined silica could be expected to show similar increases. However, the K_2O/Al_2O_3 ratio falls with depth, and at a lower level of significance so does the combined SiO_2/Al_2O_3 ratio (Table 5.5). Although small these changes are variations in clay mineral species. At first sight the falling K_2O/Al_2O_3

ratio might be assigned to leaching of potassium from the micaceous minerals with depth. If this were so the combined SiO_2/Al_2O_3 ratio should show little or no change. The ratio does change (Table 5.5) which means that leaching of K^+ can be eliminated*. In the tip samples the changes in clay mineral compositional ratios are presumably too small to be detected by X-ray diffraction. The underground samples show that as ~~the~~ grain size increases (in some of the coarser non-marine roof rocks), so too does the kaolinite content (see also Taylor, 1971). On the other hand in some of the high clay content floor-measures illite is the dominant clay mineral type.

Within the tip therefore, it would seem logical that one or both of the following conditions obtained:

1) During the early stages of underground exploitation roof measures were preferentially extracted, but the balance was gradually redressed once the seam was developed.
2) The fine fraction (enhanced illite) was concentrated by changing washery practice.

It is of interest to note that the compositional difference between U4 and S.P.T. samples can be explained by increased kaolinite in the former (Section 5.15).

5.5 Water sample analysis and tip permeability

During the sinking of the first borehole two falling head permeability tests were carried out, using the conventional falling-head principle. The borehole lining is pulled back a known distance and the hole topped-up with water. The fall in head (measured with an electronic dip-meter) is timed and a graph plotted. From Hvorslev's (1949) formula (condition C, Lamb and Whitman, 1969, p.284) the mean coefficient of permeability (k_m) is calculated.

* The illite shape factors of U4 samples (Table 5.7) are low and are not symptomatic of degraded and disordered illite (c.f. Brancepeth Table 4.6).

TABLE 5.6

Ground-water analyses

Element		Yorkshire Main (1) concentration, mg/litre (ppm)	Yorkshire Main (1) relative proportions Ca, Mg, Na, K by weight	Coal Measures Sandstones. East Midlands mean values (2) relative proportions Ca, Mg, Na, K by weight
Si	(aa)	7		
Al	(aa)	< 1		
Fe	(S)	5		
Ca	(aa)	660	19	17
Mg	(aa)	428	12	3
Na	(fp)	2,355	68	79
K	(fp)	36	1	1
Mn	(aa)	2		
Total Ca, Mg, Na, K, mg/litre =		3,479		32,086

pH = 7.2

(1) Analyst, V.A. Somogyi Methods (aa) atomic absorption, (S) spectrophotometer, (fp) Flame photometer

(2) figures from Downing and Howitt (1969).

Figure 5.5

Permeability (field and laboratory) plotted against porosity of materials

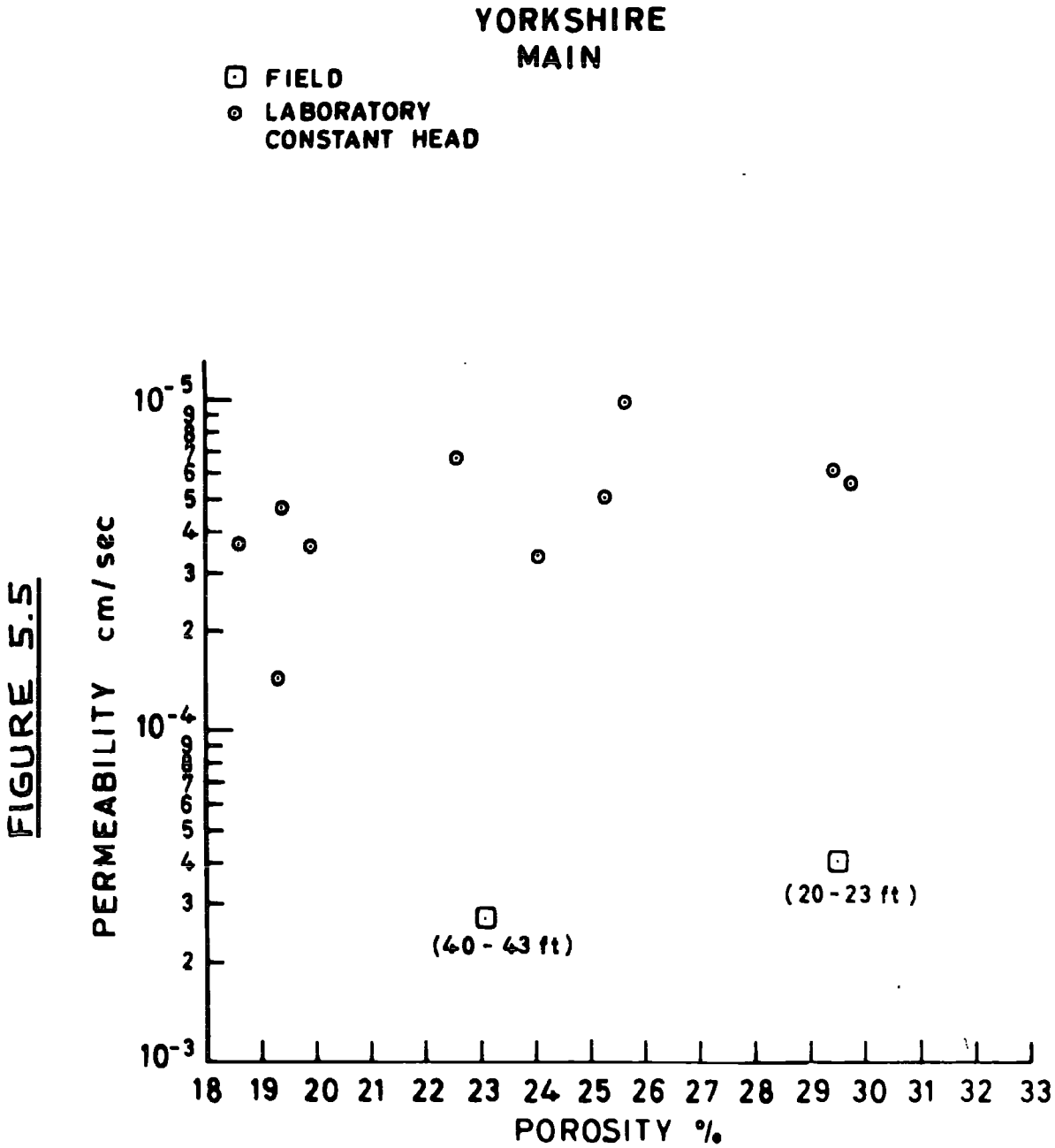

FIGURE 5.5

$$k_m = \frac{\pi D}{11(t_2-t_1)} \log_e \frac{H_1}{H_2}$$

where: D = diameter of exposed section of borehole = diameter of standpipe

H_1= piezometric head for time = t_1 (sec)

H_2= " " " time = t_2 (sec)

(other dimensions in centimetres)

The two values obtained (3.97×10^{-3} cm/sec- 20 to 23 ft; 2.68×10^{-3} cm/sec - 40 to 43 ft) are about an order of magnitude greater than the mean permeability of recompacted U4 samples (Fig. 5.5, Table 5.1). Single borehole field measurements are not usually regarded as precise, but it should also be mentioned that the laboratory values took about 100 hours before an equilibrium value could be obtained (see Fig. 2.5 for fragmental shale). De-airing is the main problem with these constant-head tests, plus the fact that the standard equipment is on the small side for this size of 'aggregate'.

It is the order of results which is important, the range 10^{-3} to 10^{-5} cm/sec being designated by Terzaghi and Peck (1967) as 'low permeability'. The writer had a christmas-tree constructed and concreted into the second borehole so that temperature measurements, water table measurements and gas samples could be taken periodically. After 12 months a water sample was taken for analysis (Table 5.6). One good reason for checking the composition of the standing water in the tip was the occasional reference to high Na^+ ion concentrations in colliery spoils (e.g. Watkins, 1959; Weeks, 1969).

The Yorkshire Main groundwater (Table 5.6) exhibits a low iron content which is supporting evidence for pyrite and iron-rich carbonate stability, as is low aluminium content for clay stability. The silica figure for this tip is well within the expected range for normal groundwaters (see Chapter 4,

Section 4.6, a)). However, the contents of sodium, calcium, magnesium and potassium are higher than normal (see White et al., 1963) and require further comment. Carbonate decomposition could account for calcium and magnesium, but this is unlikely because iron and manganese are not high. Gypsum could be the source of calcium, although this does not explain the high magnesium content. Alternatively all four elements could have been leached from the clay minerals, but why the predominance of sodium over potassium? Similarly, a jarosite origin raises the same question. The evidence so far presented on mineral stability, together with these anomalies, makes it very unlikely that the four elements have in fact been leached from the tip minerals.

One important possibility is connate water, trapped within the voids when the sediments were originally deposited. Comparison with the data of White et al., (1963) shows that this tip water is of intermediate composition between waters in which there is a meteoric component and waters believed to be mainly connate. It is also of interest to note that the cation proportions can be compared with detailed analyses of other Carboniferous groundwaters (see mean values for Coal Measures sandstones of the East Midlands, Table 5.6). The cation proportions of the tip water and the groundwaters are very similar, though the latter are more saline. Hence, there is evidence for suggesting that the chemistry of the water within this great tip complex at Yorkshire Main Colliery is controlled largely by the connate water released from the debris, with some dilution by meteoric water. The low permeability of the spoil is certainly compatible with this contention.

5.6 Liquid and plastic limits

From the Casagrande plasticity chart (Fig. 5.6) it is readily apparent that twelve of the thirteen spoil samples are split into two groups (ML/OL and CL) by the 'A' line. The remaining sample* from near the 50 ft

* See S.P.T. profile on Fig. 2.7

FIGURE 5.6

CASAGRANDE CLASSIFICATION
BRANCEPETH & YORKSHIRE MAIN

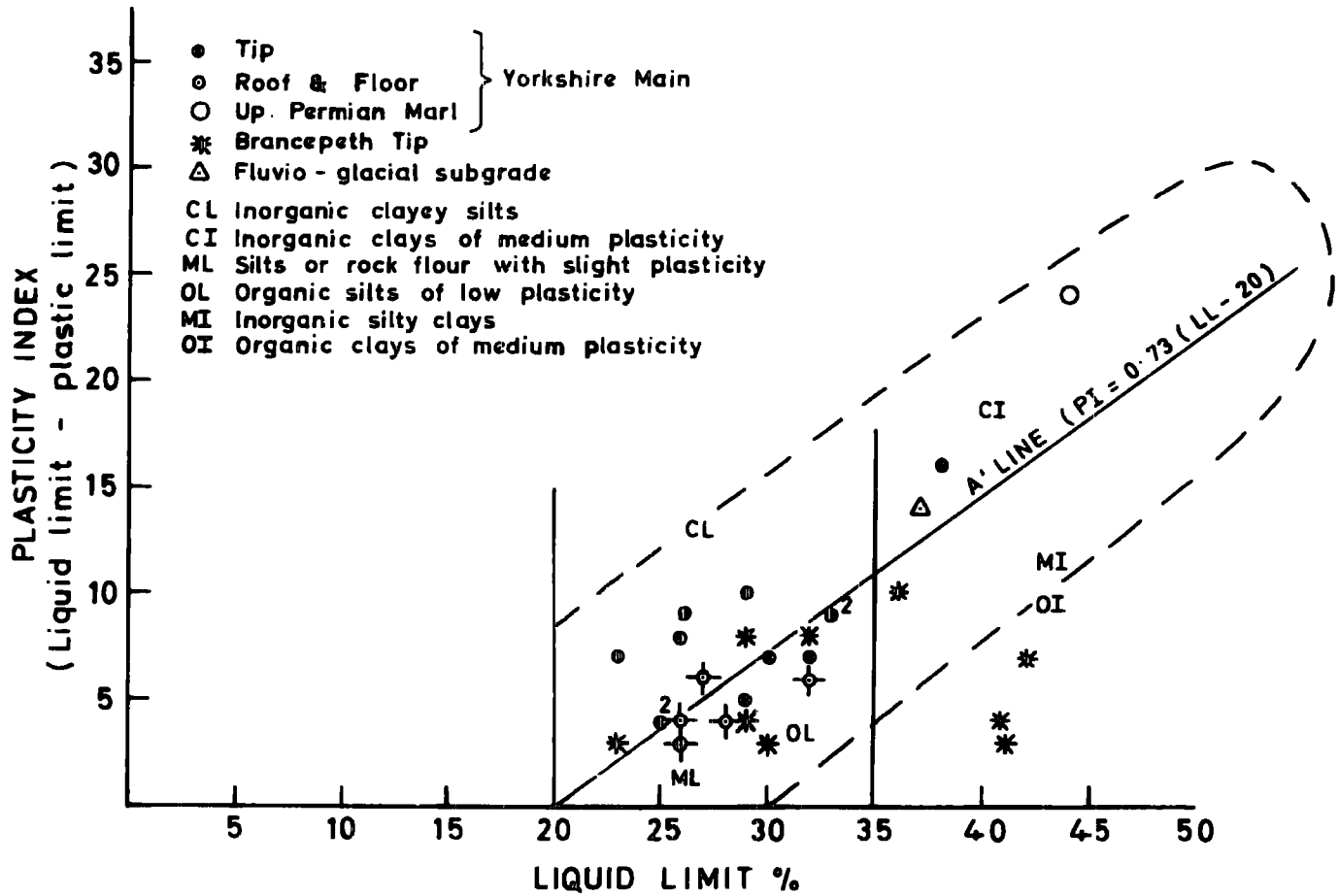

Note: 95 per cent of all results collated by N.C.B. lie within the dashed line.

FIGURE 5.6

FIGURE 5.7

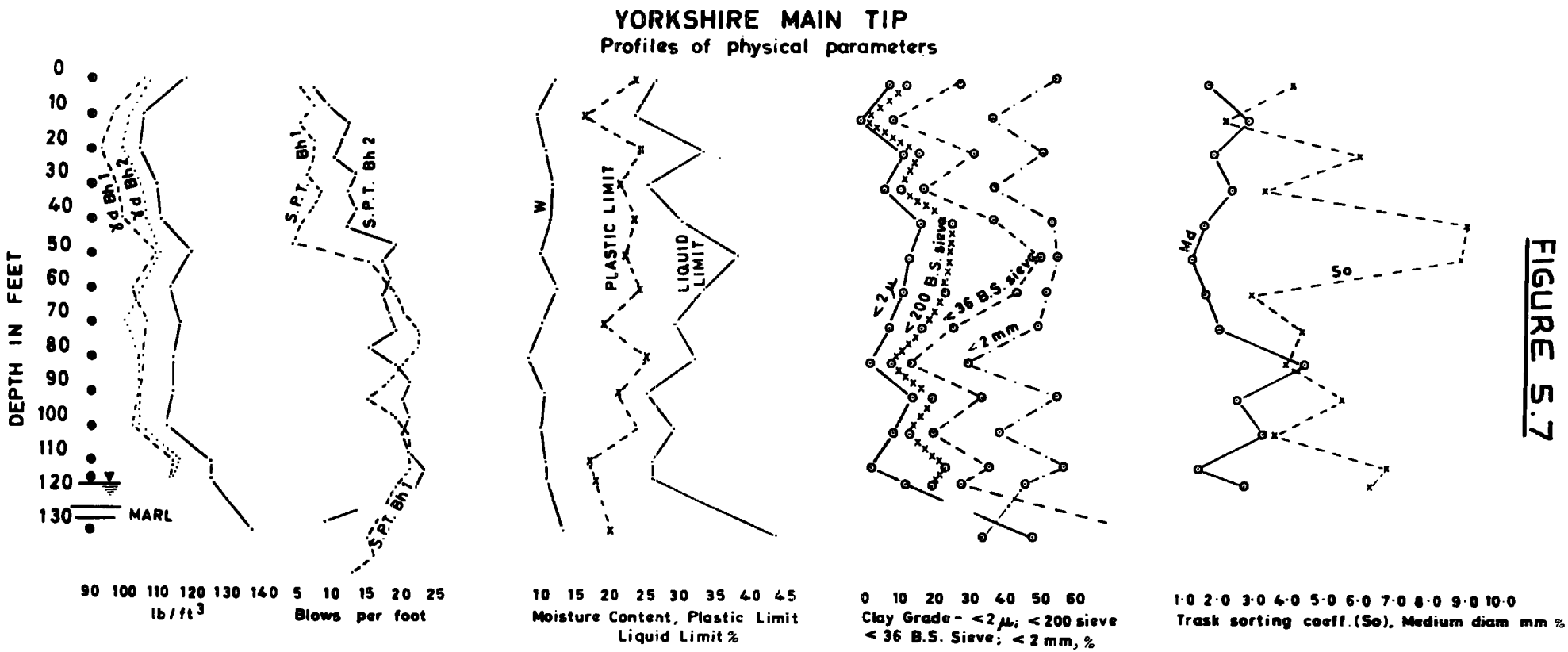

FIGURE 5.7

TABLE 5.7

Properties of Yorkshire Main discard

Sample	Bulk density, Bh 1. lb/ft^3	Dry density, Bh 1. lb/ft^3	Dry density, Bh 2. lb/ft^3	Permeability, cm/sec, x 10^{-4}	Moisture Content %	Specific Gravity	Organic Carbon %	Liquid Limit
A	117	105	107	3.36	11.4	2.21	10.06	26
B	105	96	101	5.53	9.1	2.20	11.77	23
C	104	94	100	6.04	10.3	2.14	11.37	33
D	109	97	104	5.16	11.4	2.09	9.90	25
E	110	99	106	-	10.9	2.06	16.96	30
F	119	109	110	1.42	9.6	2.16	6.64	38
G	113	102	105	9.78	11.7	2.19	11.01	33
H	116	106	100	6.63	10.0	2.19	6.18	29
I	114	105	104	4.71	8.0	2.09	8.57	32
J	114	104	104	-	10.2	2.12	10.92	25
K	112	102	104	3.64	9.9	2.04	17.80	29
L	126	114	116	-	10.6	2.23	9.10	26
M	125	113	114	3.70	10.6	2.22	9.29	26
Subgrade	137							

(table 5.7 continued over page)

TABLE 5.7 (continued)

Sample	Plastic Limit	Plasticity Index	Illite shape Factor	% less than 2 microns	% less than B.S.36 sieve	% less than 2 mm	Median diameter	Trask sorting coefficient
A	23	3	0.179	8.5	28.5	56.0	1.60	4.00
B	16	7	0.208	0.0	9.0	37.5	2.75	2.10
C	24	9	0.163	12.0	32.0	52.0	1.75	5.90
D	21	4	0.208	6.5	18.0	38.0	2.30	3.20
E	23	7	0.186	17.0	37.5	54.5	1.50	10.00
F	22	16	0.086	13.5	51.0	55.5	1.30	9.80
G	24	9	0.089	12.0	44.0	53.0	1.55	2.90
H	19	10	0.189	7.5	26.0	50.0	2.00	4.30
I	25	7	0.250	2.0	14.0	30.0	4.50	2.90
J	21	4	0.182	14.0	34.0	55.5	1.50	5.50
K	24	5	0.175	8.5	20.0	39.0	3.25	3.60
L	17	9	0.171	2.0	36.0	57.0	1.40	6.70
M	18	8	0.135	12.0	28.0	46.0	2.75	6.30

'boundary' is of higher plasticity (Fig. 5.7) and falls within the CI (medium plasticity) group. On Figure 5.6 the fabricated samples of Barnsley Bed roof and floor measures are also shown. These latter samples (Section 5.10b) are believed to be the parent materials of the tip samples. These fabricated samples tend to be mainly silty in character (ML) and it is of interest to record that the one with the highest liquid limit contains floor material which on Figure 5.2 is the sample with the highest mixed-layer clay content.

5.7 Density considerations with respect to the evolution of the tip

Both the bulk and dry densities of this spoil (Table 5.7) are higher than Brancepeth, this being partly a function of the lower organic carbon content of the Yorkshire Main U4 samples (see Section 5.9). The mean moisture content (10.3%) coincides with the modal values of English and Scottish spoils (N.C.B. Technical Handbook, 1970, Fig. 5.8). Turning to the density* and Standard Penetration Test (S.P.T.) profiles (Fig. 5.7) it can be seen that the dry densities of samples from the two boreholes (approximately 10 ft apart), vary by up to 7 lb/ft^3, particularly in the upper 50 ft of discard. It will be shown that the borehole 1 densities exhibit a significant density increase with depth (Table 5.10). The S.P.T. values of borehole 1 show that this material is very loose indeed. Standard Penetration Test values in granular materials give a measure of relative density, with values of 4 to 10 being designated loose and 10 to 30, medium dense. The scant evidence to date infers that comparisons between tips may be misleading (compare S.P.T./densities of Aberfan, Bishop et al., 1969, p.61, with the Yorkshire Main/results - Fig. 5.7). In a similar manner to the natural rocks of the in situ section (Chapter 3), it is more than likely that the intactness and strength of the individual fragments control the resulting penetration values. The Yorkshire Main S.P.T. profiles

* Bh.2 bulk densities are excluded because it was found that the discard in some of these U4's was in the process of drying out. Bulk densities were determined on total U4 content, dry densities from sub-samples.

Figure 5.8

Particle size distributions relating to Yorkshire Main tip.

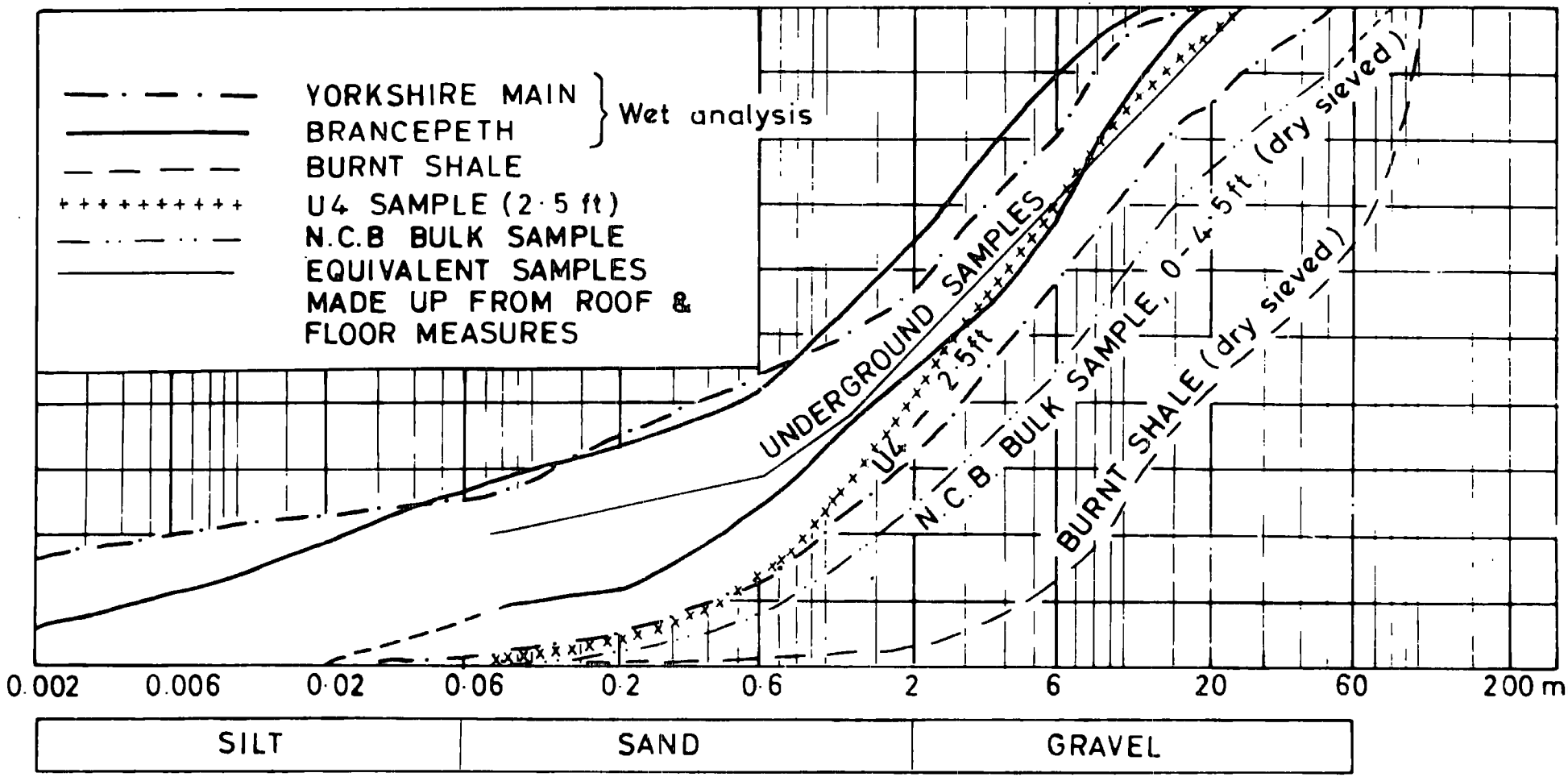

FIGURE 5.8

FIGURE 5.9

YORKSHIRE MAIN

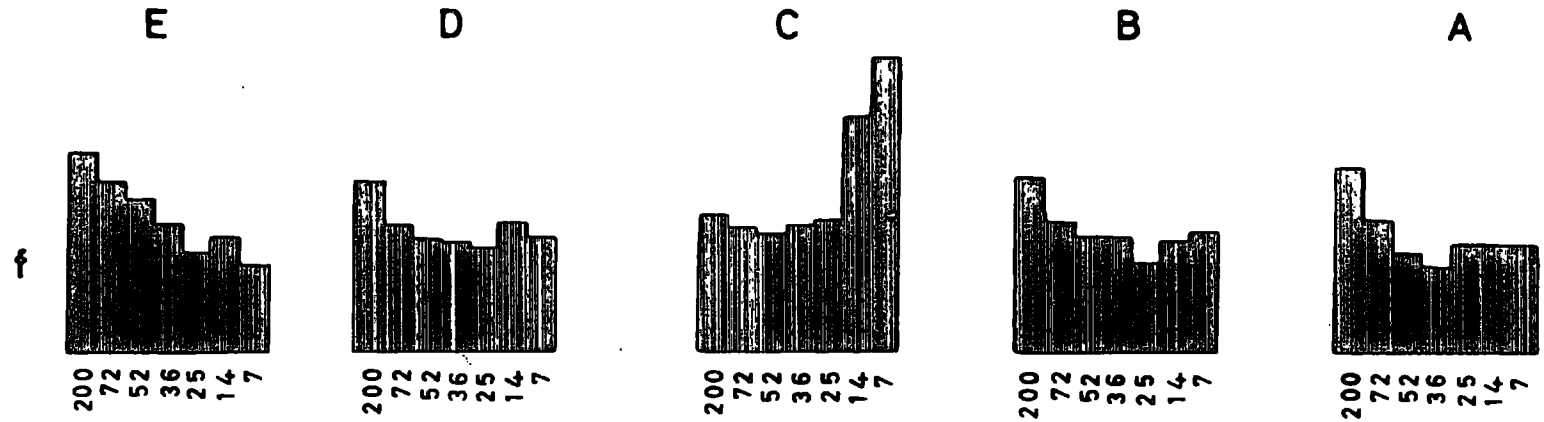

B.S. sieve sizes shown beneath histogram

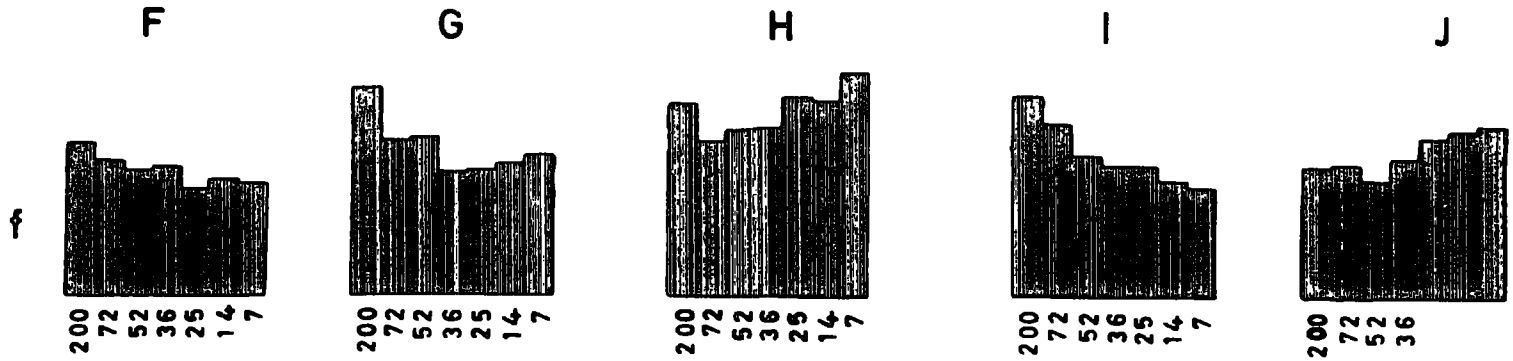

Organic carbon determinations at 375° C
(Relative weight percentages)

FIGURE 5.9

highlight two features which may well have an important bearing on the evolution of the tip. In the first place the 1:1250 N.C.B. plan of the tip, drawn from aerial survey data, shows quite clearly that the upper 50 ft of spoil represents a restricted area of discard. In other words, a time break or change in tipping procedure is almost certainly involved. Both the S.P.T. profiles and the change in densities bring out this feature very well. Moreover, the particle size and grading parameters (Fig. 5.7) show a somewhat similar trend. Whatever the reason for this particular change it has not been detected in the chemistry and mineralogy. The change that was recorded in the chemistry occurred around 90 ft. Here again the borehole 1 S.P.T. profile is in line with such a change. A more indistinct change in the borehole 2 profile could well be a reflection of the same phenomenon, the difference in level being attributed to the difficulty in ensuring that one is sampling the same horizon, even though the boreholes are close together, and were purposely set out along the 'strike' of the ridge. It is probably not fortuitous that the particle size parameters in particular (Fig. 5.7), also favour this interpretation. Taking all the evidence into consideration we can therefore reasonably suggest that the tip can be sub-divided into three stages.

5.8 Particle size distribution

The Brancepeth work showed that the highest frequency of clay grade material was 8 per cent. Some 62 per cent of the Yorkshire Main samples have a less than 2 micron fraction in excess of this figure. On Figure 5.8 the overall grain size distributions of the Yorkshire Main and Brancepeth wet analysed material are superimposed. They are remarkably similar for so varied a material, but for Yorkshire Main the increased percentages of fine material (silt and clay), as well as coarse sand and gravel sizes, are evident. The other grading curves shown on Figure 5.8 will be discussed later in the text.

One very important conclusion to be drawn from Figure 5.7 is that for all grain size levels there is no systematic increase in fines with the age of the tip. In line with the chemistry and the more tentative evidence from Brancepeth, progressive degradation with age and depth of burial is remote.

5.9 Specific gravity (G_s) and organic carbon content

The range of organic carbon in the U4 samples (Table 5.7) is much more restricted than that of Brancepeth (Yorkshire Main mean - 10.74% $\pm$ 3.26 std. dev.; Brancepeth mean - 19.91% $\pm$ 9.46 std. dev.). It will immediately be apparent that coal is concentrated in the S.P.T. samples (see Table 5.4). This will be referred to again in Section 5.15. Concentration of coal in the smaller sample sizes is mirrored in part by the tendency for coal to be concentrated on the finer sieve sizes (Fig. 5.9); this feature was of course noted in the Brancepeth material as well (Fig. 4.4).

The mean specific gravity is 2.15 which compares with 2.04 for Brancepeth; the absence of samples with a specific gravity of less than 2.0 is indirectly a reflection of the lower coal content of the Yorkshire Main heap. Whereas quartz content governed G_s in the in situ rocks (Chapter 3), organic carbon controls this physical property in the two spoil heaps. (negative correlation at the 99.9% significance level for Brancepeth, 95% for Yorkshire Main, Table 5.10).

5.10 Triaxial compression tests

a) Colliery discard

In a similar manner to Brancepeth the consolidated-drained triaxial tests were carried out at a rate of strain of 0.00012 in/minute. With the larger (8 in long x 4 in diameter) samples (Table 5.1) the rate of strain was reduced for tests that ran overnight. Saturation under a back-pressure of 50 lb/in^2 was again used and only one specimen failed to attain at least 90 per cent saturation. It will be observed (Table 5.8) that all

TABLE 5.8

Triaxial test data

Sample	σ'_{3f} lb/in^2	$(\sigma_1 - \sigma_3)_f$ lb/in^2	Linear strain %	volumetric strain %	Specimen dry density lb/ft^3
a) Yorkshire Main tip					
A	7.1	24.8	2.2	-1.3	105.0
	19.9	57.0	4.0	-1.5	103.6
	29.0	72.0	9.0	-2.8	104.7
	46.8	108.6	9.5	-2.4	105.4
B	9.0	40.0	6.0	-1.1	97.6
	19.6	49.2	8.7	-2.5	98.2
	28.0	79.6	10.0	-3.9	94.0
	47.3	110.4	12.2	-4.2	95.7
C	9.0	29.6	4.0	-0.5	90.7
	19.9	54.8	7.0	-1.3	94.3
	28.3	84.4	8.2	-2.4	88.0
	47.1	112.8	11.3	-2.8	88.9
D	9.4	20.0	7.1	-1.6	97.7
	18.5	60.4	9.8	-1.8	96.4
	29.0	64.0	8.9	-2.7	98.5
	41.1	96.0	8.7	-2.8	97.0

Sample	σ'_{3f} lb/in^2	$(\sigma_1 - \sigma_3)_f$ lb/in^2	Linear strain %	volumetric strain %	Specimen dry density lb/ft^3
E	5.5	24.4	4.2	-0.7	100.4
	19.0	55.8	7.5	-3.5	98.6
	22.8	66.4	6.2	-4.2	97.5
F	10.0	33.4	7.0	-0.2	107.5
	19.0	73.6	5.8	-1.1	112.7
	30.0	94.0	6.5	-2.7	107.4
	47.8	126.8	8.0	-3.1	107.0
G	10.0	30.6	8.8	-1.2	91.3
	20.0	56.8	7.7	-1.9	90.7
	30.0	83.4	11.3	-2.5	93.4
	46.2	129.4	10.9	-1.3	90.2
H	10.0	32.2	8.0	-0.5	107.2
	17.0	58.4	7.5	-0.9	103.6
	30.0	82.0	8.0	-1.2	105.5
	49.0	110.4	8.3	-1.6	106.8
I	10.0	30.0	2.9	-1.2	100.0
	19.8	75.2	8.1	-2.2	101.2
	30.0	99.2	8.3	-4.0	99.7
	40.0	140.0	8.9	-4.2	98.3

Sample	σ'_{3f} lb/in^2	$(\sigma_1 - \sigma_3)_f$ lb/in^2	Linear strain %	volumetric strain %	Specimen dry density lb/ft^3
J	10.0	28.6	6.7	-0.6	105.5
	17.2	49.4	7.1	-2.2	101.7
	26.2	67.4	9.0	-3.9	104.3
K	10.0	38.6	3.0	-0.3	100.7
	19.0	50.6	7.5	-0.7	103.2
	29.0	94.2	6.4	-1.8	101.6
	46.0	113.4	7.2	-2.2	102.1
L	8.8	13.6	4.4	-1.1	113.2
	18.8	54.0	6.2	-2.3	113.6
	28.2	80.6	8.5	-3.7	113.5
M	9.0	35.4	2.5	-0.4	114.4
	20.0	48.4	7.3	-1.3	112.8
	28.0	90.8	8.7	-2.7	113.5
	49.0	116.4	9.0	-3.2	113.7
Subgrade	5.0	29.4	4.4	+0.2	121.4
	10.0	63.8	6.2	-0.7	120.1
	20.0	80.6	5.1	-1.4	120.1
	30.0	117.6	9.0	-2.1	121.3

Sample	σ'_{3f} lb/in^2	$(\sigma_1 - \sigma_3)_f$ lb/in^2	linear strain %	volumetric strain %
b) Fabricated specimens from underground measures				
R1A-R1F	7.8	29.6	7.0	-2.1
	27.0	85.2	11.2	-3.6
	37.8	95.6	12.0	-4.6
F1A-F1C	8.5	32.4	3.4	-1.7
	18.7	62.8	8.0	-3.6
	35.0	100.0	11.8	-2.9
	46.9	131.4	8.0	-5.4
R2A-R2G	6.0	24.0	8.0	-1.1
	19.0	44.4	8.0	-3.6
	28.3	73.6	8.4	-4.2
	36.2	102.2	11.6	-4.3
R2A-R2E	9.0	27.2	4.0	-0.9
	15.0	34.6	7.5	-1.2
	22.4	68.6	6.2	-3.0
	45.0	90.6	6.0	-3.2
F2A-F2C	8.6	14.4	7.5	-0.9
	15.0	40.0	10.0	-2.7
	40.0	70.0	9.0	-4.0
	46.0	78.4	11.5	-3.9

Initial dry density = 110 lb/ft^3

TABLE 5.9

Triaxial Shear Strength Parameters

YORKSHIRE MAIN TIP

Sample	N-Ø	ϕ' (c'=0)	ϕ' degrees	c' lb/in^2	r*	t*	Significance* level	U	Significance with respect to c'=0
All data	47	35.0	33.5	2.15	a)0.9918 b)0.9982	53.2219 114.3358	99.9% 99.9%	2.7243	99-99.9%
2'6"- 4'0"	2	33.5	30.5	3.41	a)0.9994 b)0.9992	41.5763 35.8364	99.9% 99.9%	5.1571	95-98%
12'6"- 14'0"	2	34.0	30.0	5.25	a)0.9953 b)0.9980	14.4886 22.4100	> 99.0% > 99.0%	2.8097	80-90%
22'6"- 24'0"	2	34.5	32.0	3.19	a)0.9968 b)0.9990	17.5628 31.1587	> 99.0% > 99.0%	1.8671	70-80%
32'6"- 34'0"	2	33.0	32.5	0.76	a)0.9898 b)0.9982	9.8044 23.6544	> 98.0% > 99.0%	0.2781	10-20%
42'6"- 44'0"	1	37.0	33.5	2.98	a)0.9999 b)0.9993	63.5676 27.3563	> 98.0% > 95.0%	11.6075	90-95%
52'6"- 64'0"	2	36.5	33.5	4.57	a)0.9949 b)0.9986	13.9746 26.3056	> 99.0% > 99.0%	1.8579	70-80%
62'6"- 64'0"	2	35.5	32.5	0.63	a)1.0000 b)1.0000	160.7255 206.1987	99.9% 99.9%	2.9410	90-95%
72'6"- 74'0"	2	34.0	29.5	5.44	a)0.9955 b)0.9979	14.9023 21.7313	> 99.0% > 99.0%	2.9523	90-95%

(Table 5.9 continued over page)

82'6"- 84'0"	2	37.0	35.0	2.96	a)0.9962 b)0.9991	16.2505 32.4513	> 99.0% 99.9%	1.2353	60-70%
92'6"- 94'0"	1	35.0	33.0	1.56	a)0.9988 b)0.9997	20.7622 43.9969	> 95.0% > 98.0%	1.9414	60-70%
102'6"-104'0"	2	35.5	32.5	3.65	a)0.9920 b)0.9983	11.1440 23.9260	> 99.0% > 99.0%	1.3074	60-70%
112'6"-114'0"	1	35.5	39.5	-3.71	a)0.9993 b)0.9989	27.2445 20.8872	> 95.0% > 95.0%	-4.3299	80-90%
117'6"-119'0"	2	34.5	32.0	3.49	a)0.9905 b)0.9978	10.1601 21.1603	> 99.0% > 99.0%	1.1528	60-70%
Permian marl	2	43.0	39.0	4.31	a)0.9966 b)0.9987	17.0145 28.1430	> 99.0% > 99.0%	2.2053	80-90%
2'6"- 92'6" (for slope stability)	36	35.0	33.5	2.35	a)0.9921 b)0.9982	47.5052 100.9384	> 99.9% > 99.9%	2.7977	99-99.9%
2'6"- 44'0"	17	34.0	31.5	3.25	a)0.9946 b)0.9984	39.4415 72.9416	> 99.9% > 99.9%	3.5939	99-99.9%
52'6"- 84'0"	14	36.0	34.0	2.82	a)0.9931 b)0.9985	31.7152 68.0243	> 99.9% > 99.9%	1.9527	90-95%
92'6"-119'0"	12	35.0	34.0	1.30	a)0.9917 b)0.9983	26.7888 59.0514	> 99.9% > 99.9%	0.9264	60-70%
FABRICATED UNDERGROUND SAMPLES									
All samples	17	33.5	33.0	0.94	a)0.9783 b)0.9955	19.4534 43.2780	> 99.9% > 99.9%	0.4750	30-40%

(Table 5.9 continued over page)

All samples less R2A-R2E set.	13	34.0	34.0	0.57	a)0.9780 b)0.9955	16.9052 37.9115	>99.9% >99.9%	0.2428	10-20%
R1A-R1F	1	35.5	33.0	3.51	a)0.9950 b)0.9987	9.9936 19.6454	> 90.0%+ > 95.0%	1.4588	
F1A-F1C	2	36.5	34.0	3.32	a)0.9998 b)0.9996	67.5489 49.6491	99.9% 99.9%	6.2016	95-98%
R2A-R2G	2	35.0	35.0	0.41	a)0.9966 b)0.9993	17.0134 38.6465	> 99.0% 99.9%	0.2405	10-20%
R2A-R2E	2	32.5	29.5	3.23	a)0.9966 b)0.9964	17.0134 16.5068	99.0% 99.0%	1.1992	60-70%
F2A-F2C	2	28.0	26.5	2.02	a)0.9923 b)0.9979	11.3631 21.8828	> 99.0% > 99.0%	1.0955	60-70%

*a) for reduced major axis regression c', Ø'

b) for y = mx (c'=0)

+below 95%(probably significant) confidence level

the volumetric strains are negative and conform with those of Aberfan tests (Bishop et al., 1969, p.58-59). The Permian marl which exhibits more elevated shear strength parameters than the tip discard (Table 5.9) does show evidence of over-consolidation (Table 5.8).

The statistical treatment of the results (Table 5.9) reveals that this spoil is rather different from Brancepeth. The composite results demonstrate that a cohesion value of greater than zero is statistically valid at a very high level of significance. It is of importance to record that from the acceptable values (not including the sample with a negative intercept) the chances that c' is greater than zero (at an arbitrary probability of greater than 50 per cent) is borne out by 92 per cent of the samples. On the other hand in the Brancepeth case the percentage is reduced to 50 for the same arbitrary level. In summary the evidence suggests that Yorkshire Main on the whole is a more cohesive spoil.

b) Fabricated equivalent roof and floor measures

These samples were made up from the fresh parental rocks from underground (Fig. 5.1). The way in which the fabricated samples were prepared was to separate out the size range smaller than a $1\frac{1}{2}$ in B.S. sieve but retained on a 1 in sieve. The individual bulk samples were then made up by mixing the aggregates on a weight basis and in proportion to their underground thicknesses (thickness measurements of individual beds from Figure 5.1). For example, sample F1A - F1C consisted of material from beds F1A, F1B and F1C. The aggregate was then put through a crusher and finally graded according to the 'average' particle size distribution shown on Figure 5.8. These equivalent roof and floor samples were made up to the average tip moisture content of 10 per cent and left in polythene bags overnight. Triaxial specimens (3 in long by $1\frac{1}{2}$ in diameter) were statically compacted to the mean borehole 2 dry density of 105 lb/ft^3.

The triaxial tests (under back-saturation) were carried out in a like manner to the tip samples. The composite shear strength results (Table 5.9)

suggest that this material is possibly more granular in behaviour than the tip itself, but it is of interest to see that the sub-division into roof and floor samples, respectively, produces a much greater range of shear strength parameters than is shown by the tip samples. The mudstone R2F, R2G has a marked effect on the roof measures parameters from the eastern district (Fig. 5.1), and it is suspected that the very low $\emptyset'$ angle of the F2A- F2C sample is a function of the high mixed-layer clay content of the F2C horizon. All the results however, will be considered in Section 5.14 because they have a very important bearing on the evidence relating to the lack of degradation in the spoil-bank.

5.11 Correlation of physical and mechanical data

Having gathered together the physical and mechanical data it is now feasible to consider the inter-relationships in the light of the tentative conclusions drawn from Brancepeth. The Yorkshire Main results can best be itemised as follows:

1) Borehole 1 bulk and dry densities not unexpectedly increase with depth of burial. Cross-correlations between densities of boreholes 1 and 2 infer that approximately the same sample horizons are in fact being sampled.

2) The negative correlation between G_s and organic carbon confirms the Brancepeth findings. The level of correlation is probably lower because the coal content of the Yorkshire Main U4's is also lower than Brancepeth.

3) Plastic limit again follows liquid limit positively, but a new positive relationship also emerges, relating plasticity index to liquid limit. Although this relationship is largely due to one specimen (see Fig. 5.6) it has also been recorded for a large batch of spoil samples from the Wimpey Central Laboratory. It could be an expression of Terzaghi and Peck's (1967) contention that samples from the same soil horizon (common parental material in the case of spoil) have a tendency to define a line which is parallel to the 'A' line.

TABLE 5.10

Correlation matrix - physical and mechanical data

	ϕ_1' (c'=0)	ϕ_2' r.m.a.	c' r.m.a.	Bulk density	Dry density, Bh.1.	Dry density, Bh.2.	Moisture content	Specific gravity	Organic carbon	Liquid limit	Plastic limit	Plasticity index	Median diameter	Depth
ϕ_1' (c'=0)														
ϕ_2' r.m.a.			-99			+95								
c' r.m.a.						+99								+95
Bulk density						+99								+99
Dry density, Bh.1.													-95	
Dry density, Bh.2.									-95		-95			
Moisture content											+95	+99		
Specific gravity														
Organic carbon														
Liquid limit														
Plastic limit														
Plasticity index														
Median diameter														
Depth														

r= 0.5529 for $\pm$ 95% confidence level

r= 0.6835 for $\pm$ 99% confidence level

4) In this spoil the two statistical ϕ' values (ϕ'_1 and ϕ'_2) correlate positively just below the 95 per cent confidence level. However, because of the greater range of cohesion values, ϕ'_1 and c' correlate negatively at a very high confidence level. This is a logical correlation which could be expected from the Mohr envelope geometry. The positive association between borehole density and ϕ'_2 is also a correlation which could reasonably be expected, but as more test samples were extracted from borehole 1 than from borehole 2 a wider selection of results is necessary before placing too much emphasis on the relationship.

5) Natural moisture content and median diameter correlate negatively at the 95 per cent confidence level. Once again the relationship is worth bearing in mind for future statistical work. The propensity for hold water may well be a function of the grain size of tip materials.

5.12 Slope stability analyses

a) Slope profile and geophysical survey

From the tip cross-section which coincides with the erosion gulley marked A on Plate 5.1 (Fig. 5.10) it is clear that the extended platform of spoil at toe of the heap may represent the remains of a 'boot' produced by slumping at some earlier stage in the tip's evolution. Many of the features of this tip conform with those often associated with heaps in which slumping has occurred (N.C.B. Technical Handbook, 1970, pp. 2-4). On the other hand the platform (which has obviously been regraded) conforms reasonably well in level to the junction between the first and second phases of tip construction, which have previously been postulated from the chemistry and certain physical parameters. It can also be seen on Figure 5.10 that the water level in a deeply entrenched ponded area adjacent to the line of section (southern toe of tip) is at the same level as that of the tip itself.

FIGURE 5.10

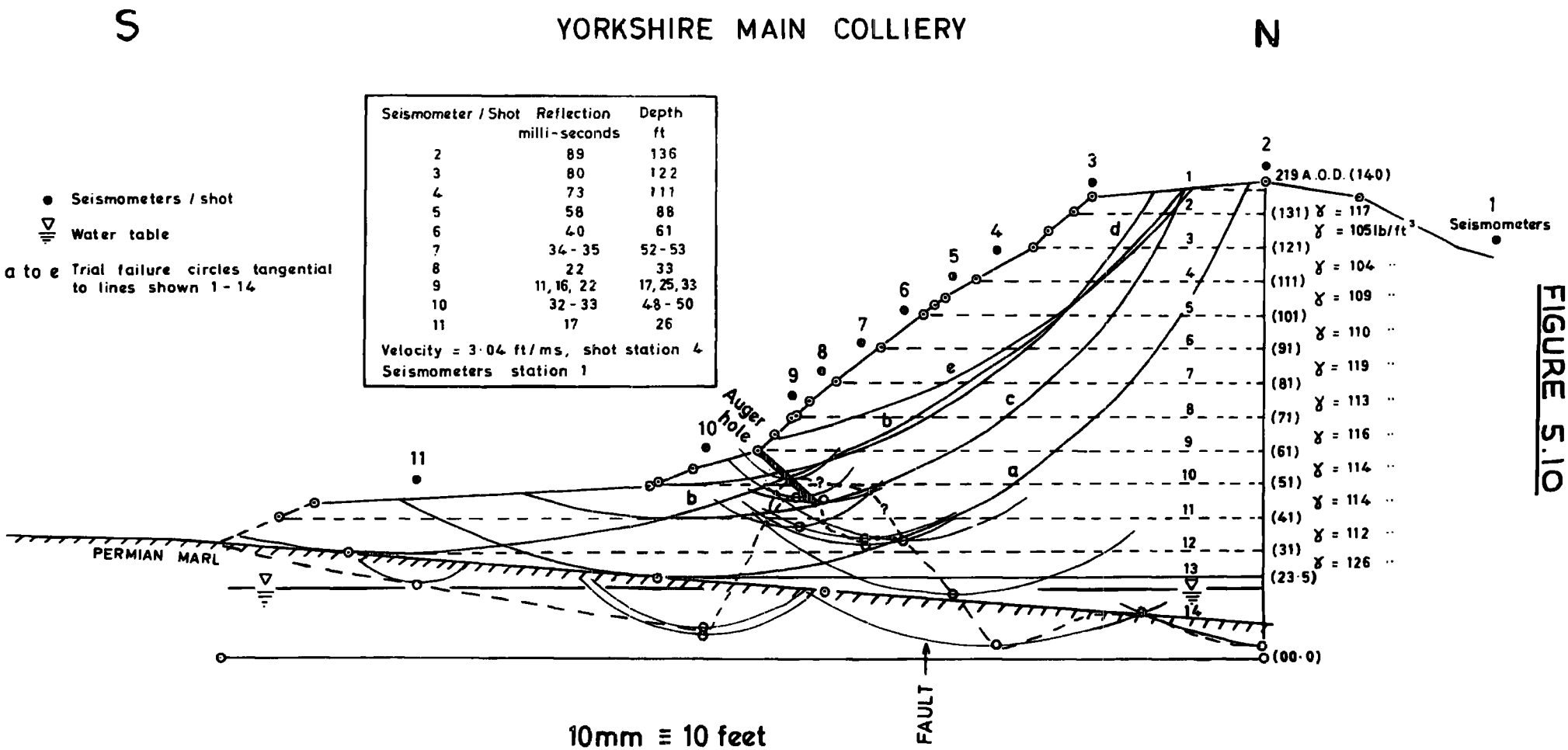

FIGURE 5.10

FIGURE 5.11

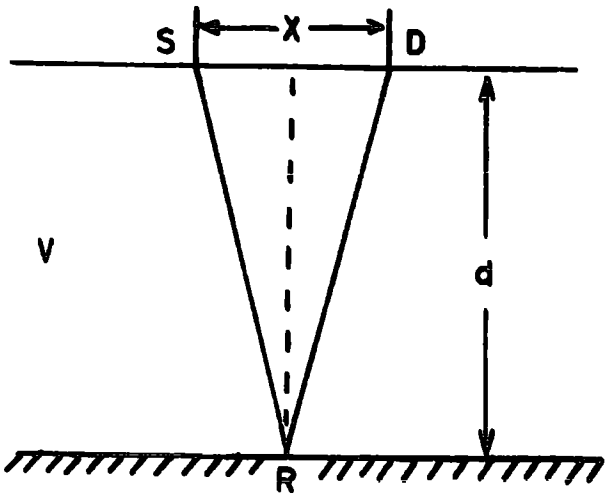

SIMPLE REFLECTION PATH

FIG. 5.11

In the diagram,

S = shot point
R = reflection point
and D = detector position.

The time T for the reflected wave to arrive at the detector after the initiation of elastic wave is given by

$$T = 2\,\frac{\overline{SR}}{V}$$

$$= \frac{2}{V}\sqrt{d^2 + \left(\frac{X}{2}\right)^2} \qquad \ldots\ldots(1)$$

or

$$d = \frac{1}{2}\left(V^2T^2 - X^2\right)^{1/2} \qquad \ldots\ldots(2)$$

where d = depth to the reflecting horizon
X = distance between shot point and detector
V = velocity of the overlying material

If in equation (1), X is much smaller than d, the effect of irregularity in depth due to the horizontal distance is negligibly small.

Hence

$$T = \frac{2d}{V}$$

or

$$d = \frac{VT}{2} \qquad \ldots\ldots(3)$$

TABLE 5.11

Slope stability analyses

Trial circle	Shear strength parameters used (ref.Table 5.9)	x co-ordinate ft	y co-ordinate ft	Tangential to line No.	Factor of Safety
a	c'Ø' composite	170	200	14	2.125
b	Ø' composite	255	336	14	1.923
c	c'Ø' composite	170	200	11	1.729
d	c'Ø' composite	180	220	10	1.562
e	c'Ø' composite (upper tip)	185	270	9	1.585

Because of this somewhat unusual profile it was decided to carry out a simple geophysical survey along the traverse using a Huntec FS3 hammer seismograph in the reflection mode (see Figure 5.11). Using bundles of six 'star-brand' I.C.I. detonators as a seismic source some twelve repeatable velocities were obtained for the spoil (3040 ft/sec). The seismometers and seismograph unit were at position 1, the shot station being station 4 (Fig. 5.10). Having ascertained a velocity it was possible to use a large excavation close to the borehole positions in order to try and calibrate any reflecting horizons with the known borehole data. A consistent reflection at 136 ft was obtained from eight shots on two different occasions. This depth conforms with the junction between the marl and the underlying dense sand.

The resulting profile, which was re-checked on a separate occasion, is interesting because it suggests that there has been either considerable heave of the subgrade, possibly in response to some earlier slumping, or, a wedge of more compact materials has been emplaced during an earlier stage in the tip's history. To try and resolve this question an inclined auger hole was put down (Fig. 5.10). Between 8.5 ft and 24.5 ft (maximum penetration distance) both normal and burnt shale was encountered, together with patches of Permian marl. At 24.5 ft the hole was in dense unburnt spoil.

Hence, the undulation is made up of materials which are greatly different from the borehole spoil, and the writer is inclined to believe that it is a 'heave' phenomenon. Whatever its origin it is now acting as a compacted 'key' which will afford support to the steeply inclined upper slope.

b) Factor of safety - limit equilibrium analyses

If we assume that the stabilizing key of compacted materials beneath the upper slope is absent, it can still be demonstrated from the series of trial failure circles (and conditions), shown on Table 5.11, that the overall stability of the slope is not in question.

The slope has been divided up into component layers according to the borehole density profile (Fig. 5.10). The shear strength parameters used in the computer program conform with the more realistic composite parameters for the total slope, and the upper slope, respectively. The values of c', ϕ' and density for the Permian marl are given on Tables 5.7 and 5.9.

Considering first of all the complete slope (circle a, Fig. 5.10), the extended platform of spoil forming the toe of the slope acts as a component that is resisting failure, so the factor of safety (F) is correspondingly high (2.125). By taking a toe circle for the overall slope (circle b) and a frictional hypothesis ($\phi'=35°$, $c'=o$), the factor of safety is only marginally reduced (1.923).

The upper slope is treated first of all as though subject to a base failure (assigning line 11 as its subgrade - Fig. 5.10). Once again the factor of safety is high (1.729). Even when trial toe failures are taken for lines 10 and 9, the resulting order for F is above the acceptable level for populated areas (F=1.5). In fact the limiting condition for a toe failure to occur in the upper slope involves a mass of spoil that is no thicker than the maximum depth of the erosion channels, namely 10 feet.

Possible failure zones are therefore extremely superficial and the morphological features of these failures can be demonstrated by the erosion gulley shown as B on Plate 5.1. The vertical depth of this particular gulley is 10 ft near the crest, 6 ft in the middle section and 3.5 ft adjacent to the platform of spoil which forms the toe of the spoil-heap. By the time that erosion by run-off has cut a channel with near-vertical sides approximately 6 ft deep, shallow seated rotational failures occur on each wall of the gulley. The loci of the centroids of the spoil above the failure planes move diagonally towards each other and in places the failed spoil from each wall forms an apparently composite mass. However, erosion during wet periods rapidly removes this spoil as a mud-run. On Plate 5.1

TABLE 5.12

Compaction tests, Yorkshire Main

U4 samples used Depth ft	Maximum dry density lb/ft^3	Optimum Moisture Content %	Bh. 1 dry density lb/ft^3	% optimum	Bh. 2 dry density lb/ft^3	% optimum	Borehole Depths (density) ft
0.0 - 4.5*	107	12	105	98	107	100	2.5 - 4.0
47.5 - 49.0 plus 57.5 - 59.0	107	9	109	102	110	110	52.5 - 54.0
67.5 - 69.0 plus 77.5 - 79.0	108	10	106	98	100	93	72.5 - 74.0
77.5 - 79.0 plus 87.5 - 89.0	108	12	105	97	104	96	83.5 - 84.0
97.5 - 99.0 plus 108.5 -109.0	113	10	102	90	102	92	102.5 -106.0

*N.C.B. bulk sample

Mean maximum dry density, 108.6 lb/ft^3
Mean dry density, Bh.1, 103.4 " - 95% optimum
Mean dry density, Bh.2, 105.7 " - 97% optimum

the scars of these superficial failures can be seen in the middle and upper section of the gulley (marked B). At the top of the gulley a mass of failed loose spoil can be observed, and this will ultimately be eroded.

5.13 Compaction characteristics

Also related to overall stability is the state of compaction of the spoil. The low standard compaction tests (B.S. 1377/1967) can be compared with the borehole densities which bracket the U4 materials used for compaction (Table 5.12). The maximum dry densities attained are at least 7 lb/ft^3 higher than Brancepeth (see Table 4.19), and organic matter of low specific gravity is primarily responsible for this difference. What is very marked in the Yorkshire Main tip is the uniformity in maximum dry density (107 to 108 lb/ft^3) down to the 90 ft level. The data imply that the normal civil engineering compaction standard (95 per cent maximum) has been achieved to a depth of 60 ft below the tip plateau. This of course is under natural conditions of aerial ropeway emplacement. The lowest percentage is 90, like Brancepeth; once again the low relative density (83%) of Aberfan is emphasized. Taking the evidence of both tips into account (Brancepeth and Yorkshire Main), together with the field reclamation densities at Brancepeth, it is reasonably clear that 90 per cent maximum dry density can be expected for tips which are about 50 years in age. Moreover, it would seem extremely unlikely that mechanical compaction will achieve a higher level under normal spoil-heap conditions. From a safety aspect however, the 90 per cent level could be achieved by compaction throughout the emplacement stage when failures may well occur in the spoil which will be in its loosest state.

5.14 Shear strength characteristics with respect to degradation

The shear strength characteristics of the tip materials can be used to confirm that progressive weathering is not taking place with age or depth of burial within the heap. Even more convincingly comparisons can

TABLE 5.13

F-value on differences between regression lines (Chow test)

Samples	F-value	Degrees of Freedom	Variance Ratio at 5% significance level
1. 2.5 to 44.0ft vs. 52.5 to 84.0ft	5.809	2,31	Significantly different
2. 52.5 to 84.0ft vs. 92.5 to 119.0ft	1.149	2,26	Not significantly different
3. 2.5 to 44.0ft vs. 92.5 to 119.0ft	1.586	2,29	" " "
4. All tip samples vs. 'Upper slope' samples(to 92.5ft)	0.011	2,83	" " "
5. All tip samples vs. All underground fabricated samples	1.805	2,64	" " "
6. All tip samples vs. All underground fabricated samples, less R2A-R2E	1.004	2,60	" " "
7. All underground fabricated samples vs. underground samples, less R2A-R2E	0.036	2,30	" " "
8. 8in long triaxial samples vs. 3in long triaxial samples	0.937	2,45	" " "

TABLE 5.14

Comparison of shear strength parameters - Spoil - heap and fabricated samples.

a) composite parameters

	Fabricated underground			Spoil-heap		
	ϕ' (c'=0)	ϕ'	c'	ϕ' (c'=0)	ϕ'	c'
All samples	33.5°	33.0°	0.94 lb/in^2			
				35°	33.5	2.15 lb/in^2
less R2A-R2E	34.0°	34.0°	0.57 lb/in^2			

b) equivalent fabricated samples related to output of eastern and western districts

1/6 [2(R1A to R1F) + 2(F1A to F1C) + (R2A to R2G) + (F2A to F2C)]

Fabricated underground			Spoil-heap		
ϕ' (c'=0)	ϕ'	c'	ϕ' (c'=0)	ϕ'	c'
34.5°	32.5°	2.68 lb/in^2	35°	33.5°	2.15 lb/in^2

be drawn between the strength of fabricated samples from underground and the composite strength of the tip materials.

In the first instance the tip itself can be sub-divided into three sections, for which historical evidence has been considered in the previous Sections. Similar divisions were also used by Spears, Taylor and Till (1971) to show by a rigorous statistical method (Fisher's L.S.D. test) that Al_2O_3 was the only oxide whose mean value varied significantly in the three parts into which the tip was divided. In terms of shear strength the three sections (Table 5.9) exhibit $\emptyset'$ values within the range 31.5° to 34.0°, with cohesions of 1.30 lb/in^2 to 3.25 lb/in^2. Chow's (1960) test applied to the Mohr circle top points (Table 5.13) establishes an important statistical fact. The $\frac{1}{2}(\sigma'_1+\sigma'_3)$ vs. $\frac{1}{2}(\sigma_1-\sigma_3)$ points for the specimens tested in the upper 44 ft differ significantly from those between 52.5 ft to 84.0 ft (central section of the tip). On the other hand the results for the central section and those for the lower section belong to the same regression model. What is more important however, is that theupper and lower section results are not significantly different. In other words, although the upper and middle sections may be different there is no statistical difference between the youngest (upper section) and the older (lower section). Independent evidence based on triaxial shear strength evidence partially confirms that variations with age are not systematic.

Probably the most convincing evidence that the overall strength characteristics are not susceptible to degradation processes is the compatability between the shear strength parameters of the fabricated fresh underground samples with those of the tip (Table 5.14). The underground samples which were subject to a certain degree of slaking during preparation, have slightly lower parameters than those of the tip. Two approaches have been used:

a) Composite parameters (Tables 5.13 and 5.14a)

b) Calculated parameters, which are dependent on the underground locations

(Fig. 5.1) and the National Coal Board's records relating the fabricated samples to output proportions (Table 5.14b).

The general conclusions that can be drawn from the data discussed in this chapter are that most of the discard reached its level of degradation relatively quickly. Moreover, once deeply buried in the tip the material appears to have changed very little.

5.15 Sample representability

Having concluded that long-term degradation processes in tips are relatively unimportant with respect to mechanical properties in particular, the Yorkshire Main investigations enable preliminary data to be evaluated with respect to another aspect of prime importance - the representability of samples.

The large bulk sample excavated in the vicinity of borehole 2 demonstrates that particle size distributions of U4 samples are not representative of the coarser grain sizes. The comparison of the dry sieved bulk sample with an equivalent U4 driven by the writer is shown on Figure 5.8. Hence, it is logical to compare the U4 particle size distributions on a relative and not an absolute basis. Shear strength comparisons are more promising, however. Large size in situ shear box tests carried out by the National Coal Board and Messrs. George Wimpey & Co. Ltd. have yielded shear strength parameters that compare favourably with those obtained from 8 in long by 4 in diameter U4 specimens (Mr. G. McKechnie Thomson - personal communication). Most of the present writer's tests on tip materials have of necessity been carried out on smaller 3 in long by $1\frac{1}{2}$ in diameter specimens. This disparity in size does not appear greatly to influence the results; the variance ratio test (Table 5.13) provides confirmatory evidence on this point. All discard materials must by their nature be remoulded to varying degrees and it is thus not altogether surprising that sample size is not a major factor from a strength view-point.

TABLE 5.15

Student t-test on U4 chemistry vs. S.P.T. chemistry

	U4		S.P.T.			
	Mean,	Std.Dev.	Mean,	Std.Dev.	t-value	Significance
SiO_2	49.60	4.99	53.41	3.73	2.5812	Significantly different (>98%)
Al_2O_3	27.24	1,11	23.36	1.44	8.2866	" " (99.9%)
Fe_2O_3	8.43	2.40	8.56	1.80	0.1825	Not significantly different
MgO	1.72	0.17	1.85	0.21	2.0087	" " "
CaO	2.88	1.06	2.95	1.27	0.1517	" " "
Na_2O	0.75	0.16	0.68	0.18	1.1727	" " "
K_2O	4.57	0.37	4.40	0.23	1.6686	" " "
TiO_2	1.06	0.10	1.17	0.10	3.1478	Significantly different (>99%)
MnO	0.15	0.04	0.13	0.04	1.3529	Not significantly different
S	3.40	1.91	3.25	3.16	0.1584	" " "
P_2O_5	0.18	0.14	0.14	0.06	1.3242	" " "

We have already seen that organic carbon tends to be concentrated on the smaller sieve sizes (Figs. 4.4 and 5.9). The major difference in the chemistry of S.P.T. samples and U4 samples concerns this component (S.P.T. mean, 23.97% (Sheffield); U4 mean, 10.74%). There are two possibilities which may equally well be responsible:

1) Driving of the S.P.T. sampler breaks down large coal fragments with the result that the small coal produced is concentrated in the split spoon sampler.

2) Small coal concentrates naturally with the finer size fraction and this is preferentially sampled during the driving of the S.P.T. split-spoon.

The present writer prefers the second hypothesis for which there is circumstantial evidence from the organic carbon histograms (Figs. 4.4 and 5.9). The tendency to concentrate fine grained materials in the split-spoon sampler has previously been mentioned and this is borne out by direct comparison of the normalized S.P.T. and U4 chemistry (Table 5.3). Further processing of this data (Student t-test, Table 5.15) shows that it is the major component means, SiO_2 and Al_2O_3 which differ significantly in the two types of sample. The total silica includes quartz, but in the component rock types alumina is a reflection of the clay minerals present. Total silica is higher in the S.P.T. samples, but alumina is lower. If we first of all assume that quartz does not vary in the two sample sizes then the total silica/alumina ratio is higher in the S.P.T. samples than in the U4's. A low ratio may be symptomatic of enhanced kaolinite. The better ratio is K_2O/Al_2O_3 because it is not affected by other minerals like quartz. In this case the U4 samples have a lower mean ratio than the S.P.T. samples, and this suggests that illite is being concentrated in the smaller sized sampler. This agrees reasonably well with the contention that the S.P.T. sampler pushes aside the larger cobble sized rocks (mainly siltstone roof

rocks, with slightly enhanced kaolinite), and therefore concentrates the smaller illitic minerals. The differences are not major ones, and all other elements and oxides (bar titania which has clay mineral affinities), are not significantly different (Table 5.15).

CHAPTER 6

GENERAL SUMMARY AND CONCLUSIONS

Since the Aberfan disaster considerable resources have been devoted to the question of colliery tip stability. The present writer has concentrated upon time-dependent weathering effects. Because little research has been carried out on the weathering of coal-bearing rocks in Britain, let alone colliery tips themselves, the subject has been treated in as much detail as possible and an attempt has been made to collate as much of the existing data as feasible. Inevitably the size of the thesis has grown accordingly.

The more common argillaceous rocks associated with coal seams slake rapidly when exposed to water; the behaviour of the Yorkshire Main underground material would suggest that the level of degradation reached is attained relatively rapidly, and in the case of washery discard breakdown will have commenced prior to tipping. The factors which control the immediate breakdown are a) geological structures, b) overall mineralogical composition (ratio of equant habit minerals like quartz to clay minerals, and grain size), c) presence of expanding clay minerals, particularly if montmorillonite is a mixed-layer component. Capillary pressures leading to air breakage have been shown to be an important breakdown mechanism but intraparticle swelling of expanding clay minerals may well blanket the effects of air-breakage. Ionic dispersive and chemical dissolution processes cited in the literature are considered to be long-term processes and judging from the present grain size distributions of both in situ and colliery tip debris, breakdown to a fundamental grain size is by no means complete.

The geographical variation in the clay mineralogy of the rocks associated with exploitable seams in Britain implies that kaolinite is dominant in the northern coalfields. Kaolinite is an 'inert' clay mineral so breakdown due to interlayer swelling should on average be at a minimum in these coalfields. The incipient rank association obtained from analysis of the

end-over-end breakdown tests from the National Coal Board's records is not reflected in the clay mineralogy. The real problem in trying to establish such relationships is in matching the rock samples from the various coalfields - mineralogy, macro and micro-structure, grain size.

An investigation of a drift-free non-weathered-weathered sequence of Coal Measures cyclothemic rocks in the East Pennine coalfield has shown very clearly that structural changes due to weathering of the detrital mineral complement over a period of about 10,000 years are very small indeed. The clay mineral chlorite is apparently partly decomposed within the zone characterized by lithorelicts in a silty and clayey matrix (below the sub-soil level and down to a depth of 6 to 8 ft below ground level). Very minor changes were detected in the 10 Å minerals but these were so small that they are almost completely masked by the natural mineralogical variations within the profile.

Large-scale oxidation of the non-detrital mineral siderite is limited to a depth of about 3 ft below ground level in this sequence, whereas pyrite is decomposed to a depth of 6 to 8 ft below ground level. Volumetric expansion of pyrite during decomposition is not a primary control on breakdown because the depth of clay-silt development is as great in strata with a low original pyrite content as it is in rocks which contained up to about 9 per cent originally.

Physically and mechanically the in situ rocks provide a useful 'yard-stick' for understanding the behavioural characteristics of colliery spoil, although there are of course important differences. In the natural strata the density variations with depth cannot necessarily be ascribed to weathering, but through the Yorkshire Main tip there is a statistically valid increase in density with depth. Increasing quartz content is mirrored by increasing specific gravity in the natural rock samples. From the two

colliery tips that have been investigated it is very clear that coal content controls specific gravity in that there is an inverse statistical relationship between organic carbon and specific gravity. In both Brancepeth and Yorkshire Main tips there are reasons for believing that coal tends to be concentrated in the smaller sieve sizes (Figs. 4.4 and 5.9) and these high coal content fines are apparently concentrated in Standard Penetration Test samples, but not in the U4 samples (see Chapter 5, Section 5.15).

The Casagrande plasticity chart classification shows that the liquid and plastic limits of the natural strata are in line with the visual descriptions and the concept of 'coarsening upwards' within a cyclothem. From a rheological point of view the quartz content has an important influence, and beyond about 44 per cent sliding rather than flow is undoubtedly taking place in the liquid limit apparatus. For dominantly granular materials the usefulness of limits is somewhat debateable because only the smaller grain sizes (less than 36 B.S. sieve) are considered. However, certain of the samples from the partly burnt Brancepeth tip are virtually 'non-plastic' and the classification chart helps to differentiate between the partly burnt spoil of Brancepeth and the non-burnt spoil from Yorkshire Main tip. From the separate evidence of both the latter tips there is statistical evidence in support of the liquid and plastic limits of tip materials showing a positive association. The positive association of plasticity index and liquid limit in the Yorkshire Main material (Table 5.10) favours Terzaghi and Peck's (1967) contention that samples from the same horizon (in this case common parental material) tend to define a straight line that is roughly parallel to the 'A' line. A similar correlation has recently been obtained by the writer for some 42 samples of tip materials, from the Wimpey Central Laboratory.

Turning now to shear strength comparisons it is very evident that cohesion is the parameter that is affected most by *in situ* weathering. The limitation of the Coulomb-Navier strength criterion and Mohr circle presentation at low normal pressures is demonstrated by the exceedingly high ϕ values exhibited by weathered and non-weathered siltstones (verging on sandstones) and transitional seatearths (Chapter 3, Table 3.11). It is of interest to note that the calcarious Cambrian shales cited by Underwood (1967, Table 2) have a ϕ value of 64 degrees. Here again, it is not unreasonable to infer that these latter rocks will also have high compressive to tensile strength ratios.

The range of ϕ' values (36° - 45.5°) for transitional partly weathered fragmental mudstone-siltstone, typical seatearth and mudstone specimens from the *in situ* section is rather higher than the ϕ' values (34.5°- 35°) for compacted shale fill used in the Burnhope and Balderhead dams. However, the fissile dark marine shale (with low deformation modulii in both the weathered and unweathered state) is the horizon which over the last 10,000 years or so has been subject to the greatest degradation; its peak ϕ' value is only 26 degrees. This value is lower than that of tailings (Bishop *et al.*, 1969) and fine grained coal (Fig. 4.10). The bulk of the material found in average tips comprises argillaceous rocks which means that low shear strength shales such as the marine horizon at Wales are an important element in any consideration of colliery tips which involve a time factor. Aberfan showed that the strength of spoil can fall considerably (possibly from ϕ' = 39.5° to ϕ'_r = 17.5°) when subjected to large strains. However, geological, hydrological and topographical circumstances played a major part in the sequence of events which led up to the 1966 disaster. More relevant to the current work is the question of degradation of spoil with time.

Brancepeth tip has been subject to all the processes of combustion and

regrading that are likely to affect the overall stability of the spoil. The mineralogy shows that kaolinite is decomposing and quartz is undoubtedly being lost with the fine fraction; it has been confirmed that it is this fraction which is the most susceptible to combustion processes. Comparisons between the normalized chemical means of the partly burnt shale of Brancepeth and the unburnt spoil of Yorkshire Main (Table 6.1), emphasize that leaching of the clay mineral oxides K_2O, Na_2O, and MgO is apparent in the former tip, with the weight percentage of the associated rutile being affected also. Moreover, a high sulphate and Fe^{3+}- mineral content is evident at Brancepeth, and in general the mineralogy bears little resemblance to that of the parental rocks.

Bearing in mind the fact that all the Brancepeth triaxial samples were extracted from within 17 ft of the free surface it is of considerable import that the composite $\emptyset'$ is 35.5° and also that the three upper samples have a $\emptyset'$ value which is only some 3.5 degrees higher than that of the lower (older) samples. The granularity of the spoil is emphasized by the deformation characteristics of the spoil, but there is minor evidence (enhanced cohesion of the burnt shale and the reciprocal association of the parameter and ferrous iron) which implies that subsequent fusion (cementation) cannot be wholly ignored. The variance ratio test(F-test; Chow, 1960) showed that the Mohr circle 'top points' for the upper spoil samples and those for the lower samples do in fact belong to the same regression model. In contrast, the residual $\emptyset'$ value for the oldest spoil sample (21°), conforms with previously determined residual values for colliery spoil and is at least 8° lower than the lowest peak value. Comminution and clay mineral hydration are considered to be the principal means by which the residual value is attained, without invoking chemical weathering as envisaged by Bishop et al., (1969). It is important to

FIGURE 6.1

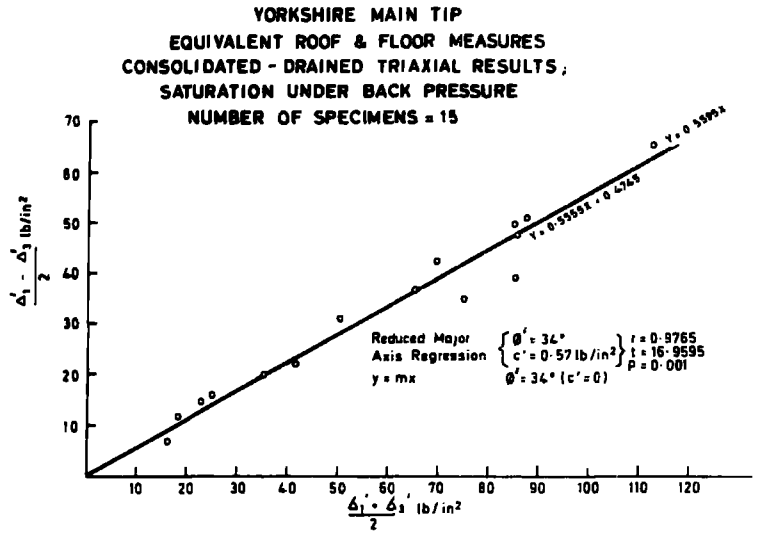

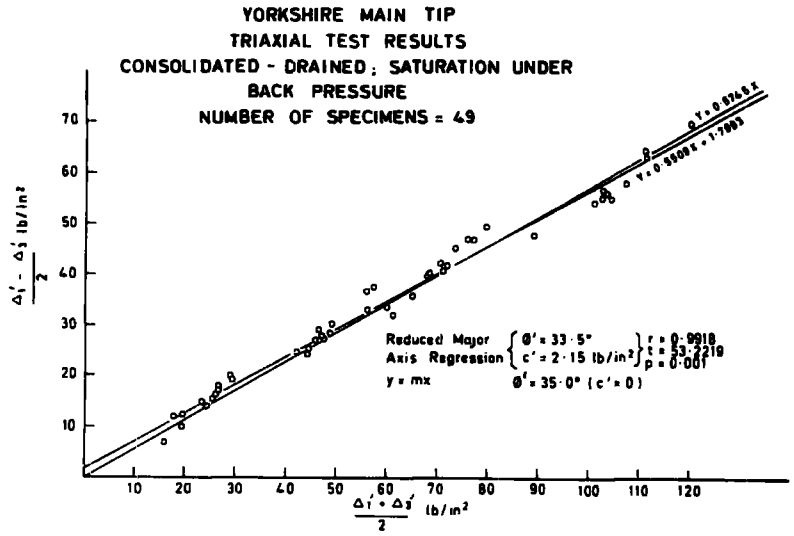

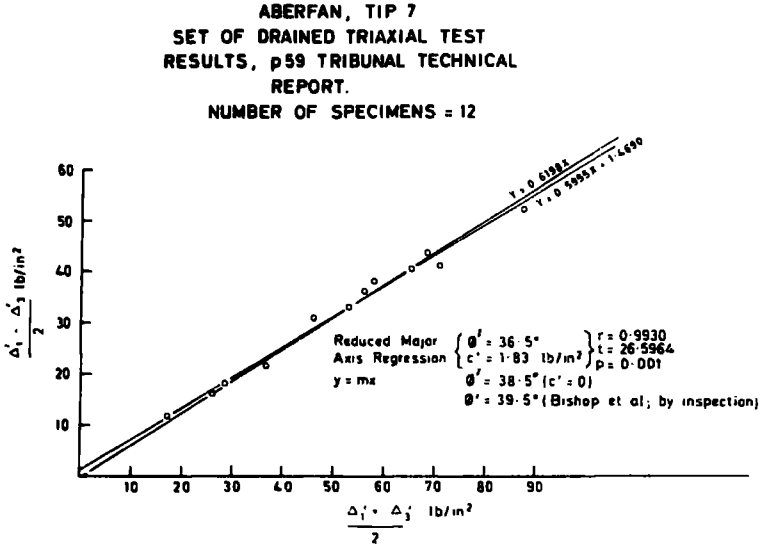

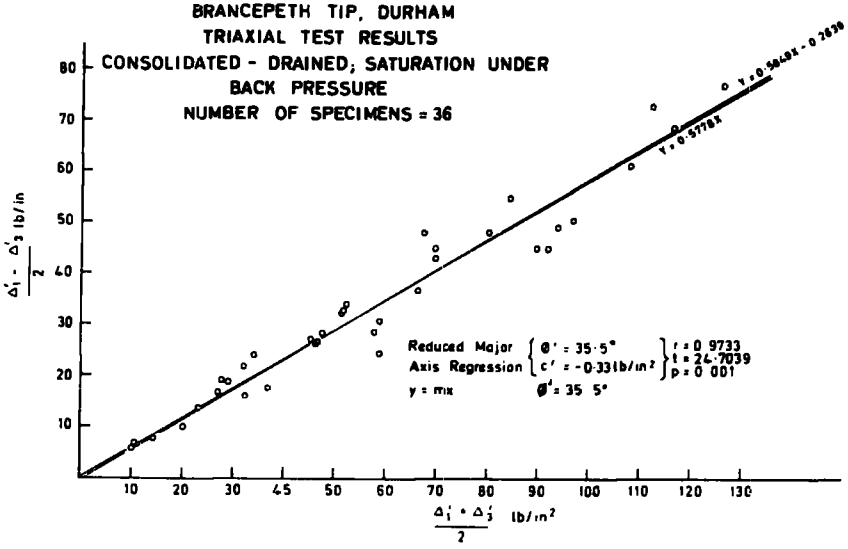

FIGURE 6.1

note that the order of residual $\emptyset'$ is by no means as low as the 11° which has been obtained for clay partings (Fig. 3.11; also Stimpson and Walton, 1970). For weathered-unweathered Coal Measures rocks the residual $\emptyset'$ value is a function of the quartz/clay minerals ratio (Fig. 3.11), which indirectly is in accord with Skempton's (1964) work.

The chemistry of the Yorkshire Main spoil infers that chemical weathering is of negligible importance, the most convincing evidence being that elements and minerals susceptible to leaching do not vary in abundance through the 50 year-old tip. Although small changes in physical and chemical properties have been detected through the tip, these are thought to be original differences in the discard at the time of tipping, and probably reflect changes in mining practice and stages in the evolution of the tip, for which some evidence exists.

Sample size is important and it has been demonstrated that both chemical and physical differences exist between bulk samples, U4's and S.P.T. samples. On a statistical basis however, the shear strength characteristics of small size triaxial samples are not significantly different from the larger (8 in long by 4 in diameter) size samples. Possibly the most convincing evidence that the strength of this unburnt spoil is not decreasing with age is the parity in shear strength parameters of fabricated fresh samples of equivalent roof and floor measures from underground with those of the tip itself (Fig. 6.1, Tables 5.9, 5.14). If we compare the regression models of the Mohr circle top points (Fig. 6.1, Table 6.2) for Aberfan (Bishop et al., 1969, p.59), Brancepeth and Yorkshire Main it is pertinent to record that the 100-year-old relatively superficial partly burnt spoil (Brancepeth) is not significantly different from the recent Aberfan material. The two older tips (Brancepeth and Yorkshire Main) are not significantly different, but Aberfan and Yorkshire Main are statistically different.

TABLE 6.1

Comparison of normalized chemistry ; U 4 samples of Brancepeth and Yorkshire Main

	Brancepeth (9 samples)		Yorkshire Main (13 samples)				
	Mean,	Standard Deviation	Mean,	Standard Deviation	t,	Significance,	Level
SiO_2	47.92	4.410	49.60	4.993	0.7747	Not sig.	Different
Al_2O_3	27.66	1.623	27.24	1.106	0.6870	" "	"
Fe_2O_3	10.44	2.320	8.43	2.398	1.8654	" "	"
MgO	0.98	0.269	1.72	0.166	7.5896	Different	> 99.9%
CaO	3.10	2.257	2.88	1.060	0.2852	Not sig.	different
Na_2O	0.38	0.120	0.75	0.163	5.5893	Different	> 99.9%
K_2O	3.30	0.578	4.57	0.373	5.9809	Different	> 99.9%
TiO_2	1.27	0.121	1.06	0.099	4.2809	Different	> 99.9%
MnO	0.17	0.235	0.15	0.045	0.3058	Not sig.	different
S	4.69	1.987	3.40	1.909	1.4604	" "	"
P_2O_5	0.09	0.077	0.18	0.139	1.6868	" "	"

TABLE 6.2

Variance Ratio (F-test) on differences between regression lines; Aberfan, Brancepeth and Yorkshire Main

Comparisons	F-value	Degrees of freedom	Significance at 5% level
Aberfan (Technical Reports, 1969, drained tests, p.59) vs. Yorkshire Main	5.508	2,57	Significantly different
Aberfan vs. Brancepeth	1.480	2,44	Not significantly different
Brancepeth vs. Yorkshire Main	0.487	2,81	Not significantly different

It is therefore concluded that the unburnt spoil is not subject to degradation and strength loss over a 50 year period. Somewhat more tentatively it is also reasonable to conclude that more ancient spoil, which has been subject to major combustion-induced changes, is not necessarily susceptible to strength loss of any magnitude or importance. A relevant feature of Figure 5.2 is the comparison between the clay mineralogy of the Yorkshire Main tip samples with the tailings samples from other areas, particularly from the standpoint of mixed-layer clay and subsequent breakdown. The content of this clay fraction in other areas is no higher than at Yorkshire Main, and in fact the highest mixed-layer percentages for tailings sample are from the National Coal Board's Doncaster Area which includes Yorkshire Main Colliery. In many cases the content is much lower, and therefore as no trouble has been experienced from this source at Yorkshire Main it would be anticipated that the same will generally be true of other areas. There may, however, be problematic tips in districts, such as South Staffordshire, where it has been demonstrated that associated measures have a high content of mixed-layer mica. Although samples from existing washeries show that this clay has been diluted by more 'inert' species it could be that this is not always the case, especially if the spoil has not been slaked in a washery, prior to emplacement.

BIBLIOGRAPHY

AITCHISON, G.D., 1960. 'Relationship of moisture stress and effective stress functions in unsaturated soils.' Conf. on Pore Pressure and Suction in Soils, Butterworths, London. 47-52.

AKROYD, T.N.W., 1957. 'Laboratory testing in soils engineering.' Soil Mechanics Ltd., London. 233pp.

ANON, 1960. 'Structures do not settle in this shale, but watch out for heave.' Engineering News-Record. 164, 46-48.

ATTEWELL, P.B., AUCOTT, J.W. and BURGESS, A.S., 1969. 'Computerized data processing from an X-ray texture-goniometer. Mineralog. Mag. 37, 428-430.

BADGER, C.W., CUMMINGS, A.D. and WHITMORE, R.L., 1956. 'The disintegration of shales in water.' J. Inst. Fuel, 29, 417-423.

BARDOSSY, G., 1959. 'The geochemistry of Hungarian bauxites.' Acta Geologica, Acad. Scient. Hung., 6, 1-47.

BECKETT, P.J., CUMMINGS, A.D. and WHITMORE, R.L., 1958. 'Interfacial properties of coal-measure shales in water.' Proc. Conf. on Science in the Use of Coal, Sheffield University, Paper 12, 14-19.

BERKOVITCH, I., MANACKERMAN, M. and POTTER, N.M., 1959. 'The shale breakdown problem in coal washing. Part 1 - assessing the breakdown of shales in water.' J. Inst. Fuel. 32, 579-589.

BISHOP, A.W., 1955. 'The use of the slip circle in the stability analysis of slopes.' Geotechnique, 5, 7-17.

BISHOP, A.W., ALPAN, I., BLIGHT, G.E. and DONALD, I.B., 1960. 'Factors controlling the strength of partly saturated cohesive soils.' Proc. Research Conf. on Shear Strength of Cohesive Soils. 503-532 (A.S.C.E.).

BISHOP, A.W. and HENKEL, D.J., 1962. 'The measurement of soil properties in the triaxial test.' Edward Arnold, London, 228 pp.

BISHOP, A.W., HUTCHINSON, J.N., PENMAN, A.D.M. and EVANS, H.E., 1969. 'Geotechnical investigation into the causes and circumstances of the disaster of 21st October, 1966. Item 1, 1-80.' A selection of Technical reports submitted to the Aberfan Tribunal. Welsh Office, London, H.M.S.O.

BJERRUM, L., 1967. 'Mechanism of progressive failure in slopes of over-consolidated plastic clays and clay-shales.' Proc. A.S.C.E. (J. Soil Mech. Div.), 93, SM5, 1-49.

BRADLEY, W.F. and GRIM, R.E., 1948. 'Colloidal properties of layer silicates.' J. Phys. Colloid Chem., 52, 1404-1413.

BRAY, A., 1951. 'The decomposition of iron pyrite from coal seams.' Proc. Geol. Ass., 62, 136-9.

BRITISH STANDARD 1377, 1967. 'Methods of testing soils for civil engineering purposes.' British Standards Institution,London, 233 pp.

BROWN, G., 1961. 'The X-ray identification and crystal structures of clay minerals.' Mineralogical Society, London. 544 pp.

CARR, J., 1947/8. 'A particular treatment of spoil bank fires in the South Derbyshire coalfield.' Trans. Inst. Min. Engrs., 107, 169-184.

CARROLL, D. and STARKEY, H.C., 1958. 'Effect of sea-water on clay minerals.' Proc. 7th National Conference on Clays and Clay Minerals. Pergamon Press, 80-101.

CARTLEDGE, G.H., 1928. 'Studies in the periodic system.' J. Chem. Soc. America. 2855-2872.

CASAGRANDE, A., 1965. 'The role of the "calculated risk" in earthwork and foundation engineering'. Proc. A.S.C.E. (J. Soil Mech. Div.), 91, SM4, 1-40.

CASAGRANDE, A. 1971. 'On liquefaction phenomena', (Reporters: P.A. Green and P.A.S. Ferguson). Geotechnique, 21, 197-202.

CHANDLER, R.J., 1969. 'The effect of weathering on the shear strength of Keuper Marl.' Geotechnique, 19, 321-334.

CHAPMAN, H.D., 1965. 'Cation exchange capacity.' In: Methods of soil analysis.' Part 2 (Ed. Black, C.A.) American Society of Agronomy. 15 771-1572 pp.

CHILDS, E.C., 1969. 'An introduction to the physical basis of soil water phenomena.' John Wiley and Sons Ltd., London 493 pp.

CHOW, G.C., 1960. 'Tests of equality between sets of coefficients in two linear regressions.' Econometrica. 28, 591-605.

CIVIC TRUST 1964. 'Derelict land.' 70pp.

CONNELLY, R., 1970. 'X-ray fabric analysis of laboratory sedimented muscovite clay.' Unpublished M.Sc. Dissertation in Engineering Geology, University of Durham.

COSGROVE, M.E. and HODSON, F., 1963. 'Jarosite from Meal Bank quarry, Ingleton, Yorkshire. Proc. Yorks. geol. Soc., 32, 229-84.

CRÁMER, H., 1946. 'Mathematical methods of statistics.' Princeton University Press. 575pp.

CRONEY, D.,COLEMAN, J.D. and BLACK, W.P.M., 1958. 'The movement and distribution of water in soil in relation to highway design and performance.' Highway Research Board, Special Report No.40, Washington, D.C.

CRONEY, D., COLEMAN, J.D. and BRIDGE, P.M., 1952. 'The suction and moisture held in soil and other porous materials.' Road Research Technical Paper No.24. London H.M.S.O.

CURTIS, C.D., 1967. 'Diagenetic iron minerals in some British Carboniferous sediments.' Geochim. Cosmochim. Acta, 31, 2103-2109.

DEERE, D.V., HENDRON, A.J., PATTON, F.D. and CORDING, E.J., 1967. 'Design of surface and near surface construction in rock.' Proc. 8th Symposium Rock Mech., Minnesota, 237-302.

DE KEYSER, W., 1939. 'A study of kaolin in some Belgian clays.' Ann. Mines Belg., 40, 711.

DOWNING, R.A. and HOWITT, F., 1969. 'Saline ground-waters in the Carboniferous rocks of the English East Midlands in relation to the geology.' Q. Jl. Engng. Geol. 1, 241-269.

DUFF, P. McL.D., and WALTON, E.K., 1962. 'Statistical basis for cyclothems: a quantitative study of the sedimentary succession in the East Pennine Coalfield.' Sedimentology, 1, 235-255.

DURUM, W.H. and HAFFTY, J., 1963. 'Implications of the minor element content of some major streams of the world.' Geochim. et Cosmochim. Acta, 27, 1-11.

EDWARDS, W. and STUBBLEFIELD, C.J., 1948. 'Marine bands and other faunal marker horizons in relation to the sedimentary cycles of the Middle Coal Measures of Nottinghamshire and Derbyshire.' Q. Jl. geol. Soc. Lond., 103, 209-260.

ELLIOTT, R.E., 1968. 'Facies, sedimentation successions and cyclothems in productive Coal Measures in the East Midlands, Great Britain. Mercian Geol., 2, 351-372.

FISHER, R.A. and YATES, F., 1948. 'Statistical Tables for biological, agricultural and medical research.' Oliver and Boyd, London. 112 pp.

FRANCOMBE, M.H. and ROOKSBY, H.P., 1959. 'Structure transformations effected by the dehydration of diaspore, goethite and delta ferric oxide.' Clay Miner. Bull., 4, 1-14.

FRANKLIN, J.A., 1970. 'Suggested methods for determining the slaking, swelling, porosity, density and related rock index properties.' Research Report D12, Rock Mechanics Project, Imperial College, London.

GILKES, R.J., and HODSON, F., 1971. 'Two mixed-layer mica-montmorillonite minerals from sedimentary rocks.' Clay Minerals, 9, 125-137.

GILLOTT, J.E., 1968. 'Clay in engineering geology.' Elsevier Publishing Co. Amsterdam, 296 pp.

GLOVER, H.G., 1967. 'Acidic drainage from colliery spoil heaps.' National Coal Board Internal Report.

GOLDSCHMIDT, V.M., 1937. 'The principles of the distribution of chemical elements in minerals and rocks.' J. Chem. Soc. (London), 655-672.

GORDON, M., and TRACEY, J.I., 1952. 'Origin of Arkansas bauxite deposits: Problems of clay and laterite genesis.' American Instit. Min and Met. Eng., New York, 244 pp.

GRIFFIN, O.G., 1954. 'A new internal standard for quantitative X-ray analysis of shales and mine dusts.' Research Report No.101. Safety in Mines Research Establishment, Ministry of Fuel and Power, Sheffield.

GRIM, R.E., 1968. 'Clay Mineralogy', McGraw-Hill, New York, 596 pp.

GRIM, R.E. and BRADLEY, W.F., 1940. 'The effect of heat on illite and montmorillonite.' J. Amer. ceram. Soc., 23, 242-248.

GROVES, A.W., 1951. 'Silicate analyses.' Allen and Unwin, London, 336 pp.

GUNEY, M., 1968. 'Oxidation and spontaneous combustion of coal. Review of individual factors.' Colliery Guard. 105-110 (January); 137-143 (February).

HAEFELI, R., 1948. 'The stability of slopes acted upon by parallel seepage.' Proc. 2nd Int. Conf. Soil Mech. (Rotterdam) 1, 57-62.

HARTLEY, J., 1957. 'Jarosite from Carboniferous shales in Yorkshire.' Trans. Leeds Geol. Assoc., 7, 19-23.

HAZEN, A., 1892. 'Some physical properties of sands and gravels, with special reference to their use in filtration.' 24th Annual Report of the State Board of Health of Massachusetts, Public Document No.34, Boston. Wright and Potter Printing Co., (1893), 553 pp.

HENDRON, A.J., 1968. 'Mechanical properties of rock'. In: 'Rock mechanics in engineering practice.' (Eds. Stagg, K.H. and Zienkiewicz, O.C.). John Wiley and Sons, London, 21-53.

HINCKLEY, D.N., 1962. 'Variability in crystallinity values among the kaolin deposits of the coastal plain of Georgia and South Carolina.' Proc. 11th National Conference on Clays and Clay Minerals. Pergamon Press, 229-235.

HOEK, E., 1970. 'Estimating the stability of excavated slopes in opencast mines. Trans. Instn. Min. Metall. (Sect. A: Min. Industry) 79, 109-132.

HOLLAND, J.G. and BRINDLE, D.W., 1966. 'A self-consistent mass absorption correction for silicate analysis by X-ray fluorescence'. Spectrochim. Acta, 22, 2083-2093.

HORSLEY, R.V., 1951-1952. 'Oily collectors in coal floatation.' Trans. Instn. Min. Engrs., 111, 886-894.

HORTON, A.E., MANACKERMAN, M., and RAYBOULD, W.E., 1964. 'The shale breakdown problem in coal washing. Part 2 - some causes of shale breakdown and means for its control.' J. Inst. Fuel. 37, 52-58.

HUDDLE, J.W. and PATTERSON, S.M., 1961. 'Origin of Pennsylvanian underclay and related seat rocks.' Bull. geol. Soc. Am., 72, 1643-1660.

HUTCHINSON, J.N., 1967. Discussion: 214-215. Proc. Geotechnical Conf., Oslo, 2, 293 pp.

HVORSLEV, M.J., 1949. 'Time lag in observation of ground-water levels and pressures.' U.S. Army Waterways Experiment Station, Vicksburg,Miss.

ILIEV, I.G., 1966. 'An attempt to estimate the degree of weathering of intrusive rocks from their physico-mechanical properties.' Proc. 1st Cong. Internat. Soc. Rock Mech. 1, 109-114.

IMBRIE, J., 1956. 'The place of biometrics in taxonomy'. Bull. Amer. Mus. Nat. Hist. 108: 2; 211-252.

JACKSON, M.L., 1964. 'Chemical composition of soils p.71-141. In: 'Chemistry of the soil' (Editor. Bear, F.E.). Reinhold Publishing Corporation, New York. 515 pp.

JOHNSON, S.J., 1969. 'Engineering properties and behavior of clay-shales.' Speciality Session No.10. Proc. 7th Int. Conf. Soil Mech., Mexico City, 3, 483-488.

JONES, G.I., 1970. 'The effects of weathering on the strength of some British Coal Measure rocks.' Unpublished M.Sc. Dissertation in Engineering Geology, University of Durham.

JONES, O.T., 1951. 'The distribution of coal volatiles in the South Wales coalfield and its probable significance.' Q.Jl. geol. Soc. Lond., 107, 51-83.

KARDOS, L.T., 1964. 'Soil fixation of plant nutrients.' p.369-394. In: Bear, F.E., 'Chemistry of the Soil.' Reinhold Publishing Corp. New York, 515 pp.

KEELING, P.S., 1962. 'Some experiments on the low-temperature removal of carbonaceous material from clays.' Clay Miner. Bull., 5, 155-158.

KENNARD, M.F., KNILL, J.L. and VAUGHAN, P.R., 1967. 'The geotechnical properties and behaviour of Carboniferous shale at the Balderhead Dam.' Q. Jl. Engng Geol., 1, 3-24.

KENNEY, T.C., 1967. 'The influence of mineral composition on the residual strength of natural soils.' Proc. Geotechnical Conf., Oslo, 1, 123-129.

KITTLEMAN, L.R., 1964. 'Applications of Rosin's distribution in size-frequency analysis of clastic rocks.' J. sedim. Petrol., 33, 483-502.

KNILL, J.L. and JONES, K.S., 1965. 'The recording and interpretation of geological conditions in the foundations of the Roseires, Kariba and Latiyan dams.' Geotechnique, 15, 94-124.

KNOX, G., 1927. 'Landslides in South Wales valleys.' Proc. S. Wales Institute of Engrs, 43, 161-233.

KRAUSKOPF, K.B., 1959. 'The geochemistry of silica in sedimentary environments: Silica in Sediments, Soc. Economic palae. and Min., Symposium 7, 4-18.

KRAUSKOPF, K.B., 1967. 'Introduction to geochemistry.' McGraw-Hill, New York, 721 pp.

KRYNINE, D.P., 1941. 'Soil mechanics, its principles and structural applications.' McGraw-Hill, New York, 451 pp.

KUYL, O.S. and PATIJN, R.J.H., 1961. 'Coalification in relation to depth of burial and geothermic gradient.' Congr. Avan. Études Stratigraph. Géol. Carbonifère, Compte Rendu, 4, Heerlen, 1958, 2, 357-365.

LAMBE, T.W. and WHITMAN, R.V., 1969. 'Soil mechanics.' John Wiley & Sons, New York, 553 pp.

LEWES, V.B., 1912. 'The carbonisation of coal.' John Allan and Co., London, 315 pp.

LEWIS, W.A. and CRONEY, D., 1966. 'The properties of chalk in relation to road foundations and pavements.' Proc. Symposium on Chalk in Earthworks and Foundations. Institution of Civil Engineers, London, Paper 3, 27-41.

LITTLE, A.L. and PRICE, V.E., 1958. 'The use of an electronic computer for slope stability analysis.' Geotechnique, 8, 113-120.

LIVINGSTONE, D.A., 1963. 'Chemical composition of rivers and lakes.' U.S. Geol. Surv. Prof. Paper 440-G, 64 pp.

LOMTADZE, V.D., 1955. 'Stages of development of properties of clayey rocks during their lithification. Dokl. Akad. Nauk S.S.S.R., 102, 819-822 (in Russian).

LOUGHNAN, F.C., 1962. 'Some considerations in the weathering of silicate minerals.' J. sedim. Petrol., 32, 284-290.

LOUGHNAN, F.C., 1969. 'Chemical weathering of silicate minerals.' Elsevier Publishing Company, Amsterdam, 154 pp.

MACKENZIE, R.C., 1970. 'Differential thermal analysis.' Academic Press, London, 775 pp.

MEAD, W.J., 1938. 'Engineering geology of damsites.' Trans. 2nd Int. Cong. Large Dams, 4, 183.

MEIGH, A.C., 1968. 'Foundation characteristics of Upper Carboniferous rocks.' Q. Jl. Engng. Geol. 1, 87-114.

MERING, J., 1946. 'On the hydration of montmorillonite.' Trans. Faraday Soc. 42B, 205-219.

MIELENZ, R.C. and KING, M.E., 1955. 'Physical-chemical properties and engineering performance of clays.' Bull. Div. Mines Calif. 169, 196-254.

MILLER, R.L. and KAHN, J.S., 1962. 'Statistical analysis in the geological sciences.' John Wiley, New York, 483 pp.

MILLOT, G., 1970. 'Geology of Clays.' Springer-Verlag, New York, 429 pp.

MINISTRY OF TRANSPORT, 1969. 'Specification for road and bridge works.' 3rd Edition, H.M.S.O., London.

MOORE, L.R., 1968. 'Some sediments closely associated with coal seams.' pp. 105-123. In: Coal and Coal-bearing strata (Eds. Murchison, D.G. and Westoll, T.S.). Oliver and Boyd, Edinburgh, 448 pp.

MORGENSTERN, N.R., 1967. 'Shear strength of stiff clay.' Proc. Geotechnical Conf., Oslo, 2, 59-69.

MORGENSTERN, N.R. and PRICE, V.E., 1965. 'The analysis of the stability of general slip surfaces.' Geotechnique, 15, 79-93.

MORONEY, M.J., 1956. 'Facts from figures.' Penguin Books, 472 pp.

MÜLLER, G., 1967. 'Diagenesis in argillaceous sediments.' pp.127-177 In: Diagenesis in sediments (Eds. Larsen, G. and Chilinger, G.V.). Elsevier Publishing Company, Amsterdam, 551 pp.

MURRAY, H.H. and LYONS, S.C., 1956. 'Degree of crystal perfection of kaolinite.' Clays and Clay Minerals (Editor, A. Swineford). Publication 456, Nat. Acad. Sci., Nat. Res. Coun., Washington, 31-40.

NAKANO, R., 1967, 'On weathering and change of properties of Tertiary mudstone related to landslide.' Soil & Fdn. 7, 1-14.

NATIONAL COAL BOARD, 1968. 'Spoil tip management.' Revised edition. National Coal Board, Production Department, 71 pp.

NATIONAL COAL BOARD, JOINT WORKING PARTY ON SOIL MECHANICS TESTING, 1969. 'Technical memorandum relating to British Standard 1377: 1970, National Coal Board, London.

NATIONAL COAL BOARD - TECHNICAL HANDBOOK, 1970. 'Spoil heaps and Lagoons.' 2nd Draft, N.C.B., London, 233 pp.

NELSON, A., 1955. 'Effects of landslides on mining operations in the United Kingdom.' Min. J. 244, 41-42.

NELSON, A. and NELSON, K.D., 1960. 'Soil mechanics in colliery practice.' Colliery Guard., 200, 65-72, 95-99, (Jan. 1960).

NICHOLLS, G.D. and LORING, D.H., 1960. 'Some chemical data on British Carboniferous sediments and their relationship to the clay mineralogy of these rocks.' Clay Miner. Bull., 4, 196-207.

NICHOLLS, G.D., 1962. 'A scheme for recalculating the chemical analyses of argillaceous rocks for comparative purposes.' Am. Miner., 47, 34-46.

PADERES, A.G.Y.E., 1967. 'The physical-mechanical behaviour of weathered rock.' Unpublished M.Sc. Dissertation in Engineering Geology, University of Durham.

PEARSON, G.M. and WADE, E., 1967. 'The physical behaviour of seat-earths.' Proc. Geol. Soc. Lond. no.1637, 24-33.

PETTIJOHN, F.J., 1957. 'Sedimentary rocks.' (2nd Edition). Harper Bros., New York, 718 pp.

PHILPOTT, K.D., 1970. 'Suction and swelling pressure of certain argillaceous materials.' Unpublished M.Sc. Dissertation in Engineering Geology, University of Durham.

PHILLIPS, D.W., 1938-1944. 'Microscopical evidence of shearing in argillaceous rocks.' Proc. Yorks.geol. Soc., 24, 67-69.

PITT, G.J. and FLETCHER, M.F., 1955. 'The application of X-ray and spectrographic analyses to the problem of breakdown of shales in water.' C.R.E.1. Report No.1251. National Coal Board, Scientific Department, 1-12.

POLYNOV, B.B., 1937. 'Cycle of weathering.' (Trans. A.Muir). Murby,London, 220 pp.

PRICE, D.G., MALKIN, A.B., and KNILL, J.L., 1969. 'Foundations of multi-storey blocks on the Coal Measures with special reference to old mine workings.' Q. Jl. Engng. Geol. 1, 271-322.

PRICE, N.J., 1958. 'A study of rock properties in conditions of triaxial stress.' Proc. Conf. on Mech. Properties Non-metallic Brittle Materials, Butterworths Scientific Publications, London, 106-122.

PRICE, N.J., 1959. 'Mechanics of jointing in rocks.' Geol. Mag. 96, 149-167.

PRICE, N.J., 1960. 'The compressive strength of Coal Measure rocks.' Colliery Engng., July 1960, 283-292.

PURTON, M.J., and YOUELL, R.F., 1969. 'An X-ray investigation of some argillaceous rocks from the Skipton Anticline, Yorkshire.' Clay Minerals, 8, 29-37.

RAYBOULD, W.E., 1966. 'Washery water clarification.' J.Coal Prepn. 2, 9-13.

READ, H.H. and WATSON, J., 1962. 'An introduction to geology.' Vol. 1. MacMillan, London, 267 pp.

REEVES, M.J., 1971. 'Geochemistry - mineralogy of British Carboniferous seatearths from northern coalfields.' Unpublished Ph.D. thesis, University of Durham.

RICHARDSON, G. and FRANCIS, E.H., 1971. 'Fragmental Clayrock (FCR) in coal-bearing sequences in Scotland and north-east England.' Proc. Yorks. geol. Soc., 38, 229-260.

SCHULTZ, L.G., 1958. 'The petrology of underclays.' Bull. geol. Soc. Am., 69, 363-402.

SCHULTZ, L.G., 1949. 'A direct method of determining preferred orientation on the Geiger counter spectrometer.' J. Appl. Phys. 20, 1030-1033.

SHAPIRO, L., 1960. 'A spectrophotometric method for the determination of FeO in rocks.' U.S. Geol. Surv. Prof. Paper 400-B, 496-497

SCHEIDIG, A., 1931. 'Tests on the deformation of sand and their application to the settlement analysis of buildings.' Unpublished M.Sc. thesis, Vienna. In: Terzaghi, K and Peck, R.B., 1967. 'Soil mechanics in engineering practice.' (2nd Edition). John Wiley, New York.

SHERWOOD, P.T., and RYLEY, M.D., 1970. 'The effect of sulphates in colliery shale on its use for roadmaking.' RRL Report LR 324, Road Research Laboratory, Ministry of Transport.

SIEVER, R., 1962. 'Silica solubility, 0-200°C, and the diagenesis of siliceous sediments.' J.Geol., 70, 127-150.

SKEMPTON, A.W., 1964. 'Long-term stability of clay slopes.' Geotechnique, 14, 77-101.

SKEMPTON, A.W., 1970. 'The consolidation of clays by gravitational compaction.' Q. Jl. geol. Soc. Lond., 125, 373-411.

SMITH, G.N., 1968. 'Coal spoil heaps and their stability:' Part 2. Ground Engineering, 1, 42-45.

SPEARS, D.A., 1964. 'The major element geochemistry of the Mansfield Marine Band in the Westphalian of Yorkshire.' Geochim. cosmochim. Acta, 28, 1679-1696.

SPEARS, D.A., 1969. 'A laminated marine shale of Carboniferous age from Yorkshire, England.' J. sedim. Petrol., 39, 106-112.

SPEARS, D.A., 1970. ' A kaolinite mudstone (tonstein) in the British Coal Measures.' J. sedim. Petrol., 40, 386-394.

SPEARS, D.A., TAYLOR, R.K. and TILL, R., 1971. 'A mineralogical investigation of a spoil heap at Yorkshire Main Colliery.' Q. Jl. Engng Geol., 3, 239-252.

SPENCER, E., 1967. 'A method of analysis of the stability of embankments assuming parallel inter-slice forces.' Geotechnique, 17, 11-26.

SPENCER, G.S., 1969. 'Correlation of residual shear strength and liquid limit.' In: Johnson, S.J. (Reporter). Engineering properties and behavior of clay-shales. Speciality Session No.10. Proc. 7th Int. Conf. Soil Mech., Mexico City, 3, 488.

STIMPSON, B. and WALTON, G., 1970. 'Clay mylointes in English Coal Measures - their significance in opencast slope stability.' Research Report, D.16, Rock Mechanics Project, Imperial College, London.

STRAKHOV, N.M., BRODSKAYA, N.G., KNYAZEVA, L.M., RAZZHIVINA, A.N., RATEEV, M.A., SAPOZHNIKOV, D.G., and SHISHOVA, E.S., 1954. 'Formation of sediments in recent basins.' Izd. Akad. Nauk S.S.S.R., Moscow, 791 pp.

TAYLOR, J.H., 1964. 'Some aspects of diagenesis.' Advan. Sci., 22, 417-436.

TAYLOR, R.K., 1967. 'Methylene blue adsorption by fine grained sediments.' J. sedim. Petrol., 37, 1221-1230.

TAYLOR, R.K., 1968. 'Site investigations in coalfields - the problem of shallow mine workings.' Q. Jl. Engng. Geol. 1, 115-134.

TAYLOR, R.K., 1969. Panel contribution: 'Engineering properties and behaviour of clay-shales.' Speciality Session 10, Proc. 7th Int. Conf. Soil Mechs. Found. Eng., 3, 483-488.

TAYLOR, R.K., 1971. 'The petrography of the Mansfield Marine Band cyclothem at Tinsley Park, Sheffield.' Proc. Yorks. geol. Soc., 38, 299-328.

TAYLOR, R.K. and SPEARS, D.A., 1970. 'The breakdown of British coal measure rocks.' Int. J. Rock Mech. Min. Sci., 7, 481-501.

TEICHMÜLLER, M. and TEICHMÜLLER, R., 1967. 'Diagenesis of coal (coalification).' In: Diagenesis in sediments (Eds. Larsen, G. and Chilingar, G.V.). Elsevier Publishing Company, Amsterdam, 391-415.

TERZAGHI, K., 1936. 'The shearing resistance of saturated soils.' Proc. First Int. Conf. Soil Mech., Harvard, 1, 54-56.

TERZAGHI, K., 1941. 'Undisturbed clay samples and undisturbed clays.' J. Boston Soc. civ. Eng. 28, 211-231.

TERZAGHI, K. and PECK, R.B., 1948. 'Soil mechanics in engineering practice.' (1st Edition), John Wiley & Sons, New York, 566 pp.

TERZAGHI, K. and PECK, R.B., 1967. 'Soil mechanics in engineering practice.' (2nd Edition), John Wiley and Sons, New York, 729 pp.

TILL, R. and SPEARS, D.A. 1969. 'The determination of quartz in sedimentary rocks using an X-ray diffraction method.' Clays and Clay Minerals, 17, 323-327.

TOURTELOT, H.A., 1962. 'Preliminary investigation of the geologic setting and chemical composition of the Pierre Shale.' U.S. Geological Survey, Prof. Paper 390.

TREWIN, N.H., 1968. 'Potassium bentonites in the Namurian of Staffordshire and Derbyshire.' Proc. Yorks. geol. Soc., 37, 73-91.

TROSTEL, L.J. and WYNNE, D.J., 1940. 'Determination of quartz (free silica) in refractory clays.' J. Am. Ceram. Soc., 23, 18-22.

TRUEMAN, A.E. (Editor), 1954. 'The coalfields of Great Britain.' 396 pp. Arnold, London.

UNDERWOOD, L.B., 1967. 'Classification and identification of shales.' Proc. A.S.C.E. (J. Soil Mech. Div.), 93, SM6, 97-116.

VAN KREVELEN, D.W., 1961. 'Coal.' Elsevier Publishing Co., Amsterdam, 514 pp.

WARD, W.H., BURLAND, J.B. and GALLOIS, R.W., 1968. 'Geotechnical assessment of a site at Mundford, Norfolk, for a large proton accelerator.' Geotechnique, 18, 399-431.

WATKINS, G.L., 1959. 'The stability of colliery spoilbanks.' Colliery Engng. 36, 493-497.

WEEKS, A., 1969. 'A preliminary investigation into certain mineralogical and chemical aspects of Tip 7 of Merthyr Vale Colliery at Aberfan.' Item 1, Appendix 3, 51-55. 'A selection of Technical reports submitted to the Aberfan Tribunal. Welsh Office, London, H.M.S.O.

WELSH OFFICE, 1969. ' A selection of Technical reports submitted to the Aberfan Tribunal' London H.M.S.O., 217 pp.

WELLER, J.M., 1930. 'Cyclical sedimentation of the Pennsylvanian period and its significance.' Journ. Geol. 38, 97-135.

WHITE, D.E., HEM, J.D. and WARING, G.A., 1963. 'Chemical composition of subsurface waters.' (Data of Geochemistry, Chapter F). U.S. Geol. Surv. Prof. Paper 440-F, 67 pp.

WHITE, W.A., 1961. 'Colloid phenomena in sedimentation of argillaceous rocks.' J. sedim. Petrol. 31, 560-570.

WILSON, M.J., 1965a. 'The origin and geological significance of the South Wales underclays.' J. sedim. Petrol., 35, 91-99.

WILSON, M.J., 1965b. 'The underclays of the South Wales coalfield east of the Vale of Neath.' Min. Engr., 124, 389-404.

WINMILL, T.F., 1915-1916. 'Atmospheric oxidation of iron pyrites.' Pt.IV Trans. Instn. Min. Engrs., 51, 500.

WOODLAND, A.W., 1968. 'Field geology and the civil engineer.' Proc. Yorks. geol. Soc., 36, 531-578.

YODER, H.S. and EUGSTER, H.P., 1955. 'Synthetic and natural muscovites.' Geochim. cosmochim. Acta., 8, 225-280.

APPENDIX 1

X-ray fluorescence spectrometry

X-ray fluorescence analysis involves the measurement of observed intensities of fluorescent radiation (peak above background) and the subsequent calculation of the concentration of the element which is fluorescing in the sample. In the current work Si, Al, Fe,Mg, Ca, Na, K, Ti, S, P and Mn were determined by this means. A very detailed analysis of operating conditions, precisions and detection limits of major elements of Carboniferous sediments, determined by the Philips 1212 automatic spectrometer is given by Reeves (1971), a research student under the partial supervision of the present writer. It is therefore not proposed to discuss the use of this very rapid and powerful analytical tool in detail but rather to point out the way in which the method has been adopted for such diverse materials as colliery spoils.

Direct proportionality between fluorescent intensity and concentration does not apply, the three causes of deviations being:

(a) Spectrograph instability (electronic)

(b) Heterogeneity in samples, principally surface effects and segregations

(c) Absorption and enhancement effects related to the chemical nature of the sample.

The first two sources of error can in practice be reduced to negligible proportions (see Holland and Brindle, 1966) and it is (c), the so-called matrix effects, which give rise to the major source of error. Absorption problems are common to all quantitative X-ray methods and possibly the simplest method of reducing the matrix effects is to use standards which are of similar chemical composition to the unknown. Thirty-two reliable wet analysed standards of Coal Measures rocks have now been acquired and for the analyses of the <u>in situ</u> weathered- non-weathered sequence the approximate analysis of the unknowns was upgraded by close range calibration i.e. chosing

standards which bracketed the unknowns over a very restricted range. The preliminary calibration data shown on Table A1.1(partly after Reeves (1971) who used the same standards as the present writer), demonstrates that for the elements Na and Mg the count rates are low, and in general that of Na is so near the limit of detection that the quantitative Na_2O percentage by X.R.F. methods must be questioned. At a very early stage of this work when only twelve wet analysed standards were available the writer had two analyses checked by wet analytical methods (Table A.1.2). The comparative results show good agreement especially for Na and it is clear that little would be gained from determining the element by an alternative method. Table A1.2 demonstrates that the X.R.F. CaO determinations are systematically low and at the time the correlation coefficient for this oxide was little better than sodium; this has now been rectified. One other feature of Table A1.1is the high SiO_2 and Al_2O_3 intercepts which may be a function of the range of the data used in the calibration. Over the calibration ranges shown it is probable that the linear relationship is accurately defined and hence the intercept is unimportant. For the in situ rocks the reliability of the standards was confirmed in that the sum of the major elements, plus CO_2, C and H_2O was within the range 99 to 102.5 per cent.

The good agreement between wet analysis and the X.R.F. processing method of Holland and Brindle (1966) justifies the use of their self-consistent mass absorption correction. Using the wide spectrum of standards available their matrix correction procedure has the added advantage that organic C, CO_2 and H_2O need not necessarily be known. Hence for all other analyses the normalized oxides and elements were obtained after Holland and Brindle (1966). In certain cases the analyses have then been re-computed to include CO_2, organic C and H_2O.

TABLE A1.1

X-ray fluorescence analysis.

Preliminary calibration of major element standards

Element/ oxide	Slope c.p.s./%	Intercept	Range %	Correlation Coefficient	Precision* %
SiO_2	260	8.0	40 - 75	0.97	1
Al_2O_3	390	2.0	10 - 35	0.94	1
Fe_2O_3	1300	-0.1	0 - 15	0.92	4
MgO	70	0.4	0 - 50	0.99	5
CaO	1280	-0.1	0 - 15	0.99	6
Na_2O	15	0.3	0 - 10	0.96	7
K_2O	3200	0.1	0 - 5	0.99	1
TiO_2	7500	0.05	0 - 3	0.99	1
MnO	-	-	0 - 0.4	0.99	2
S	120	-0.05	0 - 5	0.98	2
P_2O_5	440	0.05	0 - 1	0.98	2

Tungsten tube for Mn, chromium for all other elements.
* 32 samples - duplicate runs over a period of 18 months.

TABLE A1.2

Comparison of X.R.F. and wet chemical analyses

	Sample H 13 A1		Sample H 13 A2	
	Lower Coal Measures			
Oxide	Wet Chemical	X.R.F.*	Wet Chemical	X.R.F.*
SiO_2	61.36	61.00	61.11	61.08
Al_2O_3	24.63	24.50	24.90	24.45
Fe_2O_3	5.98	6.54	6.40	6.73
MgO	2.08	2.24	1.93	2.04
CaO	0.82	0.42	0.57	0.39
Na_2O	0.42	0.36	0.35	0.34
K_2O	3.55	3.50	3.61	3.57
TiO_2	1.13	1.22	1.09	1.15
P_2O_5	0.12	0.11	0.10	0.08
MnO	0.03	0.04	0.08	0.07

Wet analyst: V.A. Somogyi

* Using computer program of Holland and Brindle (1966) with 12 wet analysed Coal Measures standards.

Cation exchange capacity

Cation exchange in sediments is a reversible reaction because the cations held on clay mineral surfaces and within the lattices can be reversibly exchanged with those of salt solutions and acids. There are numerous methods of achieving the exchange and they vary in degree of accuracy. In the current work a method which does not involve acid leaching and which is essentially quick with respect to sodium, potassium, magnesium and calcium has been used (Chapman, 1965).

The cation exchange capacity tends to vary with the method used - it is dependent to a certain extent on the nature of the replacing cation. In the current work it is therefore more specific to define the exchange capacity of a particular cation as that which is extractable with 1.0 N NH_4OAc (ammonium acetate).

15 ml of 1.0 N NH_4OAc (pH7) was added to 0.5g of dried sediment which had previously been thoroughly washed in distilled water to remove extraneous cations. After standing for 24 hours the suspension was then filtered and washed through with a further 15 ml of NH_4OAc. The exchangeable sodium and potassium in the filtrate were determined by flame photometer and calcium and magnesium by atomic absorption. The availability of correct tubes limited the atomic absorption determinations to two cations only. Full details of the standards used and conversion to milliequivalents per 100g are given by Connelly (1970) and Taylor (1967), respectively.

APPENDIX 2

X-ray diffraction quantitative curves

The calibration curves for quantitative mineralogical studies have been developed by R.G. Hardy, using boehmite as an internal standard (Griffin, 1954). The present writer found that good repeatability was obtained with boehmite (Taylor, 1967) because its mass absorption coefficient at the Cu Kα wavelength is of the same order as the clay minerals and quartz i.e. the standards are homogeneous. Boehmite as a 10 per cent addition by weight has a high 6.18 Å reflection so that a small addition causes little loss in sensitivity. The boehmite 6.18 Å peak is close to 7.0 Å kaolinite plus chlorite, 10 Å mica and also to the 4.26 Å quartz reflection. The 14 Å chlorite peak is a little remote and hence it is advocated that chlorite (which in any case is a minor constituent) should be treated as a semi-quantitative estimate. Till and Spears (1969) developed a boehmite-quartz determinative method which involves removing the clay minerals by ignition at 950°C. The reason for adopting this modification is that illite 4.5 Å does overlap with quartz 4.26 Å close to the base-line. Small peak area adjustments can be made however, and judging from the precision of the Brancepeth results there is little advantage in determining quartz from separate preparations.

Standards were made up (Table A 2.1) using quartz, illite, kaolinite, chlorite and a matrix of charcoal, ankerite and pyrite. The matrix composition is an attempt to simulate coal and its immediate mineralogical associates. The matrix composition was kept constant and the percentage of clay minerals and quartz varied within the ranges shown on Table A 2.1. Smear mounts were then made up and the samples run under suitable instrumental conditions (Table A 2.1). The intensity ratios of mineral to the 10 per cent boehmite addition were determined by areal measurement of the respective

peaks using a polar planimeter. In order to correct the kaolinite peak for chlorite (7Å reflection = kaolinite + chlorite), twice the area of the 14Å chlorite peak was subtracted from the 7Å peak area (relative intensities of 14Å and 7Å penninite peaks (see Brown, 1961.).

The resulting calibration curves are shown on Figure A1.1; for the greater portion of the distributions least squares linear regression lines are logically the 'best fit'.

TABLE A2.1

X-ray calibration data (standards)

Mineral	Source	Impurity weight %	Range weight %
Quartz	Madagascar	-	2.97 - 32.10
Illite	Le Puy-en-Velay (France)	3.5 chlorite	7.41 - 53.60
Kaolinite	Cornwall	6.0 Illite	2.70 - 65.66
Chlorite (Penninite)	Switzerland	-	3.50 - 10.10

Matrix concentration (constant at 17%)

Mineral	Source	Concentration
Charcoal	Analar	10%
Ankerite	Cow Green	5%
Pyrite	Cornwall	2%

X-ray diffraction instrumentation conditions

1 Kilowatt diffractometer (PW1010/1051 generator)

Cu radiation, Ni filtered

40 kV, 20 m A

Slits - 1° Div., 0.1° Rec., Scatter 1°

Scan speed 1°/min.

FIG A 2.1

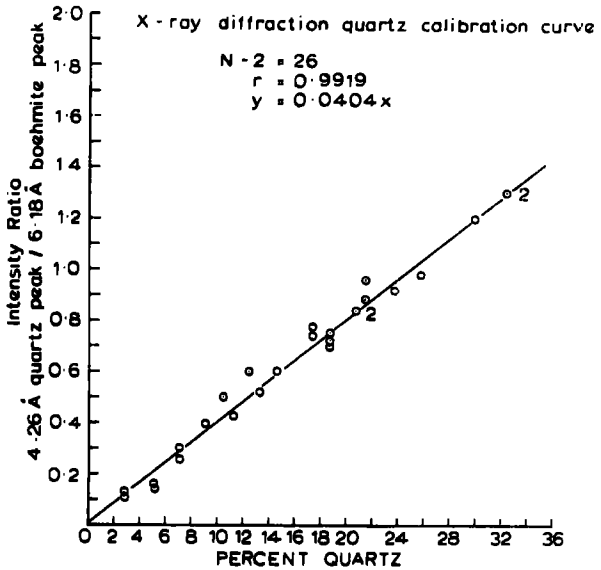

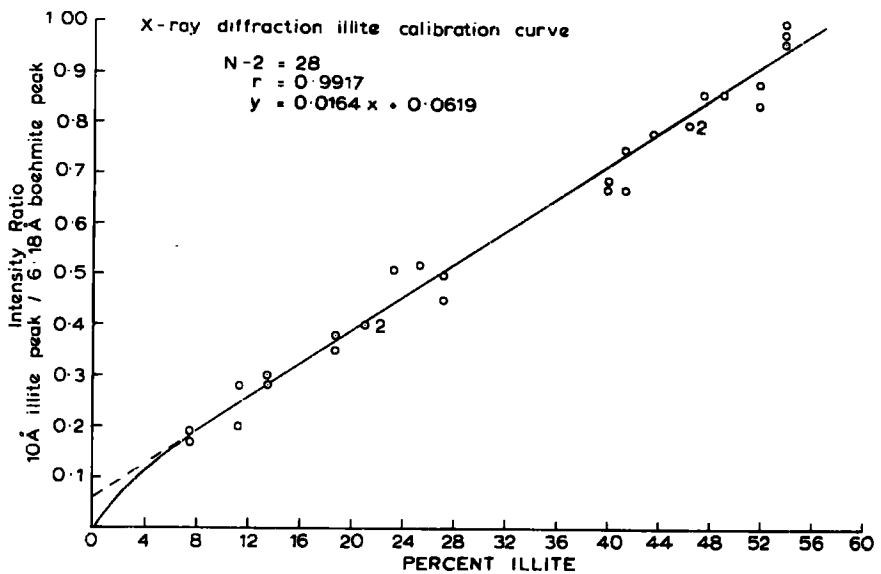

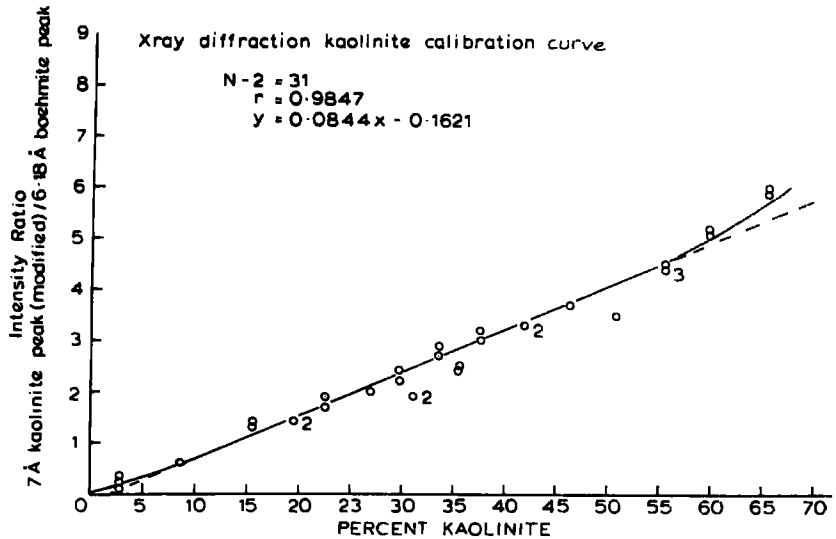

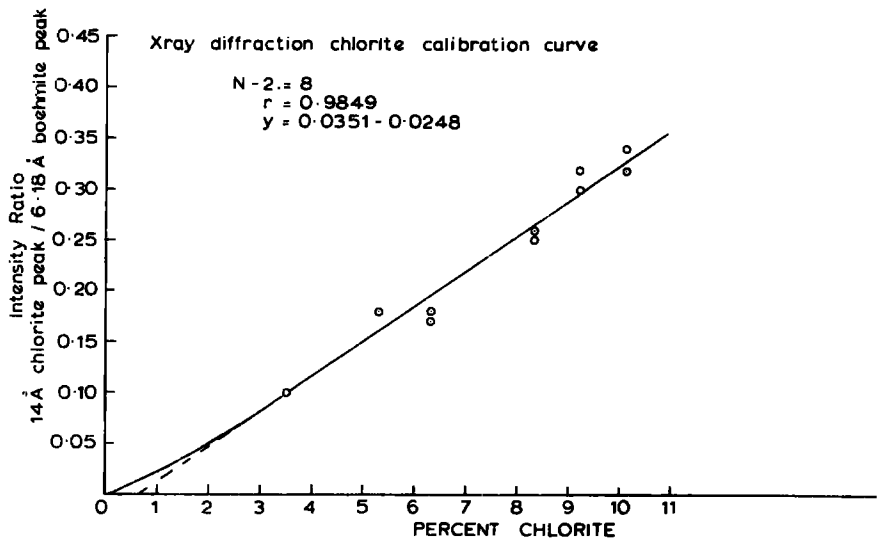

FIGURE A2.1

APPENDIX 3

Triaxial tests - back-saturation

The triaxial tests as applied to soils have reached a highly sophisticated level (see Bishop and Henkel, 1962) and standard undrained tests with pore pressure measurement, and fully drained tests are becoming more common in the commercial field. One feature concerning the tests carried out on colliery spoil requires elaboration in that the use of a back pressure to ensure full saturation (Bishop et al., 1960) is a refinement that is important when dealing with partly saturated soils.

From Figure A3.1 it can be seen that the cell pressure (minimum principal stress, σ_3) is applied to the sample via a pressure control. In our case, a conventional self-compensating mercury-water control (Bishop and Henkel, 1962, p.48) is used. The writer constructed a portable trolley-mounted system which is suitable for application of constant back pressure to the sample via the basal porous disc (basal connection, Fig. A3.1). The cell pressure and the pore pressure (i.e. back pressure) are increased in small steps of 5 lb/in^2 with time for equalization being allowed at each stage. Full saturation can be checked by measuring the pore pressure (standard Wykeham Farrance manual pore pressuremeasuring device) via the upper porous disc connection (Figure A3.1). A high back pressure (50 lb/in^2) was necessary tobring the majority of samples to near full saturation and consequently if the required effective pressure across the sample, σ_3' is say, 30 lb/in^2 the back pressure may well be 50 lb/in^2 and the cell pressure 80 lb/in^2. The sample is then sheared under drained conditions under constant back pressure at a rate of strain sufficiently low to avoid any significant build up in pore pressure. By utilising a double klinger cock system drainage of the sample can also be facilitated via the upper porous plate. The axial load (Fig. A3.1) at failure is converted to a stress

FIG. A3.1.

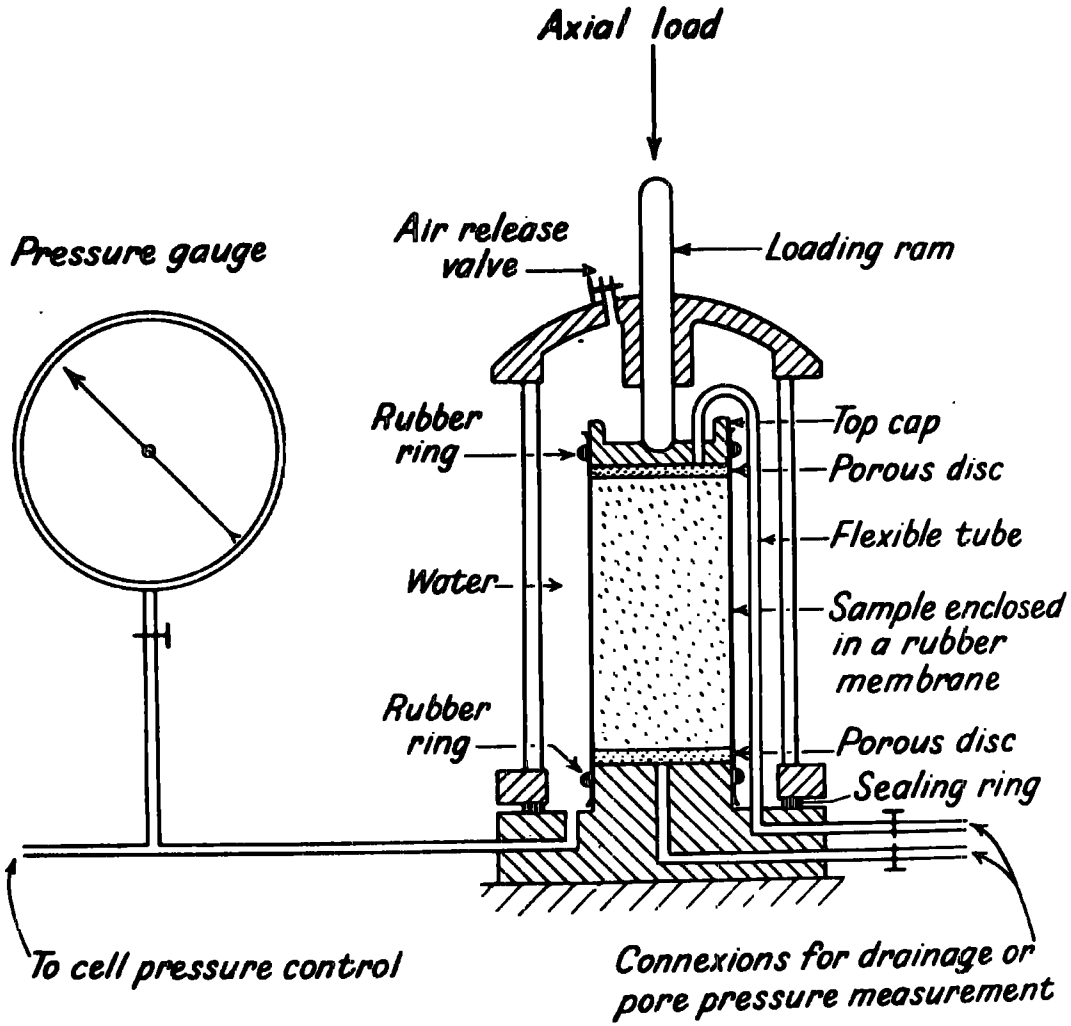

FIGURE A3.1

Diagrammatic layout of the triaxial test

difference component ($\sigma_1 - \sigma_3$) in that:

$$(\sigma_1 - \sigma_3) \text{ at failure} = \frac{\text{axial load x proving ring constant}}{\text{cross sectional area of sample at failure}}$$

The value of ($\sigma_1 - \sigma_3$) is of course the diameter of the respective Mohr circle.

APPENDIX 4

Slope stability analysis

The simplified Bishop Method of Slices (Bishop, 1955) was developed from the conventional Method of Slices which may well under-estimate the factor of safety (F), by over 20%.

In the Bishop method the moment about O (Fig. A4.1) of the weight of soil contained within the circular failure zone is equated with the moment of the shear forces acting on the slip surface. The following expression for the factor of safety (F) is obtained.

$$F = \frac{1}{\Sigma W \sin\alpha} \Sigma \left[\left\{ c'b + \tan\phi' \left[W(1-\bar{B} + (X_n - X_{n+1}) \right] \right\} \frac{\sec\alpha}{1 + \frac{\tan\phi' \tan\alpha}{F}} \right]$$

It is assumed that $(X_n - X_{n+1}) = 0$

$$\text{Hence } F = \frac{1}{\Sigma W \sin\alpha} \Sigma \left[\left\{ c'b + W(1-\bar{B}) \tan\phi' \right\} \frac{1}{\cos\alpha + \frac{\tan\phi' \sin\alpha}{F}} \right]$$

Notation used by Bishop (1955) - to be read in conjunction with Figure A4.1

When: E_n and E_{n+1} are the resultants of the horizontal forces on each side of slice

X_n and X_{n+1} are vertical shear forces

W total weight of slice

P total normal force acting on base of slice

S shear force acting along base of slice

h is the height of the slice

b is the breadth of the slice

l is the length of the base arc of the slice

α is the angle between the base of the slice and the horizontal

x is the horizontal distance of the slice from the centre of rotation

R is the radius of the circular arc

FIG. A4.1

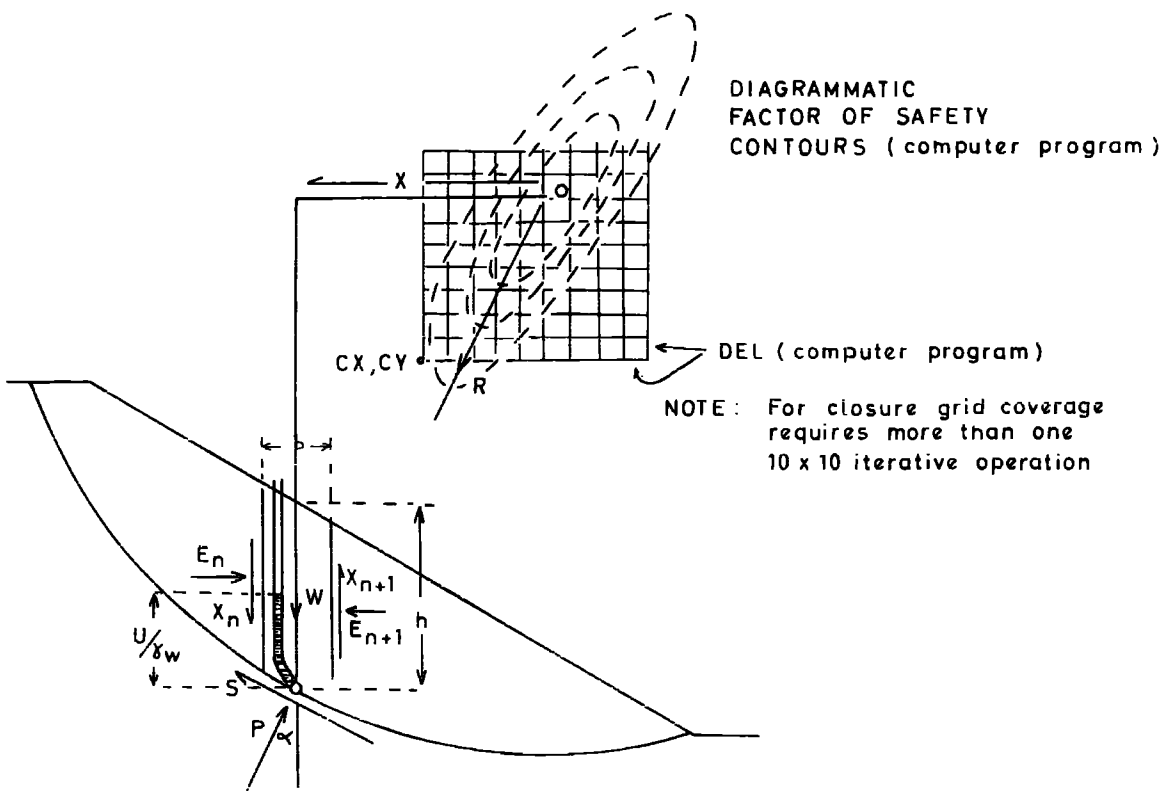

To show forces and dimensions used in Bishop Simplified Method of Slices analysis. Diagrammatic grid and Factor of Safety contours refer to computer program.

u is the pore pressure

γ_w is the density of water

$\bar{B} = u/\frac{W}{b}$

c' = effective cohesion

ϕ' = effective angle of shearing resistance

As F appears on both sides of the equation the solution has to be obtained by a process of successive approximation. Convergence is very rapid and the method lends itself to computer analysis (Little and Price, 1958). The simplifying assumption that the inter-slice forces can be neglected has been studied in detail by Spencer (1967) who showed that they are remarkably insensitive. The remarkable accuracy of the Bishop Simplified Method (even for non-circular failure surfaces) can be judged from the fact that computed factors of safety are usually less than 2 per cent in error when compared with complex methods such as Morgenstern and Price (1965), whose analytical method is well beyond the capabilities of any user with no previous computing experience. Even with the current program a considerable amount of work is required to arrive at the minimum factor of safety, but the co-ordinate input system and the representation of the water table (phreatic line) by a downward curving parabola which can be constructed by well-established methods (see Krynine 1941, p.66), has resulted in an exceedingly simple and versatile program.

The operation of the program which was originally written as a student project by Mr. R.G. Roberts in Fortran IV can be best explained by reference to the Brancepeth slope profile (Fig. 4.13), the sample data input sheet for Brancepeth (Table A4.1) and Figure A4.1.

The slope is first divided into a signified number of vertical slices (ideally between 32 and 64 according to Spencer, 1967). On the data input (Table A4.1) this is signified as EN. The width of each slice is determined

TABLE A4.1

1. NL = (10) EXAMPLE; CIRCLE (9) BRANCEPETH FIGURE 4.13

2.

t	c		φ		γ	t	c	φ		γ
	lb/in^2	lb/ft^2	o	rads	lb/ft^3		lb/ft^2	o	rads	lb/ft^3
(1)	0	-	35.5	.6196	100	(7)	0	35.5	.6196	107
(2)	0	-	35.5	.6196	100	(8)	0	35.5	.6196	103
(3)	0	-	35.5	.6196	98	(9)	144	31.5	.5498	131
(4)	0	-	35.5	.6196	89	(10)	144	31.5	.5498	131
(5)	0	-	35.5	.6196	103					
(6)	0	-	35.5	.6196	105					

3.

	X(I.J.)	Y(I.J.)		X(I.J.)	Y(I.J.)
1.1	0	282	7.2	315	77.5
1.2	10	280	8.1	0	85
2.1	0	275	8.2	332.5	67.5
2.2	20	275	9.1	0	42
3.1	0	207	9.2	567.5	12
3.2	84	207	10.1	0	28
4.1	0	190	10.2	610	0
4.2	107.5	185			
5.1	0	152			
5.2	170	142.5			
6.1	0	105			
6.2	282.5	92			
7.1	0	95			

4. NIX = 16

5.

QX	J = 1	J = 2	QX	J = 1	J = 2
1	0	282	9	247.5	102
2	10	280	10	282.5	92
3	20	275	11	310	82
4	84	207	12	375	42
5	100	192	13	427.5	32
6	155	152	14	465	22
7	187.5	132.5	15	567.5	12
8	225	112	16	610	10

6. CX = 340 CY = 185 DEL = 10

7. KL = 9 KZ = 9

8. WID = 610 EN = 40

9. JHRED = 1

10. NPOIN 8

11.

PX	J = 1	J = 2	PX	J = 1	J = 2
1	0	95	5	427.5	32
2	266	82	6	465	22
3	317.5	68	7	567.5	12
4	375	42	8	610	10

in the program from the overall slope dimension, WID (Table A4.1, No.8; dimension shown on Fig. 4.13). Now the number of stratum lines is signified (NL) and also their x and y co-ordinates, X(I.J), Y(I.J) - see Table A4.1 and Figure 4.13. These are of course related to the origin (0,0) of the scale drawing (e.g. Fig.4.13). Similarly, the number of points used to determine the surface profile of the slope are signified (NIX), together with respective x and y co-ordinates QX, (J=1, J=2) - Table A4.1, Nos. 4 and 5. Hence, an algebraic computer picture is built up from the previously prepared graphical one. The x co-ordinate of the centre line of each slice is calculated by the computer and the initial failure surface located by stipulating the co-ordinates of its centre, and the failure line to which it is tangential (CX,CY (co-ordinates); KL,KZ (line number) - TableA4.1, Nos. 6 and 7). A reasonable approximation by trial and error is involved initially.

The y co-ordinates of the centre line of each slice are now calculated and for each slice in turn the area of each stratum that lies within the slice and the failure circle boundary is found. Because the number of slices are large the area is calculated from the known slice width multiplied by the respective stratum thickness. These areas are transformed into weights by multiplying by the respective stratum bulk density (γ , TableA4.1, No.2). The table of weights is stored by the computer as these values are used for all calculations.

The pore pressure parameter $\bar{B}$ is expressed as $\bar{B} = u/\frac{W}{b}$ (Bishop, 1955 and notation, Fig. A4.1). The pore pressure u acting on the base of the slice is given by $u = h_1 \gamma_w$ where h_1 is the height of the phreatic line above the base of the slice and γ_w is the density of water. Most of the work carried out on slope stability in this country has involved the use of average values of $\bar{B}$ for each soil stratum in the slope, and the use of

an 'average' parameter has probably been a method of expediting design, because it can be estimated from the triaxial test. In the current program the pore pressure is treated realistically with JHRED = 1 being called when a water table is approximated by a specified number of co-ordinates, NPOIN with x and y values, shown as PX, (J = 1, J = 2) on Table A4.1, Nos. 8 and 9. The value of $\bar{B}$ is therefore calculated for each slice and all the factors required to build up the Newton Raphson iterative equation are now assembled as cohesion, c' and ϕ' (in radians) are already included in the input data (Table A4.1, No.2).

The equation is of the form:

$$F1 = FO\left\{1 - \frac{\Sigma W \sin\alpha - \Sigma \left[\dfrac{c'b + W(1-\bar{B})\tan\phi'}{FO\cos\alpha + \tan\phi'\sin\alpha}\right]}{\Sigma W \sin\alpha - \dfrac{\Sigma\left[c'b + W(1-\bar{B})\tan\phi'\right]\tan\phi'\sin\alpha}{(FO\cos\alpha + \tan\phi'\sin\alpha)^2}}\right\}$$

where F1 is a better approximation of the factor of safety obtained from an initial approximation, FO. The computer iterates from a value of FO which is set early in the program and tests to see if each new F1 is closer than 10^{-3} to the previous one. When this condition has been fulfilled the factor of safety is printed out, together with circle radius, circle centre co-ordinates, grid numbers and failure line number. It has already been mentioned that the initial circle centre co-ordinates are given to the computer (CX and CY). When the first factor of safety is printed out the value of CX is updated by a specified increment DEL (Table A4.1, No.6). When CX has been updated 9 times the computer resets CX to its original value and updates CY by the increment DEL. Eventually a 10 by 10 grid of circle centres is formed and if each factor of safety is appended to its respective grid intersection they can be contoured in order to determine the minimum (diagrammatic on Fig. 4.1). The program usually has to be run

several times before contour 'closure' is ensured.

The writer has gradually updated the program, and for JHRED=0 (i.e. no water table) the comparison with Bishop et al., (1969, p.65) is within 0.3% (F= 1.281 for $\emptyset'=35°$ soil types 1 and 2, circle 2, Bishop et al.; F=1.277, this work). Expressing their pore pressure ratio in terms of a water table (p.65) the factor of safety is within 1.26% (F= 1.271 for $\emptyset'= 38°$ soil types 1 and 2, circle 2, Bishop et al.; F= 1.255 for similar conditions, this work).